DISSERTATION

STRUCTURAL VARIATIONS IN METAL ION COMPLEXES OF THE LIGAND $EGTA^{4-}$

Submitted by

Cynthia Karen Schauer

Department of Chemistry

In partial fulfillment of the requirements

for the Degree of Doctor of Philosophy

Colorado State University

Fort Collins, Colorado

Fall, 1985

COLORADO STATE UNIVERSITY

October 17, 1985

WE HEREBY RECOMMEND THAT THE THESIS PREPARED UNDER OUR SUPERVISION BY CYNTHIA KAREN SCHAUER ENTITLED STRUCTURAL VARIATIONS IN METAL ION COMPLEXES OF THE LIGAND $EGTA^{4-}$ BE ACCEPTED AS FULFILLING IN PART REQUIREMENTS FOR THE DEGREE OF DOCTOR OF PHILOSOPHY.

Committee on Graduate Work

Anthony J. Jr
C. Michael Elliott
[illegible]
[illegible]
Advisor

[illegible]
Department Head

ABSTRACT OF DISSERTATION

STRUCTURAL VARIATIONS IN

METAL ION COMPLEXES OF THE LIGAND $EGTA^{4-}$

Structural studies of several metal ion complexes with the tetraanion of the octadentate ligand, H_4EGTA (3,12-bis(carboxymethyl)-6,9-dioxa-3,12-diazatetradecanedioic acid), as well as the structure of H_4EGTA, have been performed by single crystal X-ray diffraction. Of particular interest was the structural basis for the large preference for $EGTA^{4-}$ to bind calcium ion rather than magnesium ion ($K(CaL^{2-}) \tilde{=} 10^6(K(MgL^{2-}))$, a preference which is similar to that exhibited by intracellular calcium binding proteins.

The alkaline earth compounds, $Ca[Ca(EGTA)]\cdot(22/3)H_2O$, $Sr[Ca(EGTA)]\cdot 6H_2O$, $Mg[Sr(EGTA)(OH_2)]\cdot 7H_2O$, $Mg[Ba(EGTA)]\cdot(8/3)H_2O\cdot(1/3)(CH_3)_2CO$, and $[Mg_2(EGTA)(OH_2)_6]\cdot 5H_2O$, have been structurally characterized. $[Ca(EGTA)]^{2-}$ is eight-coordinate and utilizes the full octadentate chelating capability of the $EGTA^{4-}$ ligand. The ether oxygen atoms are bound at a shorter distance than the amine nitrogen atoms. $EGTA^{4-}$ is octadentate toward both the strontium and barium ions, which are nine- and ten-coordinate, respectively. The magnesium complex is

dinuclear, utilizing each end of the $EGTA^{4-}$ ligand as a tridentate iminodiacetate ligand; the ether oxygen atoms are not involved in coordination to the metal ion.

Structures of $EGTA^{4-}$ chelates of metal ions that are commonly used as spectroscopic probes for calcium ion binding sites have also been determined. The cadmium chelate in $Sr[Cd(EGTA)]\cdot 7H_2O$ is eight-coordinate, like $[Ca(EGTA)]^{2-}$, but the amine nitrogen atoms are bound at shorter distances than the ether oxygen atoms. The metal ions in the structures of tripositive lanthanide ion complexes, $Ca[Er(EGTA)(OH_2)]_2\cdot 12H_2O$ and $Ca[Nd(EGTA)(OH_2)]_2\cdot 9H_2O$, are nine- and ten-coordinate, respectively.

To further explore coordination modes of the $EGTA^{4-}$ ligand with smaller metal ions, where the ligand is not likely to be octadentate, structures of manganese and copper complexes of $EGTA^{4-}$ were determined. $Sr[Mn(EGTA)]\cdot 7H_2O$ is isomorphous with the cadmium compound. As a result, the Mn(II) ion is eight-coordinate. The copper complex crystallizes as a dinuclear species, $[Cu_2(EGTA)(OH_2)_2]\cdot 2H_2O$, in which each end of the $EGTA^{4-}$ ligand binds a copper(II) ion in a tetradentate fashion; the ether oxygen atom is bound in the apical position of the square pyramidal coordination sphere.

Cynthia Karen Schauer
Department of Chemistry
Colorado State University
Fort Collins, CO 80523
Fall, 1985

ACKNOWLEDGEMENTS

I would like to thank Professor Oren Anderson for support and encouragement over the course of this research (especially near the end),and for re-sparking my interest in learning. I would also like to thank Professors Jack Norton and Steve Strauss for many stimulating and helpful discussions during the past four years.

I feel very lucky to have my two classmates, Joe and Mike, as good friends. Joe, your cheerful and laid-back approach to life has been very pleasant to work around the past three years. Joe and I are still the reigning shuffleboard champions, right Mike. I have especially enjoyed the friendly interactions with the graduate students of the inorganic division during my stay at CSU, and I am grateful for their support over the last few months. Patty and Kim were always ready for a late-night bull session, sometimes even about chemistry. To my fellow motorcycle mama, Lucille: too bad we didn't have time for just one last ride; thanks for trying, though.

I am also indebted to the Bernsteins (Elliott, Barbara, Jephta, and Becky), who provided me a place to live while I completed my dissertation.

My parents have always been there when anything was needed. Mom deserves special thanks for typing several of the tables which appear in the appendices of this thesis, and for helping with proofreading.

Lastly, I would like to acknowledge my husband, Mark, who, in taking a job 1000 miles away while I completed my thesis, probably did the best thing for our marriage. Thanks for being near the phone when I needed you, and giving me some perspective when I needed it most.

TABLE OF CONTENTS

LIST OF TABLES

LIST OF FIGURES

LIST OF ABBREVIATIONS

BAPTA^{4-} 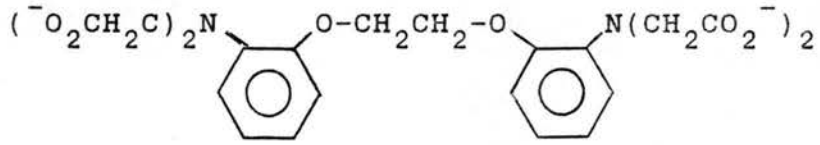

DCTA4- 

DTPA^{5-} $(^{-}O_2CH_2C)_2N\text{-}CH_2CH_2\text{-}N(CH_2CO_2^{-})\text{-}CH_2CH_2\text{-}N(CH_2CO_2^{-})_2$
CH_2
CO_2^{-}

EEDTA^{4-} $(^{-}O_2CH_2C)_2N\text{-}CH_2CH_2\text{-}O\text{-}CH_2CH_2\text{-}N(CH_2CO_2^{-})_2$

EDTA^{4-} $(^{-}O_2CH_2C)_2N\text{-}CH_2CH_2\text{-}N(CH_2CO_2^{-})_2$

EGTA^{4-} $(^{-}O_2CH_2C)_2N\text{-}CH_2CH_2O\text{-}CH_2CH_2\text{-}O\text{-}CH_2CH_2\text{-}N(CH_2CO_2^{-})_2$

IDA^{2-} $HN(CH_2CO_2^{-})_2$

MIDA^{2-} $H_3CN(CH_2CO_2^{-})_2$

NTA^{3-} $N(CH_2CO_2^{-})_3$

ODA^{2-} $O(CH_2CO_2^{-})_2$

ODTA^{4-} $(^{-}O_2CH_2C)_2N\text{-}(CH_2)_8\text{-}N(CH_2CO_2^{-})_2$

CHAPTER 1

INTRODUCTION

Many structural investigations have been performed on metal complexes of $EDTA^{4-}$ and $EDTA^{4-}$-like hexadentate ligands (see Table 1.1).[1-44] Despite this fact, very few structural results are available for complexes of polycarboxylate chelating ligands with more than six binding sites, in which the full chelating potential of the ligand is realized.[45-47] The tetraanion of the ligand H_4EGTA (3,12-bis(carboxymethyl)-6,9-dioxa-3,12-diazatetradecanedioic acid, see below) is potentially octadentate and contains three ligand atom types, including two neutral

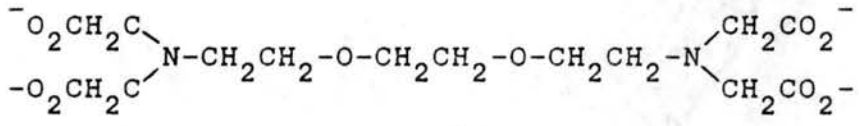

$EGTA^{4-}$

tertiary amine nitrogen atoms, two ether oxygen atoms, and four anionic carboxylate groups.

The results presented in this dissertation have been gathered in an attempt to attain a detailed understanding of the metal-binding preferences of $EGTA^{4-}$. Among various types and sizes of metal ions, significant differences might be expected in the manner in which the metals are bound by a flexible polydentate ligand such as $EGTA^{4-}$.

Table 1.1 Metal Complexes of $EDTA^{4-}$ and Related Ligands Characterized by X-Ray Diffraction

Complex	Reference
$[Ca(EDTA)]^{2-}$	1
$[Mg(EDTA)(OH_2)]^{2-}$	2,3
$[Cd(HEDTA)]^{-}$	4
$[Cd(EDTA)(OH_2)]^{2-}$	5
$[Ba(EDTA)]^{2-}$	6
$[Pr(EDTA)(OH_2)_3]^{-}$	7
$[Gd(EDTA)(OH_2)_3]^{-}$	7
$[Sm(EDTA)(OH_2)_3]^{-}$	7,8
$[Dy(EDTA)(OH_2)_3]^{-}$	9
$[La(HEDTA)(OH_2)_4]$	10,11
$[La(EDTA)(OH_2)_3]^{-}$	10,12
$[Tb(EDTA)(OH_2)_3]^{-}$	10
$[Er(EDTA)(OH_2)_2]^{-}$	13
$[Nd(EDTA)(OH_2)_3]^{-}$	14
$[Yb(EDTA)(OH_2)_2]^{-}$	11
$[Ni(EDTA)]^{2-}$	15-19
$[Ni(HEDTA)(OH_2)]^{-}$	20
$[Ni(H_2EDTA)(OH_2)]$	21
$[Co(EDTA)(OH_2)]^{2-}$	22-24
$[Mn(HEDTA)(OH_2)]^{-}$	25
$[Co(EDTA)]^{-}$	26
$[Cr(HEDTA)(OH_2)]$	27
$[Mn(EDTA)]^{-}$	28,29

Table 1.1 (continued)

$[Fe(EDTA)(OH_2)]^{2-}$	30,31
$[Fe(DCTA)(OH_2)]^{2-}$	32
$[Cu(EDTA)]^{2-}$	33,34
$[Cu(H_2EDTA)(OH_2)]$	35
$[In(EDTA)(SO_3)]^{3-}$	36
$[Rh(HEDTA)(OH_2)]$	37
$[VO_2(EDTA)]^{3-}$	38
[Sb(HEDTA)]	39
$[Sn(H_2EDTA)]$	40
$[Sn(EDTA)(OH_2)]$	41
$[Ga(HEDTA)(OH_2)]$	42
$[Al(EDTA)]^{-}$	43
[Zr(EDTA)]	44

Such differences might be based on the metal ion's coordination number or ligand atom preferences, or on steric constraints associated with organizing the polydentate ligand about the various metal ions. Structures of the chelates formed between $EGTA^{4-}$ and the alkaline earth metal ions (Mg^{2+}, Ca^{2+}, Sr^{2+}, and Ba^{2+}), other dipositive metal ions (Mn^{2+}, Cu^{2+}, and Cd^{2+}), and tripositive lanthanide metal ions (Nd^{3+} and Er^{3+}) have been determined in the course of this research; those results are described in subsequent chapters of this dissertation.

$EGTA^{4-}$ is of particular interest among the amino-polycarboxylate ligands because it exhibits a very large preference for binding calcium ion rather than magnesium ion ($K(CaL^{2-}) \tilde{=} 10^{6}(K(MgL^{2-})^{48}$). This calcium-binding preference is similar to that exhibited by intracellular calcium-binding proteins. Calcium-binding proteins, such as troponin C and calmodulin, are known to play a central role in the regulation of many important biological processes.[49-59] Troponin C plays a fundamental role in muscle contraction,[60] while the seemingly ubiquitous calmodulin has been found to regulate ATPase activity,[61] exocytosis,[62,63] and other cellular functions.[51-54] The mechanism for such regulation is thought to involve a change in the conformation of the regulatory protein on binding of the calcium ion. To bind calcium ion in the intracellular environment, where magnesium ion is typically present in thousand-fold excess, such calcium-binding

proteins clearly must possess a binding site which is highly selective for calcium ion over magnesium ion. As a result of the calcium-binding selectivity of $EGTA^{4-}$, it is used extensively as a calcium ion buffer in biological studies of these calcium-binding proteins.[64] Additionally, both the calcium-binding proteins[65] and $EGTA^{4-}$ [48] prefer to bind calcium ion over strontium and barium ions, although these preferences are not important in nature.

The structurally characterized binding sites of the calcium-binding proteins contain only oxygen atom donors. As yet, no high resolution structural information is available for the calcium-selective binding sites of troponin C[66] or calmodulin.[67] However, a single crystal X-ray diffraction study of carp muscle parvalbumin, another calcium-binding protein, has revealed two highly selective calcium-binding domains, commonly referred to as "EF hands".[68] In the first site (located between helical sections C and D), the calcium ion is bound by six ligand atoms, including oxygen atoms from unidentate carboxylate groups of aspartic (Asp) and glutamic (Glu) acid residues, a serine hydroxyl group, and an amido oxygen atom of a phenylalanine residue. In the second site (located between helical sections E and F), the calcium ion is bound by eight ligand atoms, including both unidentate and bidentate Asp and Glu residues, an amido oxygen atom of a lysine residue, and the oxygen atom of a single water molecule. Kretsinger's proposal that similar domains perform the

highly selective calcium complexation characteristic of troponin C and calmodulin has received apparent confirmation from low-resolution X-ray diffraction results in the case of calmodulin.[67] In nature, therefore, it appears that homologous domains which complex calcium rather than magnesium in a highly selective fashion are used repeatedly.

Similarities exist between the coordination environment seen in the calcium-binding proteins and the coordination environment provided by the $EGTA^{4-}$ ligand. Six of the eight potential binding sites of $EGTA^{4-}$ are provided by neutral and anionic oxygen donors. Additionally, the overall charge of the $EGTA^{4-}$ ligand is identical to the charge of the protein calcium-binding domains. However, the remaining two binding sites are nitrogen donors, and, consequently, $EGTA^{4-}$ cannot be regarded as a faithful "model" for the binding sites of calcium-binding proteins. Despite this fact, it is likely that an understanding of the structural aspects of alkaline earth binding which are associated with the high degree of calcium-binding selectivity seen for $EGTA^{4-}$ will allow at least a partial understanding of the features which must be employed in the binding sites of calcium-binding proteins. It is this consideration that has led to the determination of the structures of the alkaline earth (Mg^{2+}, Ca^{2+}, Sr^{2+}, and Ba^{2+}) complexes of $EGTA^{4-}$ reported in this dissertation.

In studies of calcium-binding proteins, cadmium ion[69,70] and tripositive lanthanide ions[71-74] are commonly substituted for calcium ion to obtain spectroscopic information on the metal ion binding site (see Chapter 6). The structures of the cadmium and lanthanide ion chelates of $EGTA^{4-}$ have been studied in this research, in an attempt to determine the nature and magnitude of the structural changes which occur upon binding these probe metal ions to a highly calcium-selective site. The $EGTA^{4-}$ ligand provides a reference calcium-selective environment, and, unlike the proteins, a detailed evaluation of the structural differences between the calcium ion complex and the probe ion complexes is possible.

To explore some of the structural variations possible with smaller metal ions, structures of the Mn^{2+} and Cu^{2+} chelates of $EGTA^{4-}$ were determined. Certainly, eight-coordination is not common for these metal ions, and structural information on these chelates will help define the metal ion size at which the transition occurs from eight-coordination to a lower coordination number. In addition, information on how the $EGTA^{4-}$ ligand achieves lower coordination numbers in which the octadentate chelating ability of the ligand is not fully utilized will be established.

CHAPTER 2

EXPERIMENTAL

Preparation and Characterization of Compounds

General

All chemicals were used as purchased: H_4EGTA (J.T. Baker), $Mg(OH)_2$ (Alfa), $Ba(OH)_2 \cdot 8H_2O$ (MCB), $Sr(OH)_2 \cdot 8H_2O$, (Alfa), $Er_2(CO_3)_3$ (17.8% H_2O, Alfa), $Nd_2(CO_3)_3$ (1.0% H_2O, Alfa), $MnCO_3$ (Baker), $CdCO_3$ (Fisher) and $CuCO_3$ (Mallinckrodt). All preparations were performed in aqueous solution utilizing distilled water from the tap.

NMR spectra were taken on a Bruker WP-200SY, a Bruker WP-270SY, or a JEOL FX-100 spectrometer. IR spectra were taken on a Perkin Elmer 983 spectrometer.

Preparations and Crystallizations

H_4EGTA (1). Single crystals of 1 suitable for X-ray diffraction studies were obtained by slow cooling of a hot aqueous 0.26 M solution of H_4EGTA. The D_4EGTA for the infrared experiments was prepared by dissolving H_4EGTA in hot 99% D_2O. Cooling of a saturated solution yielded crystalline D_4EGTA.

Ca[Ca(EGTA)]·(22/3)H_2O (2). Calcium hydroxide (0.148 g, 2.00 mmol) was added to an aqueous slurry (20 mL) of H_4EGTA (0.385 g, 1.00 mmol). The solid materials dissolved on warming. The pH of the resultant solution was adjusted to 9, using a small amount of solid $Ca(OH)_2$. After addition of approximately 30 mL of acetone, single crystals suitable for X-ray diffraction studies were grown by slow cooling of the warm solution to refrigerator temperature. The resulting clear, colorless plates were characterized by the structure determination. Dissolution of the crystals allowed ^1H NMR and ^{13}C NMR spectra of the complex to be obtained. ^1H NMR (D_2O, 200 MHz, pH 9, DDS standard; δ, ppm): (2.82, t, 4, J_{HH} = 4.7 Hz), (3.25, AB_q, 8, J_{AB} = 14 Hz), (3.62, t, 4, J_{HH} = 4.7 Hz), (3.77, s, 4). ^{13}C NMR (D_2O, 68 MHz, pH 9, DDS standard; δ, ppm): (58.89, t, $^1J_{CH}$ = 137 Hz), (63.25, t, $^1J_{CH}$ = 136 Hz), (69.52, t, $^1J_{CH}$ = 144 Hz), (70.51, t, $^1J_{CH}$ = 146 Hz), (181.91, s).

Sr[Ca(EGTA)]·6H_2O (3). Calcium hydroxide (0.074 g, 1.00 mmol) and strontium hydroxide octahydrate (0.265 g, 1.00 mmol) were added to an aqueous slurry (15 mL) of H_4EGTA (0.380 g, 1.00 mmol). The pH was adjusted to 8 utilizing solid $Ca(OH)_2$. The volume of the above solution was reduced to 10 mL by evaporation, and 25 mL of acetone was then added. Slow cooling of the solution to room temperature yielded crystals suitable for X-ray

diffraction studies. This compound gave a ^{1}H NMR spectrum identical with that of **2**.

Mg[Sr(EGTA)(H_2O)]·$7H_2O$ (**4**). Magnesium hydroxide (0.058 g, 1.00 mmol), and strontium hydroxide octahydrate (0.265 g, 1.00 mmol) were added to an aqueous slurry (30 mL) of H_4EGTA (0.380 g, 1.00 mmol). Upon heating and stirring, a cloudy solution of neutral pH was obtained. Addition of acetone to a total volume of 75 mL induced precipitation of **4** as a powder. Single crystals of **4** suitable for X-ray diffraction experiments were grown by slow diffusion of acetone (over a period of two to three weeks) into filtered 2-4 mL samples of a 0.09 M solution prepared from the isolated powder. The clear, colorless single crystals were characterized by the X-ray structure determination, and by the ^{1}H NMR spectrum. ^{1}H NMR spectra of the magnesium, strontium, and barium complexes of $EGTA^{4-}$ have been previously reported;[75] these spectra qualitatively resemble the spectrum of the free $EGTA^{4-}$ ligand. The ^{1}H NMR spectrum of **4** (in D_2O) also qualitatively resembled the spectrum of the free ligand.

Mg[Ba(EGTA)]·(8/3)H_2O·(1/3)$(CH_3)_2CO$ (**5**). Magnesium hydroxide (0.058 g, 1.00 mmol), and barium hydroxide octahydrate (0.315 g, 1.00 mmol) were added to an aqueous slurry (25 mL) of H_4EGTA (0.380 g, 1.00 mmol), yielding a cloudy solution of approximately neutral pH upon stirring and heating. The volume of the solution was reduced to 5

mL, and addition of acetone to a total volume of 15 mL induced precipitation of 5 as a powder. Single crystals of 5 suitable for X-ray diffraction studies were grown through repeated recrystallization by vapor diffusion of acetone into 2 mL aliquots of an 0.08 M solution of the barium complex. The complex was characterized by the structure determination and by NMR spectroscopy (see above).

[Mg_2(EGTA)(OH_2)$_6$]·5H_2O (6). Magnesium hydroxide (0.116 g, 2.00 mmol) was added to an aqueous slurry (20 mL) of H_4EGTA (0.380 g, 1.00 mmol). This mixture was stirred and heated overnight, and the pH of the resulting solution was adjusted to 9 by addition of a small amount of solid $Mg(OH)_2$. Clear, colorless crystals suitable for X-ray diffraction were obtained as a result of slow evaporation of the above solution. The compound was characterized by the X-ray structure determination, as well as by NMR spectroscopy (see above).

Sr[Cd(EGTA)]·7H_2O (7). Strontium hydroxide octahydrate (0.265 g, 1.00 mmol) and cadmium carbonate (0.172 g, 1.00 mmol) were added to an aqueous slurry (6 mL) of H_4EGTA (0.380 g, 1.00 mmol), yielding a solution of approximately neutral pH upon warming. Addition of approximately 14 mL of acetone, followed by slow cooling of the solution to room temperature, resulted in isolation of single crystals suitable for the X-ray diffraction study. The compound was characterized by the structure determination, as well as by

NMR spectroscopy. The ^{1}H NMR spectrum of $[Cd(EGTA)]^{2-}$ has been previously reported.[76] The ^{1}H NMR spectrum of **7** agreed with the literature spectrum.

Ca[Er(EGTA)(OH_2)]$_2\cdot 11H_2O$ (**8**). $Er_2(CO_3)_3$ (17.8% H_2O) (0.626 g, 2.00 mmol) and H_4EGTA (0.760 g, 2.00 mmol) were dissolved in 500 mL of boiling water. $Ca(OH)_2$ (1.00 mmol, 0.074 g) was added and the volume was reduced to 8 mL. Vapor diffusion of acetone into the above solution, after filtration, yielded crystalline material. Crystals suitable for X-ray diffraction were obtained by vapor diffusion of acetone into 2.5 mL of a 0.02 M solution of **9**. The compound was characterized by the X-ray structure determination, as well as by ^{1}H NMR spectroscopy. ^{1}H NMR(D_2O, 200 MHz, pH 7, D_2O standard; δ, ppm): (-14.1, $\Delta\nu_{1/2} \tilde{=}$ 440 Hz, 2), (4.5, $\Delta\nu_{1/2} \tilde{=}$ 510 Hz, 4), (11.5, $\Delta\nu_{1/2} \tilde{=}$ 560 Hz, 2), (19.8, $\Delta\nu_{1/2} \tilde{=}$ 310 Hz, 2), (23.2. $\Delta\nu_{1/2} \tilde{=}$ 310 Hz, 2), (34.5, $\Delta\nu_{1/2} \tilde{=}$ 570 Hz, 6), (51.3, $\Delta\nu_{1/2} \tilde{=}$ 940 Hz, 2).

Ca[Nd(EGTA)(OH_2)]$_2\cdot 9H_2O$ (**9**). $Nd_2(CO_3)_3$ (1% H_2O) (0.956 g, 4.00 mmol) and H_4EGTA (1.520 g, 4.00 mmol) were added to 350 mL of water and heated at reflux temperature overnight. After addition of $Ca(OH)_2$ (0.148 g, 2.00 mmol), and filtration, the volume of the solution was reduced to 10 mL. Vapor diffusion attempts with solutions of varying concentrations initially yielded non-crystalline material. Single crystals suitable for X-ray diffraction were

eventually obtained by vapor diffusion of acetone into 3 mL of a 0.020 M solution of **8** (prepared from the isolated non-crystalline material) over a period of a month. The compound was characterized by the X-ray structure determination, as well as by NMR spectroscopy. ^{1}H NMR (D_2O, 200 MHz, pH 8, DDS standard; δ, ppm): (-1.10, $\Delta\nu_{1/2} \tilde{=}$ 18 Hz, 4), (0.84, $\Delta\nu_{1/2} \tilde{=}$ 42 Hz, 4), (2.38, $\Delta\nu_{1/2} \tilde{=}$ 42 Hz, 4), (3.22, $\Delta\nu_{1/2} \tilde{=}$ 24 Hz, 4), (6.73, $\Delta\nu_{1/2} \tilde{=}$ 51 Hz, 4).

Sr[Mn(EGTA)]·7H_2O (10). $MnCO_3$ (0.230 g, 1.00 mmol) and H_4EGTA (0.380 g, 1.00 mmol) were dissolved in 10 mL of boiling water. $Sr(OH)_2 \cdot 8H_2O$ (0.530 g, 1.00 mmol) was added, and the solution of approximately neutral pH was filtered. The volume of the solution was increased to 20 mL. Addition of approximately 30 mL of acetone to the warm solution, followed by slow cooling to room temperature, yielded crystals suitable for X-ray diffraction studies. The compound was characterized by the X-ray structure determination, as well as by EPR spectroscopy and by magnetic susceptibility.

[Cu_2(EGTA)(OH_2)$_2$]·2H_2O (11). $CuCO_3$ (0.248 g, 2.00 mmol) and H_4EGTA (0.380 g, 1.00 mmol) were dissolved in 15 mL of water. The volume of the resultant solution was reduced to 10 mL; slow evaporation of the solvent yielded crystals suitable for X-ray diffraction studies. The compound was characterized by the X-ray structure determination.

Variable Temperature NMR Studies

Variable temperature proton NMR spectra were obtained on solutions of the disodium salts of $[Ca(EGTA)]^{2-}$ (pH = 9, 0.1 M) and $[Cd(EGTA)]^{2-}$ (pH = 9, 0.1 M) on a Bruker WP-200SY spectrometer equipped with a variable temperature probe. The pH values of the solutions were chosen to assure that the concentrations of HML^{-} species were negligible.

^{113}Cd NMR Studies

The natural abundance ^{113}Cd NMR spectrum of a solution of $Na_2[Cd(EGTA)]$ (pH = 9) was recorded at 44.4 MHz on a Bruker 200 MHz spectrometer, utilizing 10 mm tubes and a tunable broad-band probe. A 0.10 M $Cd(ClO_4)_2$ solution was used to provide a reference signal.

The solid state ^{113}Cd NMR spectra of an unenriched sample of $Sr[Cd(EGTA)]\cdot 7H_2O$ were obtained on a Nicolet NT-200 spectrometer at 44.4 MHz, using solid $Cd(ClO_4)_2\cdot 6H_2O$ as a reference. Standard cross-polarization conditions (contact time = 2 ms), with a 1 second delay between scans and a ^{1}H decoupling field of 42 kHz, were utilized. Both the non-spinning and the magic angle spinning experiments were performed; rotor speeds of approximately 1.8 kHz were utilized in acquisition of the magic angle spinning spectrum.

Magnetic Susceptibilities and EPR Studies

Solid state magnetic susceptibilities were measured at room temperature by the Faraday method, using a Cahn-Ventron 7600 magnetic susceptibility system (model RTL minibalance). $Hg[Co(SCN)_4]$ was used as the calibrant. The measured susceptibilities were corrected for diamagnetic contributions using Pascal's constants.

EPR solution and solid state spectra were obtained on a Varian E-9 X-band spectrometer. $[Mn(EGTA)]^{2-}$ was doped into the lattice of $Sr[Cd(EGTA)]\cdot 7H_2O$ at the 1% level for the solid state spectrum. The solution spectra were taken on an approximately 1 m<u>M</u> solution of $[Mn(EGTA)]^{2-}$.

<u>X-Ray Structure Determinations</u>

General X-Ray Experimental

The orientation matrix utilized for data collection was obtained by a least squares fit of the cell constants to the setting angles for high angle reflections centered on a Nicolet <u>R3m</u> diffractometer. Cell parameter standard deviations which were not greater than 0.03% of the associated parameters were considered acceptable. Axis lengths, axial symmetry, and crystal quality were confirmed by axial photographs taken on the diffractometer. In addition, crystal quality was examined utilizing omega scans of reflections at relatively high 2θ angles along

each axis. Any crystal that showed an abnormal reflection profile was rejected.

Data collection for all structures was performed operating in the bisecting geometry and utilizing a graphite-monochromatized Mo K_{α} source. Intensities of the reflections were measured by $\theta/2\theta$ scans; the scan width typically used was 1.0 degree below $K_{\alpha 1}$ to 1.0 degree above $K_{\alpha 2}$. Crystal stability in the beam was monitored by measurement of the intensities of three control reflections at regular intervals; when necessary, the data were scaled to correct for degradation of the crystal over the course of the experiment. For low temperature data collection, the standard set-up provided by Nicolet XRD was utilized. A flow rate of 30 cfh with a nozzle heater setting of 2.0 yielded a temperature of -130° C as measured with an iron-constantan minithermocouple placed at the center of the goniostat. All computer programs for diffractometer operations were provided by Nicolet XRD corporation.

All subsequent computations, including data reduction, structure solution, structure refinement, and graphical presentation of structural results, were performed utilizing the SHELXTL library of crystallographic routines[77] on the Data General Eclipse S140 computer in the chemistry department X-ray laboratory at Colorado State University. During data reduction, Lorentz and polarization corrections were applied to the data. The

method of absorption correction (if any) is detailed for each individual case below.

Neutral atom scattering factors[78] with anomalous scattering contributions[79] were utilized in all structure factor computations. Refinement of the structural model was performed utilizing a block cascade least squares algorithm. Refinement was always on $\underline{F}$ (the function minimized was $\sum_{hkl} \underline{w}_{hkl} (|\underline{F}_o| - |k\underline{F}_c|)^2$), utilizing a maximum of 103 parameters per cycle. When hydrogen atoms were included in the structural model, unless stated otherwise, they were placed in idealized positions (C-H = 0.96 Å) and were given thermal parameters that were 20% higher than the equivalent isotropic $\underline{U}$ for the carbon atoms to which the hydrogen atoms were bound. The residuals $\underline{R}$, $\underline{R}_w$, $\underline{R}_g$, and GOF that are reported in the "Crystallographic Parameters and Refinement Results" table for each structure take the following forms:

$$\underline{R} = \frac{\sum |(\underline{F}_o - \underline{F}_c)|}{\sum \underline{F}_o}$$

$$\underline{R}_w = \frac{\sum |\sqrt{\underline{w}}(\underline{F}_o - \underline{F}_c)|}{\sum \underline{F}_o}$$

$$\underline{w} = [\sigma^2(\underline{F}) + |\underline{g}|\underline{F}^2]^{-1}$$

$$\underline{R}_g = \left\{ \frac{\sum \underline{w}(\underline{F}_o - \underline{F}_c)^2}{\sum \underline{w}(\underline{F}_o)^2} \right\}^{1/2}$$

$$GOF = \left\{ \frac{\sum \underline{w}(\underline{F}_o - \underline{F}_c)^2}{N_{data} - N_{parameters}} \right\}^{1/2}$$

In addition, the value for g utilized in the statistical weighting scheme defined above is reported, along with the slope of a normal probability plot.[80]

Experimental Details for Individual Structures

$\underline{H_4EGTA}$ (1). The crystallographic parameters for 1, together with the details of the X-ray diffraction experiment and subsequent computations, are shown in Table 2.1. The cell dimensions were obtained from a least squares fit of the cell constants to the setting angles for 24 reflections (2θ(ave) = 13.30°). The intensities of three control reflections (020, $\bar{4}00$, $0\bar{1}\bar{4}$, measured every 97 reflections) showed no significant variation over the course of data collection.

The structure was solved by the direct methods routine RANT. The initial E-map revealed all non-hydrogen atoms of the H_4EGTA molecule. The hydrogen atom on the amine nitrogen atom appeared in a Fourier difference map during the final stages of least squares refinement; coordinates and an isotropic thermal parameter were refined for this atom. The carboxylate hydrogen atoms were initially fixed on crystallographic inversion centers. When this constraint was removed, the protons moved slightly off the inversion centers (average displacement 3.4σ). A detailed

Table 2.1 Crystallographic Parameters and Refinement Results for H_4EGTA (1)

Mol formula	$C_{14}H_{24}N_2O_{10}$
Formula weight	380.35
μ(Mo K_α), cm^{-1}	1.19
Data collection temp, °C	20(1)
Crystal system	Triclinic
Space group	$P\bar{1}$
Cell constants (Å, deg):	
a	6.707(2)
b	6.792(2)
c	10.048(3)
α	82.23(2)
β	78.82(2)
γ	71.33(2)
V, $Å^3$	424.1
Z	1
F(000)	202
D(calc), g cm^{-3}	1.49
Crystal dimensions, mm	0.07(010-0$\bar{1}$0) x 0.12(001-00$\bar{1}$) x 0.35(100-$\bar{1}$00)
2θ range, deg	3.5-50
Variable scan speed, deg min^{-1}	2-30 (3.5° < 2θ < 40°) 1-30 (40° < 2θ < 50°)
Indices collected	-h, ±k, ±l
Reflections	1706 measured 1495 unique 1269 with $I > 2\sigma(I)$ used
No. least squares parameters	124
Data/parameters	10.2
R	0.055
R_w	0.059
R_g	0.076
GOF	1.15
g	3.5×10^{-3}
Slope of normal prob. plot	1.01

examination of a difference Fourier map with the acetate protons removed from the structural model did not reveal two resolved positions on either side of the inversion center. In addition, the observed hydrogen atom peak was elongated off the O-O axis, not along the axis as would be expected if the electron density represented two hydrogen atom positions. Consequently, the hydrogen atoms were fixed at the inversion centers in the final structural model. All non-hydrogen atoms were given anisotropic thermal parameters. At convergence (mean shift/esd < 0.10 over the last four cycles), the largest peaks in the final Fourier synthesis corresponded to +0.3 e $\mathring{A}^{-3}$; the minimum in the map was -0.4 e $\mathring{A}^{-3}$.

Final fractional atomic coordinates and anisotropic (or isotropic) thermal parameters for all atoms (including hydrogen atoms) of **1** may be found in Table A.1. Bond lengths and angles for **1** are listed in Table 3.1.

Ca[Ca(EGTA)]·(22/3)H_2O (2). Crystallographic parameters for **2**, together with details of the X-ray diffraction experiment and subsequent computations, are specified in Table 2.2. The cell dimensions were obtained from a least squares fitting of the cell constants to the setting angles for 25 reflections (2θ(ave) = 20.16°). The intensities of three control reflections ($20\bar{0}$, $0\bar{8}0$, $00\bar{5}$, measured every 100 data points) declined by an average of 11% during data collection; a correction for this decay was applied. No

Table 2.2 Crystallographic Parameters and Refinement Results for $Ca[Ca(EGTA)]\cdot(22/3)H_2O$ (**2**)

Mol formula	$C_{14}H_{20}Ca_2N_2O_{10}\cdot(22/3)H_2O$
Formula weight	588.5
μ(Mo K_α), cm^{-1}	4.90
Data collection temp, °C	20(1)
Crystal system	Monoclinic
Space group	$\underline{P}2_1/\underline{c}$
Cell constants (Å, deg):	
$\underline{a}$	24.358(4)
$\underline{b}$	16.798(4)
$\underline{c}$	19.015(4)
β	94.05(2)
$\underline{V}$, $Å^3$	7760.5
$\underline{Z}$	12
$\underline{F}$(000)	3736
D(calc), g cm^{-3}	1.51
Crystal dimensions, mm	0.15 x 0.4 x 0.4
2θ range, deg	3.5-50
Variable scan speed, deg min^{-1}	2-30
Indices collected	$+\underline{h}$, $+\underline{k}$, $\pm\underline{l}$
Reflections	14674 measured 13702 unique 9136 with $\underline{I} > 2.5\sigma(\underline{I})$ used
No. least squares parameters	973
Data/parameters	9.4
$\underline{R}$	0.068
$\underline{R}_w$	0.073
$\underline{R}_g$	0.093
GOF	1.89
$\underline{g}$	1.2×10^{-3}
Slope of normal prob. plot	1.47

correction was made for absorption, due to the small average value of μt (see Table 2.2).

Based on the systematic absences, the space group was determined to be $\underline{P}2_1/\underline{a}$. Conversion to the standard space group $\underline{P}2_1/\underline{c}$ required multiplication of the vectors ($\underline{h}$, $\underline{k}$, $\underline{l}$) and ($\underline{a}$, $\underline{b}$, $\underline{c}$) by the transformation matrix (0 0 1)/(0 -1 0)/(1 0 0). Twelve formula units were required per cell, in order to achieve a resonable calculated density. Due to the rarity of such a result in $\underline{P}2_1/\underline{c}$, attempts were made to find alternate cells using TRACER;[81] none were discovered. The structure was solved using the direct methods routine SOLV. The initial E-map revealed the presence of the six calcium ions. Subsequent Fourier difference electron density maps revealed all non-hydrogen ligand atoms, the oxygen atoms of water molecules coordinated to the calcium counterions, and the oxygen atoms of occluded water molecules.

Resolvable disorder was seen at one position (C34) of the ethylene backbone of one of the EGTA ligands. Refinement of site occupancy factors (x and 1-x) for the fractional atoms at these two positions yielded a value of 0.62(1) (0.38(1)) for C34 (C34'). Large thermal parameters were seen for oxygen atoms of three of the water molecules of crystallization (w21, w22, and w23); refinement of site occupancy factors for these atoms yielded values less than unity for w22 and w23 (0.81(3) and 0.21(2)) respectively); for convenience, these site

occupancy factors were fixed at values of 0.8 and 0.2. Interpretation of residual electron density peaks as oxygen atoms of occluded water molecules was terminated at a level of 1 e $\mathring{A}^{-3}$. Although many of the hydrogen atoms bound to the water molecules were visible in the final electron density map, such atoms were not included in the structural model. In the final model, all non-hydrogen atoms were given anisotropic thermal parameters. The refinement converged ($(shift/esd)_{ave} < 0.068$ over the last 10 cycles) to yield the residual indices shown in Table 2.2. In the final difference electron density map, the highest peaks (1 e $\mathring{A}^{-3}$) occurred in the vicinity of the disordered occluded water molecules; the minimum in the map was -0.5 e $\mathring{A}^{-3}$.

Final fractional atomic coordinates and anisotropic (or isotropic) thermal parameters for all atoms (including hydrogen atoms) may be found in Table A.2. Metric parameters relevant to the coordination of the $[Ca(EGTA)]^{2-}$ anions and the partially aquated calcium counterions, as well as to the interionic interactions between these species, may be found in Table 4.1(a, b, and c). Bonding and conformational parameters for the $EGTA^{4-}$ ligands (Table 4.2 and Table 4.3, respectively) together with the inter-ring torsion angles (Table 4.4) have also been compiled. Displacements of atoms from selected least squares planes (Table B.1) have been tabulated, as have hydrogen bonding distances (Table C.1).

Sr[Ca(EGTA)]·6H_2O (3). Crystallographic parameters for 3, together with details of the X-ray diffraction experiment and subsequent computations, are specified in Table 2.3. The cell dimensions were obtained using 25 reflections (2θ(ave) = 21.98°). The intensities of three control reflections ($\bar{1}\bar{1}4$, $\bar{3}10$, 030) showed no significant trends over the course of data collection. An empirical absorption correction was applied to the raw data, utilizing the intensity profiles for fifteen reflections measured as a function of ψ ($\Delta\psi$ = 15°). The range of transmission factors exhibited for the complete data set was ± 8% of the mean value.

The space group was unambiguously determined to be $P2_1/n$ by the systematic absences. The structure was solved by the direct methods routine SOLV. The initial E-map clearly revealed the positions of the strontium and calcium ions. Subsequent Fourier difference maps revealed the positions of all non-hydrogen atoms of the $EGTA^{4-}$ ligand and the oxygen atoms of six water molecules (four of which were bound to the strontium ion). In the final structural model, all non-hydrogen atoms were given anisotropic thermal parameters. At convergence ($(shift/esd)_{ave} < 0.02$ over the last three cycles), the largest peaks in the final difference electron density map corresponded to hydrogen atoms of water molecules (0.5 e $\AA^{-3}$); the minimum in the map was -0.4 e $\AA^{-3}$.

Table 2.3 Crystallographic Parameters and Refinement Results for $Sr[Ca(EGTA)]\cdot 6H_2O$ (3)

Mol formula	$C_{14}H_{20}CaN_2O_{10}Sr\cdot 6H_2O$
Formula weight	612.11
μ(Mo K_α), cm^{-1}	25.49
Data collection temp, °C	20(1)
Crystal system	Triclinic
Space group	$P\bar{1}$
Cell constants (Å, deg):	
a	8.410(1)
b	11.282(2)
c	13.833(2)
α	88.60(1)
β	73.88(1)
γ	78.45(1)
V, $Å^3$	1234.6
Z	2
F(000)	632
D(calc), g cm^{-3}	1.65
Crystal dimensions, mm	0.48(100-$\bar{1}$00) x 0.18(001-00$\bar{1}$) x 0.22(010-0$\bar{1}$0)
2θ range, deg	3.5-50
Variable scan speed, deg min^{-1}	2-30
Indices collected	$\pm h$, $\pm k$, $+l$
Reflections	4087 measured 3888 unique 3152 with $I > 2\sigma(I)$ used
No. least squares parameters	307
Data/parameters	10.3
R	0.040
R_w	0.039
R_g	0.049
GOF	1.55
g	4.6×10^{-4}
Slope of normal prob. plot	1.19

Final fractional atomic coordinates and anisotropic thermal parameters for all atoms (including hydrogen atoms) may be found in Table A.3. Metric parameters relevant to the coordination of the $[Ca(EGTA)]^{2-}$ anion and the partially aquated strontium counterion, as well as to the interionic interactions between these species, may be found in Table 4.5(a, b, and c). Bonding and conformational parameters for the $EGTA^{4-}$ ligands (Table 4.6 and Table 4.7, respectively), together with the inter-ring torsion angles (Table 4.8) have also been compiled. Displacements of atoms from selected least squares planes (Table B.2) have been tabulated, as have hydrogen bonding distances (Table C.2).

$Mg[Sr(EGTA)(OH_2)_2]\cdot 6H_2O$ **(4)**. Crystallographic parameters for **4**, together with details of the X-ray diffraction experiment and subsequent computations, are specified in Table 2.4. The cell dimensions reported for **4** were obtained from a least squares fit of the cell constants to the setting angles for twenty-five reflections (2θ(ave) = 17.33°). The intensities of the three standard reflections ($00\bar{8}$, 800, and $0\bar{8}0$, measured every 97 reflections), declined by an average of 6% during data collection. An empirical absorption correction was applied to the raw data, utilizing the intensity profiles for nine reflections measured as a function of ψ ($\Delta\psi$ = 15°). The range of

Table 2.4 Crystallographic Parameters and Refinement Results for $Mg[Sr(EGTA)(OH_2)]\cdot 7H_2O$ (**4**)

Mol formula	$C_{14}H_{20}MgN_2O_{10}Sr\cdot 8H_2O$
Formula weight	632.37
μ(Mo K_α), cm^{-1}	22.90
Data collection temp, °C	20(1)
Crystal system	Orthorhombic
Space group	Pccn
Cell constants (Å):	
a	21.331(4)
b	16.799(4)
c	14.372(2)
V, $Å^3$	5149.8
Z	8
F(000)	2624
D(calc), g cm^{-3}	1.63
Crystal dimensions, mm	0.40(100-$\bar{1}$00) x 0.14(011-0$\bar{1}\bar{1}$) x 0.20(122-$\bar{1}\bar{2}\bar{2}$)
2θ range, deg	3.5-50
Variable scan speed, deg min^{-1}	2-30
Indices collected	+h, -k, -l
Reflections	5086 measured 4571 unique 2832 with $I > 2\sigma(I)$ used
No. least squares parameters	327
Data/parameters	8.7
R	0.053
R_w	0.048
R_g	0.060
GOF	1.61
g	4.2×10^{-4}
Slope of normal prob. plot	1.18

transmission factors exhibited for the complete data set was ± 20% of the mean value.

The space group was unambiguously determined to be Pnaa by the systematic absences. Conversion to the standard space group given in Table 2.4 was carried out by multiplication of the vectors (h, k, l) and (a, b, c) by the matrix (0 0 1)/(0 -1 0)/(1 0 0). The position of the strontium ion was established by analysis of the Patterson map. The two largest peaks in the subsequent difference Fourier electron density map appeared on the special positions (0, 0, 1/2) and (1/4, 1/4, z), of $\bar{1}$ and 2 symmetry, respectively. These peaks were identified as the magnesium counterions (each with a site occupancy factor of 1/2, to total one magnesium counterion per $[Sr(EGTA)]^{2-}$ unit). All non-hydrogen atoms of the $EGTA^{4-}$ ligand, together with the oxygen atoms of eight water molecules (one bound to the strontium ion, one bound to each of the magnesium ions, and five occluded lattice water molecules), were revealed in subsequent difference maps. In the final structural model, all non-hydrogen atoms were given anisotropic thermal parameters. At convergence ($(shift/esd)_{ave} < 0.01$ over the last three cycles), the largest peaks in the final difference electron density map corresponded to hydrogen atoms of water molecules (0.6 e $\mathring{A}^{-3}$); the minimum in the map was -0.6 e $\mathring{A}^{-3}$.

Final fractional atomic coordinates and anisotropic (or isotropic) thermal parameters for all atoms (including

hydrogen atoms) may be found in Table A.4. Metric parameters relevant to the coordination of the $[Sr(EGTA)]^{2-}$ anion, the magnesium counterions, and the interionic interactions between these species may be found in Table 5.2(a, b, and c). Bonding and conformational parameters for the $EGTA^{4-}$ ligands (Table 5.3 and Table 5.4, respectively) have also been compiled. Distances of atoms from selected least squares planes have been tabulated (Table B.3), as have hydrogen bonding distances (Table C.3).

Mg[Ba(EGTA)]·(8/3)H_2O·(1/3)$(CH_3)_2CO$ (5). Crystallographic parameters for 5, together with details of the X-ray diffraction experiment and subsequent computations, are specified in Table 2.5. The cell dimensions for 5 were obtained from a least squares fit of the cell constants to the setting angles for twenty-five reflections (2θ(ave) = 23.18°). The intensities of the three standard reflections ($\bar{6}0\bar{1}$, 0 0 $\overline{10}$, and $\bar{5}\bar{8}0$, measured every 297 reflections) declined by an average of 4% during data collection. An empirical absorption correction was applied to the raw data, utilizing the intensity profiles for eleven reflections as a function of ψ ($\Delta\psi$ = 15°). The range of transmission factors exhibited for the complete data set was $\pm$ 5% of the mean value. Two symmetry-equivalent octants of data were collected; equivalent reflections

Table 2.5 Crystallographic Parameters and Refinement Results for $Mg[Ba(EGTA)]\cdot(8/3)H_2O\cdot(1/3)(CH_3)_2CO$ (5)

Mol formula	$C_{14}H_{20}BaMgN_2O_{10}\cdot(8/3)H_2O \cdot(1/3)(CH_3)_2CO$
Formula weight	605.35
μ(Mo K_α), cm^{-1}	18.95
Data collection temp, °C	-130(1)
Crystal system	Orthorhombic
Space group	$\underline{Pca}2_1$
Cell constants (Å):	
$\underline{a}$	21.801(5)
$\underline{b}$	15.444(2)
$\underline{c}$	20.115(4)
$\underline{V}$, $Å^3$	6772.4
$\underline{Z}$	12
$\underline{F}$(000)	3640
D(calc), g cm^{-3}	1.78
Crystal dimensions, mm	0.50 x 0.38 x 0.35
2θ range, deg	3.5-50
Variable scan speed, deg min^{-1}	5-30
Indices collected	$-\underline{h}$, $+\underline{k}$, $\pm\underline{l}$
Reflections	17756 measured 8478 unique 7845 with $\underline{I} > 2.5\sigma(\underline{I})$ used
No. least squares parameters	872
Data/parameter ratio	9.3
$\underline{R}$	0.023
$\underline{R}_w$	0.024
$\underline{R}_g$	0.030
GOF	0.99
$\underline{g}$	4.6×10^{-4}
Slope of normal prob. plot	0.85

were averaged to give the final data set utilized in the crystallographic computations.

The observed systematic absences demanded that the space group must be either Pcmb or the noncentrosymmetric alternative, $Pc2_1b$. Statistical analysis of the data gave a weak indication that $Pc2_1b$ was the correct choice ($|(E^2-1)|$(ave) = 0.84 for $\sin(\theta/\lambda)$ = 0.15 - 0.50). A reasonable calculated density was obtained utilizing Z = 12 (See Table 2.5). A value of Z = 12 in the centrosymmetric space group would imply that one barium complex occupies a general position in the asymmetric unit, and that a second barium complex occupies a special position of symmetry m, 2, or $\bar{1}$, all of which seemed unlikely. No crystallographic symmetry would be imposed on any barium complex in the non-centrosymmetric space group, where three $[Ba(EGTA)]^{2-}$ complex anions would occupy general positions in the asymmetric unit.

If the correct space group were Pcmb, the Patterson synthesis would show quadruple strength Harker line peaks at (0, 1/2 $\pm$ 2y, 0)(type 1), (1/2 $\pm$ 2x, 1/2, 0)(type 2), and (1/2, 0, $\pm$ 2z)(type 3) for each of the two unique barium ions; in $Pc2_1b$, only the latter two peaks would be expected to be present for the three unique barium ions. In the Patterson map, no multiple strength peaks of type 1 were observed; type 2 peaks were observed for two of the barium ions, and type 3 peaks were found for all three barium ions. Additionally, all possible cross peaks

between three barium ions were observed, as expected for $\underline{Pc}2_1\underline{b}$. Consequently, the non-centrosymmetric space group was chosen. Conversion to the standard space group $\underline{Pca}2_1$ required multiplication of the vector ($\underline{h}$, $\underline{k}$, $\underline{l}$) for each reflection by the transformation matrix (-1 0 0)/(0 0 1)/(0 1 0). A corresponding axial transformation was also performed.

The positions of two of the three unique barium ions were established by analysis of the Patterson map. The subsequent difference Fourier map revealed the position of the remaining barium ion, as well as the three magnesium counterions. Repeated difference Fourier syntheses established initial positions for all non-hydrogen atoms of three $EGTA^{4-}$ ligands, oxygen atoms of eight water molecules (six of which were bound to the three magnesium counterions, two of which occurred as occluded water molecules), and a single acetone molecule of solvation. The site occupancy factor for the atoms comprising the acetone molecule was refined; the final value of this parameter was 0.90(1). A factor, ndf, which multiplies the imaginary component of the atomic scattering factors ($\Delta\underline{f}$") was refined; convergence at a value of -0.93(2) indicated that the inverted structure was correct, and the atomic coordinates were appropriately transformed. The final structural model utilized anisotropic thermal parameters for all non-hydrogen atoms. At convergence $((\text{shift/esd})_{ave} < 0.03$ over the last nine cycles), the largest peaks in the

final difference electron density map (1 e $\mathring{A}^{-3}$) occurred in the immediate vicinities of barium ions; the minimum in the map was -0.5 e $\mathring{A}^{-3}$.

Final fractional atomic coordinates and anisotropic (or isotropic) thermal parameters for all atoms (including hydrogen atoms) may be found in Table A.5. Metric parameters relevant to the coordination of the $[Ba(EGTA)]^{2-}$ anions, the magnesium counterions, and the interionic interactions between these species may be found in Table 5.6(a, b, and c). Bonding and conformational parameters for the $EGTA^{4-}$ ligands (Table 5.7 and Table 5.8, respectively), together with inter-ring torsion angles (Table 5.9) have also been compiled. Distances of atoms from selected least squares planes (Table B.4) have also been tabulated, as have hydrogen bonding distances (Table C.4).

$\underline{[Mg_2(EGTA)(OH_2)_6]\cdot 5H_2O}$ **(6)**. Crystallographic parameters for **6**, together with details of the X-ray diffraction experiment and subsequent computations, are specified in Table 2.6. The cell dimensions for **6** were obtained from a least squares fitting of the cell constants to the setting angles for twenty-five reflections (2θ(ave) = 15.70°). The intensities of the three standard reflections ($00\bar{8}$, $\bar{5}0\bar{3}$, 080, measured every ninety-seven reflections) showed no significant trends over the course of data collection. No

Table 2.6 Crystallographic Parameters and Refinement Results for $[Mg_2(EGTA)(OH_2)_6]\cdot 5H_2O$ (6)

Mol formula	$C_{14}H_{20}Mg_2N_2O_{10}\cdot 11H_2O$
Formula weight	623.10
μ(Mo K_α), cm^{-1}	1.70
Data collection temp, °C	20(1)
Crystal system	Orthorhombic
Space group	$\underline{Pna2}_1$
Cell constants (Å):	
$\underline{a}$	14.098(2)
$\underline{b}$	12.396(3)
$\underline{c}$	15.925(3)
$\underline{V}$, $Å^3$	2783.2
$\underline{Z}$	4
$\underline{F}$(000)	1328
D(calc), g cm^{-3}	1.49
Crystal dimensions, mm	0.24(100-$\bar{1}$00) x 0.46(010-0$\bar{1}$0) x 0.22(001-00$\bar{1}$)
2θ range, deg	3.5-58
Variable scan speed, deg min^{-1}	2-30
Indices collected	-$\underline{h}$, +$\underline{k}$, -$\underline{l}$
Reflections	4168 measured 3846 unique 2914 with $\underline{I} > 2.5\sigma(\underline{I})$ used
No. least squares parameters	371
Data/parameter ratio	7.9
$\underline{R}$	0.055
$\underline{R}_w$	0.057
$\underline{R}_g$	0.073
GOF	1.65
$\underline{g}$	1.0×10^{-3} (fixed)
Slope of normal prob. plot	1.30

absorption correction was performed, due to the small average value of μt.

The systematic absences determined the space group to be either Pbnm or the noncentrosymmetric alternative, $Pbn2_1$. The structure was solved by the direct methods routine RANT in the noncentrosymmetric space group. Transformation of the data to the standard space group $Pna2_1$ required multiplication of the vectors (h, k, l) and (a, b, c) by the transformation matrix (0 1 0)/(-1 0 0)/(0 0 1). The initial E-map revealed the magnesium ion positions, all non-hydrogen atoms of the $EGTA^{4-}$ ligand, and the oxygen atoms of several water molecules present in the structure (eleven were eventually found, six of which were bound to the magnesium ions). Disorder was apparent in the diether portion of the chain. The site occupancy factors for C8 (C8') and O6 (O6') were refined to a values of 0.75(1) (0.25(1)). Hydrogen atoms of the $EGTA^{4-}$ ligand were included in the model as described above, with the exception of this disordered portion. The parameter ndf (see discussion for 5) was unsuccessfully refined (ndf = 2.2(9), see above), indicating that anomalous scattering by the magnesium ions was not sufficient to make a definitive determination of the enantiomorph. The final structural model utilized anisotropic thermal parameters for all non-hydrogen atoms. At convergence $((shift/esd)_{ave} < 0.03$ over the last four cycles) the largest peaks (0.5 e

$\mathring{A}^{-3}$) corresponded to hydrogen atoms of water molecules; the minimum in the map was -0.3 e $\mathring{A}^{-3}$.

The positions of the magnesium ions are approximately centrosymmetrically related. This may account for the fact that the usual statistical test indicated a centrosymmetric space group. If the correct space group choice were Pnam, the two halves of the dinuclear magnesium complex would be related by a mirror plane or an inversion center. In the observed structure (as solved in the noncentrosymmetric space group), a single oxygen atom and the adjacent carbon atom in the diether portion of the $EGTA^{4-}$ ligand were found to be disordered. Such a disorder would not obey the requisite $\underline{m}$ or $\bar{1}$ symmetry in the centrosymmetric space group. In addition, the conformation of the diether backbone is such that mirror or inversion symmetry is impossible.

Final fractional atomic coordinates and anisotropic (or isotropic) thermal parameters for all atoms (including hydrogen atoms) may be found in Table A.6. Metric parameters relevant to the coordination of the magnesium ions may be found in Table 5.10. Bonding and conformational parameters for the $EGTA^{4-}$ ligands (Table 5.11 and Table 5.12, respectively) have also been compiled. Distances of atoms from selected least squares planes (Table B.5) have been tabulated, as have hydrogen bonding distances (Table C.5).

Sr[Cd(EGTA)]·7H_2O (7). Crystallographic parameters for 7, together with details of the X-ray diffraction experiment and subsequent calculations, are given in Table 2.7. The cell dimensions reported were obtained from a least squares fit of the cell constants to the setting angles of twenty-four reflections (2θ(ave) = 18.8°). The intensities of three standard reflections (12 0 0, 040, 0 0 12, measured every 100 reflections) showed no significant trends over the course of the data collection. An empirical absorption correction was performed, utilizing the intensity profiles obtained for fourteen reflections as a function of ψ ($\Delta\psi$ = 15°). The range of transmission factors exhibited for the complete data set was ± 6% of the mean value.

Analysis of the Patterson map established the positions of the strontium and cadmium ions. Subsequent Fourier difference electron density maps revealed all non-hydrogen ligand atoms, together with the oxygen atoms of seven water molecules (four of which were bound to the partially aquated strontium cation). In the final structural model, all non-hydrogen atoms were given anisotropic thermal parameters. At convergence ($(\text{shift/esd})_{ave} < 0.052$ over the last 4 cycles) the final difference electron density map exhibited a highest peak (0.67 e Å^{-3}) in the immediate vicinity of the cadmium ion and a minimum of -0.35 e Å^{-3}.

Final fractional atomic coordinates and anisotropic (or isotropic) thermal parameters for all atoms (including

Table 2.7 Crystallographic Parameters and Refinement Results for $Sr[Cd(EGTA)]\cdot 7H_2O$ (7)

Mol formula	$C_{14}H_{20}CdN_2O_{10}Sr\cdot 7H_2O$
Formula weight	702.46
μ(Mo K_α), cm^{-1}	31.70
Data collection temp, °C	20(1)
Crystal System	Monoclinic
Space group	$\underline{P}2_1/\underline{n}$
Cell constants (Å, deg):	
$\underline{a}$	16.814(4)
$\underline{b}$	8.454(2)
$\underline{c}$	17.614(5)
β	97.34(2)
$\underline{V}$, $Å^3$	2483.3
$\underline{Z}$	4
$\underline{F}$(000)	1416
D(calc), g cm^{-3}	1.88
Crystal dimensions, mm	0.38(001-00$\bar{1}$) x 0.40(100-$\bar{1}$00) x 0.44(010-0$\bar{1}$0)
2θ range, deg	3.5-50
Variable scan speed, deg min^{-1}	2-30
Indices collected	$\pm\underline{h}$, $+\underline{k}$, $-\underline{l}$
Reflections	4882 measured 4394 unique 3713 with $\underline{I} > 2.5\sigma(\underline{I})$ used
No. least squares parameters	316
Data/parameters	11.8
$\underline{R}$	0.032
$\underline{R}_w$	0.036
$\underline{R}_g$	0.048
GOF	1.21
$\underline{g}$	1.0×10^{-3}
Slope of normal prob. plot	1.00

hydrogen atoms) may be found in Table A.7. Metric parameters relevant to the coordination of the $[Cd(EGTA)]^{2-}$ anion, the partially aquated strontium counterion, and to the interionic interactions between these species may be found in Table 6.1(a, b, and c). Bonding and conformational parameters for the $EGTA^{4-}$ ligands (Table 6.2 and Table 6.3, respectively), together with the inter-ring torsion angles (Table 6.4) have also been compiled. Distances of atoms from selected least squares planes (Table B.6) have been tabulated, as have hydrogen bonding distances (Table C.6).

$\underline{Ca[Er(EGTA)(OH_2)]_2 \cdot 12H_2O \cdot (CH_3)_2CO}$ (8). Crystallographic parameters for 8, together with details of the X-ray diffraction experiment and subsequent computations, are shown in Table 2.8. The reported cell dimensions were obtained from a least squares fit of the cell constants to the setting angles for 25 reflections (2θ(ave) = 21.46°). The intensities of the three control reflections ($0\bar{4}0$, 105, 503, measured every 97 reflections) showed no significant trends over the course of the data collection. An analytical absorption correction was applied to the data, utilizing the crystal dimensions reported in Table 2.8. The range of transmission factors exhibited for the complete data set was $\pm$ 13% of the mean value.

The systematic absences indicated the space group was either the centrosymmetric space group, $\underline{P2_1/m}$, or the

Table 2.8 Crystallographic Parameters and Refinement Results for $Ca[Er(EGTA)(OH_2)]_2 \cdot 12H_2O \cdot (CH_3)_2CO$ (8)

Mol formula	$C_{28}H_{40}CaEr_2N_4O_{20} \cdot 14H_2O \cdot (CH_3)_2CO$
Formula weight	1437.53
μ(Mo K_α), cm^{-1}	35.45
Data collection temp, °C	-130(1)
Crystal system	Monoclinic
Space group	$\underline{P}2_1$
Cell constants (Å, deg):	
$\underline{a}$	12.710(2)
$\underline{b}$	12.157(2)
$\underline{c}$	17.765(3)
β	105.79(1)
$\underline{V}$, $Å^3$	2641.5
$\underline{Z}$	2
$\underline{F}(000)$	1428
D(calc), g cm^{-3}	1.81
Crystal dimensions, mm	0.48(010-0$\bar{1}$0) x 0.08(001-00$\bar{1}$) x 0.14(100-$\bar{1}$00)
2θ range, deg	3.5-50
Variable scan speed, deg min^{-1}	2-30
Indices collected	$\pm\underline{h}$, $-\underline{k}$, $+\underline{l}$
Reflections	5075 measured 4905 unique 4711 with $\underline{I} > 2\sigma(\underline{I})$ used
No. least squares parameters	664
Data/parameters	7.1
$\underline{R}$	0.027
$\underline{R}_w$	0.028
$\underline{R}_g$	0.035
GOF	1.21
$\underline{g}$	4.9×10^{-4}
Slope of normal prob. plot	1.05

non-centrosymmetric space group, $\underline{P}2_1$. Statistical analysis of the data strongly indicated that the non-centrosymmetric space group was the correct choice ($|E^2-1|$(ave) = 0.75 for sin (θ/λ) = 0.15 - 0.50). This would require that there be two unique $[Er(EGTA)]^-$ complex anions in the asymmetric unit. The Patterson synthesis supported the assignment of $\underline{P}2_1$ as the space group, with a strong indication that two unique heavy atoms occupy the asymmetric unit. The heavy atom positions predicted by the direct methods routine SOLV were in agreement with the atomic postions predicted from the peaks present in the Patterson map. The Fourier difference map calculated based on phasing from the erbium ions revealed the calcium ion and several atoms of the $EGTA^{4-}$ ligand. Subsequent difference maps established initial positions for all non-hydrogen atoms of the two unique $EGTA^{4-}$ ligands, as well as the oxygen atoms of fourteen water molecules (six of which are bound to metal ions), and an acetone molecule of solvation. On refinement, w14 exhibited a relatively large thermal parameter. The site occupancy factor for this water molecule and the acetone molecule of solvation were subsequently refined, but the final refined value for both of them did not differ significantly from one. The parameter ndf refined to a value of -1.01(2), indicating that the inverted conformation was correct, and the atomic coordinates were appropriately transformed. The final structural model utilized anisotropic thermal parameters

for all non-hydrogen atoms. At convergence ($(\text{shift/esd})_{ave} < 0.01$ over the last seven cycles) the largest peaks in the final difference electron density map (1.7 e Å^{-3}) occurred in the immediate vicinity of the erbium ions; the minimum in the map was -0.7 e Å^{-3}.

Final fractional atomic coordinates and anisotropic (or isotropic) thermal parameters for all atoms (including hydrogen atoms) may be found in Table A.8. Metric parameters relevant to the coordination of the $[Er(EGTA)]^-$ anions, the partially aquated calcium counterion, and the interionic interactions between these species may be found in Table 6.5(a, b, and c). Bonding and conformational parameters for the $EGTA^{4-}$ ligands (Table 6.6 and Table 6.7, respectively), together with the inter-ring torsion angles (Table 6.8), have also been compiled. Distances of atoms from selected least squares planes (Table B.7) have been tabulated, as have hydrogen bonding distances (Table C.7).

<u>$Ca[Nd(EGTA)(OH_2)]_2 \cdot 9H_2O$ (9)</u>. Crystallographic parameters for **9**, together with details of the X-ray diffraction experiment and subsequent computations, are specified in Table 2.9. The cell dimensions for **9** were obtained from a least squares fit of the cell constants to the setting angles for twenty-five reflections (2θ(ave) = 29.76°). The intensities of the three standard reflections ($\bar{4}00$, $0\bar{6}0$, $0\bar{2}6$, measured every 97 reflection) declined by an average of 4% over the course of the data collection. An empirical

Table 2.9 Crystallographic Parameters and Refinement Results for $Ca[Nd(EGTA)(OH_2)]_2 \cdot 9H_2O$ (9)

Mol formula	$C_{28}H_{40}CaN_4Nd_2O_{20} \cdot 11H_2O$
Formula weight	1279.37
μ(Mo K_α), cm^{-1}	24.57
Data collection temp, °C	20(1)
Crystal system	Monoclinic
Space group	$\underline{P}2_1/\underline{c}$
Cell constants (Å, deg)	
$\underline{a}$	10.776(2)
$\underline{b}$	18.218(4)
$\underline{c}$	12.560(2)
β	112.14(1)
$\underline{V}$, $Å^3$	2284.0
$\underline{Z}$	2
$\underline{F}$(000)	1292
D(calc), g cm^{-3}	1.86
Crystal dimensions, mm	0.51 x 0.16 x 0.29
2θ range, deg	3.5-50
Variable scan speed, deg min^{-1}	5-30
Indices collected	$-\underline{h}$, $-\underline{k}$, $\pm\underline{l}$
Reflections	4419 measured 4047 unique 3746 with $\underline{I} > 2\sigma(\underline{I})$ used
No. least squares parameters	304
Data/parameters	12.3
$\underline{R}$	0.028
$\underline{R}_w$	0.030
$\underline{R}_g$	0.040
GOF	1.88
$\underline{g}$	2.2×10^{-4}
Slope of normal prob. plot	1.46

absorption correction was applied to the raw data, utilizing the intensity profiles for fifteen reflections as a function of ψ ($\Delta\psi$ = 15°). The range of transmission factors exhibited for the complete data set was $\pm$21% of the mean value.

The space group was unambiguously determined to be $\underline{P}2_1/\underline{c}$ based on the observed systematic absences. A reasonable calculated density was obtained utilizing two formula units per unit cell. This required that the calcium counterion be positioned on an inversion center. The coordinates of the single unique neodymium ion were established by analysis of the Patterson map, and the calcium ion was arbitrarily placed on an inversion center at (1/2, 1/2, 1/2). Subsequent Fourier difference electron density maps revealed all non-hydrogen ligand atoms and the oxygen atoms of six water molecules (two of which were bound to metal ions). The thermal parameter for w6 refined to a relatively large value. Consequently, the site occupancy factor for this molecule was refined. Convergence of this parameter occurred at a value of 0.42(1); for convenience, this value was fixed at 0.5, and was considered as one-half of a water molecule in calculating the molecular formula.

The final structural model utilized anisotropic thermal parameters on all non-hydrogen atoms. At convergence ($(\text{shift/esd})_{ave} < 0.06$ over the last three cycles), the largest peaks (1.1 e Å^{-3}) in the difference

electron density map occurred in the immediate vicinity of the neodymium ion; the minimum in the map was -0.5 e $\AA^{-3}$.

Final fractional atomic coordinates and anisotropic (or isotropic) thermal parameters for all atoms (including hydrogen atoms) may be found in Table A.9. Metric parameters relevant to the coordination of the $[Nd(EGTA)]^-$ anions and the partially aquated calcium counterion, and to the interionic interactions between these species, may be found in Table 6.9(a, b, and c). Bonding and conformational parameters for the $EGTA^{4-}$ ligands (Table 6.10 and Table 6.11, respectively), together with the inter-ring torsion angles (Table 6.12), have also been compiled. Distances of atoms from selected least squares planes (Table B.8) have been tabulated, as have hydrogen bonding distances (Table C.8).

<u>$Sr[Mn(EGTA)]\cdot 7H_2O$ (10)</u>. Crystallographic parameters for 10, together with details of the X-ray diffraction experiment and subsequent calculations, are specified in Table 2.10. Crystals of 10 were found to degrade quite rapidly upon exposure to X-radiation at room temperature. Acquisition of a low temperature data set alleviated these problems. The cell dimensions for 10 were obtained from a least squares fit of the cell constants to the setting angles for twenty-five reflections (2θ(ave) = 20.65°). The intensities of the three standard reflections ($\bar{1}\bar{1}\bar{8}$, $0\bar{4}0$, and $80\bar{2}$, measured every 97 reflections) showed no

Table 2.10 Crystallographic Parameters and Refinement Results for $Sr[Mn(EGTA)]\cdot 7H_2O$ (10)

Mol formula	$C_{14}H_{20}MnN_2O_{10}Sr\cdot 7H_2O$
Formula weight	644.98
μ(Mo K_α), cm^{-1}	28.97
Data collection temp, °C	20(1)
Crystal system	Monoclinic
Space group	$\underline{P}2_1/\underline{n}$
Cell constants (Å, deg):	
$\underline{a}$	16.535(4)
$\underline{b}$	8.415(2)
$\underline{c}$	17.457(4)
β	97.11(2)
$\underline{V}$, $Å^3$	2410.1
$\underline{Z}$	4
$\underline{F}(000)$	1324
$\underline{D}$(calc), g cm^{-3}	1.78
Crystal dimensions, mm	0.32 x 0.36 x 0.50
2θ range, deg	3.5-50
Variable scan speed, deg min^{-1}	4-30 ($3.5° < 2\theta < 40°$) 2-30 ($40° < 2\theta < 50°$)
Indices collected	$\pm\underline{h}$, $-\underline{k}$, $-\underline{l}$
Reflections	4548 measured 4087 unique 3421 with $\underline{I} > 2\sigma(\underline{I})$ used
No. least squares parameters	316
Data/parameters	10.8
$\underline{R}$	0.036
$\underline{R}_w$	0.038
$\underline{R}_g$	0.049
GOF	1.40
$\underline{g}$	6.2×10^{-4}
Slope of normal prob. plot	1.11

significant trends over the course of the data collection. An empirical absorption correction was applied to the raw data, utilizing the intensity profiles for eleven reflections as a function of ψ ($\Delta\psi$ = 15°). The range of transmission factors exhibited for the complete data set was $\pm$ 25% of the mean value. 200 reflections for which 2θ = 40 - 50° were accidently overwritten on the original data tape. This error was not discovered until the data collection crystal had been removed from the cold stream. Consequently these 200 reflections were not used in refinement of the structural model.

The structure of **10** is isomorphous with the structure of **7**. The refined atomic coordinates for **7** were utilized as starting positions for the atoms of **10** (with manganese ion occupying the position of the cadmium ion). The final structural model utilized anisotropic thermal parameters for all non-hydrogen atoms. At convergence ($(\text{shift/esd})_{ave}$ < 0.01 over the last three cycles), the largest peaks in the difference electron density map (0.7 e Å^{-3}) corresponded to the hydrogen atoms of water molecules; the minimum in the map was -0.3 e Å^{-3}.

Final fractional atomic coordinates and anisotropic (or isotropic) thermal parameters for all atoms (including hydrogen atoms) may be found in Table A.10. Metric parameters relevant to the coordination of the $[Mn(EGTA)]^{2-}$ anion, the partially aquated strontium counterion, and the interionic interactions between these species may be found

in Table 7.1(a, b, and c). Bonding and conformational parameters for the $EGTA^{4-}$ ligands (Table 7.2 and Table 7.3, respectively), together with inter-ring torsion angles (Table 7.4), have also been compiled. Distance of atoms from selected least squares planes (Table B.9) have been tabulated, as have hydrogen bonding distances (Table C.9).

$[Cu_2(EGTA)(OH_2)_2]\cdot 2H_2O$ (11). Crystallographic parameters for 11, together with details of the X-ray diffraction experiment and subsequent computations, are specified in Table 2.11. The cell dimensions for 11 were obtained from a least squares fit of the cell constants to the setting angles for twenty-five reflections (2θ(ave) = 22.04°). Crystals of 11 were generally twinned, and appropriate cleaving was necessary to obtain a single crystal fragment. The intensities of the three standard reflections ($\bar{8}00$, $\bar{1}\bar{3}5$, $\bar{1}\bar{3}2$, measured every 97 data points) showed no significant trends over the course of the data collection. An analytical absorption correction was applied to the raw data, utilizing the crystal dimensions specified in Table 2.11. The range of transmission factors observed for the complete data set was $\pm$ 8% of the mean value.

Based on the observed systematic absences, the space group was determined to be the centrosymmetric space group, C2/c, or the non-centrosymmetric space group Cc. The centrosymmetric space group choice would require that only half of the formula unit be crystallographically unique.

Table 2.11 Crystallographic Parameters and Refinement Results for $[Cu_2(EGTA)(OH_2)_2]\cdot 2H_2O$ (11)

Mol formula	$C_{14}H_{20}Cu_2N_2O_{10}\cdot 4H_2O$
Formula weight	575.47
μ(Mo K_α), cm^{-1}	20.71
Data collection temp, °C	-130(1)
Crystal system	Monoclinic
Space group	C2/c
Cell constants (Å, deg):	
a	20.962(5)
b	7.513(2)
c	13.545(2)
β	90.85(2)
V, $Å^3$	2133.0
Z	4
F(000)	1184
D(calc), g cm^{-3}	1.79
Crystal dimensions, mm	0.37(010-0$\bar{1}$0) x 0.18(001-00$\bar{1}$) x 0.11(100-$\bar{1}$00)
2θ range, deg	3.5-50
Variable scan speed, deg min^{-1}	2-30
Indices collected	-h, -k, ±l
Reflections	2073 measured 1866 unique 1670 with $I > 2\sigma(I)$ used
No. least squares parameters	145
Data/parameters	11.5
R	0.031
R_w	0.034
R_g	0.046
GOF	1.61
g	4.7×10^{-4}
Slope of normal prob. plot	1.21

Peaks in the Patterson map were consistent with a single heavy atom in the centrosymmetric space group. The positional parameters derived from analysis of the Patterson map were in agreement with a copper ion position predicted by the direct methods routine RANT. The subsequent difference Fourier electron density map revealed all non-hydrogen ligand atoms, as well as the oxygen atoms of two occluded water molecules (one of which was bound to the copper ion). In the final structural model, all non-hydrogen atoms were given anisotropic thermal parameters. At convergence ($(shift/esd)_{ave} < 0.001$ over the last two cycles), the largest peaks in the difference electron density map (0.7 e $\mathring{A}^{-3}$) corresponded to hydrogen atoms of water molecules; the minimum in the map was -0.3 e $\mathring{A}^{-3}$.

Final fractional atomic coordinates and anisotropic (or isotropic) thermal parameters for all atoms (including hydrogen atoms) may be found in Table A.11. Metric parameters relevant to the coordination of the copper ions may be found in Table 7.5. Bonding and conformational parameters for the $EGTA^{4-}$ ligands (Table 7.6 and Table 7.7, respectively) have also been compiled. Distances of atoms from selected least squares planes (Table B.10) have been tabulated, as have hydrogen bonding distances (Table C.10).

CHAPTER 3

H_4EGTA

Structure of H_4EGTA (1)

To initiate a structural study of the calcium-binding selectivity of $EGTA^{4-}$, the structure of the tetraprotonated, neutral H_4EGTA ligand was determined. The molecular structure and numbering scheme for H_4EGTA are depicted in Figure 3.1(a). The H_4EGTA molecule is centrosymmetric in the solid state. An inversion center of the space group $P\bar{1}$ bisects the C7-C7' bond, and, thus only half of the formula unit is crystallographically unique. Bond lengths and angles are listed in Table 3.1.

H_4EGTA, like most amino-carboxylates, exists in the zwitterionic form. The unique N-H proton is clearly seen in a Fourier difference map for 1, and its position can be refined (N1-H1 = 0.89(3) Å. As expected, one carbon-nitrogen bond length (C5-N1 = 1.510(3) Å is different from the other two (C1-N1 = 1.491(2) Å, C3-N1 = 1.494(2) Å. The carbon-nitrogen bond lengths (C-N(ave) = 1.50(1) Å are longer than is typical for a C-N single bond (~1.47 Å, which is consistent with the presence of a formal positive charge on the nitrogen atom.[82]

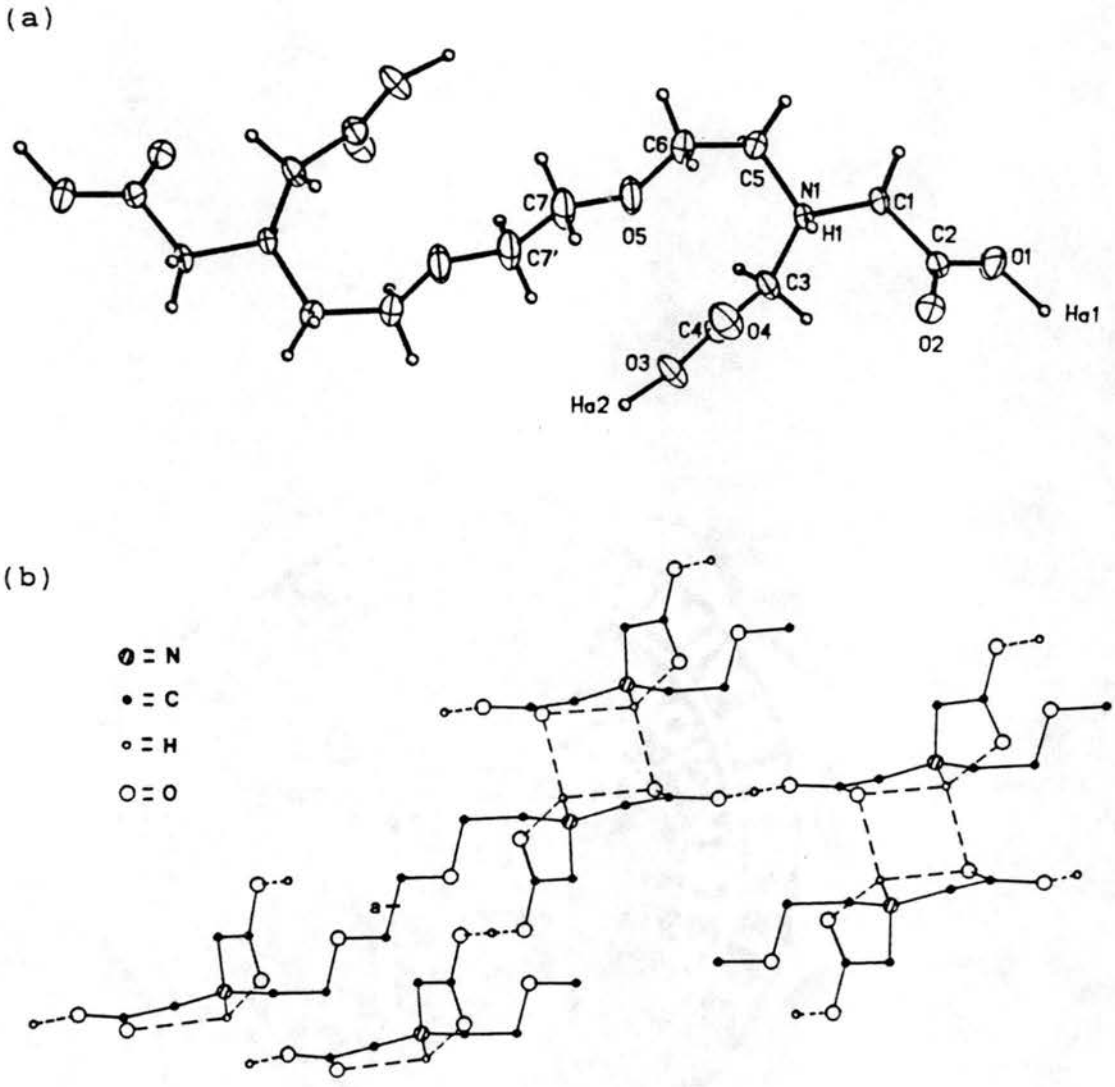

Figure 3.1 (a) A thermal ellipsoid plot (45%) depicting the numbering scheme for H_4EGTA. Ha1 and Ha2 are shared with other H_4EGTA molecules in the lattice. (b) A diagram illustrating the inter- and intramolecular hydrogen bonding interactions. The inversion center for the only complete H_4EGTA molecule in the diagram is indicated by a.

Table 3.1 Bond Lengths (Å) and Angles (deg)[a] for H_4EGTA

C1-C2	1.519(3)	C1-N1	1.491(2)
C2-O1	1.278(2)	C2-O2	1.223(3)
C3-C4	1.511(3)	C3-N1	1.493(2)
C4-O3	1.285(2)	C4-O4	1.220(3)
C5-C6	1.506(3)	C5-N1	1.510(3)
C6-O5	1.415(3)	C7-O5	1.423(3)
C7-C7'	1.492(5)	O1-Ha1	1.222(2)
O3-Ha2	1.225(2)	N1-H1	0.89(3)
H1··O2	2.45(2)	H1··O4	2.27(2)
H1··O2'	2.11(2)		

C2-C1-N1	111.6(2)	C1-C2-O1	112.2(2)
C1-C2-O2	120.7(2)	O1-C2-O2	127.0(2)
C4-C3-N1	111.2(2)	C3-C4-O3	112.8(2)
C3-C4-O4	120.0(2)	O3-C4-O4	127.2(2)
C6-C5-N1	113.5(2)	C5-C6-O5	110.3(2)
O5-C7-C7'	107.9(2)	C1-N1-C3	112.1(1)
C1-N1-C5	108.7(2)	C3-N1-C5	112.8(2)
C6-O5-C7	110.8(2)	C1-N1-H1	107(1)
C3-N1-H1	107(1)	C5-N1-H1	109(1)
Ha1-O1-C2	116.2(2)	Ha2-O3-C4	114.5(2)
N1-H1··O2	100(1)	N1-H1··O4	111(2)
N1-H1··O2'	142(2)		

(a) Estimated standard deviations in the least significant digits are given in parentheses.

The two carboxylate groups exhibit very similar geometries; the chemically distinct carbon-oxygen distances average 1.282(5) Å (C2-O1 and C4-O3) and 1.222(2) Å (C2-O2 and C4-O4). The difference between the two chemically distinct sets of carbon-oxygen distances is 0.060(7) Å This value is consistent with the strongly hydrogen bonded nature of these carboxylate groups; the O···O hydrogen bond distances of 2.444(3) Å (O1···O1') and 2.450(3) Å (O3···O3') rank among the shortest that have been observed.[83] In an anionic carboxylate, these two distances would be identical, and in a non-hydrogen bonded carboxylic acid, this difference is typically 0.1 Å.[84] The hydrogen bonding between carboxylate groups appears to be symmetric, although a disordered, asymmetrically bridged structure would be difficult to distinguish crystallographically.[85]

The hydrogen atom bound to nitrogen is involved in three non-linear hydrogen bonding interactions (see Figure 3.1(b)). Two of these interactions involve the carbonyl oxygen atoms of the acetate groups attached to that nitrogen atom (N1···O2 = 2.746(2) Å and N1···O4 = 2.717(3) Å, while one involves the carbonyl group in an adjacent molecule (N1···O2'') = 2.862(2) Å The hydrogen-bond bridging pattern is very similar to that seen in H_4EDTA.[86]

Infrared Study of H_4EGTA and D_4EGTA

Correlations have been developed between O···O bond distances in hydrogen-bonded systems and the positions of

the infrared stretching and bending modes associated with the hydrogen bond.[87] The infrared spectrum of H_4EGTA appears to be consistent with these correlations.

As is characteristic of strong hydrogen bonds, there is no evidence of an O-H stretching band in the region 3500-2000 cm^{-1}. The O-H-O stretching mode typically occurs as a very broad band shifted to lower energy than that characteristic of a non-hydrogen bonded O-H group; the magnitude of the shift depends on the strength of the hydrogen bond. A broad feature which spans 1500-500 cm^{-1} (maximum at ~750 cm^{-1}) is apparent in the IR spectrum of H_4EGTA (see Figure 3.2(a)). This band is similar in breadth and position to the band identified as ν_{as}(O-H-O) in the infrared spectrum of H_4EDTA.[88] That band arises from a hydrogen bond approximately equal in strength to that in H_4EGTA. As expected, this broad feature for H_4EGTA moves to lower frequency (maximum at ~550 cm^{-1}) upon deuteration. The correlation between the position of the O-H-O stretching mode and the out of plane (γ) bending mode of the hydrogen bond would predict a γ mode for H_4EGTA at 1250 cm^{-1}. A band at 1220 cm^{-1} (which moves to 878 cm^{-1} for D_4EGTA) is observed, and is assigned to this out of plane bending motion.

Correlations are less well-developed for prediction of the position of the in-plane (δ) bending mode of O···O hydrogen bonds, since this vibration is usually strongly

Figure 3.2 (a) Infrared spectrum of H_4EGTA. The spectrum shown for the region 4000-1550 cm^{-1} was taken in fluorolube while the spectrum for the region 1550-300 cm^{-1} was taken in nujol. (b) Infrared spectrum of D_4EGTA, recorded similarly.

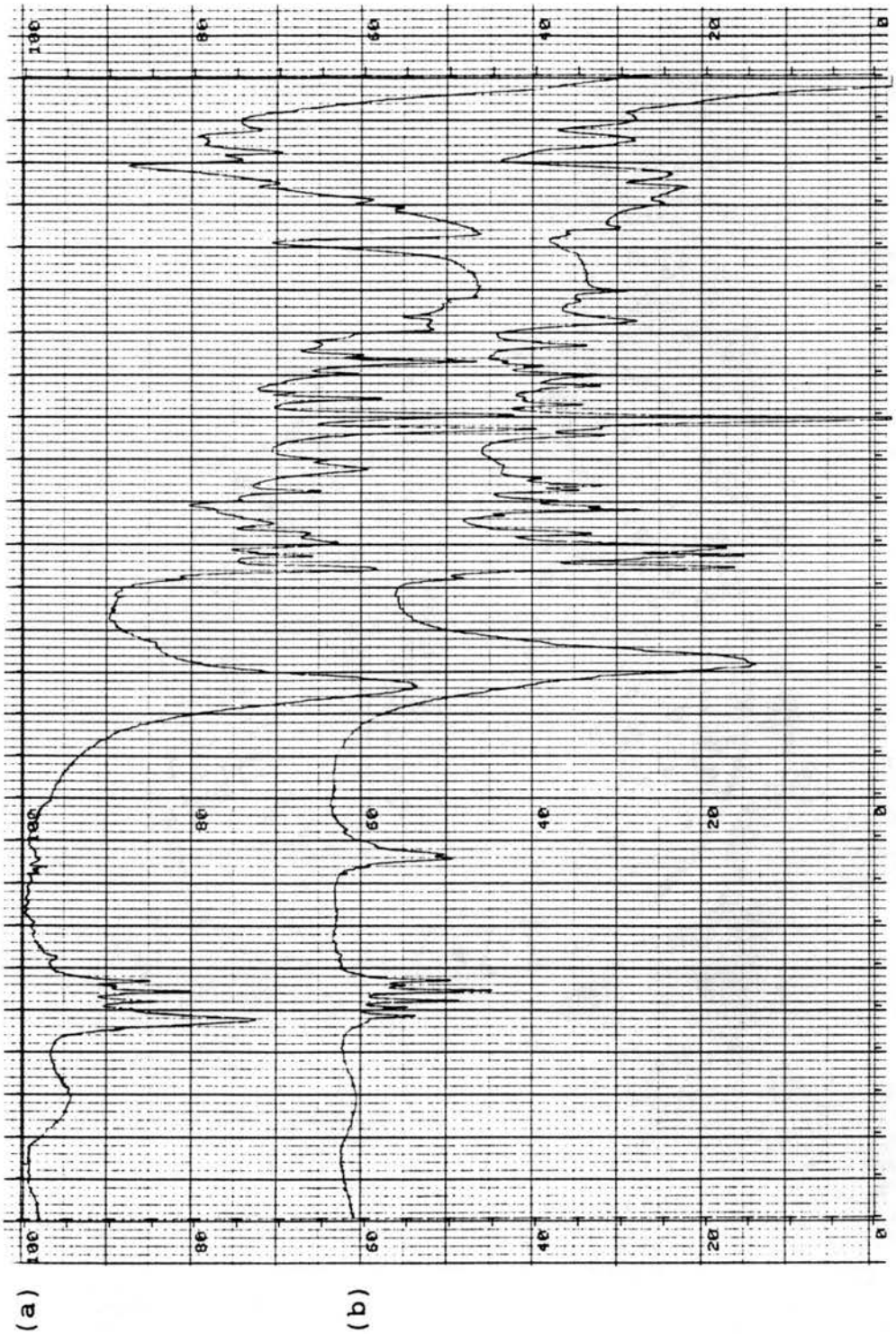
(a)
(b)
100
80
60
40
20
0
4000
3000
2000
1600
1200
800
400

coupled with at least one, and often several other, vibrations. This vibrational mode was not readily apparent in the spectrum of H_4EGTA. Upon deuteration, however, two bands appeared at 1278 cm^{-1} and 1338 cm^{-1}. Assignment of these bands as δ bands is consistent with the assignments made in other strongly hydrogen bonded systems.[83] The δ band would be expected to coincide, approximately, with the C=O stretch in H_4EGTA, based on the observed band positions for D_4EGTA; this may be why these bands were not seen in the infrared spectrum of the protonated species.

N-H (N-D) stretching and bending modes have also been identified in the infrared spectrum. Band assignments are summarized in Table 3.2.

Table 3.2 IR Band Assignments for H_4EGTA and D_4EGTA (cm^{-1})

	H_4EGTA	D_4EGTA
ν(C=O)	1741	1690
ν(C-O)	1400	1414
ν(N-H^+)	3052	2157
δ(N-H^+)	1356	--
ν(O-H-O)	1500-500 (max ~ 750)	1300- < 400 (max ~ 550)
γ(O-H-O)	1228	878
δ(O-H-O)	--	1278, 1338

CHAPTER 4

THE EIGHT-COORDINATE CALCIUM CHELATE OF $EGTA^{4-}$

Introduction

The structures of both the strontium and calcium salts of $[Ca(EGTA)]^{2-}$ will be discussed. Two different salts were structurally characterized in an attempt to assess the counterion influence on the chelate bonding and conformational parameters. Variable temperature ^{1}H NMR spectra of $[Ca(EGTA)]^{2-}$ have also been obtained, allowing discussion of the structure of the complex in solution.

Structure of $Ca[Ca(EGTA)]\cdot(22/3)H_2O$ (2)

The asymmetric unit of the unit cell contains three unique $[Ca(EGTA)]^{2-}$ complex anions (anion **a**, Ca1; **b**, Ca2; **c**, Ca3); complex anion **a**, containing Ca1, is pictured in Figure 4.1(a). Since the most commonly observed coordination number for calcium is eight,[89,90] it is not surprising that the $EGTA^{4-}$ ligand is able to utilize its full octadentate chelating capability in binding to the calcium ion in each of the $[Ca(EGTA)]^{2-}$ units. The ligand atoms about calcium in the three $[Ca(EGTA)]^{2-}$ complexes in 2 occupy the vertices of dodecahedra, which are distorted by the constraints associated with the chelate rings. A

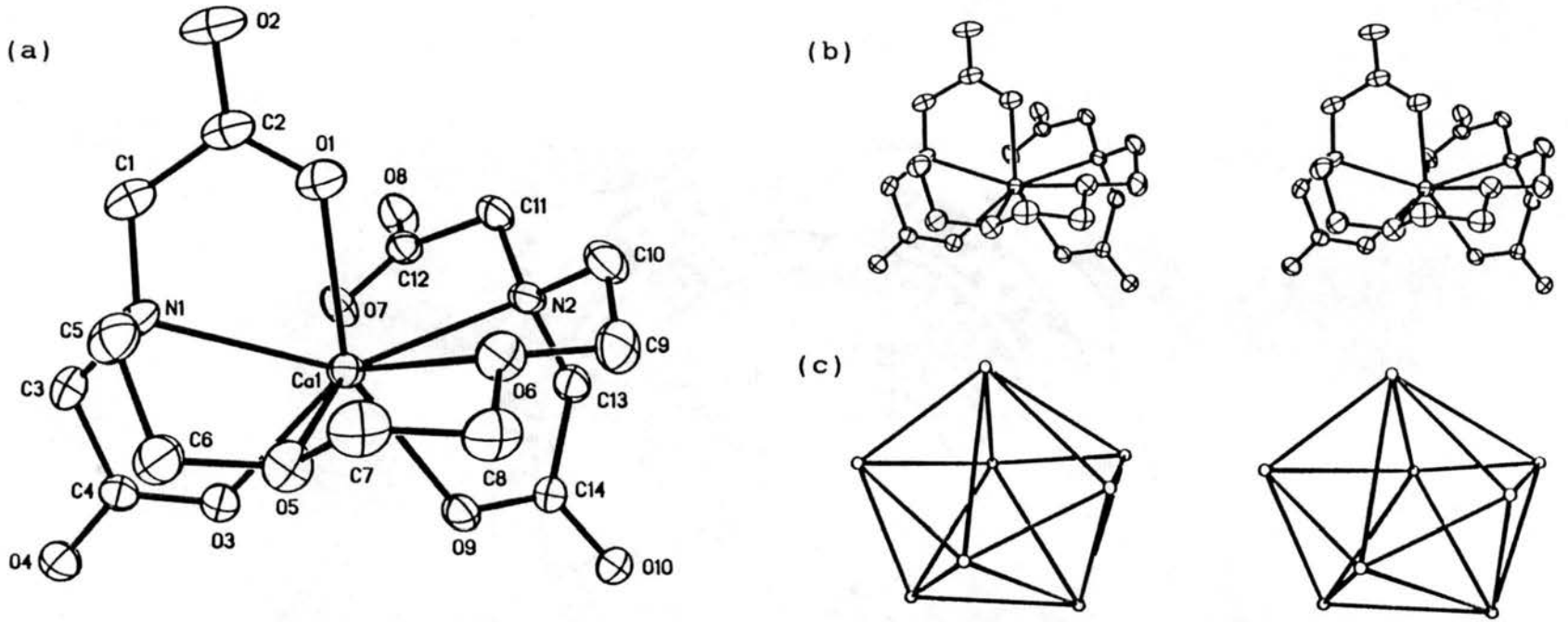

Figure 4.1 (a) A thermal ellipsoid plot (40%) of the $[Ca(EGTA)]^{2-}$ complex anion involving Ca1. The numbering scheme for the complex anions involving Ca2 and Ca3 may be derived as follows: C(n,a) = 14(n-1) + a; O(n,a) = 10(n-1) + a; N(n,a) = 2(n-1) + a; n = complex anion number, a = atom number in complex a. (b) Stereoview of $[Ca(EGTA)]^{2-}$. (c) Stereoview of the dodecahedron comprised of the ligand atoms about Ca1.

dodecahedron is formed by the orthogonal intersection of two equivalent trapezoids (each represented as BAAB). For complex **a**, for example (see Figures 4.1(b) and (c)), one trapezoid contains N2 and O6 (A sites) as well as O5 and O7 (B sites), while the second trapezoid contains O3 and N1 (A sites) together with O1 and O9 (B sites).

The three Ca^{2+} counterions are coordinated to water molecules and to the oxygen atoms of carboxylate groups that bridge between the $[Ca(EGTA)]^{2-}$ complex anions and these partially aquated counterions. Such bridging in **2** is so extensive that no truly discrete $[Ca(EGTA)]^{2-}$ complex anions exist in the solid. Three possible modes of carboxylate bridging to counterions are depicted schematically in Figure 4.2(a). All three types of bridging interactions occur in **2**; examples are displayed in Figure 4.3(a). A bridging carboxylate group is classified as type 1 if both oxygen atoms are involved in the bridge to a counterion (see, for example, carboxylate O7/O8 bridging to Ca5). If the bridging interaction only involves the carboxylate oxygen atom that <u>is</u> <u>not</u> coordinated to the calcium ion of the $[Ca(EGTA)]^{2-}$ complex, the carboxylate group is classified as type 2 (see, for example, O2 bridging to Ca6). Finally, if the bridging interaction only involves the carboxylate oxygen atom which <u>is</u> coordinated to the calcium ion of the $[Ca(EGTA)]^{2-}$ complex, the carboxylate group is classified as type 3 (see, for example, O29 bridging to Ca6). All modes of

(a)

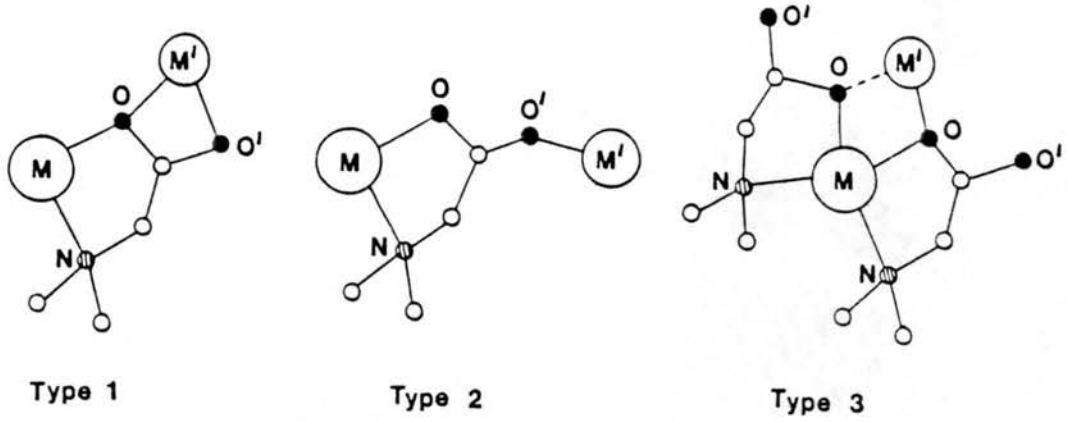

(b)

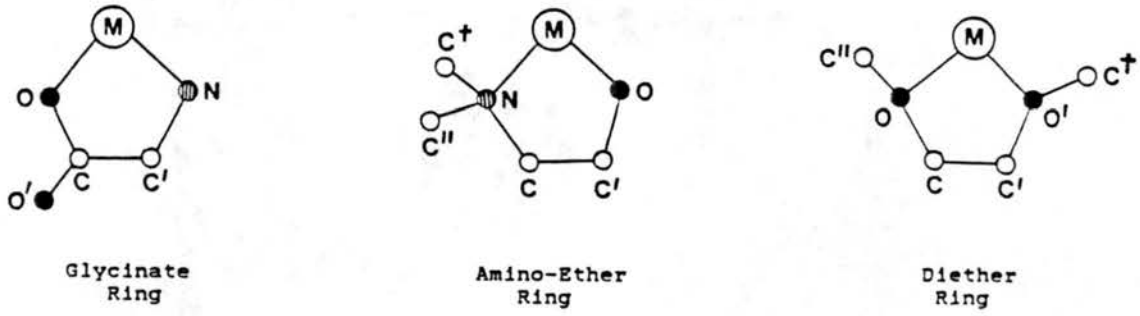

Figure 4.2 (a) Schematic diagram of the bridging modes observed in crystal structures of $EGTA^{4-}$ chelates (see text). (b) The nomenclature utilized in describing the chelate ring bonding and conformational parameters for the three ring types. Of the C" and $C^{\dagger}$ carbon atoms attached to the nitrogen atom of the amino-ether ring, C" has the lower number of the two. For the diether ring, O' is the odd numbered oxygen atom while O is even numbered.

Figure 4.3 (a) Ball and stick plot depicting all of the unique interionic interactions in the lattice of $Ca[Ca(EGTA)]\cdot(22/3)H_2O$ (2). In the two complex anions illustrated, all oxygen atoms that are involved in bridging interactions are enlarged. Hollowed bonds highlight the bridging paths between the $[Ca(EGTA)]^{2-}$ anions and the calcium counterions. (b) A stereoview of the unit cell of 2, viewed along the b axis. metal ions are drawn as large shaded spheres, oxygen atoms of water molecules molecules and carboxylate oxygen atoms are drawn as small unshaded spheres of different size. All other atoms are drawn as black dots.

(a)

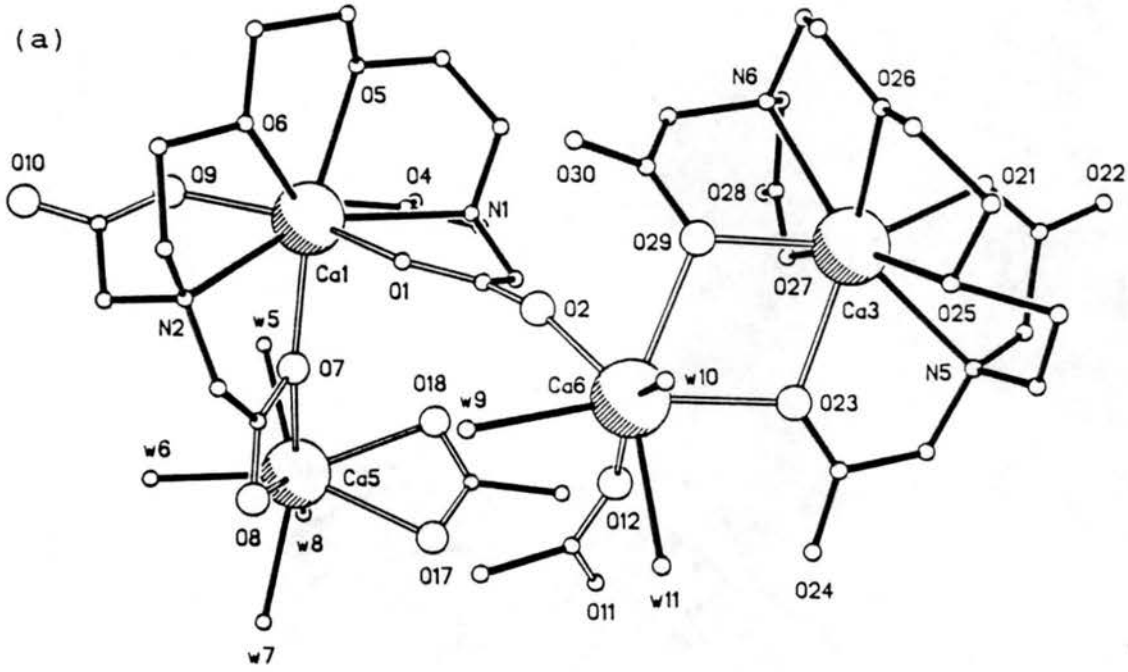
010
09
06
05
04
N1
Ca1
01
02
N2
w5
07
018
w9
Ca6
w10
w6
Ca5
08
w8
017
012
011
w11
w7
N6
026
030
028
021
022
029
027
Ca3
025
023
N5
024

(b)

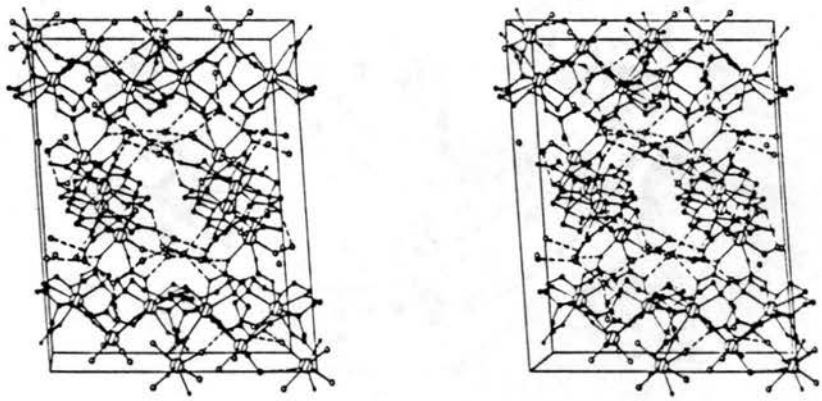

bridging seen in 2, including the planar Ca6-023-Ca3-029 bridge, have been previously observed.[90,91]

Complexes a and b are involved in identical bridging patterns, and appear to be related to each other by an approximate non-crystallographic two-fold axis passing through Ca5. Three of the four carboxylate groups in each of these two $[Ca(EGTA)]^{2-}$ complex anions act as external donors, bridging to all three calcium counterions (Ca4, Ca5, and Ca6). Two of these three carboxylate groups are involved in type 1 interactions (O7/O8 and O9/O10) while the remaining group (O1/O2) acts as a type 2 bridging group. In complex anion c (involving Ca3), only two of the four carboxylate groups are involved in bridging to counterions. Both of these groups (O23/O24 and O29/O30) bridge in a type 3 manner; together, they allow the $[Ca(EGTA)]^{2-}$ anion containing Ca3 to function as a bidentate ligand toward Ca6 (see Figure 4.3(a)).

Of the three unique Ca^{2+} counterions, two are eight-coordinate (Ca4 and Ca5), and exhibit very similar ligand arrays. Each of these ions is coordinated to two type 1 bridging carboxylate groups from the Ca1 and Ca2 complex anions (O7/O8 and O17/O18 for Ca5, for example), and to four water molecules. The oxygen atoms of these complex cations are arranged about Ca4 and Ca5 in distorted dodecahedral arrays. Significant differences exist in the geometric arrangement of ligand atoms about Ca4 and Ca5, however. For Ca4, in each of the two trapezoids comprising

the dodecahedron, a bidentate carboxylate group occupies the A sites, while water molecules occupy the B sites. For Ca5, on the other hand, a bidentate carboxylate group occupies an A and a B site in each trapezoid.

The third counterion, Ca6, is only seven-coordinate. Among the ligands about Ca6 are three water molecules and the oxygen atoms of four bridging carboxylate groups, two of type 2 and two of type 3. The ligand atoms bound to Ca6 occupy the vertices of a distorted monocapped trigonal prism, with triangular faces outlined by O29, O23, and w10, and by O2, O12, and w9. Water molecule w11 caps the rectangular w10-O23-O12-w9 face (see Figure 4.3(a)). The lower coordination number for Ca6 may be due to the greater steric requirements of the unidentate carboxylate bridging groups (types 2 and 3) compared to bidentate carboxylate bridging groups (type 1).

In the solid state, $[Ca(EGTA)]^{2-}$ anions and partially aquated Ca^{2+} counterions are linked into an extended network. The individual units of this network are connected into a polymeric chain by bridging carboxylate groups, as described above. These chains are propagated parallel to the bc-plane (see Figure 4.3(b)). In addition to those interactions, hydrogen bonds connect carboxylate groups and coordinated water molecules to occluded solvent water molecules. Every carboxylate oxygen atom in 2 is involved in an interaction with a metal ion or a water molecule. Of the roughly twenty-two water molecules

Table 4.1 Metal-Ligand Distances (Å) and Angles (deg)[a] for $Ca[Ca(EGTA)]\cdot(22/3)H_2O$

(a) Complex Ions

Complex a		Complex b		Complex c	
Ca1-N1	2.617(5)	Ca2-N3	2.613(5)	Ca3-N5	2.575(6)
Ca1-N2	2.603(5)	Ca2-N4	2.602(5)	Ca3-N6	2.567(5)
Ca1-O1	2.375(5)	Ca2-O11	2.347(4)	Ca3-O21	2.379(5)
Ca1-O3	2.386(4)	Ca2-O13	2.374(4)	Ca3-O23	2.412(4)
Ca1-O5	2.502(4)	Ca2-O15	2.550(4)	Ca3-O25	2.426(6)
Ca1-O6	2.473(4)	Ca2-O16	2.477(4)	Ca3-O26	2.483(5)
Ca1-O7	2.404(4)	Ca2-O17	2.392(4)	Ca3-O27	2.365(5)
Ca1-O9	2.365(4)	Ca2-O19	2.375(4)	Ca3-O29	2.397(5)
N1-Ca1-N2	144.9(2)	N3-Ca2-N4	142.7(1)	N5-Ca3-N6	147.0(2)
N1-Ca1-O1	66.3(2)	N3-Ca2-O11	65.8(1)	N5-Ca3-O21	67.1(2)
N2-Ca1-O1	83.0(2)	N4-Ca2-O11	80.8(1)	N6-Ca3-O21	87.0(2)
N1-Ca1-O3	66.3(1)	N3-Ca2-O13	66.7(1)	N5-Ca3-O23	66.7(2)
N2-Ca1-O3	135.5(1)	N4-Ca2-O13	138.6(1)	N6-Ca3-O23	130.2(2)
O1-Ca1-O3	131.2(2)	O11-Ca2-O13	131.5(1)	O21-Ca3-O23	132.8(2)
N1-Ca1-O5	70.4(1)	N3-Ca2-O15	69.1(1)	N5-Ca3-O25	69.8(2)
N2-Ca1-O5	132.4(1)	N4-Ca2-O15	132.4(1)	N6-Ca3-O25	132.0(2)
O1-Ca1-O5	96.4(1)	O11-Ca2-O15	94.4(1)	O21-Ca3-O25	88.3(2)
O3-Ca1-O5	78.3(1)	O13-Ca2-O15	77.4(1)	O23-Ca3-O25	84.9(2)
N1-Ca1-O6	120.2(1)	N3-Ca2-O16	117.4(1)	N5-Ca3-O26	123.9(2)
N2-Ca1-O6	66.6(1)	N4-Ca2-O16	67.7(1)	N6-Ca3-O26	67.0(2)
O1-Ca1-O6	79.3(1)	O11-Ca2-O16	77.4(1)	O21-Ca3-O26	79.7(2)
O3-Ca1-O6	136.5(1)	O13-Ca2-O16	135.0(1)	O23-Ca3-O26	136.3(2)
O5-Ca1-O6	66.5(1)	O15-Ca2-O16	65.2(1)	O25-Ca3-O26	65.1(2)
N1-Ca1-O7	94.8(1)	N3-Ca2-O17	95.2(1)	N5-Ca3-O27	91.3(2)
N2-Ca1-O7	65.6(1)	N4-Ca2-O17	66.0(1)	N6-Ca3-O27	66.7(2)
O1-Ca1-O7	86.6(1)	O11-Ca2-O17	87.6(1)	O21-Ca3-O27	88.1(2)
O3-Ca1-O7	86.3(1)	O13-Ca2-O17	87.5(1)	O23-Ca3-O27	83.7(2)
O5-Ca1-O7	161.9(1)	O15-Ca2-O17	161.5(1)	O25-Ca3-O27	160.7(2)
O6-Ca1-O7	131.4(1)	O16-Ca2-O17	133.0(1)	O26-Ca3-O27	132.6(2)
N1-Ca1-O9	143.9(1)	N3-Ca2-O19	147.0(1)	N5-Ca3-O29	138.2(2)
N2-Ca1-O9	68.6(1)	N4-Ca2-O19	68.1(1)	N6-Ca3-O29	70.2(2)

Table 4.1 (continued)

O1-Ca1-O9	149.7(2)	O11-Ca2-O19	147.2(1)	O21-Ca3-O29	154.5(2)
O3-Ca1-O9	78.6(1)	O13-Ca2-O19	80.9(1)	O23-Ca3-O29	72.4(1)
O5-Ca1-O9	95.3(1)	O15-Ca2-O19	98.7(1)	O25-Ca3-O29	98.6(2)
O6-Ca1-O9	79.9(1)	O16-Ca2-O19	81.1(1)	O26-Ca3-O29	81.0(2)
O7-Ca1-O9	90.8(1)	O17-Ca2-O19	89.2(1)	O27-Ca3-O29	92.8(2)

(b) Counterions

Counterion 1		Counterion 2		Counterion 3	
Ca4-w1	2.393(5)	Ca5-O7	2.526(4)	Ca6-O2	2.325(5)
Ca4-w2	2.437(4)	Ca5-O8	2.485(4)	Ca6-O12	2.381(4)
Ca4-w3	2.430(5)	Ca5-O17	2.525(4)	Ca6-O23	2.407(5)
Ca4-w4	2.386(4)	Ca5-O18	2.470(5)	Ca6-O29	2.473(4)
Ca4-O9a	2.540(4)	Ca5-w5	2.485(5)	Ca6-w9	2.452(6)
Ca4-O10a	2.461(4)	Ca5-w6	2.395(5)	Ca6-w10	2.408(7)
Ca4-O19a	2.542(4)	Ca5-w7	2.467(5)	Ca6-w11	2.469(5)
Ca4-O20a	2.447(4)	Ca5-w8	2.392(5)		

w1-Ca4-w2	98.6(2)	O7-Ca5-O8	52.1(1)	O2-Ca6-O12	75.6(2)
w1-Ca4-w3	154.5(2)	O7-Ca5-O17	93.9(1)	O2-Ca6-O23	114.9(2)
w2-Ca4-w3	88.5(1)	O8-Ca5-O17	83.8(1)	O12-Ca6-O23	82.5(1)
w1-Ca4-w4	87.8(2)	O7-Ca5-O18	84.9(1)	O2-Ca6-O29	75.6(2)
w2-Ca4-w4	153.6(2)	O8-Ca5-O18	117.3(2)	O12-Ca6-O29	127.3(1)
w3-Ca4-w4	96.7(2)	O17-Ca5-O18	52.5(1)	O23-Ca6-O29	71.2(1)
w1-Ca4-O9a	129.2(1)	O7-Ca5-w5	75.4(1)	O2-Ca6-w9	77.9(2)
w2-Ca4-O9a	74.8(1)	O8-Ca5-w5	119.8(2)	O12-Ca6-w9	97.2(2)
w3-Ca4-O9a	76.3(1)	O17-Ca5-w5	132.0(2)	O23-Ca6-w9	166.5(2)
w4-Ca4-O9a	81.3(1)	O18-Ca5-w5	79.7(2)	O29-Ca6-w9	118.3(2)
w1-Ca4-O10a	76.9(1)	O7-Ca5-w6	98.3(2)	O2-Ca6-w10	128.7(2)
w2-Ca4-O10a	77.5(1)	O8-Ca5-w6	84.7(2)	O12-Ca6-w10	153.5(2)
w3-Ca4-O10a	128.6(1)	O17-Ca5-w6	152.8(2)	O23-Ca6-w10	93.8(2)
w4-Ca4-O10a	79.2(1)	O18-Ca5-w6	152.6(2)	O29-Ca6-w10	74.9(2)
O9a-Ca4-O10a	52.3(1)	w5-Ca5-w6	74.9(2)	w9-Ca6-w10	80.5(2)
w1-Ca4-O19a	79.3(1)	O7-Ca5-w7	130.1(1)	O2-Ca6-w11	143.3(2)
w2-Ca4-O19a	75.9(1)	O8-Ca5-w7	78.0(1)	O12-Ca6-w11	75.8(2)

Table 4.1 (continued)

w3-Ca4-O19a	78.7(1)	O17-Ca5-w7	77.7(1)	O23-Ca6-w11	83.4(2)
w4-Ca4-O19a	130.5(1)	O18-Ca5-w7	122.4(2)	O29-Ca6-w11	140.9(2)
O9a-Ca4-O19a	141.7(1)	w5-Ca5-w7	143.7(2)	w9-Ca6-w11	83.5(2)
O10a-Ca4-O19a	140.9(1)	w6-Ca5-w7	75.9(2)	w10-Ca6-w11	77.7(2)
w1-Ca4-O20a	77.5(1)	O7-Ca5-w8	155.3(2)		
w2-Ca4-O20a	127.9(1)	O8-Ca5-w8	151.4(2)		
w3-Ca4-O20a	78.8(1)	O17-Ca5-w8	96.3(2)		
w4-Ca4-O20a	78.4(1)	O18-Ca5-w8	83.6(2)		
O9a-Ca4-O20a	145.6(1)	w5-Ca5-w8	81.1(2)		
O10a-Ca4-O20a	146.4(1)	w6-Ca5-w8	82.5(2)		
O19a-Ca4-O20a	52.2(1)	w7-Ca5-w8	74.2(2)		

(c) Interionic Angles

Ca6-O2-C2	164.9(4)	C14-O10-Ca4b	94.1(3)	C28-O19-Ca4a	90.5(3)
Ca1-O7-Ca5	146.9(2)	Ca6-O12-C16	140.9(4)	C28-O20-Ca4a	94.9(3)
Ca5-O7-C12	90.7(3)	Ca2-O17-Ca5	144.8(2)	Ca3-O23-Ca6	108.5(2)
Ca5-O8-C12	92.9(3)	Ca5-O17-C26	91.1(3)	Ca6-O23-C32	127.8(4)
Ca1-O9-Ca4b	146.7(2)	Ca5-O18-C26	93.9(3)	Ca3-O29-Ca6	106.8(2)
C14-O9-Ca4b	89.9(3)	Ca2-O19-Ca4a	146.1(2)	Ca6-O29-C42	121.2(4)

(a) Estimated standard deviations in the least significant digits are given in parentheses.

contained in the asymmetric unit, eleven are not bound to calcium. These occluded solvent molecules knit together the polymeric $[Ca(EGTA)]^{2-}$-Ca^{2+} counterion chains in the a direction. Complex anion c is involved in bridging interactions to only one cation (Ca6), and therefore functions as a side group on the polymer chain. These side groups extend out from the chain in the a direction, and function to stitch the chains together by hydrogen bonding to water molecules coordinated to cations on the opposite chain. Undoubtedly, the extensive hydrogen bonding network is an extremely important factor in the stability of crystals of **2**.

The Ca-O(carboxylate) bond distances observed are a function of the bridging/nonbridging nature of the carboxylate group. Metal-ligand distances and angles describing the bonding in the complex anions and the counterions, as well as the interionic interactions between them, may be found in Table 4.1. Ca-O(carboxylate) bond lengths in the $[Ca(EGTA)]^{2-}$ anions are, with the exception of type 2 bridging interactions, shorter than Ca-O(carboxylate) bond lengths for the calcium counterions. For example, carboxylate group O7/O8, which is involved in a type 1 bridge, bonds at a shorter distance to Ca1 (Ca1-O7 = 2.404(4) Å) than to the Ca5 counterion (Ca5-O7 = 2.526(4) Å, Ca5-O8 = 2.485(4) Å). In addition, for type 1 carboxylate bridges, the oxygen atom that is not bonded to the chelated Ca^{2+} ion bonds at a shorter distance to the

calcium counterion than does the oxygen atom which is simultaneously bound to both metal ions.

Carboxylate groups involved in type 2 interactions do not exhibit as regular a pattern of bond lengths as do the type 1 carboxylate bridges. Of the two type 2 interactions, one carboxylate group (O11/O12) bonds at a shorter distance to the chelated calcium ion (Ca2-O11 = 2.347(4) Å) than to the associated calcium counterion (Ca6-O12 = 2.381(4) Å), while for the other carboxylate group (O1/O2), the reverse is true (Ca1-O1 = 2.375(4) Å, Ca6-O2 = 2.325(5) Å). For the two type 3 bridging interactions which form a planar Ca_2O_4 unit, the bridge involving O23 is approximately symmetric (Ca3-O23 = 2.412(4) Å, Ca6-O23 = 2.407(5) Å), while the bridge involving O29 is asymmetric, with O29 binding at a shorter distance to the chelated calcium ion (Ca3-O29 = 2.397(5) Å, Ca6-O29 = 2.473(4) Å). Additionally, the carboxylate oxygen atoms involved in the type 3 bridges are bound at the longest distances to Ca3 of the four carboxylate ligands. Type 1 and type 2 bridging interactions are seen in the structure of $Ca[Ca(EDTA)]\cdot H_2O$,[1] and similar bond length/bridge type patterns are seen.

Examination of structural reviews of all Ca-O interactions[89,90] reveals that all Ca-O(carboxylate) distances observed for 2 (2.325(5)-2.542(4) Å) fall within the normal ranges for seven- and eight-coordinate calcium ions. In addition, Ca-O(water) distances in 2 span a range

(2.386(4)-2.485(5) Å) which is typical of seven- and eight-coordinate aquated calcium ions.[89,90]

The question of whether the $EGTA^{4-}$ ligand utilizes the ether oxygen atoms in coordinating to various metal ions, including calcium, has been disputed.[75,92,93] A study of the rate of ligand exchange between $[Ca(EGTA)]^{2-}$ and free $EGTA^{4-}$ suggested a mechanism in which the ether oxygen atoms were not bound to the metal.[92] In the solid state, however, the ether oxygen atoms of all three independent $[Ca(EGTA)]^{2-}$ complexes are strongly coordinated (Ca-O(ether,ave) = 2.50(3) Å). Given the chelating nature of the $EGTA^{4-}$ ligand, it seems likely that these ether oxygen atoms remain bound in solution. The abnormally short Ca3-O25 distance of 2.426(6) Å was omitted in calculating this average; this distance has clearly been influenced by the δ/λ disorder present in the A5 chelate ring (see below). All of the Ca-O(ether) distances (with the exception of Ca3-O25) fall within the range observed previously for Ca-O(ether) bonds. In eight-coordinate $[Ca(ODA)]\cdot H_2O$[94] (ODA = 3-oxapentanedioic acid), a short Ca-O(ether) distance of 2.431(3) Å was seen, while in nine-coordinate $[Ca(222)Br]^{+}$ ((222) = 4,7,13,16,21,24-hexaoxa-1,10-diazabicyclo[8.8.8]hexaeicosane), the Ca-O(ether) distances span the range from 2.487(7) Å to 2.551(7) Å,[95] essentially the same range of Ca-O(ether) distances seen in **2** (2.473(4)-2.550(4) Å).

The Ca-N distances in **2** (Ca-N = 2.567(5)-2.617(5) Å) are slightly shorter than those seen previously in the eight-coordinate $EDTA^{4-}$ complex of Ca^{2+} (Ca-N = 2.623(7), 2.711(8) Å)[1] and the six coordinate NTA^{3-} complex of Ca^{2+} (Ca-N = 2.629(2) Å).[1] In addition, the Ca-N bonds in complex **c** (Ca-N(ave) = 2.570(6) Å) are significantly shorter than those for complexes **a** and **b** (Ca-N(ave) = 2.609(7)Å). As described above, O23 and O29 of complex **c** are involved in type 3 bridging interactions. As a result, these two atoms are brought into closer proximity than would otherwise be possible. The O23-O29 distance in complex **c** is 3.190(6) Å, which is significantly shorter than the corresponding distances (O3-O9 = 3.279(6) Å, O13-O19 = 3.298(6) Å) in complexes **a** and **b**. Simultaneous binding of O23 and O29 to Ca6 thus appears to act to tighten the bonding of the $EGTA^{4-}$ ligand to Ca3.

The chelate ring bonding and conformational parameters for **2** may be found in Tables 4.2 and 4.3, respectively. The conformations of the five-membered chelate rings in the $[Ca(EGTA)]^{2-}$ complex anions can be analyzed in a manner similar to that employed for other metal complexes of non-peptide polyamino-polycarboxlic acids in a recent review.[45] This same method has been used to analyze the conformations of steroids.[96] The ring conformation is evaluated by computation of ring asymmetry parameters, based on summations involving the torsion angles characteristic of each chelate ring. The diagram below illustrates the

Table 4.2 Chelate Ring[a] Bonding Parameters[b] for $Ca[Ca(EGTA)]\cdot(22/3)H_2O$

Glycinate Rings

	C-C'	C'-N	C-O	C-O'	C-C'-N	O-C-O'	C'-C-O	C'-C-O'	Ca-N-C'	Ca-O-C
G1	1.504(9)	1.466(8)	1.254(8)	1.249(8)	112.1(5)	124.0(6)	118.1(5)	117.9(6)	105.7(3)	123.2(4)
G2	1.503(9)	1.460(7)	1.272(7)	1.240(7)	115.0(5)	124.2(6)	117.6(5)	118.1(5)	111.0(3)	125.9(4)
G3	1.527(8)	1.456(7)	1.261(7)	1.247(7)	109.5(5)	122.8(5)	118.6(5)	118.6(5)	106.1(3)	121.3(3)
G4	1.514(8)	1.479(8)	1.261(7)	1.243(7)	114.0(5)	123.4(5)	118.1(5)	118.2(5)	107.5(3)	123.2(3)
G5	1.515(9)	1.478(8)	1.265(7)	1.252(7)	111.4(5)	123.4(6)	117.9(5)	118.6(5)	105.6(3)	123.0(4)
G6	1.497(8)	1.475(8)	1.267(7)	1.257(7)	113.6(5)	123.5(5)	118.8(5)	117.6(5)	110.6(3)	125.3(4)
G7	1.500(8)	1.460(7)	1.269(7)	1.260(7)	109.3(5)	121.6(5)	118.7(5)	119.7(5)	105.4(3)	121.0(4)
G8	1.515(8)	1.457(8)	1.254(7)	1.255(7)	114.8(5)	122.3(5)	119.6(5)	118.1(5)	109.6(3)	123.4(3)
G9	1.516(11)	1.461(10)	1.257(9)	1.247(10)	113.3(6)	125.2(7)	118.1(7)	116.7(7)	107.8(4)	122.7(5)
G10	1.492(10)	1.470(9)	1.273(8)	1.240(7)	113.3(6)	124.1(6)	118.4(5)	117.5(6)	109.7(4)	122.8(4)
G11	1.528(10)	1.451(8)	1.262(9)	1.239(9)	113.0(5)	125.0(7)	117.1(6)	117.8(6)	105.8(4)	121.2(4)
G12	1.498(9)	1.474(9)	1.270(8)	1.250(8)	114.8(5)	124.3(6)	117.3(5)	118.2(6)	105.4(3)	118.8(4)

Amino-Ether Rings

	C-C'	C-N	C'-O	C-C'-O	C'-C-N	C"-N-C[†]	C-N-C"	C-N-C[†]	Ca-N-C	Ca-O-C'
A1	1.496(9)	1.474(8)	1.452(8)	110.6(5)	113.5(5)	113.3(5)	110.5(5)	111.1(5)	104.8(4)	112.8(3)
A2	1.519(9)	1.467(7)	1.422(8)	105.3(5)	111.9(5)	110.3(4)	112.1(4)	110.9(5)	109.6(3)	119.0(3)
A3	1.501(9)	1.464(8)	1.435(7)	111.2(5)	112.8(5)	111.9(4)	110.9(5)	111.0(5)	106.6(3)	113.0(3)
A4	1.514(8)	1.484(8)	1.418(7)	107.8(5)	109.6(5)	109.8(4)	112.1(5)	111.5(4)	108.2(3)	116.6(4)
A5	1.288(20)	1.457(11)	1.536(17)	112.3(12)	118.0(10)	110.7(6)	111.1(7)	110.1(6)	107.4(5)	109.3(6)
A6	1.503(10)	1.461(8)	1.430(9)	106.6(5)	112.1(5)	110.9(5)	111.8(5)	112.0(5)	110.7(4)	117.7(4)

Diether Rings

	C-C'	C'-O'	C-O	C'-C-O	C-C'-O'	C'-O'-C[†]	C"-O-C	Ca-O-C	Ca-O'-C'
E1	1.490(10)	1.431(8)	1.444(8)	107.5(5)	107.8(5)	112.8(5)	112.4(5)	113.3(3)	115.8(3)
E2	1.491(9)	1.422(7)	1.418(8)	108.8(5)	106.8(5)	114.3(4)	113.2(5)	114.4(3)	116.7(3)
E3	1.469(16)	1.421(10)	1.408(12)	109.2(8)	106.5(8)	114.3(6)	125.8(8)	118.4(6)	115.9(5)

(a) Chelate ring nomenclature is described in Figure 4.2(b). Rings within each series are numbered with increasing oxygen number.

(b) Bond lengths are given in Ångstroms and bond angles are given in degrees. Estimated standard deviations in the least significant digits are given in parentheses.

Table 4.3 Chelate Ring[a] Conformational Parameters[b] for $Ca[Ca(EGTA)]\cdot(22/3)H_2O$

Glycinate Rings

	Ring Type	Bridging[c] Interaction	N-Ca-O-C	Ca-O-C-C'	O-C-C'-N	C-C'-N-Ca	C'-N-Ca-O	ΔC_s,min[d] ΔC_s,max	ΔC_2,min ΔC_2,max
G1	δ	2	-16.7(4)	-0.3(7)	31.1(8)	-40.6(5)	29.2(3)	13.0(N) 46.0(C)	11.7(O) 59.8(N)
G2	λ	0	7.8(4)	1.9(7)	-18.0(8)	22.8(6)	-15.6(3)	8.8(N) 24.7(O)	4.5(O) 32.7(N)
G3	δ	1	-20.6(4)	2.4(7)	32.6(7)	-45.6(5)	34.5(3)	11.6(N) 53.0(C)	16.3(O) 68.0(N)
G4	δ	1	-2.1(4)	-14.8(6)	32.5(7)	-30.8(5)	17.6(3)	2.3(C') 37.4(O)	13.8(O) 50.3(C')
G5	δ	2	-25.8(4)	12.3(7)	22.8(7)	-39.8(5)	32.8(3)	5.4(N) 52.6(C)	12.4(C) 61.8(N)
G6	λ	0	5.8(4)	6.1(7)	-21.9(8)	24.6(6)	-16.0(3)	7.3(C') 28.1(O)	4.2(O) 36.4(C')
G7	δ	1	-16.5(4)	-4.3(7)	38.0(7)	-46.9(5)	33.2(3)	18.0(N) 52.5(O)	9.3(O) 68.5(N)
G8	δ	1	-4.1(4)	-7.5(7)	22.0(8)	-23.0(6)	14.4(3)	4.9(C') 27.0(O)	5.9(O) 35.4(C')
G9	λ	0	17.0(6)	-3.6(10)	-23.9(12)	35.0(9)	-26.3(5)	7.9(N) 41.6(C)	14.7(O) 52.1(N)
G10	δ	3	-11.6(4)	-2.8(7)	26.0(8)	-33.2(6)	23.0(4)	12.5(N) 36.1(O)	6.6(O) 47.8(N)
G11	λ	0	26.3(5)	-13.5(8)	-21.5(9)	39.8(6)	-33.0(4)	5.9(N) 52.9(C)	11.1(C) 61.6(N)
G12	λ	3	-2.9(4)	24.4(7)	-43.5(8)	36.1(6)	-17.8(3)	7.0(C') 45.9(O)	13.4(Ca) 63.7(C')

Amino-Ether Rings

	Ring Type		O-Ca-N-C	Ca-N-C-C'	N-C-C'-O	C-C'-O-Ca	C'-O-Ca-N	ΔC_s,min ΔC_s,max	ΔC_2,min ΔC_2,max
A1	δ		18.9(3)	-48.4(6)	62.5(7)	-39.4(6)	10.6(4)	17.6(C) 65.5(Ca)	8.7(Ca) 88.6(C)
A2	λ		-15.1(4)	44.9(6)	-59.2(7)	45.1(6)	-17.5(4)	21.8(C') 67.7(Ca)	1.7(Ca) 85.9(C')

Table 4.3 (continued)

A3	δ	20.0(3)	-48.9(5)	61.6(7)	-38.3(6)	9.6(4)	15.8(C) 65.1(Ca)	10.5(Ca) 88.3(C)
A4	λ	-18.3(3)	48.0(5)	-62.5(6)	44.8(6)	-14.7(4)	21.4(C) 69.6(Ca)	3.4(Ca) 90.0(C)
A5	λ	-3.4(5)	33.8(12)	-56.8(14)	47.9(12)	-20.1(7)	11.6(C') 60.1(Ca)	15.5(Ca) 83.3(C')
A5′	δ	-3.4(5)	-27.2(14)	50.9(17)	-49.7(15)	30.8(10)	2.7(C') 61.7(N)	22.0(N) 82.1(C')
A6	λ	15.0(4)	-44.1(6)	57.6(7)	-43.4(6)	16.2(4)	22.1(C') 65.7(Ca)	1.0(Ca) 83.2(C')

Diether Rings

	Ring Type	O'-Ca-O-C	Ca-O-C-C'	O-C-C'-O'	C-C'-O'-Ca	C'-O'-Ca-O	ΔC_s,min ΔC_s,max	ΔC_2,min ΔC_2,max
E1	δ	18.8(4)	-48.1(6)	59.9(6)	-44.1(6)	14.3(4)	19.7(C) 69.3(Ca)	4.3(Ca) 88.4(C)
E2	δ	14.1(4)	-43.3(6)	58.8(6)	-47.8(6)	19.2(4)	18.7(C') 68.6(Ca)	4.8(Ca) 87.4(C')
E3	λ	-12.2(7)	40.6(11)	-54.5(10)	45.8(8)	-19.4(5)	16.2(C') 65.1(Ca)	6.3(Ca) 82.6(C')

(a) Chelate ring nomenclature is described in Figure 4.2(b). Rings within each series are numbered with increasing oxygen number.
(b) Torsion angles are given in degrees. Estimated standard deviations in the least significant digits are given in parentheses.
(c) The bridge types are schematically depicted in Figure 4.2(a). Type 0 implies no interaction.
(d) The symmetry unique atom of the summation is given in parentheses.

torsion angles of interest for five-membered rings of C_s and C_2 symmetry (envelope and half-chair conformers, respectively); the +/- signs refer to the signs of the torsion angles. The symmetry-unique atom is the atom of the ring through which the mirror plane or two-fold axis passes. If a ring has perfect C_s symmetry, ΔC_s must

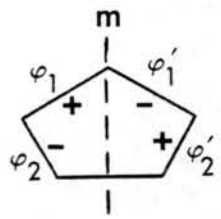

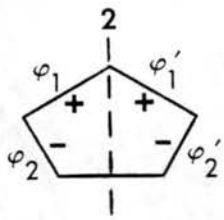

$$\Delta C_s = \{[\sum_{i=1}^{2} (\phi_i + \phi_i')^2]/m\}^{1/2} \qquad \Delta C_2 = \{[\sum_{i=1}^{2} (\phi_i - \phi_i')^2]/m\}^{1/2}$$

equal zero. The greater the deviation of ΔC_s from zero, the greater the distortion of the chelate ring from ideal C_s symmetry. The quantity ΔC_2 similarly represents the deviation of a ring from ideal C_2 symmetry. Any atom in the chelate ring may be taken to be the symmetry-unique atom (through which the imagined symmetry element passes) for purposes of such summations.

In polyamino-polycarboxylate complexes, the minimum asymmetry parameter calculated for ethylenediamine chelate rings usually is ΔC_2, with the metal ion as the symmetry-unique atom. The value of this ΔC_2 parameter is typically less than 10°.[45] In **2**, the amino-ether and diether chelate rings behave similarly. The minimum asymmetry parameters for these ring types in **2** always correspond to a half-chair

conformation associated with the metal atom; the value of this parameter ranges from 1.0-10.6°, discluding rings the disorded rings, A5 and A5' (See Table 4.3). The ether oxygen atoms in the diether rings of complexes **a** and **b** each utilize one lone pair to bind to the calcium ion. On the basis of the observed ring conformations, the lone pairs not used in coordination must be on opposite sides of the ring plane. The ring conformations may be classified as δ or λ, based on the sign of the N-C-C'-O torsion angle (see Table 4.3). The amino-ether ring A5 (complex **c**) exhibits a δ/λ disorder, which may be a consequence of the accumulated strain created by intermolecular interactions involving complex **c** (see above).

Glycinate chelate rings in polyamino-polycarboxylate complexes exhibit a wider range of preferred conformations than do ethylenediamine rings, due to the planarity of the carboxylate group. Both half-chair and envelope conformers occur among the glycinate rings, and a variety of symmetry-unique atoms are observed. A carbon or an oxygen atom is usually the symmetry-unique atom for the half-chair conformation, while a nitrogen atom or the metal ion is usually the symmetry-unique atom for the envelope conformation. The range and distribution of values for the minimum asymmetry parameters is similar to that seen for the ethylenediamine rings. In **2**, seven of the twelve glycinate chelate rings exhibit envelope conformations; the symmetry-unique atoms are either N or C' (see Table 4.3).

Among the five half-chair conformers, the oxygen atom is always the symmetry-unique atom.

In addition to the conformational parameters of the individual rings, inter-ring torsion angles, which describe the orientation of the rings with respect to each other, are listed in Table 4.4. N1, O1, and O3 of the N1 iminodiacetate end of the $EGTA^{4-}$ ligand are approximately coplanar with the metal ion (see Figure 4.1(a)). In contrast, the metal ion does not lie near the plane formed by N2, O7, and O9. The "meridional" and "bent" arrangements of these chelating ligand terminii are reflected in the inter-ring torsion angles. For the meridional arrangement of the iminodiacetate unit, the torsion angles about the N-C bonds of the glycinate ring with respect to the amino-ether carbon atom both approach 90°; the torsion angles about the N-C bond of the glycinate ring with respect to the opposite glycinate carbon atom both approach 180°. As expected, the two torsion angles with respect to the amino-ether carbon atom, for the bent arrangement of the iminodiacetate unit, take on values approaching 90° and 180°. Likewise, the torsion angles with respect to the glycinate ring carbon atom now also approach values of 90° and 180° (see Table 4.4).

The orientation of the N-O(ether)-O(ether)-N belt can also be assessed by inter-ring torsion angles. A low level of torsional strain typical in cryptand and crown ether complexes is characterized by inter-ring torsion angles

Table 4.4 Inter-ring Torsion Angles[a] for $Ca[Ca(EGTA)]\cdot(22/3)H_2O$

	complex a	complex b	complex c[b]
C2-C1-N1-C5	72.3(6)	75.3(6)	-82.4(9)
C4-C3-N1-C5	-93.5(6)	-93.5(6)	84.7(8)
C12-C11-N2-C10	-165.2(5)	-164.4(4)	160.4(6)
C14-C13-N2-C10	89.0(5)	96.8(6)	-84.4(6)
C2-C1-N1-C3	-162.3(5)	-160.1(5)	154.9(7)
C4-C3-N1-C1	141.5(5)	142.1(5)	-152.1(6)
C12-C11-N2-C13	70.5(6)	71.1(6)	-74.0(7)
C14-C13-N2-C11	-146.0(5)	-138.4(5)	150.1(5)
C1-N1-C5-C6	-161.9(5)	-163.4(5)	152(1)/91(1)
C3-N1-C5-C6	71.5(7)	71.6(6)	-86(1)/-146(1)
C11-N2-C10-C9	162.4(5)	163.8(5)	-161.7(6)
C13-N2-C10-C9	-73.6(6)	-72.6(6)	73.2(7)
C5-C6-O5-C7	90.2(6)	93.8(6)	-103(1)/-171(1)
C10-C9-O6-C8	-174.3(5)	-174.2(5)	175.5(6)
C6-O5-C7-C8	-177.5(5)	-174.7(5)	-171(1)/159(1)
C9-O6-C8-C7	174.1(5)	171.3(5)	-172.4(7)

(a) Torsion angles are given in degrees. Estimated standard deviations in the least significant digits are given in parentheses.

(b) In cases where two torsion angles are given, the first one corresponds to the torsion angle involving C34 while the second one corresponds to the torsion angle involving C34'.

which approach 180°.[97] Three of the torsion angles which describe the belt are near 180°, while the remaining torsion angle is near 90°. This deviation from ideality is necessitated by the constraints of wrapping the $EGTA^{4-}$ ligand about the calcium ion.

Structure of $Sr[Ca(EGTA)]\cdot H_2O$(3)

The structure of 3 is much simpler than that of 2; there is only one formula unit per asymmetric unit. As in the case of 2, the counterion interacts extensively with the complex anion. These interactions, however, do not influence the arrangement of the $EGTA^{4-}$ ligand about the calcium ion; a thermal ellipsoid plot of 3 is indistinguishable from a thermal ellipsoid plot of one of the complex anions in 2. Oxygen atoms from bridging carboxylate groups contribute five of the nine ligand atoms surrounding the strontium counterion. The remaining positions are occupied by water molecules. Two of the four carboxylate groups of the $[Ca(EGTA)]^{2-}$ anion are involved in bridging interactions. One carboxylate group (O9/O10) functions simultaneously as a type 1 and a type 2 donor to two symmetry-related strontium ions (see Figure 4.4(a)). The other bridging carboxylate group (O7/O8) acts solely as a type 1 donor; this type 1 bridge is quite asymmetric (Sr-O8 = 2.613(3) Å, Sr-O7b = 3.215(3) Å). The nine ligand atoms about strontium occupy the vertices of a slightly twisted tri-capped trigonal prism. The triangular faces of

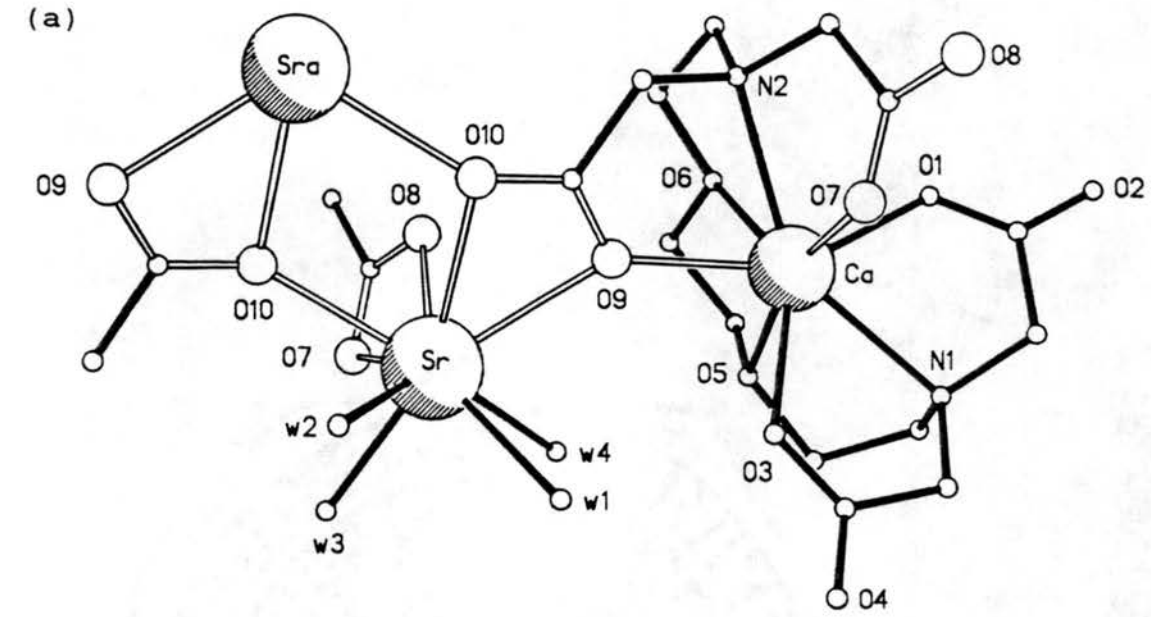

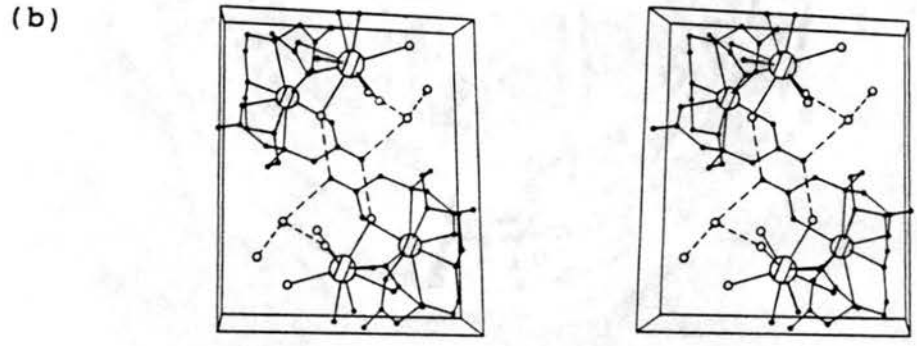

Figure 4.4 (a) Ball and stick plot depicting all the unique interionic interactions in the lattice of $Sr[Ca(EGTA)]\cdot 6H_2O$ (3). Conventions regarding ionic radii of the atoms are the same as in Figure 4.3(a). (b) Unit cell of 3 viewed along a.

the prism are composed of two sets of atoms: O10, O8b, and O10a, and w3, w1, and w4. The prism is capped by atoms O9, w2, and O7b (see Figure 4.4(a)).

3, like 2, is held together in the solid state by carboxylate bridges between metal ions and by hydrogen bonding. Two occluded water molecules participate in hydrogen bonding with carboxylate groups and coordinated water molecules to link the polymeric cation/anion chains, which are propagated parallel to the a-axis (see Figure 4.4(b)). As in 2, all carboxylate oxygen atoms are involved in at least one interaction with a metal ion or a water molecule.

Except for the long bond to O7b (see above), the bridging bond lengths to strontium range from 2.588(4) Å to 2.703(3) Å (see Table 4.5). Despite the fact that O10 is involved in both a type 1 and a type 2 bridge, the type 2 bridge exhibits the shortest Sr-O(carboxylate) distance (2.588(3) Å). The average Sr-O(carboxylate) distance seen in $Mg[Sr(EGTA)(OH_2)]\cdot 7H_2O$ is 2.67(6) Å (see Chapter 5), with a range of 2.588(4)-2.722(5) Å. This range agrees well with the range of Sr-O(carboxylate) distances seen for 3 (discluding the very long bond to O7b. The water molecules are bound more tightly, on average, than the bridging carboxylate groups ($Sr-OH_2$(ave) = 2.60(5) Å, Sr-O(carb, ave) = 2.65(6) Å).

The different bridging interactions in 3 were not observed to influence the mean metal-ligand bonding

Table 4.5 Metal-Ligand Distances (Å) and Angles (deg)[a] for $Sr[Ca(EGTA)]\cdot 6H_2O$

(a) Complex Ion

Ca-N1	2.599(4)
Ca-N2	2.586(3)
Ca-O1	2.387(3)
Ca-O3	2.377(3)
Ca-O5	2.493(3)
Ca-O6	2.528(3)
Ca-O7	2.373(3)
Ca-O9	2.369(4)
N1-Ca-N2	147.0(1)
N1-Ca-O1	66.0(1)
N2-Ca-O1	86.5(1)
N1-Ca-O3	66.8(1)
N2-Ca-O3	132.3(1)
O1-Ca-O3	131.7(1)
N1-Ca-O5	70.6(1)
N2-Ca-O5	131.3(1)
O1-Ca-O5	92.5(1)
O3-Ca-O5	81.3(1)
N1-Ca-O6	119.3(1)
N2-Ca-O6	67.1(1)
O1-Ca-O6	76.0(1)
O3-Ca-O6	138.7(1)
O5-Ca-O6	65.5(1)
N1-Ca-O7	94.7(1)
N2-Ca-O7	66.0(1)
O1-Ca-O7	89.9(1)
O3-Ca-O7	84.2(1)
O5-Ca-O7	162.5(1)
O6-Ca-O7	131.7(1)
N1-Ca-O9	143.3(1)
N2-Ca-O9	68.5(1)
O1-Ca-O9	148.3(1)
O3-Ca-O9	79.9(1)
O5-Ca-O9	90.1(1)
O6-Ca-O9	76.5(1)
O7-Ca-O9	96.9(1)

(b) Counterion

Sr-O9	2.697(3)
Sr-O10	2.703(3)
Sr-w1	2.608(5)
Sr-w2	2.653(3)
Sr-w3	2.526(3)
Sr-w4	2.595(3)
Sr-O7a	3.215(3)
Sr-O8a	2.613(3)
Sr-O10a	2.588(4)
O9-Sr-O10	48.1(1)
O9-Sr-w1	74.9(1)
O10-Sr-w1	99.9(1)
O9-Sr-w2	113.1(1)
O10-Sr-w2	84.4(1)
w1-Sr-w2	70.4(1)
O9-Sr-w3	153.3(1)
O10-Sr-w3	157.9(1)
w1-Sr-w3	95.1(1)
w2-Sr-w3	85.5(1)
O9-Sr-w4	74.9(1)
O10-Sr-w4	122.0(1)
w1-Sr-w4	70.4(1)
w2-Sr-w4	135.7(1)
w3-Sr-w4	78.4(1)
O9-Sr-O7a	112.0(1)
O10-Sr-O7a	117.4(1)
w1-Sr-O7a	135.6(1)
w2-Sr-O7a	132.9(1)
w3-Sr-O7a	58.3(1)
w4-Sr-O7a	69.7(1)
O9-Sr-O8a	76.8(1)
O10-Sr-O8a	75.2(1)
w1-Sr-O8a	145.1(1)
w2-Sr-O8a	141.1(1)
w3-Sr-O8a	101.1(1)
w4-Sr-O8a	82.9(1)
O7a-Sr-O8a	43.4(1)
O9-Sr-O10a	117.5(1)
O10-Sr-O10a	72.1(1)
w1-Sr-O10a	141.1(1)
w2-Sr-O10a	71.0(1)
w3-Sr-O10a	86.0(1)
w4-Sr-O10a	146.6(1)
O7a-Sr-O10a	77.0(1)
O8a-Sr-O10a	71.3(1)

(c) Interionic Angles

Ca-O7-Sra	158.8(1)
C12-O7-Sra	80.2(2)
C12-O8-Sra	108.6(3)
Ca-O9-Sr	143.7(1)
Sr-O9-C14	94.6(3)
Sr-O10-C14	94.5(2)
Sr-O10-Srb	107.9(1)
C14-O10-Srb	148.2(3)

(a) Estimated standard deviations in the least significant digits are given in parentheses.

parameters (the comparative data are summarized below).

	2	3
Ca-N(ave)	2.60(2)	2.592(9)
Ca-O(carb,ave)	2.38(2)	2.377(8)
Ca-O(ether,ave)	2.50(3)	2.51(2)

As implied by the very similar metal-ligand bonding parameters, the chelate ring bonding parameters are also very similar for the two structures (see Table 4.6). Bridging interactions might be expected to exert the most influence on the conformations of the glycinate rings. The δ/λ classifications of all of the individual chelate rings are identical to those assigned in **2** (see Table 4.7). The individual torsion angles and the resultant calculated asymmetry parameters differ slightly between the two structures. It is difficult to attribute these variations to specific differences in the bridging interactions, however. The manner in which the $EGTA^{4-}$ ligand wraps around the calcium ion, as assessed by the inter-ring torsion angles, also differs slightly (see Table 4.8).

There is apparently little variability in how the $EGTA^{4-}$ ligand can wrap around a metal ion (such as calcium, cadmium (see Chapter 6) or manganese (see Chapter 7)) to form an eight-coordinate chelate. This fact may explain the small differences seen between the structures of the two salts of $[Ca(EGTA)]^{2-}$. Greater influence of counterion would be expected in cases where the metal ion has the

Table 4.6 Chelate Ring[a] Bonding Parameters[b] for $Sr[Ca(EGTA)]\cdot 6H_2O$

Glycinate Rings

	C-C'	C'-N	C-O	C-O'	C-C'-N	O-C-O'	C'-C-O	C'-C-O'	Ca-N-C'	Ca-O-C
G1	1.524(6)	1.481(6)	1.256(6)	1.239(6)	111.8(4)	125.9(4)	117.8(4)	116.3(4)	106.1(2)	122.5(3)
G2	1.519(7)	1.471(5)	1.261(6)	1.246(5)	114.2(4)	124.9(4)	118.3(4)	116.8(4)	111.5(3)	125.8(3)
G3	1.524(6)	1.467(6)	1.245(5)	1.262(5)	112.3(3)	125.1(4)	118.7(4)	116.2(4)	105.4(3)	119.4(3)
G4	1.515(6)	1.470(6)	1.259(5)	1.251(6)	115.4(3)	122.5(4)	119.1(4)	118.4(4)	106.2(2)	121.4(3)

Amino-Ether Rings

	C-C'	C-N	C'-O	C-C'-O	C'-C-N	C"-N-C†	C-N-C"	C-N-C†	Ca-N-C	Ca-O-C'
A1	1.507(7)	1.464(5)	1.444(6)	110.2(3)	113.3(4)	112.0(4)	110.0(3)	111.6(3)	105.4(3)	112.3(2)
A2	1.507(6)	1.476(5)	1.414(6)	107.9(4)	112.4(4)	111.2(3)	110.7(3)	112.4(4)	110.6(2)	116.4(2)

Diether Ring

	C-C'	C'-O'	C-O	C'-C-O	C-C'-O'	C'-O'-C†	C"-O-C	Ca-O-C	Ca-O'-C'
E1	1.493(7)	1.419(5)	1.439(5)	108.3(3)	106.7(4)	112.9(4)	113.2(3)	114.3(2)	115.9(3)

(a) Chelate ring nomenclature is described in Figure 4.2(b). Rings within each series are numbered with increasing oxygen number.
(b) Bond lengths are given in Ångstroms and bond angles are given in degrees. Estimated standard deviations in the least significant digits are given in parentheses.

Table 4.7 Chelate Ring[a] Conformational Parameters[b] for $Sr[Ca(EGTA)]\cdot 6H_2O$

Glycinate Rings

	Ring Type	Bridging[c] Interaction	N-Ca-O-C	Ca-O-C-C'	O-C-C'-N	C-C'-N-Ca	C'-N-Ca-O	ΔC_s,min[d] ΔC_s,max	ΔC_2,min ΔC_2,max
G1	δ	0	-24.2(3)	10.1(4)	23.9(5)	-40.1(3)	32.2(2)	5.6(N) 51.4(C)	14.9(C) 61.4(N)
G2	λ	0	9.4(3)	-1.4(5)	-14.1(5)	20.3(4)	-15.1(3)	5.0(N) 23.7(C)	7.7(O) 30.0(N)
G3	δ	1	-32.5(4)	23.3(6)	13.8(6)	-37.4(4)	34.6(2)	10.1(Ca) 56.0(C)	7.6(C) 64.0(Ca)
G4	δ	1,2	-18.8(3)	8.1(5)	18.9(6)	-31.3(4)	24.9(2)	4.5(N) 40.2(C)	11.7(C) 47.9(N)

Amino-Ether Rings

	Ring Type	O-Ca-N-C	Ca-N-C-C'	N-C-C'-O	C-C'-O-Ca	C'-O-Ca-N	ΔC_s,min ΔC_s,max	ΔC_2,min ΔC_2,max
A1	δ	17.5(2)	-47.2(4)	63.1(4)	-41.6(4)	12.8(3)	20.4(C) 66.3(Ca)	5.2(Ca) 88.5(C)
A2	λ	-13.5(3)	42.2(5)	-57.9(5)	44.5(4)	-17.4(3)	19.9(C') 65.1(Ca)	3.2(Ca) 83.8(C')

Diether Ring

	Ring Type	O'-Ca-O-C	Ca-O-C-C'	O-C-C'-O'	C-C'-O'-Ca	C'-O'-Ca-O	ΔC_s,min ΔC_s,max	ΔC_2,min ΔC_2,max
E1	δ	18.9(3)	-48.8(4)	59.9(5)	-43.9(4)	14.7(3)	19.3(C) 69.7(Ca)	4.6(Ca) 88.8(C)

(a) Chelate ring nomenclature is described in Figure 4.2(b). Rings within each series are numbered with increasing oxygen number.
(b) Torsion angles are given in degrees. Estimated standard deviations in the least significant digits are given in parentheses.
(c) The bridge types are schematically depicted in Figure 4.2(a). Type 0 implies no interaction.
(d) The symmetry unique atom of the summation is given in parentheses.

Table 4.8 Inter-ring Torsion Angles[a] for $Sr[Ca(EGTA)]\cdot 6H_2O$

C2-C1-N1-C5	73.4(4)	C4-C3-N1-C5	-97.2(4)
C12-C11-N2-C10	-157.0(4)	C14-C13-N2-C10	89.8(4)
C2-C1-N1-C3	-161.9(3)	C4-C3-N1-C1	139.0(4)
C12-C11-N2-C13	77.3(4)	C14-C13-N2-C11	-145.5(4)
C1-N1-C5-C6	-161.1(4)	C3-N1-C5-C6	74.0(5)
C11-N2-C10-C9	158.6(4)	C13-N2-C10-C9	-76.4(5)
C5-C6-O5-C7	89.7(4)	C10-C9-O6-C8	-177.8(4)
C6-O5-C7-C8	-179.2(4)	C9-O6-C8-C7	178.2(4)

(a) Torsion angles are given in degrees. Estimated standard deviations in the least significant digits are given in parentheses.

potential for a higher coordination number than eight, and where the $EGTA^{4-}$ ligand is able to wrap about the metal ion in a more flexible manner.

Variable Temperature ^{1}H NMR Study of $[Ca(EGTA)]^{2-}$

The proton NMR spectra of $EGTA^{4-}$ and its metal complexes have been described previously.[75,92,93] Based on the splitting patterns observed in the ^{1}H NMR spectrum, qualitative statements about individual bond labilities within a metal chelate in solution can be made.[98,99] Such an analysis, however, requires that the frequency difference between the theoretically inequivalent protons be sufficiently large to observe the predicted splitting patterns.[76] This requirement has created difficulties in interpretation of the 60 MHz room temperature NMR spectrum of $[Ca(EGTA)]^{2-}$.[92] At 200 MHz, however, the same species exhibits a clear AB quartet for the (d) protons, a singlet for the (a) protons and slightly broadened triplets for the (b) and (c) protons (see Figure 4.5).

The presence of an AB pattern for the acetate protons, which has been previously disputed for $[Ca(EGTA)]^{2-}$,[92] implies that inversion at nitrogen is not occurring on the NMR time scale at room temperature. This, in turn, implies that the nitrogen atoms are not labile, since such lability would result in inversion at nitrogen and the exchange of the diastereotopic A and B protons. The observation of only one AB quartet for the acetate protons implies that

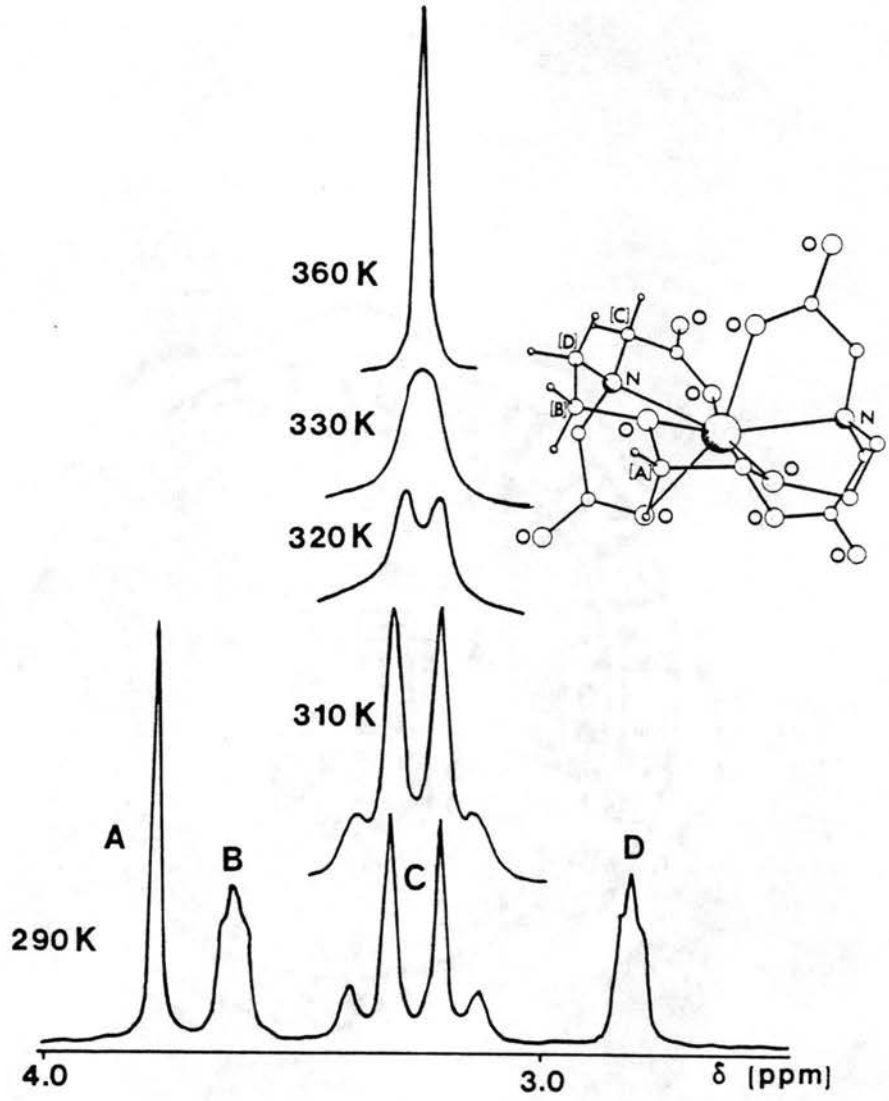

Figure 4.5 Variable temperature ^{1}H NMR spectra of $[Ca(EGTA)]^{2-}$. The assignments of the resonances are indicated on the pictured complex anion.

some metal-ligand bond labilization process that is rapid on the NMR time scale results in a higher average symmetry ($\underline{C}_{2v}$) for the complex in solution than that which is observed in the solid state ($\underline{C}_1$). This may be accomplished through breaking and reforming of Ca-O(carboxylate) bonds, which would permit rapid $\Delta \rightleftharpoons \Lambda$ interconversion between the centrosymmetrically related complex anions. In addition, δ/λ interconversion for individual five-membered chelate rings must be rapid on the NMR time scale.

The acetate AB patterns coalesce to singlets as the temperature is raised (see Figure 4.5). This high temperature behavior can be explained by the onset of additional bond-breaking processes. Such behavior implies that metal-nitrogen bond-breaking, which allows inversion at nitrogen to occur, has become rapid on the NMR time scale.

CHAPTER 5

OTHER ALKALINE EARTH COMPLEXES OF $EGTA^{4-}$

Introduction

The calcium-binding selectivity exhibited by $EGTA^{4-}$ ($K(CaL^{2-}) \tilde{=} 10^6\ K(MgL^{2-})$) is even greater than the selectivity for calcium ion exhibited by the calcium-binding proteins (see Chapter 1 and Table 5.1). Both

Table 5.1 Selected Stability Constants

$\log K\ (M^{2+} + L^{4-} \rightleftharpoons ML^{2-})$

	Mg^{2+}	Ca^{2+}	Sr^{2+}	Ba^{2+}	ref.
$EDTA^{4-}$	8.8	10.7	8.7	7.9	48
$EGTA^{4-}$	5.2	11.0	8.5	8.4	48
Calmodulin Calcium-Binding Domains	3.0	6.0-7.2			100

$EGTA^{4-}$ and the calcium-binding proteins[65] also bind calcium ion preferentially over the strontium and barium ions; $[Sr(EGTA)]^{2-}$ and $[Ba(EGTA)]^{2-}$ exhibit stability constants which are approximately three orders of magnitude lower than that for $[Ca(EGTA)]^{2-}$. The common hexadentate ligand, $EDTA^{4-}$, is also capable of calcium-selective binding. The selectivity of $EDTA^{4-}$ for binding calcium ion

over the two larger alkaline earth metal ions is similar to that of $EGTA^{4-}$, but the selectivity for binding calcium ion over magnesium ion is much smaller than for $EGTA^{4-}$ (less than two orders of magnitude difference in stability constants).

This chapter presents structural results for the magnesium, strontium, and barium ion complexes of $EGTA^{4-}$. The results contained herein, together with the previously described structural results for calcium ion complexes of $EGTA^{4-}$ (see Chapter 4), allow an understanding of the structural features (ligand atom preferences, coordination number preferences, and steric constraints) responsible for the calcium-binding selectivity of $EGTA^{4-}$. The relative enthalpic and entropic contributions to the stability constants for the $[M(EGTA)]^{2-}$ complexes ($M^{2+} = Mg^{2+}$, Ca^{2+}, Sr^{2+}, Ba^{2+}) have been measured,[101-103] but interpretation of such thermodynamic data in the absence of knowledge of the chelates' structures is difficult. This is especially true for magnesium ion, since it is unlikely that the Mg^{2+} ion is able to utilize all of the binding sites of a ligand such as $EGTA^{4-}$. With the aid of these structural results, previous interpretations of the thermodynamic data for the $EGTA^{4-}$ chelates of the alkaline earth metal ions can be re-evaluated.

Structure of a Nine-Coordinate Strontium Chelate of $EGTA^{4-}$, $Mg[Sr(EGTA)(OH_2)]\cdot 7H_2O$ (4)

The coordination number of the strontium ion in the $[Sr(EGTA)]^{2-}$ chelate in **4** is nine. In addition to the eight coordinating atoms from the $EGTA^{4-}$ ligand, a water molecule (w1) is strongly bound to the strontium ion (Sr-w1 = 2.554(5) Å, see Figure 5.1(a)). The ligand atoms about the strontium ion occupy the vertices of a highly distorted tri-capped trigonal prism, with the trigonal faces made up of O7, O6, and O9, and O1, O5, and O3. Stereoviews of the complex anion and the coordination polyhedron are shown in Figures 5.1(b) and (c), respectively. Capping of the trigonal faces is accomplished by the nitrogen atoms of the $EGTA^{4-}$ ligand. The water molecule, w1, caps the rectangular face made up of O9, O7, O3, and O1. As a consequence of the geometric constraints arising from the carboxylate bridges between $[Sr(EGTA)]^{2-}$ and Mg2 (see below and Figure 5.2(a)), one of the water molecules that is already bound to a magnesium counterion is brought into relatively close proximity to the strontium ion (Sr-w2 = 2.970(5) Å). If w2 were considered to be part of the coordination sphere of the Sr^{2+} ion, it would also cap a rectangular face (O6, O5, O7, O3).

Two crystallographically unique magnesium counterions appear in the lattice of **4**. Mg1 occupies a special position of $\bar{1}$ symmetry, while Mg2 resides on a site of 2

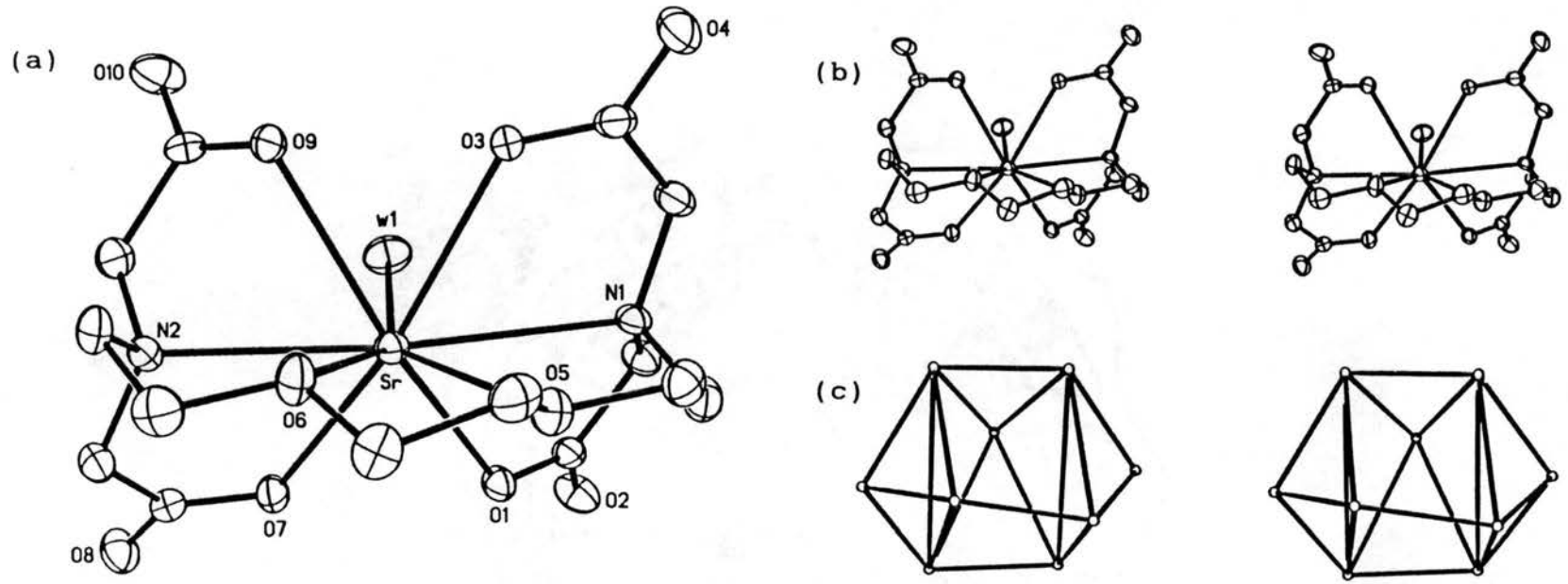

Figure 5.1 (a) A thermal ellipsoid plot (30%) of the $[Sr(EGTA)(OH_2)]^{2-}$ complex anion. For details of the numbering scheme, see Figure 4.1(a). (b) Stereoview of $[Sr(EGTA)(OH_2)]^{2-}$. (c) Stereoview of the coordination polyhedron formed by the ligand atoms about Sr (see text).

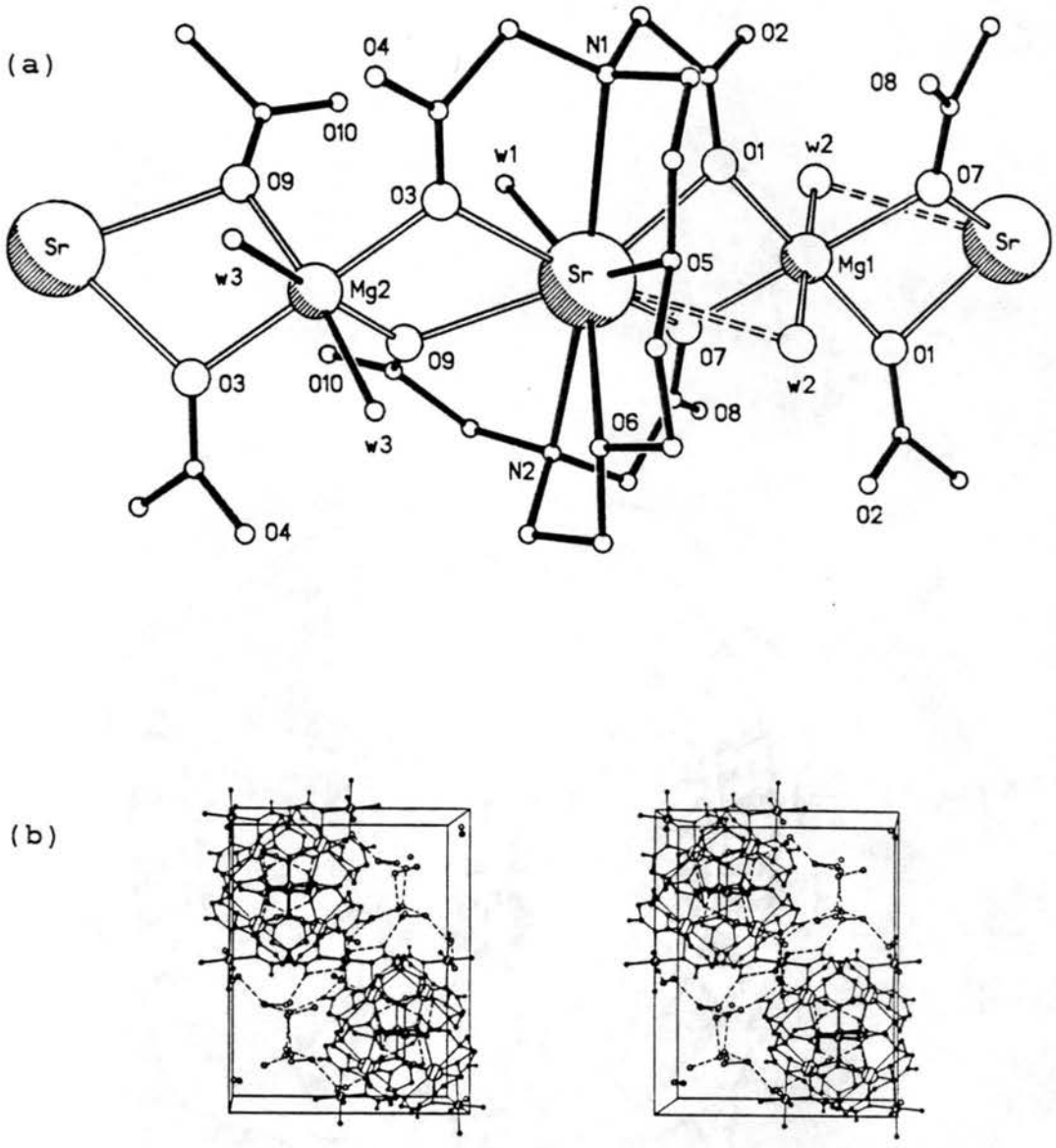

Figure 5.2 (a) Ball and stick plot depicting all the unique interionic interactions in the lattice of $Mg[Sr(EGTA)(OH_2)]\cdot 7H_2O$ (4). Conventions regarding ionic radii of the atoms are described in the caption of Figure 4.3(a). (b) Unit cell of 4 viewed along c.

symmetry. As a result, both Mg1 and Mg2 each have a site occupancy factor of one-half. The coordination sphere for each of these octahedral magnesium ions consists of two water molecules in addition to oxygen atoms of four carboxylate groups from the $[Sr(EGTA)(OH_2)]^{2-}$ complex anions. The water molecules coordinated to Mg1 occupy trans positions in the octahedral coordination sphere, as required by the crystallographic $\bar{1}$ symmetry. For Mg2, the crystallographically required two-fold site symmetry is satisfied by a cis geometry for the two water molecules.

All oxygen atoms that bridge to the magnesium ions in **4** do so via type 3 carboxylate bridges (see Figure 5.2(a)). The strontium chelate engages in two type 3 interactions to each magnesium ion. As a result, every carboxylate group bound to the strontium ion is also bound to a magnesium ion.

The range of distances observed for bridging to magnesium ions in **4** (1.978(4)-2.094(4) Å, Mg-O(carb,ave) = 2.05(5) Å, see Table 5.2) is relatively small in comparison to the corresponding ranges observed for bridging to calcium and strontium counterions in $EGTA^{4-}$ chelates (see Chapter 4). The two unique $Mg-OH_2$ distances in **4** are within the range of those previously observed.[89]

The interionic linkages between the strontium chelate and the magnesium counterions (see Figure 5.2(b)) result in the formation of criss-crossed polymeric cation-complex anion chains, each if which is propagated by the n-glide

Table 5.2 Metal-Ligand Distances (Å) and Angles (deg)[a] for $Mg[Sr(EGTA)(OH_2)]\cdot 7H_2O$

(a) Complex Ion

Sr-N1	2.891(5)	Sr-O6	2.654(5)
Sr-N2	2.802(5)	Sr-O7	2.722(5)
Sr-O1	2.588(4)	Sr-O9	2.691(4)
Sr-O3	2.693(5)	Sr-w1	2.554(5)
Sr-O5	2.605(4)	Sr-w2	2.970(5)

N1-Sr-N2	170.8(2)	O1-Sr-O9	147.6(1)
N1-Sr-O1	57.5(1)	O3-Sr-O9	60.7(1)
N2-Sr-O1	122.0(2)	O5-Sr-O9	119.7(1)
N1-Sr-O3	60.3(1)	O6-Sr-O9	80.8(1)
N2-Sr-O3	118.0(1)	O7-Sr-O9	108.9(1)
O1-Sr-O3	117.3(1)	N1-Sr-w1	76.9(2)
N1-Sr-O5	64.3(1)	N2-Sr-w1	94.0(2)
N2-Sr-O5	124.6(2)	O1-Sr-w1	76.4(1)
O1-Sr-O5	86.8(1)	O3-Sr-w1	83.3(1)
O3-Sr-O5	73.3(1)	O5-Sr-w1	140.8(2)
N1-Sr-O6	125.3(1)	O6-Sr-w1	150.4(2)
N2-Sr-O6	62.8(2)	O7-Sr-w1	77.9(2)
O1-Sr-O6	130.6(1)	O9-Sr-w1	71.3(1)
O3-Sr-O6	91.5(1)	N1-Sr-w2	99.6(1)
O5-Sr-O6	62.9(1)	N2-Sr-w2	87.0(1)
N1-Sr-O7	117.8(1)	O1-Sr-w2	60.7(1)
N2-Sr-O7	60.4(1)	O3-Sr-w2	139.7(1)
O1-Sr-O7	61.7(1)	O5-Sr-w2	66.4(1)
O3-Sr-O7	160.8(1)	O6-Sr-w2	71.4(1)
O5-Sr-O7	124.4(1)	O7-Sr-w2	58.4(1)
O6-Sr-O7	103.0(1)	O9-Sr-w2	144.3(1)
N1-Sr-O9	114.9(1)	w1-Sr-w2	128.8(1)
N2-Sr-O9	60.0(1)		

(b) Counterions

Counterion 1		Counterion 2	
Mg1-O1	1.978(4)	Mg2-O3	2.092(4)
Mg1-O7	2.094(4)	Mg2-O9	2.043(5)
Mg1-w2	2.117(4)	Mg2-w3	2.087(5)

O1-Mg1-O7	84.0(2)	O3-Mg2-O9	82.3(2)
O1-Mg1-w2	87.2(2)	O3-Mg2-w3	90.1(2)
O7-Mg1-w2	82.9(2)	O9-Mg2-w3	85.9(2)

Table 5.2 (continued)

(c) Interionic Angles

Sr-O1-Mg1	100.3(2)
Mg1-O1-C2	131.5(4)
Sr-O3-Mg2	106.6(2)
Mg2-O3-C4	124.6(4)
Sr-O7-Mg1	93.3(2)
Mg1-O7-C12	130.2(4)
Sr-O9-Mg2	108.2(2)
Mg2-O9-C14	136.5(4)
Sr-w2-Mg1	86.1(1)

(a) Estimated standard deviations in the least significant digits are given in parentheses.

parallel to the x-y plane. These chains are linked by an extensive hydrogen-bonding network; all four of the carboxylate oxygen atoms which are not involved in metal ion coordination (O2, O4, O8 and O10) form hydrogen bonds with occluded water molecules or with water molecules coordinated to magnesium ions in adjacent polymeric chains.

Magnesium ion was chosen as the counterion because of a previously observed tendency to remain as a discrete hexaaqua ion rather than form bridges to carboxylate oxygen atoms of metal chelates.[104] As noted, this was not the case in **4** (nor was it the case in **5**, see below).

Of the three types of oxygen donors to the strontium ion in **4**, the water molecule is bound to the strontium ion at the shortest distance (Sr-w1 = 2.554(5) Å). This distance agrees well with previously observed Sr-OH_2 distances.[105] As noted in Chapter 4, the calcium ion exhibits a preference to bind anionic carboxylate oxygen atoms at a shorter distance than neutral ether oxygen atoms in the $EGTA^{4-}$ chelates (Ca-O(ether,ave) - Ca-O(carb,ave) = 0.14 Å). Such a preference is not exhibited by strontium ion. The range of bonding distances observed for the four carboxylate oxygen atoms (2.588(4)-2.722(5) Å) actually encompasses the two Sr-O(ether) oxygen atom bond distances (Sr-O5 = 2.605(4) Å, Sr-O6 = 2.654(5) Å, Sr-O(carb,ave) = 2.67(6) Å, Sr-O(ether,ave) = 2.63(3) Å). The Sr-O(ether) bond distances are within the range of

distances observed in two strontium-crown ether complexes (for nine-coordinate $[Sr(benzo\text{-}18\text{-}crown\text{-}6)(H_2O)_3](ClO_4)_2$,[105] Sr-O(ether) = 2.662(5)-2.723(4) Å, Sr-O(ether,ave) = 2.68(4) Å; for two independent eight-coordinate molecules of $Sr(4'\text{-}acetobenzo\text{-}18\text{-}crown\text{-}6)(ClO_4)_2$,[106] Sr-O(ether) = 2.61(2)-2.78(2) Å, Sr-O(ether,ave) = 2.68(6) Å). The range of Sr-O(carb) distances seen for the monodentate and bidentate carboxylate groups for the nine-coordinate strontium ion in strontium malonate[107] (Sr-O(carb) = 2.512(3)-2.796(2) Å, Sr-O(carb,ave) = 2.64(11)) is even broader than in **4**.

It is difficult to assess to what degree the large range of chemically equivalent bond distances can be attributed to the bridging interactions. A recent review of the literature indicated that magnesium ion exhibits a smaller range of $Mg\text{-}OH_2$ bond distances than does calcium ion.[89] Given this fact, and the high charge to radius ratio of magnesium ion, a magnesium counterion might be expected to perturb the coordination sphere about the metal ion in a chelate more so than other counterions. In the structures of the strontium and calcium salts of the calcium chelate of $EGTA^{4-}$ (see Chapter 4), it did not appear that the variations in the bridging interactions had a large effect on the observed bond distances involving the chelated metal ions. In these structures, the counterions are more compliant than magnesium ion is likely to be; as a result, they are bonded to the oxygen atoms at distances

dictated by the steric constraints of the packing. The structural literature lacks sufficient relevant structural data for the case in which magnesium ion acts as a coordinated counterion to resolve this question.

Of the various cation-complex anion bridges observed in $Ca[Ca(EGTA)]\cdot(22/3)H_2O$(2), the double type 3 bridge most appreciably influenced the metal-ligand distances and chelate ring conformations (see Chapter 4). Double type 3 bridging is all that is observed in the lattice of **4**, and thus no comparison is possible between bridging modes available within the structure. However, one would assume that the metal-ligand distances and chelate ring conformational parameters for **4** might be influenced by these strong bridging interactions, based on the observations for **2**.

Of the four ligand atom types, the amine nitrogen atoms are bound at the longest distances to the strontium ion (Sr-N1 = 2.891(5) Å, Sr-N2 = 2.802(5) Å). These distances are very similar to those in the eight-coordinate strontium complex, $\{[N(CH_2CH_2OH)_3]_2Sr\}(NO_3)_2$, (Sr-N = 2.830(4) Å).[108]

The bonding parameters of the chelate rings in **4** are summarized in Table 5.3. The conformations of the chelate rings have been assessed as before (see Chapter 4) by the summation of various combinations of the torsion angles. The torsion angles and the resultant summations are summarized in Table 5.4. The conformations of the amino-

Table 5.3 Chelate Ring[a] Bonding Parameters[b] for $Mg[Sr(EGTA)(OH_2)]\cdot 7H_2O$

Glycinate Rings

	C-C'	C'-N	C-O	C-O'	C-C'-N	O-C-O'	C'-C-O	C'-C-O'	Sr-N-C'	Sr-O-C
G1	1.508(9)	1.453(9)	1.270(8)	1.256(9)	112.5(6)	124.0(6)	116.6(6)	119.3(6)	109.2(4)	125.2(4)
G2	1.512(10)	1.474(9)	1.242(8)	1.262(9)	114.4(5)	124.7(7)	119.1(6)	116.1(6)	112.6(4)	126.5(4)
G3	1.509(10)	1.476(9)	1.270(8)	1.249(9)	113.1(5)	125.0(6)	116.9(6)	118.0(6)	113.8(4)	124.9(4)
G4	1.528(9)	1.471(9)	1.259(8)	1.230(9)	115.7(6)	127.3(6)	117.2(6)	115.5(6)	103.4(4)	112.3(4)

Amino-Ether Rings

	C-C'	C-N	C'-O	C-C'-O	C'-C-N	C"-N-C[†]	C-N-C"	C-N-C[†]	Sr-N-C	Sr-O-C'
A1	1.501(10)	1.471(9)	1.433(9)	108.7(6)	114.3(6)	111.1(5)	109.5(5)	111.1(5)	103.0(4)	120.2(4)
A2	1.498(10)	1.483(9)	1.448(9)	107.4(6)	112.3(6)	108.9(5)	110.4(5)	110.3(5)	109.7(4)	120.3(4)

Diether Ring

	C-C'	C'-O'	C-O	C'-C-O	C-C'-O'	C'-O'-C[†]	C"-O-C	Sr-O-C	Sr-O'-C'
E1	1.464(11)	1.425(9)	1.445(9)	109.2(6)	108.8(6)	112.3(5)	111.8(5)	116.3(4)	115.6(4)

(a) Chelate ring nomenclature is described in Figure 4.2(b). Rings within each series are numbered with increasing oxygen number.

(b) Bond lengths are given in Ångstroms and bond angles are given in degrees. Estimated standard deviations in the least significant digits are given in parentheses.

Table 5.4 Chelate Ring[a] Conformational Parameters[b] for $Mg[Sr(EGTA)(OH_2)]\cdot 7H_2O$

Glycinate Rings

	Ring Type	Bridging[c] Interaction	N-Sr-O-C	Sr-O-C-C'	O-C-C'-N	C-C'-N-Sr	C'-N-Sr-O	ΔC_s,min[d] ΔC_s,max	ΔC_2,min ΔC_2,max
G1	δ	3	-36.5(5)	31.6(8)	8.6(9)	-35.5(6)	34.1(4)	3.2(Sr)	16.3(C)
								58.3(C)	68.9(Sr)
G2	λ	3	-2.2(5)	18.1(9)	-30.9(9)	27.0(7)	-13.7(4)	4.2(C')	10.3(Sr)
								33.8(Sr)	46.7(C')
G3	δ	3	-1.5(5)	-17.1(8)	35.7(8)	-35.8(7)	19.7(4)	1.8(C')	15.8(O)
								41.3(O)	56.9(C')
G4	λ	3	-45.9(4)	42.3(7)	2.3(9)	-41.1(6)	41.0(4)	3.6(Sr)	28.5(C)
								69.1(C)	85.2(Sr)

Amino-Ether Rings

	Ring Type	O-Sr-N-C	Sr-N-C-C'	N-C-C'-O	C-C'-O-Sr	C'-O-Sr-N	ΔC_s,min ΔC_s,max	ΔC_2,min ΔC_2,max
A1	δ	21.4(4)	-52.1(6)	63.7(8)	-38.2(7)	9.0(4)	14.4(C)	13.2(Sr)
							67.4(Sr)	92.1(C)
A2	δ	18.4(4)	-48.5(6)	59.8(7)	-41.5(7)	12.9(4)	18.2(C)	6.3(Sr)
							67.4(Sr)	87.5(C)

Diether Ring

	Ring Type	O'-Sr-O-C	Sr-O-C-C'	O-C-C'-O'	C-C'-O'-Sr	C'-O'-Sr-O	ΔC_s,min ΔC_s,max	ΔC_2,min ΔC_2,max
E1	λ	-16.3(4)	45.8(7)	-58.8(7)	44.9(7)	-15.7(4)	22.2(C)	.8(Sr)
							68.0(Sr)	85.7(C)

(a) Chelate ring nomenclature is described in Figure 4.2(b). Rings within each series are numbered with increasing oxygen number.
(b) Torsion angles are given in degrees. Estimated standard deviations in the least significant digits are given in parentheses.
(c) The bridge types are schematically depicted in Figure 4.2(a). Type 0 implies no interaction.
(d) The symmetry unique atom of the summation is given in parentheses.

ether rings and diether rings in **4** do not differ appreciably from those of the calcium chelates. The minimum asymmetry parameters for these rings still correspond to half-chair conformations with the metal atoms as the symmetry-unique atoms.

More appreciable conformational differences occur between the strontium and calcium chelates for the glycinate rings. This may, once again, be a consequence of the strong bridging interactions that occur between complex anions and counterions. The minimum asymmetry parameters for two of the four glycinate rings correspond to a mirror plane associated with the metal ion; this conformer was not observed for any of the glycinate rings in the calcium chelates. Additionally, the torsion angles about C-C' for G1 and G2 are unusually large (see Chapter 8).

The inter-ring torsion angles (summarized in Table 5.5) describing the mode of coordination of the glycinate rings for the strontium chelate are nearly identical to those for the calcium chelate. Thus, the iminodiacetate end involving N1 is coordinated in a "meridional" fashion, while the end involving N2 is coordinated in a "bent" fashion. The most drastic inter-ring conformational change occurs in the N-O(ether)-O(ether)-N belt, which now adopts a relatively planar configuration; thus, all the inter-ring torsion angles describing the orientation of the belt are near 180°.

Table 5.5 Inter-ring Torsion Angles[a] for $Mg[Sr(EGTA)(OH_2)]\cdot 7H_2O$

C2-C1-N1-C5	76.7(7)	C4-C3-N1-C5	-88.0(7)
C12-C11-N2-C10	-159.8(6)	C14-C13-N2-C10	76.2(7)
C2-C1-N1-C3	-160.3(5)	C4-C3-N1-C1	149.9(6)
C12-C11-N2-C13	78.9(7)	C14-C13-N2-C11	-162.4(6)
C1-N1-C5-C6	-168.2(6)	C3-N1-C5-C6	68.8(7)
C11-N2-C10-C9	77.8(7)	C13-N2-C10-C9	-161.8(6)
C5-C6-O5-C7	-179.8(6)	C10-C9-O6-C8	177.1(6)
C6-O5-C7-C8	-171.0(6)	C9-O6-C8-C7	-171.8(6)

(a) Torsion angles are given in degrees. Estimated standard deviations in the least significant digits are given in parentheses.

Structure of a Ten-Coordinate Barium Chelate of $EGTA^{4-}$, $Mg[Ba(EGTA)]\cdot(8/3)H_2O\cdot(1/3)(CH_3)_2CO$ (5)

The asymmetric unit of the unit cell contains three unique $[Ba(EGTA)]^{2-}$ complex anions (anion **a**, Ba1; **b**, Ba2, **c**, Ba3); complex anion **a**, containing Ba1, is pictured in Figure 5.3(a). Stereoviews of the complex anion and the coordination polyhedron are shown in Figures 5.3(b) and 5.3(c) respectively. The barium ion in **5** is clearly ten-coordinate, in contrast to the strontium ion in **4**. All eight ligand atoms of each $EGTA^{4-}$ ligand are bound to a barium ion. The two additional ligand atoms, in each case, are provided through bridging interactions with adjacent barium chelates in the lattice (see Figure 5.4(a), and below). The coordination geometry about the barium ions is based on a trigonal prism, similar to that of the strontium chelate. O12 caps the square face that was capped by w1 in the strontium chelate, and the tenth ligand (bridging carboxylate atom O22) caps a second square face (bounded by O6-O5-O1-O7) of the prism. In **4**, a water molecule (w2) was found in the vicinity of this tenth coordination site.

All three of the crystallographically unique magnesium counterions are octahedrally coordinated. The coordination array about each of the magnesium ions resembles that of Mg2 in **4**; a non-crystallographic two-fold axis bisects the w1-Mg1-w2 angle in Figure 5.4(a). Two of the four carboxylate groups of the $EGTA^{4-}$ ligands simultaneously act

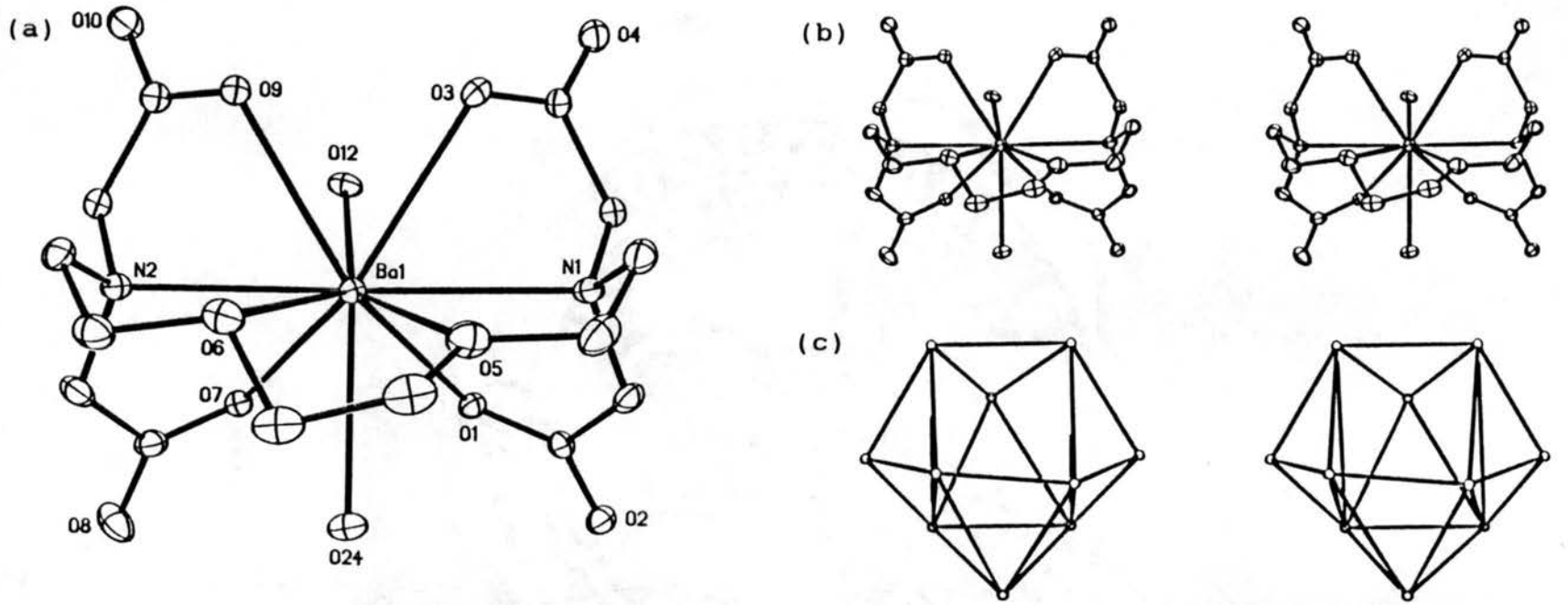

Figure 5.3 (a) A thermal ellipsoid plot (35%) of the ten coordinate $[Ba(EGTA)]^{2-}$ complex anion involving Ba1. For details of the numbering scheme of complexes involving Ba2 and Ba3, see Figure 4.1(a). (b) Stereoview of $[Ba(EGTA)]^{2-}$. (c) Stereoview of the coordination polyhedron formed by the ligand atoms about Ba1 (see text).

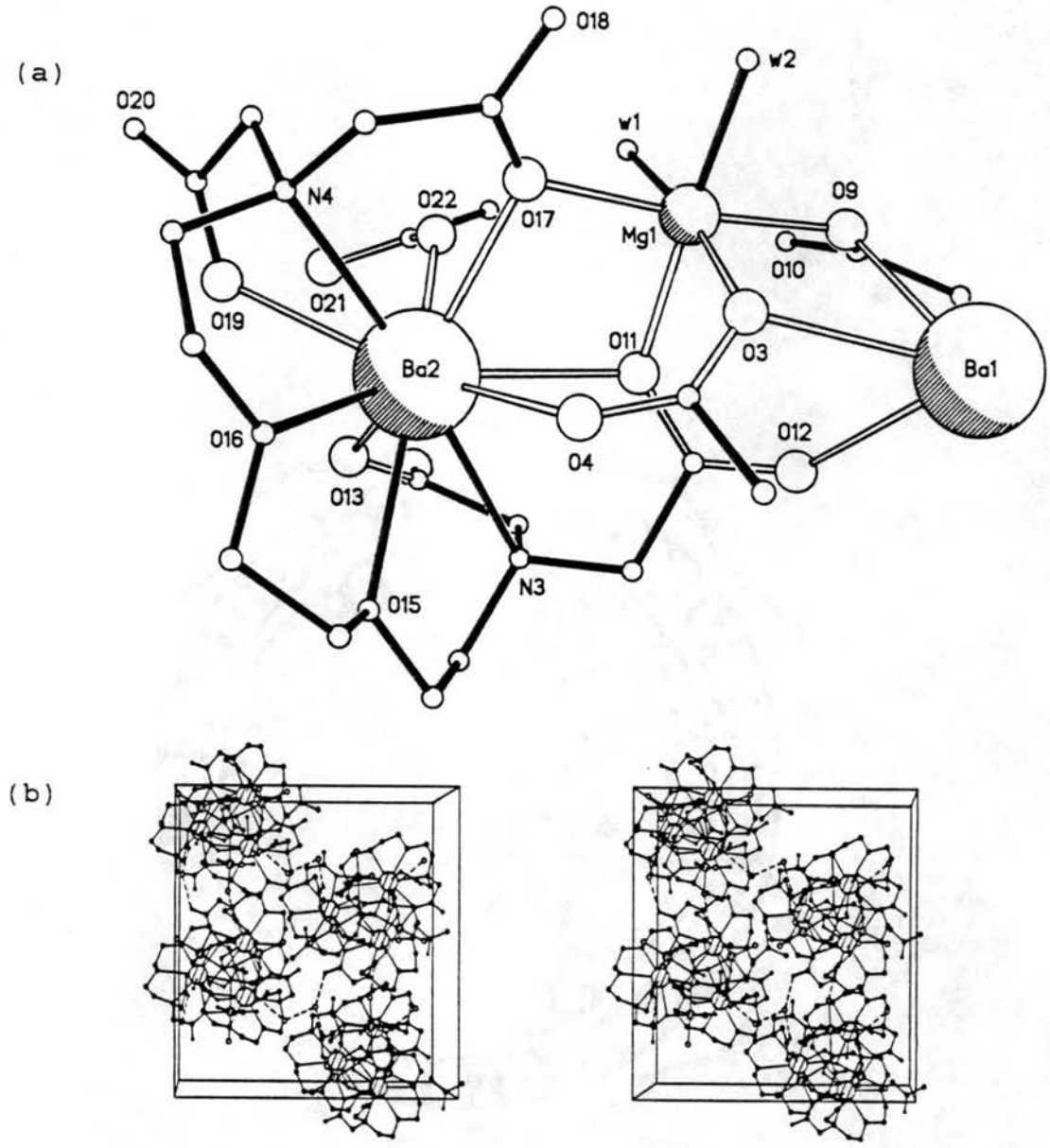

Figure 5.4 (a) Ball and stick plot depicting all the unique interionic interactions in the lattice of $Mg[Ba(EGTA)]\cdot(8/3)H_2O\cdot(1/3)(CH_3)_2CO$ (5). Conventions regarding ionic radii of the atoms are described in the caption of Figure 4.3(a). (b) Unit cell of 5 viewed along b.

as type 2 and type 3 bridging donors to adjacent barium complexes and magnesium counterions, respectively (see, for example, the carboxylate group containing O3 and O4, which is complexed to Ba1 and bridges to Mg1 and Ba2 in Figure 5.4(a)). The remaining two carboxylate groups only bridge in type 3 fashion to the magnesium counterions (see, for example, O17 bridging to Mg1). Metal-ligand bonding parameters for **5** are found in Table 5.6. The Mg-O(carb) bridging distances seen for the three unique magnesium counterions in **5** (2.057(3)-2.171(3) Å, Mg-O(carb,ave) = 2.10(4) Å) are an average of 0.06 Å longer than the Mg-O(carb) bridge distances seen in **4**.

The $[Ba(EGTA)]^{2-}$ complex anions and magnesium counterions link together to form polymeric ribbons parallel to the a-b plane (see Figure 5.2(b)). The sheets are held together in the z direction by hydrogen bonding between the eight occluded water molecules in the asymmetric unit and carboxylate oxygen atoms O14, O10, and O18. The acetone molecule of solvation is also located between these polymeric ribbons.

The Ba-O(carb) bond distances do not seem to be a function of the intra- or interchelate nature of the metal-oxygen bond. The range of intrachelate distances seen (Ba-O(carb) = 2.756(3)-2.844(3) Å, Ba-O(carb, ave) = 2.80(3) Å) is very similar to the range of interchelate distances seen (Ba-O(carb) = 2.799(3)-2.868(3) Å, Ba-O(carb, ave) = 2.83(2) Å). Surprisingly, the carboxylate groups that are

Table 5.6 Metal-Ligand Distances (Å) and Angles (deg)[a] for $Mg[Ba(EGTA)]\cdot(8/3)H_2O\cdot(1/3)(CH_3)_2CO$

(a) Complex Ions

Complex a		Complex b		Complex c	
Ba1-N1	2.863(4)	Ba2-N3	2.924(4)	Ba3-N5	2.876(4)
Ba1-N2	2.888(4)	Ba2-N4	2.935(4)	Ba3-N6	2.876(4)
Ba1-O1	2.783(3)	Ba2-O4	2.815(3)	Ba3-O14	2.814(3)
Ba1-O3	2.840(3)	Ba2-O11	2.827(3)	Ba3-O21	2.844(3)
Ba1-O5	2.807(3)	Ba2-O13	2.811(3)	Ba3-O23	2.809(3)
Ba1-O6	2.963(3)	Ba2-O15	2.832(3)	Ba3-O25	2.867(3)
Ba1-O7	2.756(3)	Ba2-O16	2.803(3)	Ba3-O26	2.790(3)
Ba1-O9	2.815(3)	Ba2-O17	2.759(3)	Ba3-O27	2.776(3)
Ba1-O12	2.839(3)	Ba2-O19	2.822(3)	Ba3-O29	2.804(3)
Ba1-O24a	2.839(3)	Ba2-O22	2.868(3)	Ba3-O2a	2.799(3)
N1-Ba1-N2	174.4(1)	N3-Ba2-N4	176.1(1)	N5-Ba3-N6	178.0(1)
N1-Ba1-O1	58.8(1)	N3-Ba2-O4	86.0(1)	N5-Ba3-O14	84.9(1)
N2-Ba1-O1	126.2(1)	N4-Ba2-O4	94.6(1)	N6-Ba3-O14	94.5(1)
N1-Ba1-O3	57.8(1)	N3-Ba2-O11	57.5(1)	N5-Ba3-O21	58.1(1)
N2-Ba1-O3	121.1(1)	N4-Ba2-O11	126.2(1)	N6-Ba3-O21	123.3(1)
O1-Ba1-O3	98.1(1)	O4-Ba2-O11	63.6(1)	O14-Ba3-O21	64.2(1)
N1-Ba1-O5	59.0(1)	N3-Ba2-O13	57.0(1)	N5-Ba3-O23	58.6(1)
N2-Ba1-O5	115.9(1)	N4-Ba2-O13	122.1(1)	N6-Ba3-O23	121.7(1)
O1-Ba1-O5	101.0(1)	O4-Ba2-O13	143.0(1)	O14-Ba3-O23	142.9(1)
O3-Ba1-O5	85.9(1)	O11-Ba2-O13	94.6(1)	O21-Ba3-O23	98.0(1)
N1-Ba1-O6	114.9(1)	N3-Ba2-O15	59.5(1)	N5-Ba3-O25	61.8(1)
N2-Ba1-O6	59.9(1)	N4-Ba2-O15	116.8(1)	N6-Ba3-O25	116.2(1)
O1-Ba1-O6	140.5(1)	O4-Ba2-O15	77.1(1)	O14-Ba3-O25	74.7(1)
O3-Ba1-O6	110.4(1)	O11-Ba2-O15	105.7(1)	O21-Ba3-O25	107.8(1)
O5-Ba1-O6	56.2(1)	O13-Ba2-O15	81.2(1)	O23-Ba3-O25	81.4(1)
N1-Ba1-O7	126.0(1)	N3-Ba2-O16	117.7(1)	N5-Ba3-O26	119.6(1)
N2-Ba1-O7	59.0(1)	N4-Ba2-O16	58.8(1)	N6-Ba3-O26	58.3(1)
O1-Ba1-O7	67.2(1)	O4-Ba2-O16	77.4(1)	O14-Ba3-O26	75.9(1)
O3-Ba1-O7	136.6(1)	O11-Ba2-O16	140.6(1)	O21-Ba3-O26	140.0(1)
O5-Ba1-O7	135.7(1)	O13-Ba2-O16	115.4(1)	O23-Ba3-O26	114.3(1)
O6-Ba1-O7	105.0(1)	O15-Ba2-O16	58.2(1)	O25-Ba3-O26	58.0(1)

Table 5.6 (continued)

N1-Ba1-O9	120.6(1)	N3-Ba2-O17	124.6(1)	N5-Ba3-O27	122.9(1)
N2-Ba1-O9	58.1(1)	N4-Ba2-O17	59.0(1)	N6-Ba3-O27	58.4(1)
O1-Ba1-O9	138.1(1)	O4-Ba2-O17	65.9(1)	O14-Ba3-O27	64.7(1)
O3-Ba1-O9	63.0(1)	O11-Ba2-O17	67.2(1)	O21-Ba3-O27	65.1(1)
O5-Ba1-O9	113.6(1)	O13-Ba2-O17	135.5(1)	O23-Ba3-O27	139.7(1)
O6-Ba1-O9	80.7(1)	O15-Ba2-O17	141.6(1)	O25-Ba3-O27	137.6(1)
O7-Ba1-O9	99.9(1)	O16-Ba2-O17	102.1(1)	O26-Ba3-O27	99.2(1)
N1-Ba1-O12	95.1(1)	N3-Ba2-O19	121.3(1)	N5-Ba3-O29	122.3(1)
N2-Ba1-O12	89.0(1)	N4-Ba2-O19	57.6(1)	N6-Ba3-O29	58.0(1)
O1-Ba1-O12	74.5(1)	O4-Ba2-O19	151.7(1)	O14-Ba3-O29	151.7(1)
O3-Ba1-O12	65.5(1)	O11-Ba2-O19	135.1(1)	O21-Ba3-O29	134.3(1)
O5-Ba1-O12	149.6(1)	O13-Ba2-O19	64.5(1)	O23-Ba3-O29	63.7(1)
O6-Ba1-O12	142.1(1)	O15-Ba2-O19	109.1(1)	O25-Ba3-O29	109.8(1)
O7-Ba1-O12	71.2(1)	O16-Ba2-O19	82.9(1)	O26-Ba3-O29	83.1(1)
O9-Ba1-O12	63.6(1)	O17-Ba2-O19	99.4(1)	O27-Ba3-O29	101.1(1)
N1-Ba1-O24a	90.9(1)	N3-Ba2-O22	94.4(1)	N5-Ba3-O2a	95.1(1)
N2-Ba1-O24a	89.6(1)	N4-Ba2-O22	88.3(1)	N6-Ba3-O2a	86.9(1)
O1-Ba1-O24a	64.4(1)	O4-Ba2-O22	127.6(1)	O14-Ba3-O2a	126.8(1)
O3-Ba1-O24a	148.5(1)	O11-Ba2-O22	72.9(1)	O21-Ba3-O2a	71.0(1)
O5-Ba1-O24a	73.0(1)	O13-Ba2-O22	64.3(1)	O23-Ba3-O2a	68.4(1)
O6-Ba1-O24a	77.3(1)	O15-Ba2-O22	145.0(1)	O25-Ba3-O2a	148.9(1)
O7-Ba1-O24a	63.3(1)	O16-Ba2-O22	142.1(1)	O26-Ba3-O2a	141.6(1)
O9-Ba1-O24a	147.2(1)	O17-Ba2-O22	71.5(1)	O27-Ba3-O2a	71.5(1)
O12-Ba1-O24a	127.2(1)	O19-Ba2-O22	62.4(1)	O29-Ba3-O2a	63.4(1)

(b) Counterions

Counterion 1		Counterion 2		Counterion 3	
Mg1-O3	2.058(3)	Mg2-O1	2.171(3)	Mg3-O13	2.057(3)
Mg1-O9	2.101(3)	Mg2-O7	2.111(3)	Mg3-O19	2.083(3)
Mg1-O11	2.154(3)	Mg2-w3	2.080(3)	Mg3-O21	2.119(3)
Mg1-O17	2.118(3)	Mg2-w4	2.083(3)	Mg3-O27	2.085(3)
Mg1-w1	2.075(3)	Mg2-O23a	2.069(3)	Mg3-w5	2.124(3)
Mg1-w2	2.040(3)	Mg2-O29a	2.071(3)	Mg3-w6a	2.085(3)

Table 5.6 (continued)

O3-Mg1-O9	90.6(1)	O1-Mg2-O7	91.4(1)	O13-Mg3-O19	93.0(1)
O3-Mg1-O11	83.6(1)	O1-Mg2-w3	88.9(1)	O13-Mg3-O21	85.5(1)
O9-Mg1-O11	92.2(1)	O7-Mg2-w3	84.7(1)	O19-Mg3-O21	93.8(1)
O3-Mg1-O17	94.0(1)	O1-Mg2-w4	173.2(1)	O13-Mg3-O27	93.4(1)
O9-Mg1-O17	173.6(1)	O7-Mg2-w4	89.2(1)	O19-Mg3-O27	171.7(1)
O11-Mg1-O17	92.7(1)	w3-Mg2-w4	97.9(1)	O21-Mg3-O27	91.9(1)
O3-Mg1-w1	170.5(1)	O1-Mg2-O23a	83.2(1)	O13-Mg3-w5	88.1(1)
O9-Mg1-w1	91.0(1)	O7-Mg2-O23a	94.8(1)	O19-Mg3-w5	86.2(1)
O11-Mg1-w1	86.9(1)	w3-Mg2-O23a	172.0(1)	O21-Mg3-w5	173.6(1)
O17-Mg1-w1	85.2(1)	w4-Mg2-O23a	90.0(1)	O27-Mg3-w5	88.7(1)
O3-Mg1-w2	93.8(1)	O1-Mg2-O29a	89.2(1)	O13-Mg3-w6a	173.0(1)
O9-Mg1-w2	86.7(1)	O7-Mg2-O29a	173.9(1)	O19-Mg3-w6a	90.1(1)
O11-Mg1-w2	177.2(1)	w3-Mg2-O29a	89.2(1)	O21-Mg3-w6a	88.1(1)
O17-Mg1-w2	88.6(1)	w4-Mg2-O29a	90.9(1)	O27-Mg3-w6a	84.1(1)
w1-Mg1-w2	95.7(1)	O23a-Mg2-O29a	91.3(1)	w5-Mg3-w6a	98.3(1)

(c) Interionic Angles

Ba1-O1-Mg2	99.5(1)	Ba2-O11-Mg1	98.5(1)	Mg3-O21-C30	124.0(3)
Mg2-O1-C2	128.7(3)	Mg1-O11-C16	126.4(3)	Ba3-O23-Mg2a	102.4(1)
C2-O2-Ba3a	134.0(3)	Ba2-O13-Mg3	101.7(1)	C32-O23-Mg2a	125.2(3)
Ba1-O3-Mg1	103.3(1)	Mg3-O13-C18	126.7(3)	C32-O24-Ba1a	135.9(3)
Mg1-O3-C4	127.0(3)	Ba2-O17-Mg1	101.5(1)	Ba3-O27-Mg3	102.9(1)
Ba1-O7-Mg2	101.9(1)	Mg1-O17-C26	130.3(3)	Mg3-O27-C40	128.5(3)
Mg2-O7-C12	126.3(3)	Ba2-O19-Mg3	100.7(1)	Ba3-O29-Mg2a	102.5(1)
Ba1-O9-Mg1	103.0(1)	Mg3-O19-C28	127.7(3)	C42-O29-Mg2a	126.3(3)
Mg1-O9-C14	125.0(3)	Ba3-O21-Mg3	99.9(1)		

(a) Estimated standard deviations in the least significant digits are given in parentheses.

engaged in the simultaneous type 2 and type 3 bridging interactions are not bound more weakly to the barium ions (Ba-O(carb) = 2.783(3)-2.844(3) Å, Ba-O(carb, ave) = 2.82(2) Å).

As in the strontium chelate (4), the metal exhibits no distinct preference for either the neutral ether oxygen atoms or the anionic carboxylate oxygen atom donors of the $EGTA^{4-}$ ligand. With the exception of one rather long Ba-O(ether) distance (Ba1-O6 = 2.963(3) Å), the observed range of distances is 2.790(3)-2.867(3) Å (Ba-O(ether, ave) = 2.82(3) Å). A conformational change in the diether ring of complex **a** is associated with the unusually long Ba1-O6 distance (see below). The Ba-O(ether) distances are also quite similar to those in ten-coordinate $[Ba(benzo\text{-}18\text{-}crown\text{-}6)(OH_2)_2](ClO_4)_2$[105] (Ba-O(ether) = 2.802(6)-2.846(5) Å, Ba-O(ether, ave) = 2.82(2) Å). In the reported structure of $Ba[Ba(EDTA)]\cdot 2.5H_2O$,[6] the extremely large variation in chemically equivalent bond lengths makes comparisons of little value. The bridging bond lengths to barium ion in $Ba[Nd(DTPA)(OH_2)]\cdot 2H_2O$[45] range from 2.72 Å to 2.85 Å, while Ba-O(carb, ave) = 2.83(7) Å, a similar range and average to that seen for **5**. The lack of any preference between the two types of oxygen donors may again be due to the strong bridging to the magnesium counterions, which may lengthen the Ba-O(carb) distances.

The amine nitrogen atoms are bound at a slightly longer distance than the oxygen atom donors (Ba-N =

2.863(4)-2.935(4) Å, Ba-N(ave) = 2.89(3) Å). These distances are shorter than those in ten-coordinate $[Ba(222)(OH_2)(SCN)]^+$ [109] (Ba-N = 2.88(1)-3.00(1) Å, Ba-N(ave) = 2.95(5) Å). This may be due to the more flexible nature of the $EGTA^{4-}$ ligand compared to the macrobicyclic cryptand.

The bonding and conformational parameters for the ligands of **5** are found in Tables 5.7 and 5.8. The δ/λ conformations of the individual rings in the three unique $[Ba(EGTA)]^{2-}$ complexes are identical, with one exception. The diether ring of complex **a** exhibits a λ configuration, whereas complexes **b** and **c** exist in δ configurations. At the same time, one of the oxygen atoms in the diether ring of complex **a** is bound at a relatively long distance to the barium ion (Ba-O6 = 2.963(3) Å (see above). Complex **a** is not involved in significantly different hydrogen bonding or bridging interactions than are complexes **b** and **c**. However, a methyl hydrogen atom from the occluded acetone molecule is found to be in van der Waals contact with a hydrogen atom bound to C7 in the diether ring in complex **a** (H7a-H43b = 2.29 Å). The conformational change (and the long Ba1-O6 bond) may be a result of this interaction.

Unusual torsion angles are seen for the diether and amino-ether rings in the barium chelates. The metal ion is no longer consistently the symmetry-unique atom associated with the two-fold axis, as it was for the strontium and calcium chelates. For the amino-ether rings in **5**, the

Table 5.7 Chelate Ring[a] Bonding Parameters[b] for $Mg[Ba(EGTA)]\cdot(8/3)H_2O\cdot(1/3)(CH_3)_2CO$

Glycinate Rings

	C-C'	C'-N	C-O	C-O'	C-C'-N	O-C-O'	C'-C-O	C'-C-O'	Ba-N-C'	Ba-O-C
G1	1.534(6)	1.460(5)	1.267(5)	1.246(5)	114.6(3)	126.2(4)	118.6(3)	115.1(3)	110.0(3)	120.1(2)
G2	1.526(6)	1.459(6)	1.269(6)	1.241(5)	115.5(4)	126.8(4)	117.0(4)	116.1(4)	104.1(2)	137.6(3)
G3	1.522(7)	1.458(6)	1.275(5)	1.254(6)	115.7(4)	125.8(4)	119.1(4)	115.1(4)	110.0(3)	119.3(3)
G4	1.511(6)	1.467(5)	1.270(5)	1.246(5)	115.0(4)	124.3(4)	118.7(4)	117.0(4)	103.3(2)	114.4(3)
G5	1.525(6)	1.461(5)	1.270(5)	1.250(5)	114.7(3)	126.4(4)	118.5(4)	115.0(4)	108.8(2)	135.4(3)
G6	1.531(6)	1.470(5)	1.273(5)	1.243(5)	114.2(3)	127.1(4)	117.4(3)	115.5(4)	106.6(2)	138.8(3)
G7	1.525(7)	1.474(6)	1.259(6)	1.256(6)	114.0(4)	124.3(4)	119.6(4)	116.1(4)	109.0(2)	123.9(3)
G8	1.538(6)	1.475(6)	1.255(5)	1.241(5)	113.7(4)	126.5(4)	117.1(4)	116.4(4)	105.0(2)	121.2(3)
G9	1.533(6)	1.466(5)	1.275(5)	1.245(5)	114.8(3)	125.4(4)	119.0(3)	115.5(3)	112.2(2)	136.8(3)
G10	1.545(6)	1.460(5)	1.270(5)	1.243(5)	116.0(4)	126.7(4)	117.1(3)	116.1(4)	105.5(2)	116.3(2)
G11	1.512(6)	1.474(5)	1.270(5)	1.249(5)	114.2(3)	125.6(4)	119.0(4)	115.4(4)	110.8(2)	121.6(3)
G12	1.519(6)	1.465(5)	1.279(5)	1.259(5)	113.7(4)	125.1(4)	120.8(10)	116.8(4)	102.3(2)	114.6(2)

Amino-Ether Rings

	C-C'	C-N	C'-O	C-C'-O	C'-C-N	C"-N-C†	C-N-C"	C-N-C†	Ba-N-C	Ba-O-C'
A1	1.502(7)	1.472(6)	1.423(6)	109.3(4)	112.4(4)	108.9(4)	111.3(3)	111.2(3)	111.0(3)	123.5(3)
A2	1.515(6)	1.474(6)	1.442(6)	108.8(4)	113.6(3)	109.5(4)	111.3(3)	110.2(3)	112.2(3)	117.1(3)
A3	1.506(7)	1.477(6)	1.406(6)	108.9(4)	112.7(4)	109.4(3)	112.3(3)	109.0(3)	110.5(3)	121.5(3)
A4	1.509(7)	1.471(6)	1.421(6)	109.6(4)	113.4(4)	110.5(4)	111.8(3)	108.6(3)	111.8(3)	124.9(3)
A5	1.514(7)	1.471(6)	1.436(6)	109.2(3)	113.2(4)	108.3(3)	110.5(3)	110.1(3)	110.2(2)	115.2(3)
A6	1.519(6)	1.466(6)	1.441(6)	107.8(4)	112.5(4)	110.7(3)	110.5(3)	110.0(3)	112.2(3)	125.9(3)

Diether Rings

	C-C'	C'-O'	C-O	C'-C-O	C-C'-O'	C'-O'-C†	C"-O-C	Ba-O-C	Ba-O'-C'
E1	1.495(7)	1.447(5)	1.439(6)	109.0(4)	109.6(4)	111.0(3)	112.4(4)	123.6(3)	104.4(3)
E2	1.480(7)	1.448(6)	1.427(6)	109.5(4)	109.0(4)	113.7(4)	111.7(3)	114.4(3)	121.3(3)
E3	1.501(8)	1.410(7)	1.425(6)	108.9(4)	110.6(4)	111.8(4)	111.0(3)	110.3(3)	122.2(3)

(a) Chelate ring nomenclature is described in Figure 4.2(b). Rings within each series are numbered with increasing oxygen number.
(b) Bond lengths are given in Ångstroms and bond angles are given in degrees. Estimated standard deviations in the least significant digits are given in parentheses.

Table 5.8 Chelate Ring[a] Conformational Parameters[b] for $Mg[Ba(EGTA)]\cdot(8/3)H_2O\cdot(1/3)(CH_3)_2CO$

Glycinate Rings

	Ring Type	Bridging[c] Interaction	N-Ba-O-C	Ba-O-C-C'	O-C-C'-N	C-C'-N-Ba	C'-N-Ba-O	ΔC_s,min[d] ΔC_s,max	ΔC_2,min ΔC_2,max
G1	λ	2,3	31.3(3)	-23.2(5)	-13.6(6)	39.7(4)	-34.0(3)	11.8(Ba) 56.5(C)	9.0(C) 64.1(Ba)
G2	λ	2,3	40.9(3)	-30.9(4)	-15.8(5)	50.5(4)	-42.7(2)	13.9(Ba) 72.6(C)	12.7(C) 82.5(Ba)
G3	δ	3	-33.6(3)	30.5(5)	4.6(6)	-33.1(4)	31.7(3)	2.3(Ba) 53.3(C)	18.3(C) 64.5(Ba)
G4	δ	3	-40.3(3)	30.7(5)	16.2(6)	-49.8(4)	42.5(2)	13.6(Ba) 71.8(C)	12.3(C) 81.7(Ba)
G5	λ	2,3	34.0(3)	-26.0(5)	-13.8(6)	42.2(4)	-36.2(2)	11.6(Ba) 60.8(C)	10.4(C) 69.2(Ba)
G6	λ	2,3	39.9(3)	-32.3(4)	-12.1(5)	45.0(4)	-40.1(2)	9.0(Ba) 67.7(C)	14.7(C) 78.7(Ba)
G7	δ	3	-21.5(3)	8.4(6)	25.0(6)	-40.6(4)	30.1(3)	7.8(N) 49.9(C)	17.9(C) 59.8(N)
G8	δ	3	-31.3(3)	16.0(5)	28.1(6)	-51.8(4)	39.1(2)	9.3(N) 66.5(C)	16.8(C) 76.8(N)
G9	λ	2,3	32.5(3)	-27.6(4)	-7.0(5)	35.8(4)	-32.7(2)	5.8(Ba) 54.1(C)	14.8(C) 64.3(Ba)
G10	λ	2,3	39.0(3)	-30.7(4)	-13.1(6)	45.7(4)	-39.7(2)	10.6(Ba) 67.4(C)	13.3(C) 77.6(Ba)
G11	δ	3	-29.3(3)	21.2(5)	13.9(5)	-38.1(4)	32.2(2)	11.7(N) 53.7(C)	8.1(C) 60.4(Ba)
G12	δ	3	-40.0(3)	27.6(5)	21.4(6)	-54.1(4)	44.7(2)	14.7(N) 75.0(C)	10.9(C) 83.2(Ba)

Amino-Ether Rings

	Ring Type		O-Ba-N-C	Ba-N-C-C'	N-C-C'-O	C-C'-O-Ba	C'-O-Ba-N	ΔC_s,min ΔC_s,max	ΔC_2,min ΔC_2,max
A1	λ		-29.1(2)	55.6(4)	-51.7(5)	22.5(5)	3.2(3)	5.4(C) 60.0(O)	21.0(O) 84.2(C)
A2	δ		21.9(2)	-53.6(4)	61.5(5)	-37.3(4)	9.0(3)	12.2(C) 67.9(Ba)	14.7(Ba) 91.5(C)

Table 5.8 (continued)

A3	λ	-21.5(2)	51.1(4)	-59.3(5)	37.3(4)	-9.0(3)	12.6(C) 66.1(Ba)	13.2(Ba) 88.4(C)
A4	δ	23.7(2)	-49.5(4)	51.0(5)	-27.7(5)	2.8(3)	3.0(C) 57.7(Ba)	21.4(Ba) 79.8(C)
A5	λ	-18.3(2)	50.3(4)	-65.0(5)	43.7(4)	-13.9(3)	20.8(C) 70.3(Ba)	5.6(Ba) 92.6(C)
A6	δ	29.4(2)	-54.7(4)	48.7(5)	-20.2(5)	-4.1(3)	7.8(C) 57.8(O)	17.8(O) 81.1(C)

Diether Rings

Ring Type		O'-Ba-O-C	Ba-O-C-C'	O-C-C'-O'	C-C'-O'-Ba	C'-O'-Ba-O	ΔC_s,min ΔC_s,max	ΔC_2,min ΔC_2,max
E1	λ	20.1(3)	5.8(5)	-51.6(5)	68.1(4)	-42.8(3)	28.6(O') 70.3(C)	11.9(O) 93.4(O')
E2	δ	28.1(3)	-56.5(4)	56.0(5)	-30.6(5)	2.5(3)	1.8(C) 65.3(Ba)	25.8(Ba) 89.7(C)
E3	δ	34.5(3)	-60.8(4)	54.4(6)	-20.9(6)	-6.4(3)	10.6(C) 65.8(O')	17.4(O') 90.4(C)

(a) Chelate ring nomenclature is described in Figure 4.2(b). Rings within each series are numbered with increasing oxygen number.
(b) Torsion angles are given in degrees. Estimated standard deviations in the least significant digits are given in parentheses.
(c) The bridge types are schematically depicted in Figure 4.2(a). Type 0 implies no interaction.
(d) The symmetry unique atom of the summation is given in parentheses.

carbon atom bound to the amine nitrogen atom is the symmetry-unique atom of an envelope ring conformation for five out of the six rings. For the one exception, ring A5, the minimum asymmetry parameter was associated with the more usual two-fold axis through the metal ion. Among the diether rings, two of the three rings (E2 and E3) are envelope conformers with a symmetry-unique carbon atom (like the majority of the amino-ether rings). Ring E1, however, is a half-chair conformer with the oxygen atom as the symmetry-unique atom.

All of these conformational irregularities appear to be associated with the fact that one of the ether oxygen atoms in the N-O-O-N belt coordinates to the barium ion through both lone pairs. This can be shown by examining the displacement of the barium ion from the plane containing the ether oxygen atom and the two carbon atoms bound to it. The displacements for rings A1, A4, and A6 (0.34, 0.21, and 0.10 Å, respectively) are quite different than for the rings A2, A3, and A5 (2.29, 1.55, and 2.09 Å, respectively). In addition, the angle the barium-O(ether) vector makes with the normal to the C-O-C plane should ideally be 90° for an ether oxygen atom which is utilizing both lone pairs in coordinating to a metal ion, and should be approximately 125° for an ether oxygen atom which is utilizing only a single lone pair in coordination to a metal ion. Although the angles seen are not ideal, these expectations are largely realized; the angles for the

ether oxygen atoms with small out of plane displacements are 97° (A1), 86° (A4), and 92° (A6), while those for the ether oxygen atoms with large out of plane displacements are 141° (A2), 127° (A3), and 137° (A5).

Examination of the structures of two barium cryptate complexes reveals that "planar" coordination of an ether oxygen atom in an N-O-O-N ring systems is not unusual. For eleven-coordinate $[Ba(322)(OH_2)_2]^{2+}$,[110] the two N-O-O-N ring systems each contain a "planar" ether oxygen atom. In ten-coordinate $[Ba(222)(OH_2)(NCS)]^{+}$,[109] one of the three N-O-O-N belts exhibits a "planar" oxygen atom. Since the cryptate complexes are not involved in interionic interactions, as are the barium chelates in 5, the adoption of a "planar" configuration at oxygen is probably necessary to relieve accumulated strain in the formation of five-membered chelate rings with a large metal ion like barium.

The inter-ring torsion angles (summarized in Table 5.9) indicate that the N-O(ether)-O(ether)-N belt is planar, as in the strontium chelate, thus permitting favorable (180°) torsion angles in the belt. The major difference between the strontium and barium chelates is that the conformations of both iminodiacetate ends of the $EGTA^{4-}$ ligand now can be described as "bent", based on the inter-ring angles.

Stereoviews of the calcium, strontium and barium complex anions are shown together in Figure 5.5. In moving

Table 5.9 Inter-ring Torsion Angles[a] for $Mg[Ba(EGTA)]\cdot(8/3)H_2O\cdot(1/3)(CH_3)_2CO$

	complex a	complex b	complex c
C2-C1-N1-C5	163.2(4)	164.9(4)	159.2(4)
C4-C3-N1-C5	-69.1(5)	-74.3(4)	-73.2(4)
C12-C11-N2-C10	-158.1(4)	-164.7(4)	-163.2(3)
C14-C13-N2-C10	70.2(5)	67.9(5)	65.3(5)
C2-C1-N1-C3	-73.8(5)	-74.0(5)	-80.2(4)
C4-C3-N1-C1	167.9(4)	162.5(4)	165.9(3)
C12-C11-N2-C13	79.9(5)	74.2(5)	74.7(4)
C14-C13-N2-C11	-167.1(2)	-169.1(4)	-172.2(4)
C1-N1-C5-C6	-67.3(5)	-70.6(5)	-74.1(4)
C3-N1-C5-C6	171.1(4)	168.0(3)	166.2(3)
C11-N2-C10-C9	70.2(5)	73.0(5)	69.5(5)
C13-N2-C10-C9	-168.1(4)	-164.8(4)	-167.9(4)
C5-C6-O5-C7	-165.9(4)	177.1(4)	170.1(4)
C10-C9-O6-C8	-157.0(4)	147.0(4)	157.3(4)
C6-O5-C7-C8	-165.8(4)	160.7(4)	170.2(4)
C9-O6-C8-C7	-164.8(4)	154.5(4)	161.5(4)

(a) Torsion angles are given in degrees. Estimated standard deviations in the least significant digits are given in parentheses.

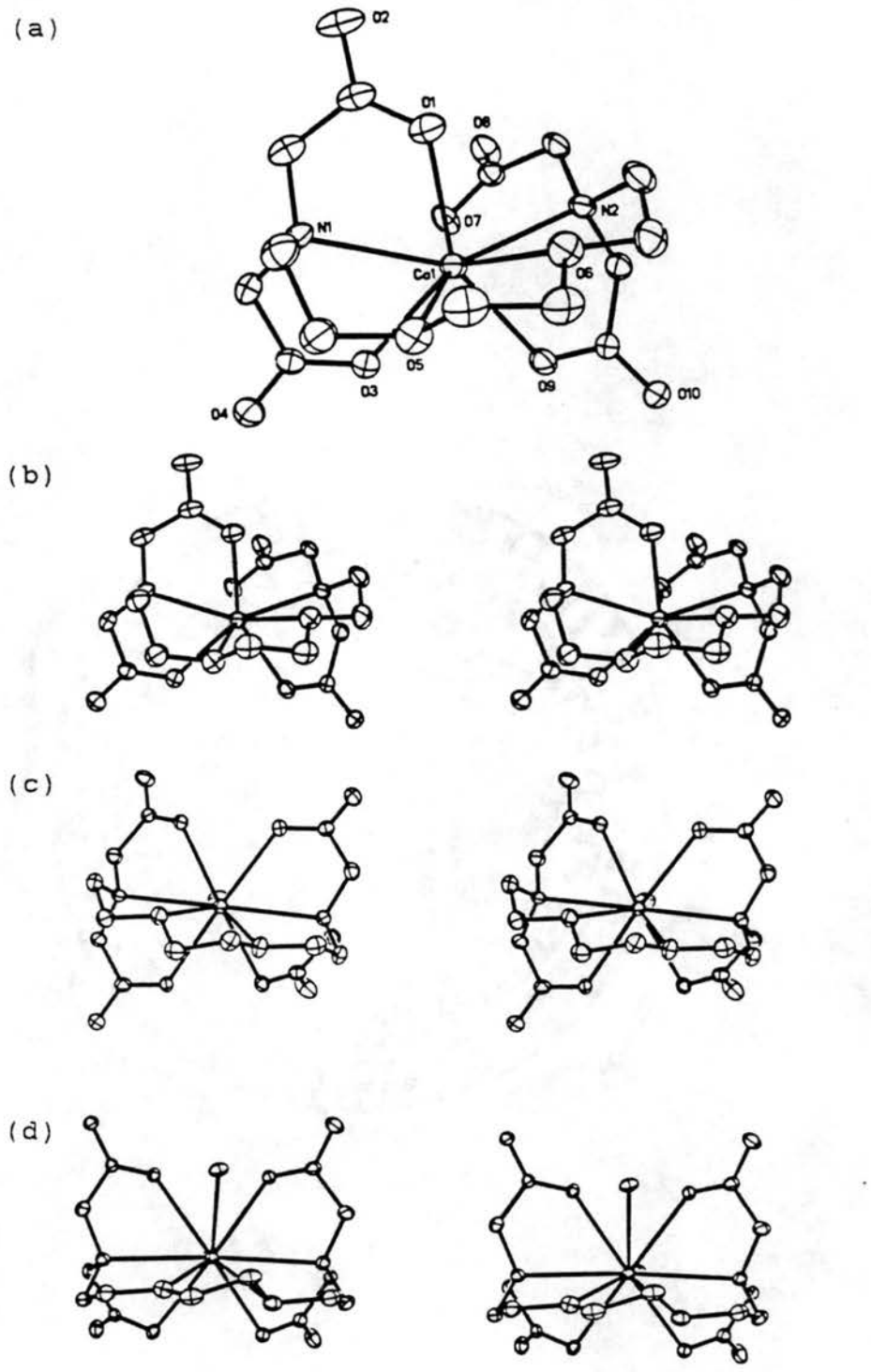

Figure 5.5 (a) Reference complex anion with numbering scheme. (b) Stereoview of $[Ca(EGTA)]^{2-}$. (b) Stereoview of $[Sr(EGTA)(OH_2)]^{2-}$. (c) Stereoview of $[Ba(EGTA)]^{2-}$.

down to strontium ion from calcium ion, enough conformational freedom is obtained to make a "planar" N-O-O-N belt possible. The further increase in size for barium ion is sufficient to allow "bent" conformations for each iminodiacetate end, without creating close intra-ligand contacts.

Structure of a Dinuclear Magnesium Complex of $EGTA^{4-}$, $[Mg_2(EGTA)(OH_2)_6]\cdot 5H_2O$ (6)

Reaction of two equivalents of a magnesium salt with $EDTA^{4-}$ yields a compound in which one magnesium ion exists as the hexaaqua cation and the other magnesium ion forms the seven-coordinate $[Mg(EDTA)(OH_2)]^{2-}$ complex anion.[104] The analogous reaction with $EGTA^{4-}$ instead yields a neutral dinuclear product, in which each end of the $EGTA^{4-}$ ligand acts as a tridentate amino-dicarboxylate ligand (see Figure 5.6(a)). Three water molecules complete the ligand array for the octahedral magnesium ions. The two oxygen atoms of each tridentate $EGTA^{4-}$ terminus occupy cis sites in each of the octahedra. Crystals of $[Mg_2(EGTA)(OH_2)_6],6H_2O$ (3) have also been isolated from a reaction mixture in which the expected stoichiometric product would have been $Rb_2[Mg(EGTA)]$. Thus, crystals of **6** are even obtained from a solution in which the dinuclear species is certainly not the predominant form in solution.

The hydrogen bonding network in the lattice of **6** is extensive, involving all water molecules and carboxylate

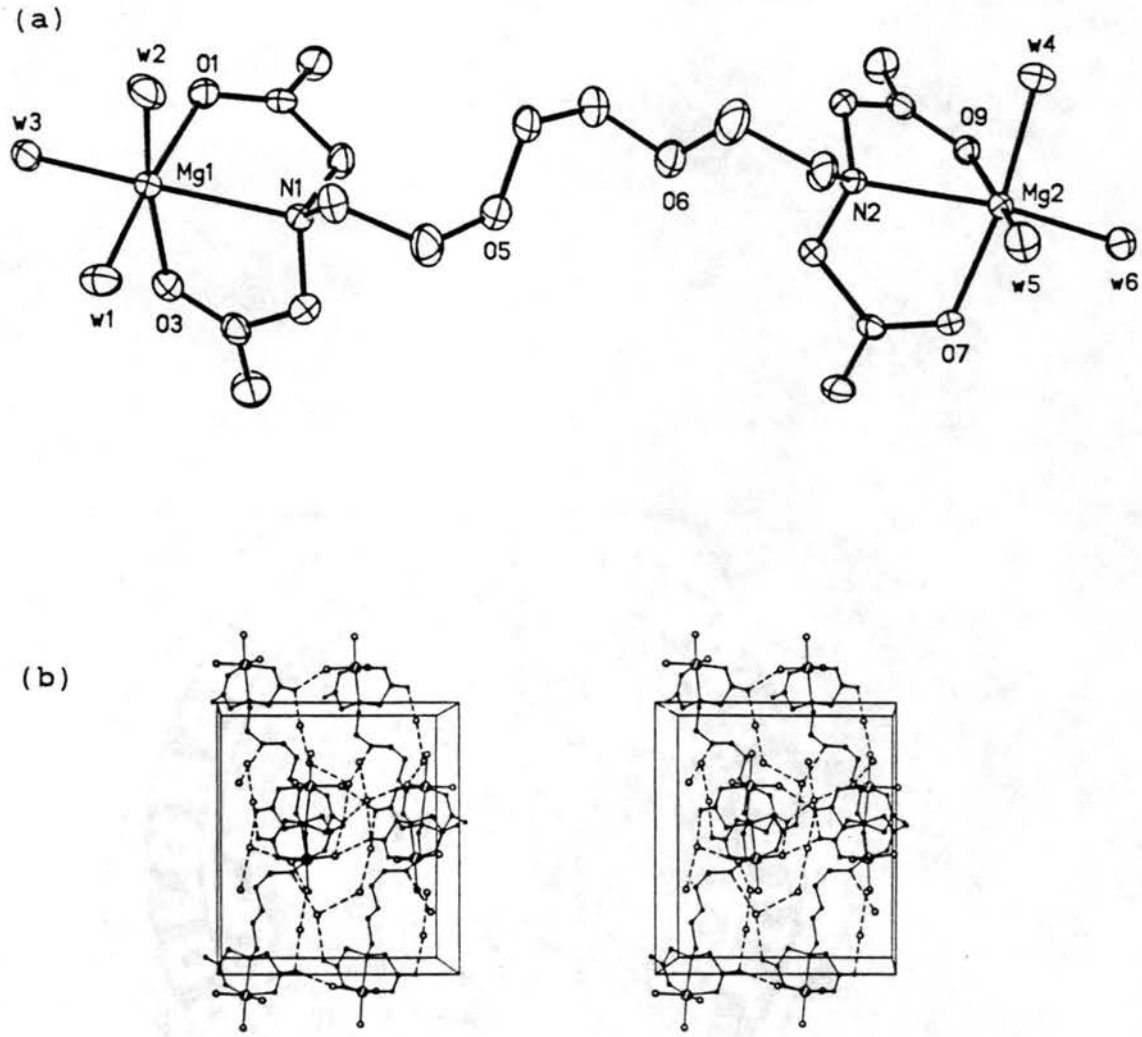

Figure 5.6 (a) A thermal ellipsoid plot (40%) of $[Mg_2(EGTA)(OH_2)_6]$. (b) Unit cell of $[Mg_2(EGTA)(OH_2)_6]\cdot 5H_2O$ viewed along b.

groups bound to the magnesium ion, in addition to the five occluded water molecules. This hydrogen bonding connects the $Mg_2(EGTA)(OH_2)_6$ complexes, which are oriented parallel to the a axis (See Figure 5.6(b)).

The bonding parameters for the magnesium ions (summarized in Table 5.10) are not unusual. The water molecules and the carboxylate oxygen atoms are bound at approximately the same distances (Mg-O(carb,ave) = 2.07(2) Å, $Mg-OH_2$(ave) = 2.05(3) Å), while the amine nitrogen atoms are bound at considerably longer distances (Mg-N(ave) = 2.30(3) Å). In seven-coordinate $[Mg(EDTA)(OH_2)]^{2-}$,[2,3] the single crystallographically unique amine nitrogen atom is bound at yet a longer distance (Mg-N = 2.378(2) Å); two of the carboxylate ligands and the single water molecule are bound at distances (Mg-O(carb) = 2.078(2) Å, $Mg-OH_2$ = 2.060(3) Å) similar to the Mg-O bond distances of **6**.

The bonding and conformational parameters for the chelate rings of **6** are summarized in Table 5.11 and 5.12. The torsion angles O-C-C'-N, C-C'-N-Mg, and C'-N-Mg-O of glycinate rings G1 and G3 are unsusually low (see Chapter 8). This planar configuration must be necessary to maintain octahedral coordination to the small magnesium ion.

Table 5.10 Metal-Ligand Distances (Å) and Angles (deg)[a] for $[Mg_2(EGTA)(OH_2)_6]\cdot 5H_2O$

(a) Complex Ions

Complex a		Complex b	
Mg1-N1	2.318(4)	Mg2-N2	2.281(4)
Mg1-O1	2.057(3)	Mg2-O7	2.047(3)
Mg1-O3	2.076(3)	Mg2-O9	2.092(3)
Mg1-w1	2.043(3)	Mg2-w4	2.095(3)
Mg1-w2	2.054(4)	Mg2-w5	2.061(3)
Mg1-w3	2.020(4)	Mg2-w6	2.025(4)
N1-Mg1-O1	78.7(1)	N2-Mg2-O7	77.8(1)
N1-Mg1-O3	76.2(1)	N2-Mg2-O9	75.6(1)
O1-Mg1-O3	95.9(1)	O7-Mg2-O9	95.6(1)
N1-Mg1-w1	96.2(1)	N2-Mg2-w4	93.8(1)
O1-Mg1-w1	173.9(2)	O7-Mg2-w4	170.7(2)
O3-Mg1-w1	86.0(1)	O9-Mg2-w4	86.1(1)
N1-Mg1-w2	94.0(2)	N2-Mg2-w5	95.5(1)
O1-Mg1-w2	89.0(1)	O7-Mg2-w5	91.8(1)
O3-Mg1-w2	167.8(2)	O9-Mg2-w5	166.9(2)
w1-Mg1-w2	88.0(1)	w4-Mg2-w5	84.9(1)
N1-Mg1-w3	165.5(2)	N2-Mg2-w6	164.4(1)
O1-Mg1-w3	91.3(1)	O7-Mg2-w6	91.2(1)
O3-Mg1-w3	94.6(2)	O9-Mg2-w6	94.7(1)
w1-Mg1-w3	94.3(2)	w4-Mg2-w6	97.8(1)
w2-Mg1-w3	96.4(2)	w5-Mg2-w6	95.9(2)

(a) Estimated standard deviations in the least significant digits are given in parentheses.

Table 5.11 Chelate Ring[a] Bonding Parameters[b] for $[Mg_2(EGTA)(OH_2)_6]\cdot 5H_2O$

Glycinate Rings

	C-C'	C'-N	C-O	C-O'	C-C'-N	O-C-O'	C'-C-O	C'-C-O'	Mg-N-C'	Mg-O-C
G1	1.516(6)	1.486(6)	1.246(6)	1.241(5)	115.1(4)	125.8(4)	119.7(4)	114.5(4)	105.5(2)	119.4(3)
G2	1.527(7)	1.464(6)	1.258(6)	1.252(6)	111.9(4)	124.9(5)	117.6(4)	117.5(4)	104.6(3)	120.1(3)
G3	1.513(6)	1.453(6)	1.262(5)	1.265(5)	114.1(4)	124.8(4)	118.9(4)	116.4(4)	106.6(3)	118.9(3)
G4	1.516(6)	1.472(5)	1.267(5)	1.241(5)	110.8(3)	124.8(4)	117.4(4)	117.8(4)	103.0(2)	117.5(3)

Amino-Ether Rings

	C-C'	C-N	C'-O	C-C'-O	C'-C-N	C"-N-C†	C-N-C"	C-N-C†	Mg-N-C
A1	1.519(8)	1.483(6)	1.425(7)	114.9(4)	116.1(4)	111.3(3)	112.9(3)	112.5(3)	109.4(3)
A2	1.546(8)	1.477(6)	1.323(8)	111.0(5)	117.4(5)	110.3(3)	113.0(3)	112.8(3)	110.5(3)

Diether Ring

	C-C'	C'-O'	C-O	C'-C-O	C-C'-O'	C'-O'-C†	C"-O-C
E1	1.483(9)	1.437(8)	1.426(6)	105.6(5)	112.3(6)	111.9(5)	113.5(4)

(a) Chelate ring nomenclature is described in Figure 4.2(b). Rings within each series are numbered with increasing oxygen number.
(b) Bond lengths are given in Ångstroms and bond angles are given in degrees. Estimated standard deviations in the least significant digits are given in parentheses.

Table 5.12 Chelate Ring[a] Conformational Parameters[b] for $[Mg_2(EGTA)(OH_2)_6]\cdot 5H_2O$

	Ring Type	Bridging[c] Interaction	Glycinate Rings N-Mg-O-C	Mg-O-C-C'	O-C-C'-N	C-C'-N-Mg	C'-N-Mg-O	ΔC_s,min[d] ΔC_s,max	ΔC_2,min ΔC_2,max
G1	δ	0	12.0(3)	-15.1(5)	8.3(6)	1.5(4)	-6.2(3)	2.6(O) 16.6(C')	6.0(N) 21.7(O)
G2	λ	0	14.2(3)	0.3(5)	-24.7(6)	32.0(4)	-24.7(3)	9.0(N) 36.9(C)	9.8(O) 48.6(N)
G3	λ	0	16.0(3)	-12.1(5)	-4.1(6)	15.3(4)	-16.0(3)	2.3(Mg) 24.9(C)	5.7(C) 29.8(Mg)
G4	λ	0	23.7(3)	-7.7(5)	-24.6(5)	39.1(4)	-33.0(2)	4.4(N) 49.9(C)	16.2(C) 61.4(N)

(a) Chelate ring nomenclature is described in Figure 4.2(b). Rings within each series are numbered with increasing oxygen number.
(b) Torsion angles are given in degrees. Estimated standard deviations in the least significant digits are given in parentheses.
(c) The bridge types are schematically depicted in Figure 4.2(a). Type 0 implies no interaction.
(d) The symmetry unique atom of the summation is given in parentheses.

Discussion

The Instability of the Magnesium Complex

It is likely that **6** is the least soluble species in solution because it is neutral. Consequently, preferential crystallization of **6** might be expected, even if it were not the predominant form in solution. There are other indications, however, that magnesium ion may only bind to one end of the $EGTA^{4-}$ ligand in solution. The equilibrium constants for protonation of a series of ML^{2-} complexes are shown in Table 5.13; abbreviations are defined, collectively, in a list in the preliminary material of this thesis. For $ODTA^{4-}$, the equilibrium constants for protonation of MgL^{2-} and CaL^{2-} are approximately equivalent. Given this fact, and the low relative affinity of calcium ion for $ODTA^{4-}$ (in comparison to $EGTA^{4-}$), it is likely that both magnesium ion and calcium ion only bind to one end of the $ODTA^{4-}$ ligand.

For $EEDTA^{4-}$, the equilibrium constants for protonation of the magnesium and calcium ion complexes are also approximately equal, but are approximately five orders of magnitude less favorable than for $[M(ODTA)]^{2-}$. The $EEDTA^{4-}$ ligand must wrap around both the calcium and the magnesium ions, in order for protonation of the $[M(EEDTA)]^{2-}$ complexes to be so relatively unfavorable. For $EGTA^{4-}$, the protonation constant for $[Mg(EGTA)]^{2-}$ is almost four orders of magnitude more favorable than for $[Ca(EGTA)]^{2-}$.

Table 5.13 Formation and Protonation Constants for Selected Ligands

$$M^{2+} + L^{4-} \rightleftharpoons ML^{2-} \;/\; ML^{2-} + H^{+} \rightleftharpoons HML^{-}$$

	EGTA[48]	EEDTA[48]	ODTA[48]	BAPTA[111]
Mg^{2+}	5.2/7.6	8.3/5.0	4.8/9.6	1.8
Ca^{2+}	11.0/3.8	10.0/4.3	4.6/10.0	7.0

An obvious explanation for this difference is that one end of the $EGTA^{4-}$ ligand is still free (i.e., uncomplexed) in the 1:1 Mg^{2+}:$EGTA^{4-}$ complex. Additionally, the equilibrium constants for complex formation of magnesium ion with $EGTA^{4-}$ and $ODTA^{4-}$ only differ by 0.4 orders of magnitude, whereas for calcium ion, the equilibrium constant for complexation with $EGTA^{4-}$ is over six orders of magnitude more favorable than with $ODTA^{4-}$. All of this evidence strongly indicates that a magnesium ion only binds to one end of the $EGTA^{4-}$ ligand, in the manner shown in the structure of 6.

Formation constants have been measured for the $EGTA^{4-}$ analogue, $BAPTA^{4-}$ (see Table 5.13). $BAPTA^{4-}$ retains the calcium selectivity characteristic of $EGTA^{4-}$, while the stabilities of its chelates have much less pH sensitivity in the physiological pH ranges.[111] During the spectrophotometric measurement of the formation constants for $BAPTA^{4-}$, the ligand spectral shift induced by magnesium ion was observed to be only half that induced by calcium ion. Much higher concentrations of magnesium ion were necessary to produce the same spectral shift as for calcium ion. These results were interpreted as being due to sequential binding of two magnesium ions, one at each end of the $BAPTA^{4-}$ ligand. Observation of the dinuclear structure of 6 with such a similar ligand supports this interpretation.

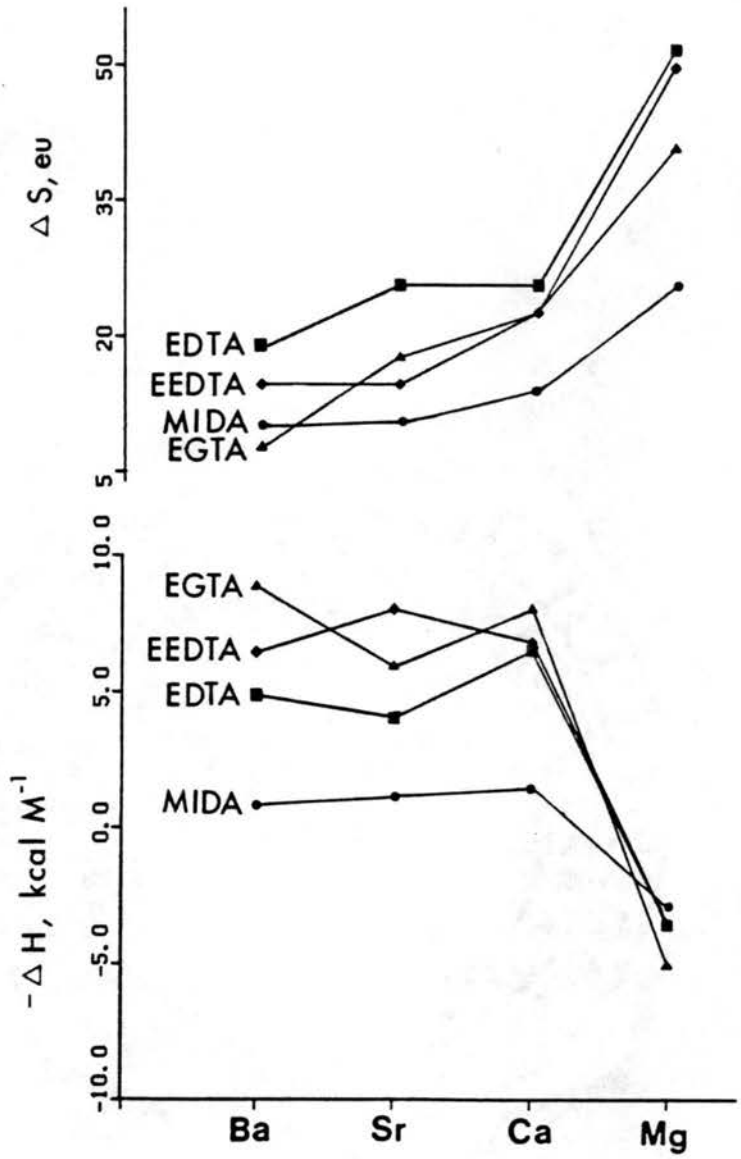

Figure 5.7 Enthalpic and entropic contributions to the stability constants for the alkaline earth metal ion complexes of selected ligands (see text).

Relative Stabilities of Other Alkaline Earth-EGTA Complexes

The relative enthalpic and entropic contributions to the stability constants of alkaline earth-$EGTA^{4-}$ complexes have been measured by several groups.[101-103] These quantities are graphically depicted in Figure 5.7 for $EGTA^{4-}$ and the related ligands $EDTA^{4-}$, $MIDA^{2-}$, and $EEDTA^{4-}$.

Formation of complexes of magnesium ion is endothermic for all of these ligands. Magnesium ion binds water molecules strongly, and when chelation does occur, the five-membered chelate rings formed are strained as a result of the small size of the metal ion; the relatively planar configuration necessitated for two of the glycinate rings in 6 is evidence for this strain.

Formation of the magnesium complex is entropy-driven for each of the ligands shown in Figure 5.7. $EDTA^{4-}$ and $EEDTA^{4-}$ complexes exhibit similar entropic contributions to the stability constants, while the entropy of formation for the $EGTA^{4-}$ complex is approximately 10 eu less favorable. This is consistent with the hypothesis that magnesium ion is only binding to one end of the $EGTA^{4-}$ ligand. Because the $EGTA^{4-}$ ligand only binds to the magnesium ion in a tridentate fashion, fewer water molecules would be released from the aquated magnesium ion upon coordination (in comparison to $EDTA^{4-}$ and $EGTA^{4-}$). Additionally, the carboxylate groups that are not involved in coordination to the metal ion would retain solvent ordering properties.

The conformational freedom retained by the uncoordinated portion of the $EGTA^{4-}$ ligand would be an offsetting effect. The entropic contributions to the stability constant might be expected to be similar for $MIDA^{2-}$ and $EGTA^{4-}$ if the magnesium ion were only binding to one end of the $EGTA^{4-}$ ligand. The fact that the entropy of formation is approximately 10 eu less favorable for the $MIDA^{2-}$ complex must indicate that coordination of magnesium ion to one end of the $EGTA^{4-}$ ligand somehow disrupts the solvent ordering properties of the other end.

The enthalpic and entropic contributions to the stability constants for formation of calcium ion chelates of $EDTA^{4-}$, $EEDTA^{4-}$, and $EGTA^{4-}$ are nearly identical. The gain in entropy attendant upon displacement of additional water molecules by the chelating ligands with more binding sites must be offset by the loss of entropy upon coordination of a ligand with a greater initial configurational entropy.

The enthalpic and entropic contributions to the stability constants for chelation of the strontium and barium ions do not seem to follow a regular pattern. Compared to the calcium ion complexes, the enthalpies of formation for $[Sr(EEDTA)]^{2-}$ and $[Ba(EGTA)]^{2-}$ seem to be unusually favorable. It is a possibility that relief of chelate ring strain for the large barium ion by the planar coordination of one of the ether oxygen atoms (see above) may explain the extra stability of $[Ba(EGTA)]^{2-}$. For this

same complex, the entropy of formation seems to be unusually low. Less conformational freedom in the chelate may be associated with this mode of binding. Structural information on barium and strontium chelates of $EEDTA^{4-}$ would be useful in evaluating this situation.

Implications for the Selectivity of Calcium-Binding Proteins

It has been suggested that magnesium ion may bind to only a subset of the ligand atoms in the highly selective calcium-binding sites in calcium-binding proteins.[65] This was put forth as an explanation of why magnesium ion is not able to induce the protein conformational changes that calcium ion propagates. The binding of magnesium ion to a subset of the possible binding sites of the $EGTA^{4-}$ is the apparent explanation of the high degree of calcium selectivity exhibited by $EGTA^{4-}$. Given this fact, it seems plausible that a similar phenomenon may permit the calcium-selective binding observed in nature.

CHAPTER 6

STRUCTURAL VARIATIONS IN CADMIUM AND LANTHANIDE CHELATES OF $EGTA^{4-}$

Introduction

Information regarding the structures of the calcium-binding sites in the native calcium-binding proteins is difficult to obtain using techniques other than X-ray crystallography, due to the calcium ion's lack of useful spectroscopic properties. Although ^{43}Ca NMR signals have been observed for several calcium-binding proteins,[112,113] expensive isotopic enrichment is required and the signals obtained are quite broad, due to the large quadrupole moment of the ^{43}Ca nucleus (I = 7/2). Consequently, more spectroscopically useful metals have been substituted in the calcium-binding sites. Cadmium(II) ion[69,70] (as a ^{113}Cd NMR probe) and various tripositive lanthanide ions (as ^{1}H NMR shift agents, as well as EPR, and luminescence probes)[71-73, 114, 115] have served in this manner as indirect spectroscopic probes of the structure of the binding sites.

Such metals, of course, may bind to the calcium-binding site in a significantly different manner than does calcium ion. X-ray crystallographic studies on the

lanthanide-substituted calcium-binding protein parvalbumin have confirmed that terbium(III) ions bind in the same domains as the calcium ions. It is clear that one of the terbium ions, when occupying the EF binding sites of parvalbumin, binds an additional sulfate ion (or water molecule), but no detailed structural comparison is possible.[116,117] To date, no detailed structural studies have explored differences in the coordination environment when such metal ions are substituted for calcium in a highly selective calcium-binding site (such as that provided by $EGTA^{4-}$). The structural studies of Cd(II), Nd(III), and Er(III) chelates of $EGTA^{4-}$ were undertaken to assess the types and magnitudes of such structural changes.

The Eight-Coordinate Cadmium Chelate of $EGTA^{4-}$

Structure of $Sr[Cd(EGTA)]\cdot 7H_2O$ (7)

The modes of coordination of the $EGTA^{4-}$ ligand to calcium ion and cadmium ion are quite similar, as can be seen by comparing Figure 6.1(a) and Figure 4.1(a). Cadmium(II), despite its slightly smaller ionic radius ($r_{Ca(II)}$ = 1.12 Å, $r_{Cd(II)}$ = 1.10 Å),[118] is still able to bind to all eight ligand atoms of the $EGTA^{4-}$ ligand. The coordination geometry about cadmium remains approximately dodecahedral.

The pattern of bridging interactions that occurs in the lattice of 7 is identical with that occurring for

(a)

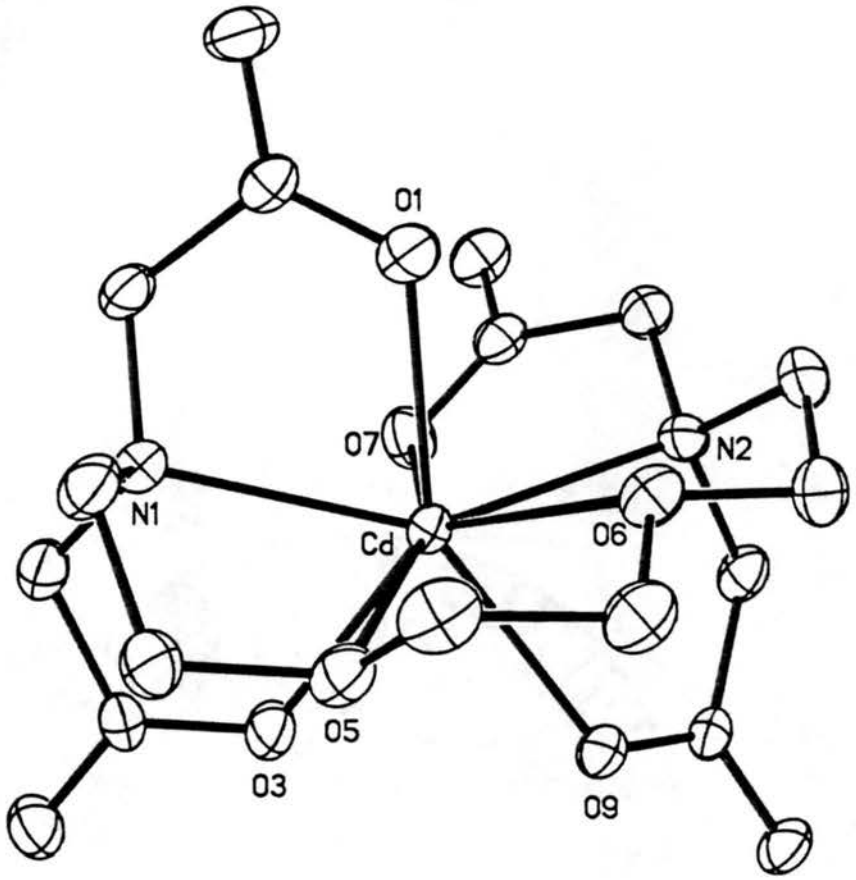

(b)

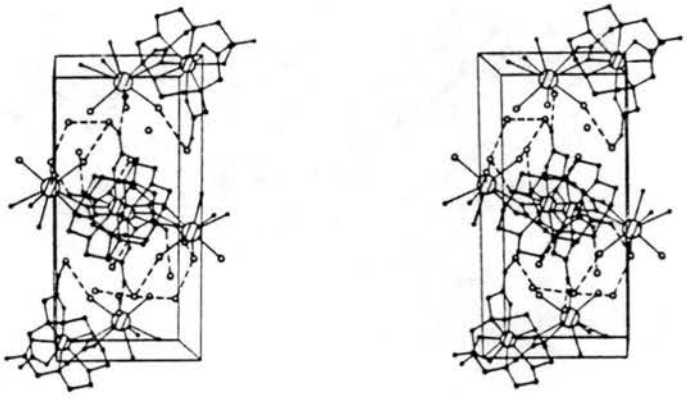

Figure 6.1 (a) A thermal ellipsoid plot (40%) of $[Cd(EGTA)]^{2-}$. (b) View of the unit cell of $Sr[Cd(EGTA)]\cdot 7H_2O$ taken along a.

$Sr[Ca(EGTA)]\cdot 6H_2O$ (3, see Chapter 4). The bridging bond distances, however, are quite different in the two complexes. The strontium ion and cadmium ion bond lengths are summarized in Table 6.1. The Sr-O7 distance, which was 3.215(3) Å in 3, is shortened to 2.995(3) Å in 7. The Sr-OH_2 distances (2.554(5)-2.734(3) Å) and the Sr-O(carb) distances (2.559(3)-2.764(3) Å) are quite different when compared in detail to the distances observed in 3; however the mean metal-ligand distances (excluding the long bond to O7) are nearly identical (Sr-L(ave) = 2.63(9) Å in 7; Sr-L(ave) = 2.62(6) Å in 3). Such differences in individual bond lengths may be taken as evidence for the compliancy of a strontium counterion. The bonding to the chelate is not sacrificed in preference to bonding to the strontium counterion; instead, the counterion makes adjustments in individual bond lengths to comply with the different bonding environment provided by the calcium and cadmium chelates. The additional water molecule in the lattice of 7 only interacts with other water molecules through hydrogen bonding interactions (see Figure 6.1(b)).

In the $[Cd(EGTA)]^{2-}$ complex anion, one Cd-O(carboxylate) bond length (Cd-O7 = 2.420(3) Å) is much longer than the other three (Cd-O1 = 2.324(3) Å, Cd-O3 = 2.347(3) Å, Cd-O9 = 2.325(3) Å). Carboxylate group O7/O8 is involved in bridging to the strontium counterion, but this involvement is less extensive than that of the carboxylate group O9/O10, which strongly interacts with two

Table 6.1 Metal-Ligand Distances (Å) and Angles (deg)[a] for $Sr[Cd(EGTA)]\cdot 7H_2O$

(a) Complex Ion

Cd-N1	2.421(4)
Cd-N2	2.437(3)
Cd-O1	2.324(3)
Cd-O3	2.347(3)
Cd-O5	2.574(3)
Cd-O6	2.585(3)
Cd-O7	2.420(3)
Cd-O9	2.325(3)

N1-Cd-N2	148.0(1)
N1-Cd-O1	71.0(1)
N2-Cd-O1	83.4(1)
N1-Cd-O3	70.6(1)
N2-Cd-O3	127.3(1)
O1-Cd-O3	140.2(1)
N1-Cd-O5	71.7(1)
N2-Cd-O5	131.1(1)
O1-Cd-O5	95.1(1)
O3-Cd-O5	82.5(1)
N1-Cd-O6	118.1(1)
N2-Cd-O6	69.6(1)
O1-Cd-O6	72.8(1)
O3-Cd-O6	136.6(1)
O5-Cd-O6	63.5(1)
N1-Cd-O7	91.8(1)
N2-Cd-O7	68.7(1)
O1-Cd-O7	90.0(1)
O3-Cd-O7	81.2(1)
O5-Cd-O7	159.9(1)
O6-Cd-O7	136.3(1)
N1-Cd-O9	139.5(1)
N2-Cd-O9	71.7(1)
O1-Cd-O9	143.9(1)
O3-Cd-O9	75.4(1)
O5-Cd-O9	82.8(1)
O6-Cd-O9	74.2(1)
O7-Cd-O9	104.2(1)

(b) Counterion

Sr-O9	2.764(3)
Sr-O10	2.696(3)
Sr-w1	2.554(5)
Sr-w2	2.734(3)
Sr-w3	2.567(4)
Sr-w4	2.555(3)
Sr-O7a	2.995(3)
Sr-O8a	2.614(3)
Sr-O10a	2.559(3)

O9-Sr-O10	47.6(1)
O9-Sr-w1	66.9(1)
O10-Sr-w1	80.9(1)
O9-Sr-w2	122.6(1)
O10-Sr-w2	92.2(1)
w1-Sr-w2	67.7(1)
O9-Sr-w3	148.3(1)
O10-Sr-w3	163.9(1)
w1-Sr-w3	102.7(1)
w2-Sr-w3	75.1(1)
O9-Sr-w4	71.9(1)
O10-Sr-w4	119.4(1)
w1-Sr-w4	78.0(1)
w2-Sr-w4	128.6(1)
w3-Sr-w4	76.7(1)
O9-Sr-O7a	110.4(1)
O10-Sr-O7a	118.1(1)
w1-Sr-O7a	153.0(1)
w2-Sr-O7a	126.0(1)
w3-Sr-O7a	64.7(1)
w4-Sr-O7a	75.8(1)
O9-Sr-O8a	74.2(1)
O10-Sr-O8a	72.9(1)
w1-Sr-O8a	141.2(1)
w2-Sr-O8a	139.8(1)
w3-Sr-O8a	110.5(1)
w4-Sr-O8a	90.3(1)
O7a-Sr-O8a	46.0(1)
O9-Sr-O10a	119.9(1)
O10-Sr-O10a	75.6(1)
w1-Sr-O10a	128.9(1)
w2-Sr-O10a	68.6(1)
w3-Sr-O10a	90.4(1)
w4-Sr-O10a	152.6(1)
O7a-Sr-O10a	76.8(1)
O8a-Sr-O10a	71.6(1)

(c) Interionic Angles

Cd-O7-Sra	159.7(1)
C12-O7-Sra	84.4(2)
C12-O8-Sra	102.1(2)
Cd-O9-Sr	148.7(1)
Sr-O9-C14	93.2(2)
Sr-O10-C14	96.5(2)
Sr-O10-Srb	104.4(1)
C14-O10-Srb	148.7(2)

(a) Estimated standard deviations in the least significant digits are given in parentheses.

different strontium counterions and still exhibits normal metal-oxygen distances. Additionally, in 3, the Ca-O7 bond is not unusually long. Thus, the bridging interactions do not seem to offer an explanation for this long distance.

Closer examination reveals that O7 is involved in a close intrachelate contact with O3 (see the space-filling plots in Figure 6.2), the atom which exhibits the next longest Cd-O(carboxylate) distance. The O3-O7 distance in 7 (3.101(6) Å), is 0.08 Å shorter than seen in 3 (O3-O7 = 3.185(6) Å). The O3-O9 contact distance is also shorter by 0.19 Å in 7 (O3-O9 = 2.858(4) Å in 7; O3-O9 = 3.046(6) Å in 3). As a consequence of these two interactions involving O3, the O7-O9 distance in 7 is increased by 0.20 Å relative to 3 (O7-O9 = 3.547(6) Å in 3 and 3.746(6) Å in 7. If O7 were bonded at a "normal" distance, it would force O3 and O7 into even closer proximity. It is difficult to understand why these intraligand contacts do not affect the Cd-O3 distance more substantially.

The $EGTA^{4-}$ ligand seems to fit much less comfortably about the smaller cadmium ion than it does about the calcium ion (as judged by the intraligand contact distances). A $[Ca(EGTA)]^{2-}$ complex would appear to have significant possibilities for distortion (creating closer intraligand contacts) and thus could possibly host a ninth ligand with some carboxylate rearrangement.

The Cd-O(carboxylate) distances in 7 appear to be shorter than those seen previously in the seven-coordinate

$[Cd(EDTA)(OH_2)]^{2-}$ complex anion,[5] where the average Cd-O(carboxylate) distance was 2.39(5) Å. The Cd-O(carboxylate) distances in 7 (Cd-O(carb, ave) = 2.35(5) Å) are also shorter than the Ca-O(carboxylate) distances seen in the $[Ca(EGTA)]^{2-}$ anion of 3 (2.377(8) Å).

More striking differences between 3 and 7 surface when the metal-nitrogen and metal-O(ether) bond lengths are compared. Cd-N(ave)(2.43(1) Å) is much shorter than Ca-N(ave)(2.592(9) Å). The cadmium-nitrogen distances in 7 are approximately equivalent to those in seven-coordinate $[Cd(EDTA)(OH_2)]^{2-}$ (Cd-N = 2.382(9), 2.414(7) Å).[5]

In contrast, Cd-O(ether) bonds are significantly longer than Ca-O(ether) distances (Cd-O(ether,ave) = 2.580(8) Å; Ca-O(ether,ave) = 2.51(2) Å). The Cd-O(ether) distances in 7 are longer than distances found between such atoms in the literature. For the seven-coordinate cadmium ion in $[Cd(ODA)]\cdot 3H_2O$,[119] Cd-O(ether) = 2.490(11) Å, while for six- and seven-coordinate cadmium ions in $Cd_2(TGM)Cl_4$[120] (TGM = tetraethylene glycol dimethyl ether), the Cd-O(ether) distances for ether oxygen atoms not involved in bridging ranged from 2.409(11) to 2.523(12) Å (Cd-O(ave) = 2.46(5) Å).

Given the differences in metal-ligand distances between $[Ca(EGTA)]^{2-}$ and $[Cd(EGTA)]^{2-}$, ligand conformational changes might be expected. As can be seen by comparison of entries in Table 6.3 and Table 4.7, the pattern of δ/λ conformations for the individual

Table 6.2 Chelate Ring[a] Bonding Parameters[b] for $Sr[Cd(EGTA)]\cdot 7H_2O$

Glycinate Rings

	C-C'	C'-N	C-O	C-O'	C-C'-N	O-C-O'	C'-C-O	C'-C-O'	Cd-N-C'	Cd-O-C
G1	1.533(6)	1.472(5)	1.267(5)	1.234(5)	112.8(3)	125.5(4)	117.9(3)	116.6(4)	104.4(2)	116.9(2)
G2	1.496(6)	1.472(5)	1.252(5)	1.251(5)	114.2(4)	123.8(4)	118.5(3)	117.6(4)	110.8(2)	120.5(3)
G3	1.526(6)	1.465(5)	1.250(5)	1.258(5)	113.6(3)	124.5(4)	119.0(4)	116.5(4)	107.4(2)	115.3(2)
G4	1.514(6)	1.467(5)	1.257(5)	1.256(5)	115.2(3)	122.5(3)	119.5(3)	118.0(3)	105.1(2)	116.5(2)

Amino-Ether Rings

	C-C'	C-N	C'-O	C-C'-O	C'-C-N	C"-N-C[†]	C-N-C"	C-N-C[†]	Cd-N-C	Cd-O-C'
A1	1.509(6)	1.485(5)	1.433(6)	110.7(4)	111.9(3)	112.1(3)	108.7(3)	111.7(3)	108.8(2)	108.7(2)
A2	1.508(6)	1.481(5)	1.427(5)	107.3(3)	113.4(3)	111.1(3)	110.0(3)	111.5(3)	111.5(2)	111.0(2)

Diether Ring

	C-C'	C'-O'	C-O	C'-C-O	C-C'-O'	C'-O'-C[†]	C"-O-C	Cd-O-C	Cd-O'-C'
E1	1.498(7)	1.419(5)	1.437(5)	107.4(3)	106.7(3)	113.2(3)	112.9(3)	115.3(2)	116.4(2)

(a) Chelate ring nomenclature is described in Figure 4.2(b). Rings within each series are numbered with increasing oxygen number.

(b) Bond lengths are given in Ångstroms and bond angles are given in degrees. Estimated standard deviations in the least significant digits are given in parentheses.

Table 6.3 Chelate Ring[a] Conformational Parameters[b] for $Sr[Cd(EGTA)]\cdot 7H_2O$

Glycinate Rings

	Ring Type	Bridging[c] Interaction	N-Cd-O-C	Cd-O-C-C'	O-C-C'-N	C-C'-N-Cd	C'-N-Cd-O	ΔC_s,min[d] ΔC_s,max	ΔC_2,min ΔC_2,max
G1	δ	O	-24.8(3)	9.5(5)	24.6(5)	-41.7(4)	33.7(2)	5.7(N) 52.8(C)	16.0(C) 63.7(N)
G2	λ	O	2.7(3)	10.6(5)	-24.7(6)	25.0(4)	-14.8(3)	3.0(C') 29.5(O)	9.0(O) 39.5(C')
G3	δ	1	-29.5(3)	19.8(5)	12.8(5)	-36.6(4)	32.9(2)	12.1(N) 52.1(C)	7.1(C) 59.5(Cd)
G4	δ	1,2	-23.1(2)	12.1(4)	17.3(5)	-33.8(4)	28.4(2)	5.6(N) 45.3(C)	8.4(C) 52.4(N)

Amino-Ether Rings

	Ring Type	O-Cd-N-C	Cd-N-C-C'	N-C-C'-O	C-C'-O-Cd	C'-O-Cd-N	ΔC_s,min ΔC_s,max	ΔC_2,min ΔC_2,max
A1	δ	20.1(2)	-49.7(4)	62.1(5)	-38.8(4)	10.1(2)	15.9(C) 66.1(Cd)	10.5(Cd) 89.4(C)
A2	λ	-13.1(2)	43.7(4)	-60.5(4)	44.5(3)	-17.8(2)	21.5(C') 66.1(Cd)	3.4(Cd) 86.0(C')

Diether Ring

	Ring Type	O'-Cd-O-C	Cd-O-C-C'	O-C-C'-O'	C-C'-O'-Cd	C'-O'-Cd-O	ΔC_s,min ΔC_s,max	ΔC_2,min ΔC_2,max
E1	δ	18.1(2)	-48.5(4)	61.2(4)	-46.7(4)	16.6(2)	22.1(C) 71.6(Cd)	1.7(Cd) 90.1(C)

(a) Chelate ring nomenclature is described in Figure 4.2(b). Rings within each series are numbered with increasing oxygen number.
(b) Torsion angles are given in degrees. Estimated standard deviations in the least significant digits are given in parentheses.
(c) The bridge types are schematically depicted in Figure 4.2(a). Type O implies no interaction.
(d) The symmetry unique atom of the summation is given in parentheses.

five-membered chelate rings are the same for $[Cd(EGTA)]^{2-}$ as for $[Ca(EGTA)]^{2-}$ in 3. The conformations, as described by the torsion angles of the amino-ether rings and the diether rings of 3 and 7, as well as the inter-ring torsion angles (see Table 6.4) also differ very little. The absence of conformational differences implies that the angles about the calcium and cadmium ions should be different.

This expectation is fully realized (see Tables 6.1, 6.2 and Tables 4.5, 4.6). For the amino-ether rings, O-Ca-N < O-Cd-N, Ca-O-C' > Cd-O-C', and Cd-N-C > Ca-N-C. These differences are as expected, given the fact that the shortening of the Cd-N bonds (compared to Ca-N) is of larger magnitude than the lengthening of the Cd-O(ether) bonds (compared to Ca-O(ether)).

The symmetry-unique atoms of the glycinate rings are not identical in the structures of 3 and 7, although differences in the individual torsion angles are quite small (see Tables 6.3 and 4.7). The shorter Cd-N bonds (relative to Ca-N) seem to dominate the angular differences between the calcium and cadmium complexes seen in the glycinate rings: Ca-O-C' > Cd-O-C', Ca-N-C' > Cd-N-C' and N-Cd-O > N-Ca-O.

Variable Temperature ^{1}H NMR Study of $[Cd(EGTA)]^{2-}$

The splitting pattern observed for the cadmium ion complex is identical with that observed for the calcium

Table 6.4 Inter-ring Torsion Angles[a] for $Sr[Cd(EGTA)]\cdot 7H_2O$

C2-C1-N1-C5	74.2(4)	C4-C3-N1-C5	-96.4(4)
C12-C11-N2-C10	-158.2(3)	C14-C13-N2-C10	87.2(4)
C2-C1-N1-C3	-161.8(3)	C4-C3-N1-C1	141.2(4)
C12-C11-N2-C13	77.9(4)	C14-C13-N2-C11	-149.7(3)
C1-N1-C5-C6	-162.8(4)	C3-N1-C5-C6	73.0(5)
C11-N2-C10-C9	162.8(4)	C13-N2-C10-C9	-73.5(4)
C5-C6-O5-C7	90.5(4)	C10-C9-O6-C8	177.5(3)
C6-O5-C7-C8	-174.3(3)	C9-O6-C8-C7	-177.0(3)

(a) Torsion angles are given in degrees. Estimated standard deviations in the least significant digits are given in parentheses.

case, except that the AB pattern is further split by the presence of 25% ^{111}Cd (I=1/2) and ^{113}Cd (I=1/2). At pH 8, the AB/ABX pattern only begins to collapse at the boiling point of the solution (~100° C). Since the coalescence temperature is much higher for $[Cd(EGTA)]^{2-}$ than for $[Ca(EGTA)]^{2-}$, while J_{AB} and δ_{AB} are of similar magnitude, the activation barrier for dissociation of the Cd-N bond must be higher than for Ca-N. This is consistent with the observed water exchange rates for the aqua complexes.[121]

^{113}Cd Solution and Solid State NMR Spectra of $[Cd(EGTA)]^{2-}$

Cd^{2+} has been used extensively in biological systems as an I = 1/2 replacement for Ca^{2+}, Mg^{2+}, and Zn^{2+} ions.[69,70] ^{113}Cd is a sensitive, relatively abundant nucleus, with a large chemical shift range of ~900 ppm (see Figure 6.3). The ^{113}Cd NMR spectra of cadmium-substituted calcium-binding proteins exhibit a characteristic chemical shift range from -85 to -130 ppm (relative to 0.1 M $Cd(ClO_4)_2$). Only recently have chemical shift values this highly shielded been reproduced by a low molecular weight compound in solution.[122] A ^{113}Cd resonance at -130 ppm has been assigned to the cadmium ion complexed within the cavity of a substituted macrocyclic crown ether which is capable of donating six ether oxygen atoms and four carboxylate oxygen atoms to the metal. One of the difficulties in achieving chemical shifts in the

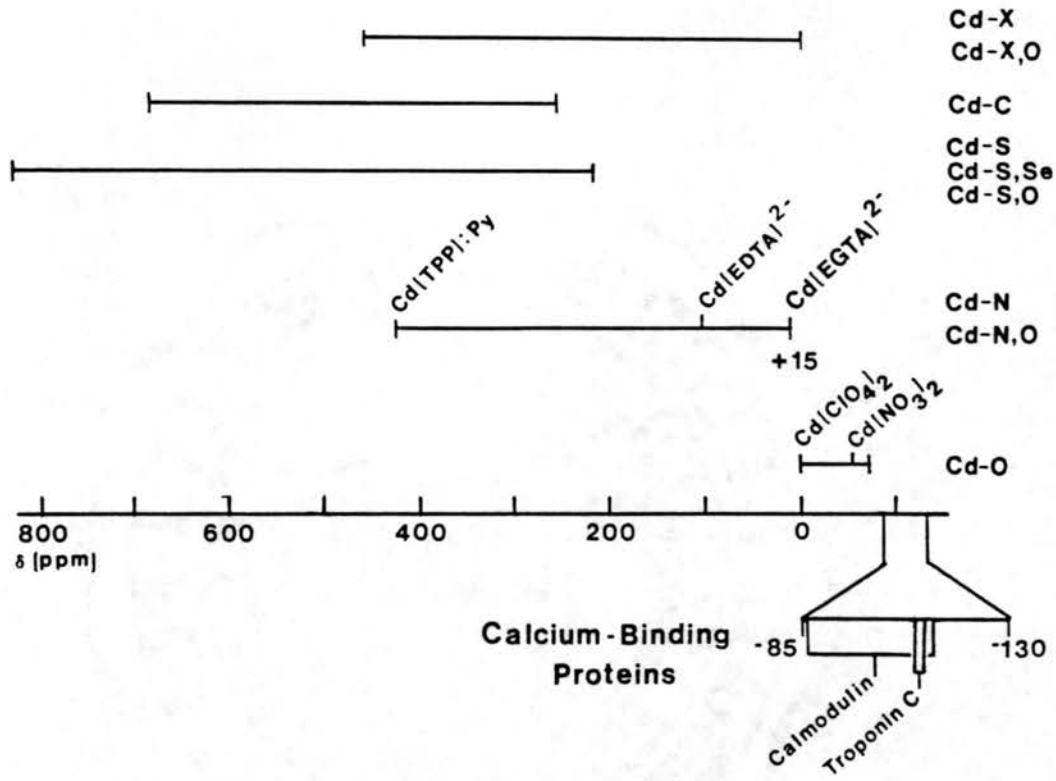

Figure 6.3 Solution ^{113}Cd NMR chemical shifts as a function of ligand atom type. Chemical shifts for calcium-binding proteins are also indicated.

range of calcium-binding proteins (which is largely circumvented by a chelating ligand) involves the dynamic processes which occur rapidly in solution. Such exchange processes result in the chemical shift value characteristic of the chelate being averaged with those of partially aquated species. To get around this bond lability problem, solid state ^{113}Cd NMR spectroscopy has been used with considerable success to reproduce signals in the chemical shift range of calcium-binding proteins for simple compounds involving oxygen-containing ligands, such as $Cd(NO_3)_2 \cdot 4H_2O$ and $Cd(OAc)_2 \cdot 2H_2O$.[123-125]

Recently, the analysis of ^{113}Cd chemical shifts has been extended by performing single crystal ^{113}Cd NMR studies.[126,127] Such studies can determine the orientation of the shielding tensor relative to a known, static molecular framework, and thus allow the determination of which interactions contribute to the individual components of the shielding tensor. In all compounds studied thus far by this method, the most highly shielded components of the tensor are oriented perpendicular to relatively long Cd-O bonds.

The solution and solid state ^{113}Cd NMR spectra of $[Cd(EGTA)]^{2-}$ have been examined. In solution, the ^{113}Cd chemical shift of the cadmium complex was found 15 ppm deshielded from the 0.1 M $Cd(ClO_4)_2$ standard. This value seems reasonable in comparison to that for $[Cd(EGTA)]^{2-}$, which exhibits a ^{113}Cd chemical shift of +85 ppm;[128] the

more shielded resonance of the $EGTA^{4-}$ complex is due to replacement of a water molecule by two ether oxygen atoms and to the higher coordination number of the $EGTA^{4-}$ chelate. This chemical shift is in agreement with results recently published for $Cd(EGTA)^{2-}$.[122] The presence of the nitrogen atoms in 7 (which are known to deshield ^{113}Cd resonances, see Figure 6.3) means that the $[Cd(EGTA)]^{2-}$ complex cannot be expected to reproduce fully the ^{113}Cd chemical shifts characteristic of Cd-substituted calcium-binding proteins, despite the presence of six oxygen atoms in the metal's primary coordination sphere.

The solid state ^{113}Cd NMR spectrum of 7 yields a chemical shift value for $[Cd(EGTA)]^{2-}$ which is free of the influence of the ligand substitution processes which affect the value obtained in solution. The metal-ligand bond-breaking processes which occur in solution (see above) must temporarily replace carboxylate oxygen atoms by water molecules, and would be expected to deshield the ^{113}Cd resonance in solution, compared to the solid state. The ^{113}Cd spectra obtained from a powder sample ground from crystals of 7 are shown in Figures 6.4(a) (magic angle spinning) and 6.4(b) (non-spinning). Surprisingly, the solid state resonance (at + 36 ppm) is deshielded by 21 ppm relative to the solution resonance. The chemical shift sensitivity of ^{113}Cd is such that the changes in the ligand binding induced by the bridging interactions to strontium counterions (see above) may be enough to cause this

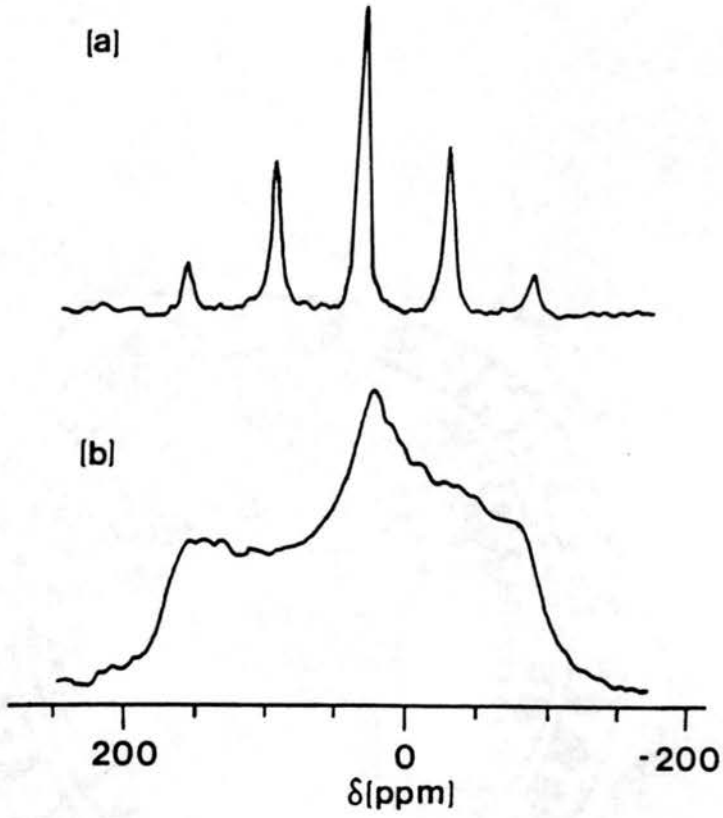

Figure 6.4 (a) Magic angle spinning ^{113}Cd NMR spectrum of $Sr[Cd(EGTA)]\cdot 7H_2O$ (7). The five line pattern is a result of spinning sideband modulated on the central resonance at + 36 ppm. (b) Non-spinning ^{113}Cd NMR spectrum of 7. Three components of the shielding tensor characteristic of a non-axially symmetric complex are evident (σ_{11} = 159 ppm, σ_{22} = 29 ppm, σ_{33} = -81 ppm). The chemical shift anisotropy spans 240 ppm.

unexpected chemical shift behavior. The position of the solid state resonance for $Na_2[Cd(EDTA)]$ is also deshielded from the solution resonance.[125]

The non-spinning pattern observed for 7 is characteristic of a non-axially symmetric complex. Three distinct elements of the shielding tensor are observed (σ_{11} = 159 ppm, σ_{22} = 29 ppm, σ_{33} = -81 ppm), and the chemical shift anisotropy spans 240 ppm. The value of the most upfield element lies in the range of chemical shifts exhibited by cadmium-substituted calcium-binding proteins. This component of the shielding tensor must be oriented so as to maximize contributions from Cd-O(ether) or Cd-O(carboxylate) bonds.

The calcium-binding sites in calcium-binding proteins contain neutral oxygen donors, in addition to the anionic carboxylate oxygen donors. The results observed for $[Cd(EGTA)]^{2-}$ imply that the low affinity of cadmium ion for neutral oxygen donors may be responsible for the large upfield shifts seen for the calcium binding sites in calcium-binding proteins.

Tripositive Lanthanide Chelates of $EGTA^{4-}$

Introduction

Of the structurally characterized $EDTA^{4-}$ chelates of the tripositive lanthanide ions, those containing metal ions larger than holmium were nine-coordinate in the solid

state,[9] while those containing smaller metal ions (i.e., metals to the right of holmium) were eight-coordinate.[13] $EGTA^{4-}$ complexes of the rare earth metal ions neodymium and erbium were chosen for structural study because a coordination number difference between the two chelates would be expected based on the EDTA results.

Structure of a Nine-Coordinate Erbium Chelate of $EGTA^{4-}$, $Ca[Er(EGTA)(OH_2)]_2 \cdot 12H_2O \cdot (CH_3)_2CO$ (8)

The calcium salt of $[Er(EGTA)]^-$ crystallizes with two unique erbium ion complexes per asymmetric unit. Erbium ion forms a nine-coordinate chelate with $EGTA^{4-}$ (see Figure 6.2(a)). The ninth coordination site is occupied by a water molecule, which is also bound to the calcium ion (see below). The ligand atoms binding to the erbium ions occupy the vertices of a distorted tri-capped trigonal prism. In complex a, the trigonal faces are formed by O1, O5, and O6, as well as by O7, O3, and O9. The square faces (O1-O3-O5-O7, O1-O7-O9-O6, and O5-O3-O9-O6) are capped by N1, N2, and w1, respectively (see Figures 6.5(b) and (c)). Complex b has the same arrangement of ligand atoms and absolute configuration as complex a.

Each $[Er(EGTA)]^-$ complex ion engages in two type 3 bridging interactions with the single calcium counterion (see Figure 6.6(a)). This eight-coordinate counterion is bound to the oxygen atoms of four water molecules, in addition to the oxygen atoms provided through the bridging

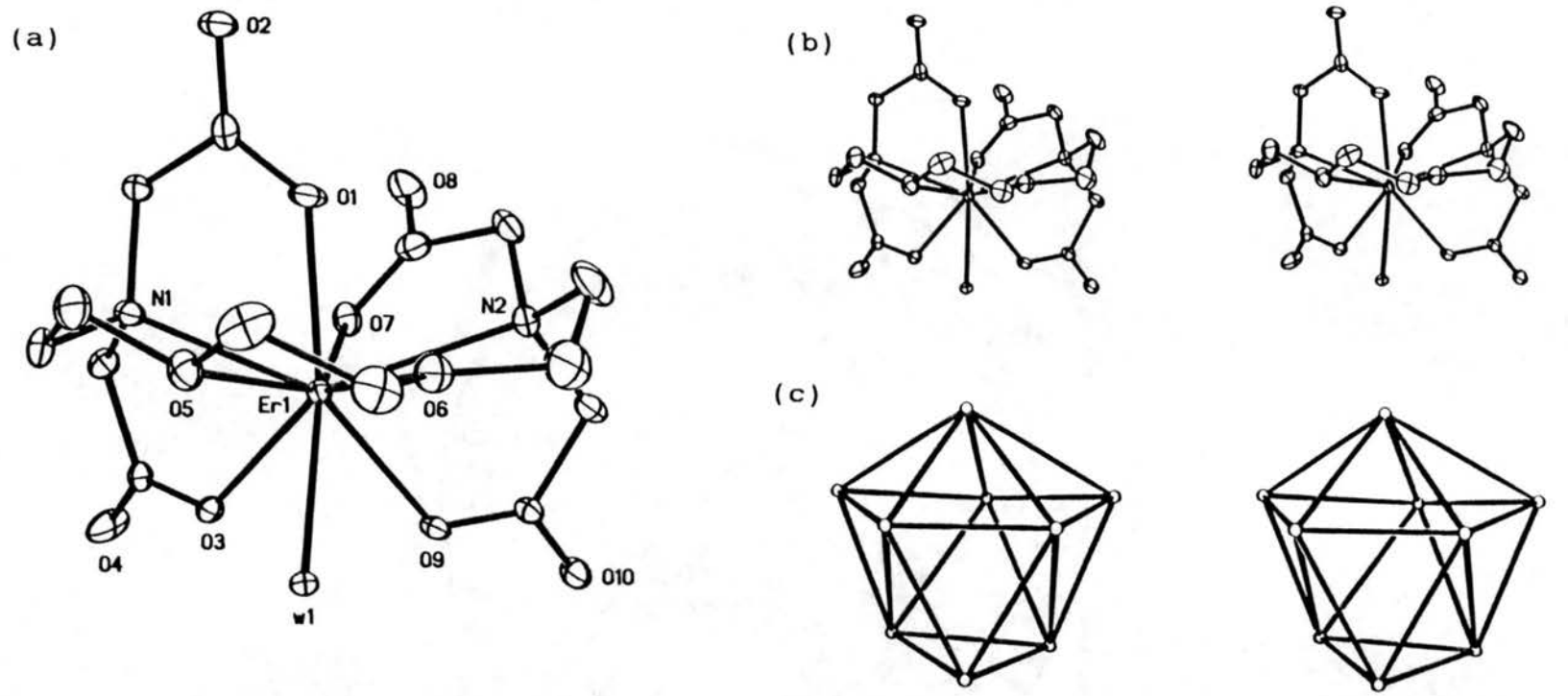

Figure 6.5 (a) A thermal ellipsoid plot (35%) of the $[Er(EGTA)(OH_2)]^-$ complex anion involving Er1. For details of the numbering scheme of the complex involving Er2, see Figure 4.1(a). (b) Stereoview of $[Er(EGTA)(OH_2)]^-$. (c) Stereoview of the coordination polyhedron formed by the ligand atoms about Er1 (see text).

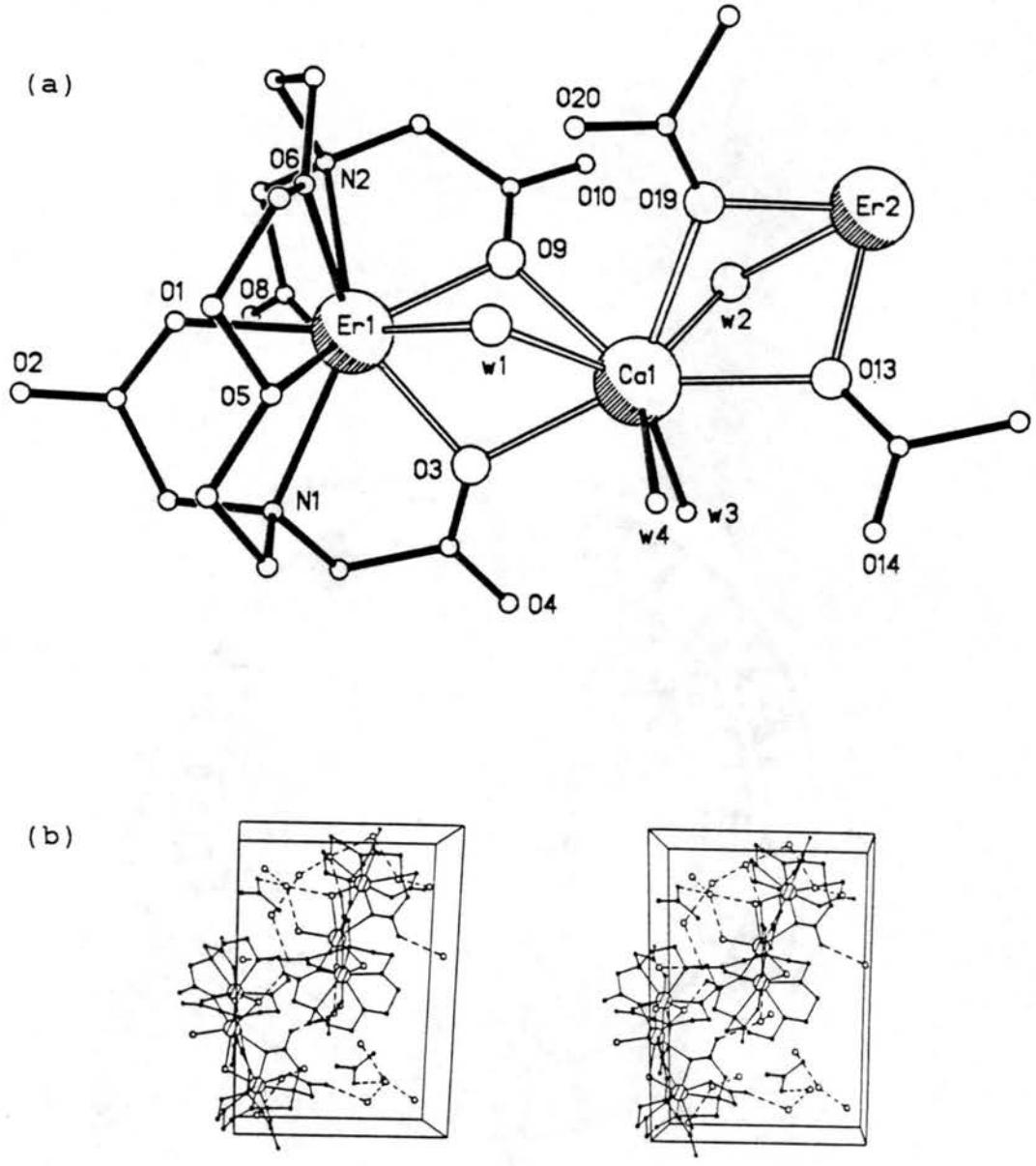

Figure 6.6 (a) Ball and stick plot depicting all the unique interionic interactions in the lattice of $Ca[Er(EGTA)(OH_2)]_2 \cdot 12H_2O \cdot (CH_3)_2CO$ (8). Conventions regarding ionic radii of the atoms are described in the caption of Figure 4.3(a). (b) Unit cell of 8 viewed along a.

interactions. Since the two complex anions of the asymmetric unit interact with the same calcium ion, discrete cation-anion trimers are formed. Additional linkages between the complex anions and the counterion occur through two bridging water molecules (w1 and w2). The ligand atoms binding to the calcium ion are located at the vertices of a distorted square antiprism, with the square faces defined by w2-w3-O9-O3 and w1-w4-O13-O19.

These discrete, trinuclear $CaEr_2$ species are held together by hydrogen bonding interactions involving occluded water molecules and all of the carboxylate oxygen atoms not coordinated to a metal ion (see Figure 6.9(b)). Even the oxygen atom of the acetone molecule of solvation is involved in a hydrogen bond with a water molecule (O21-w9 = 2.77(1) Å).

The bridging water molecules are nearly symmetrically bound between the calcium and erbium ions (Ca1-OH_2(ave) = 2.48(3) Å, Er-OH_2(ave) = 2.462(5) Å). The Er-OH_2 distances are longer than those seen in eight-coordinate $[Er(EDTA)(OH_2)_2]^-$ (Er-OH_2 = 2.32(3) Å)[13] and in eight-coordinate $[Er(HOCH_2COO)_2(H_2O)_4)]^+$ (Er-OH_2 = 2.37(1) Å, 2.28(1) Å),[129] where the water molecules are not involved in bridging interactions. The non-bridging water molecules are bound to the calcium ion at shorter distances than are the bridging water molecules (Ca-OH_2 (non-bridging) = 2.35(1) Å). A bridging water molecule has been previously observed to link two calcium ions.[89]

In all cases, the carboxylate oxygen atom involved in the type 3 bridge to calcium is bound at a shorter distance to the chelated erbium ion than to the calcium ion (Er-O(ave) = 2.33(1) Å, Ca-O(ave) = 2.48(3) Å). As was typical of the type 3 interactions in $Ca[Ca(EGTA)]\cdot(22/3)H_2O$, the bridging carboxylate oxygen atoms are bound to erbium at longer distances than for any other carboxylate atoms. The bonding parameters for the calcium ion and the erbium ion are summarized in Table 6.5.

The mean metal-ligand distances for all three classes of donor atoms of the $EGTA^{4-}$ ligand are shorter for the erbium ion chelate than for the calcium ion chelates of 2 (Er/Ca-N(ave) = 2.57(4)/2.60(2) Å, Er/Ca-O(carb,ave) = 2.31(3)/2.38(2) Å, Er/Ca-O(ether,ave) = 2.42(5)/2.50(3) Å). The mean erbium-ligand distances agree well with those observed in the $EDTA^{4-}$ complex, $[Er(EDTA)(OH_2)_2]^-$:[13] Er-N(ave) = 2.57(5) Å, Er-O(carb,ave) = 2.27(5) Å. The Er-O(ether) distances in the nine-coordinate ODA^{2-} complex of erbium ($[Er(ODA)_3]^{3-}$:[130] Er-O(carb, ave) = 2.35 Å, Er-O(ether,ave) = 2.49 Å) are substantially longer than those seen in $[Er(EGTA)(OH_2)]^-$. It appears, however, that the Er-O(ether) distances in the ODA^{2-} complex are anomalously long, since they are approximately 0.05 Å longer than would be expected, based on the isomorphous cerium structure.[131]

Despite the fact that all mean metal-ligand distances are shorter for erbium than for calcium, the erbium ion

Table 6.5 Metal-Ligand Distances (Å) and Angles (deg)[a] for $Ca[Er(EGTA)(OH_2)]_2 \cdot 12H_2O \cdot (CH_3)_2CO$

(a) Complex Ions

Complex a		Complex b	
Er1-N1	2.526(6)	Er2-N3	2.548(6)
Er1-N2	2.599(7)	Er2-N4	2.595(7)
Er1-O1	2.288(5)	Er2-O11	2.298(4)
Er1-O3	2.327(5)	Er2-O13	2.309(5)
Er1-O5	2.468(5)	Er2-O15	2.453(5)
Er1-O6	2.389(6)	Er2-O16	2.353(5)
Er1-O7	2.299(6)	Er2-O17	2.267(6)
Er1-O9	2.344(4)	Er2-O19	2.335(4)
Er1-w1	2.459(5)	Er2-w2	2.466(5)
N1-Er1-N2	133.6(2)	N3-Er2-N4	133.3(2)
N1-Er1-O1	68.9(2)	N3-Er2-O11	68.1(2)
N2-Er1-O1	76.5(2)	N4-Er2-O11	76.7(2)
N1-Er1-O3	65.8(2)	N3-Er2-O13	66.0(2)
N2-Er1-O3	131.8(2)	N4-Er2-O13	130.3(2)
O1-Er1-O3	133.7(2)	O11-Er2-O13	132.5(2)
N1-Er1-O5	68.8(2)	N3-Er2-O15	69.1(2)
N2-Er1-O5	128.5(2)	N4-Er2-O15	128.6(2)
O1-Er1-O5	72.8(2)	O11-Er2-O15	73.4(2)
O3-Er1-O5	98.9(2)	O13-Er2-O15	100.4(2)
N1-Er1-O6	129.2(2)	N3-Er2-O16	130.8(2)
N2-Er1-O6	67.2(2)	N4-Er2-O16	67.3(2)
O1-Er1-O6	76.5(2)	O11-Er2-O16	79.5(2)
O3-Er1-O6	142.9(2)	O13-Er2-O16	142.6(2)
O5-Er1-O6	66.1(2)	O15-Er2-O16	66.8(2)
N1-Er1-O7	76.7(2)	N3-Er2-O17	76.5(2)
N2-Er1-O7	67.1(2)	N4-Er2-O17	67.4(2)
O1-Er1-O7	79.4(2)	O11-Er2-O17	79.3(2)
O3-Er1-O7	81.4(2)	O13-Er2-O17	79.1(2)
O5-Er1-O7	141.5(2)	O15-Er2-O17	142.0(2)
O6-Er1-O7	132.0(2)	O16-Er2-O17	133.2(2)
N1-Er1-O9	134.1(2)	N3-Er2-O19	135.2(2)
N2-Er1-O9	68.0(2)	N4-Er2-O19	68.2(2)
O1-Er1-O9	143.8(2)	O11-Er2-O19	144.4(2)
O3-Er1-O9	71.8(2)	O13-Er2-O19	71.8(2)
O5-Er1-O9	136.3(2)	O15-Er2-O19	134.7(2)
O6-Er1-O9	95.4(2)	O16-Er2-O19	92.2(2)
O7-Er1-O9	80.8(2)	O17-Er2-O19	81.8(2)
N1-Er1-w1	111.9(2)	N3-Er2-w2	109.7(2)
N2-Er1-w1	114.5(2)	N4-Er2-w2	117.0(2)
O1-Er1-w1	138.6(2)	O11-Er2-w2	140.7(2)
O3-Er1-w1	70.3(2)	O13-Er2-w2	68.7(2)
O5-Er1-w1	69.8(2)	O15-Er2-w2	69.8(1)
O6-Er1-w1	72.7(2)	O16-Er2-w2	73.9(2)
O7-Er1-w1	142.0(2)	O17-Er2-w2	139.7(2)
O9-Er1-w1	66.8(2)	O19-Er2-w2	65.8(2)

Table 6.5 (continued)

(b) Counterions

Ca1-O3	2.466(4)
Ca1-O9	2.504(5)
Ca1-O13	2.459(5)
Ca1-O19	2.494(5)
Ca1-w1	2.501(5)
Ca1-w2	2.458(5)
Ca1-w3	2.336(6)
Ca1-w4	2.355(6)

O3-Ca1-O9	66.9(2)
O3-Ca1-O13	154.7(2)
O9-Ca1-O13	136.7(2)
O3-Ca1-O19	138.1(2)
O9-Ca1-O19	76.7(2)
O13-Ca1-O19	66.7(2)
O3-Ca1-w1	67.4(2)
O9-Ca1-w1	63.8(2)
O13-Ca1-w1	126.3(2)
O19-Ca1-w1	78.6(2)
O3-Ca1-w2	123.6(2)
O9-Ca1-w2	77.2(2)
O13-Ca1-w2	66.5(2)
O19-Ca1-w2	63.7(2)
w1-Ca1-w2	130.8(2)
O3-Ca1-w3	78.8(2)
O9-Ca1-w3	116.8(2)
O13-Ca1-w3	80.6(2)
O19-Ca1-w3	138.6(2)
w1-Ca1-w3	142.8(2)
w2-Ca1-w3	80.7(2)
O3-Ca1-w4	88.1(2)
O9-Ca1-w4	136.6(2)
O13-Ca1-w4	77.6(2)
O19-Ca1-w4	105.9(2)
w1-Ca1-w4	74.1(2)
w2-Ca1-w4	143.9(2)
w3-Ca1-w4	90.3(2)

(c) Interionic Angles

Er1-O3-Ca1	101.7(2)
Ca1-O3-C4	133.3(5)
Er1-O9-Ca1	100.1(2)
Ca1-O9-C14	134.3(4)
Er2-O13-Ca1	102.5(2)
Ca1-O13-C18	132.0(4)
Er2-O19-Ca1	100.7(2)
Ca1-O19-C28	132.9(4)
Er1-w1-Ca1	97.1(2)
Er2-w2-Ca1	98.1(2)

(a) Estimated standard deviations in the least significant digits are given in parentheses.

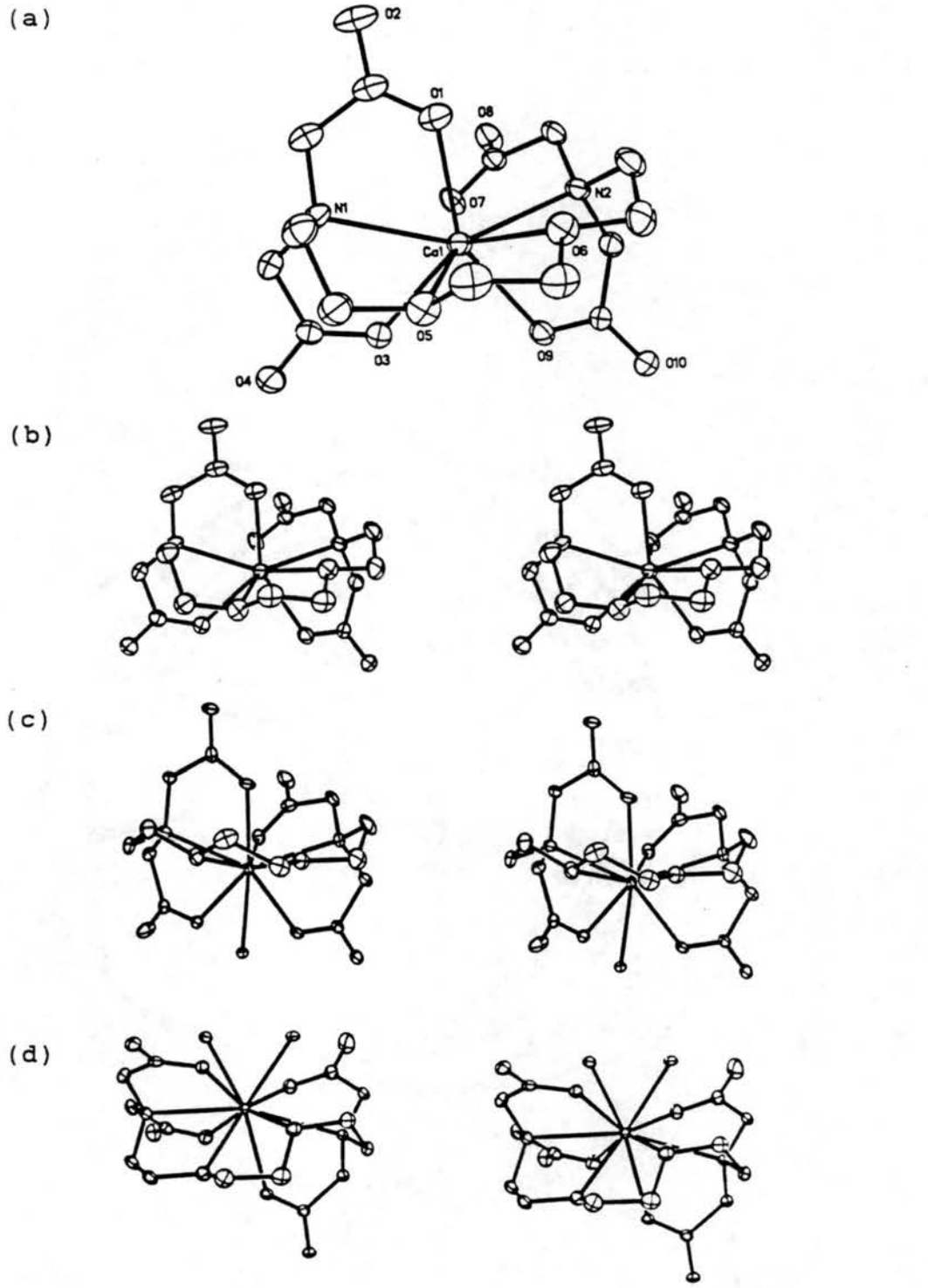

Figure 6.7 (a) Reference complex anion with numbering scheme. (b) Stereoview of $[Ca(EGTA)]^{2-}$. (c) Stereoview of $[Er(EGTA)(OH_2)]^{-}$. (d) Stereoview of $[Nd(EGTA)(OH_2)]^{-}$.

complex is nine-coordinate, while the calcium ion complex is eight-coordinate. In comparing the structures of $[Ca(EGTA)]^{2-}$ and $[Er(EGTA)]^{-}$ (see Figure 6.7(a) and (b)), it is easy to see that the room for the ninth ligand is provided by conformational rearrangement of the N-O-O-N amino-ether belt. This belt adopts a relatively planar configuration, as was seen for $[Sr(EGTA)]^{2-}$ and $[Ba(EGTA)]^{2-}$; O6 exhibits a planar bonding mode, as did O5 in $[Ba(EGTA)]^{2-}$. The extra ligand in $[Sr(EGTA)]^{2-}$, instead of being bound between the N-O-O-N belt and the two carboxylate groups as in $[Er(EGTA)]^{2-}$, is bound between four carboxylate groups. The conformational change in **7** is most evident in the O1···O5 contact distance, which, shortens to 2.8 Å in the case of erbium ion, compared to 3.6 Å in the case of calcium ion. A meridional conformation is seen for the N1-O1-O3 iminodiacetate end of the $EGTA^{4-}$ ligand, and a bent conformation is observed for the N2-O7-O9 end, as was the case for the calcium ion complex. This is apparently necessary as a result of the constraints associated with wrapping the $EGTA^{4-}$ ligand about the relatively small erbium ion. The chelate ring bonding and conformational parameters for **7** are summarized in Tables 6.6 and 6.7, respectively.

The inequivalencies in the chemically equivalent bond lengths in complex a and complex b follow the same patterns. Of the two amine nitrogen atoms in each complex anion, the nitrogen atoms N2 and N4 are bound at longer

Table 6.6 Chelate Ring[a] Bonding Parameters[b] for $Ca[Er(EGTA)(OH_2)]_2 \cdot 12H_2O \cdot (CH_3)_2CO$

Glycinate Rings

	C-C'	C'-N	C-O	C-O'	C-C'-N	O-C-O'	C'-C-O	C'-C-O'	Er-N-C'	Er-O-C
G1	1.515(12)	1.495(9)	1.282(9)	1.238(9)	112.8(6)	125.0(8)	117.3(6)	117.7(7)	109.7(5)	125.3(5)
G2	1.505(10)	1.459(11)	1.277(10)	1.223(11)	112.4(6)	125.9(6)	115.5(7)	118.6(7)	109.3(4)	124.0(4)
G3	1.530(13)	1.461(10)	1.276(10)	1.245(10)	112.7(7)	123.6(8)	117.9(7)	118.4(8)	104.7(5)	120.9(5)
G4	1.506(12)	1.471(9)	1.271(9)	1.236(8)	116.6(7)	124.4(7)	117.7(6)	117.8(7)	110.7(5)	125.4(4)
G5	1.531(11)	1.494(8)	1.263(9)	1.249(8)	110.3(6)	124.1(8)	119.5(6)	116.3(7)	111.9(5)	125.6(5)
G6	1.525(9)	1.487(9)	1.270(9)	1.231(9)	110.9(6)	125.5(6)	116.7(6)	117.7(7)	109.6(4)	124.9(4)
G7	1.517(12)	1.467(10)	1.253(10)	1.254(10)	112.7(6)	124.2(8)	118.4(7)	117.4(7)	104.4(5)	122.2(5)
G8	1.517(9)	1.502(8)	1.256(9)	1.248(8)	114.5(6)	124.6(6)	119.4(6)	116.0(7)	111.2(4)	126.2(4)

Amino-Ether Rings

	C-C'	C-N	C'-O	C-C'-O	C'-C-N	C"-N-C[†]	C-N-C"	C-N-C[†]	Er-N-C	Er-O-C'
A1	1.499(14)	1.491(11)	1.433(10)	106.4(6)	111.5(7)	110.6(6)	111.7(5)	109.1(7)	106.4(5)	117.2(5)
A2	1.483(15)	1.489(13)	1.434(12)	108.4(8)	111.5(9)	110.8(6)	110.8(6)	109.4(7)	110.4(5)	120.3(6)
A3	1.524(11)	1.470(11)	1.430(9)	106.3(6)	112.0(7)	110.1(5)	110.8(5)	109.0(6)	105.4(4)	117.7(5)
A4	1.501(12)	1.484(10)	1.446(11)	105.6(6)	111.4(6)	109.8(6)	112.2(5)	110.5(6)	108.6(5)	122.3(5)

Diether Rings

	C-C'	C'-O'	C-O	C'-C-O	C-C'-O'	C'-O'-C[†]	C"-O-C	Er-O-C	Er-O'-C'
E1	1.486(12)	1.407(12)	1.454(12)	109.5(7)	107.7(8)	117.8(7)	111.4(6)	115.7(5)	121.2(5)
E2	1.496(12)	1.445(10)	1.468(9)	106.9(6)	107.0(6)	117.1(6)	111.0(5)	115.4(4)	120.4(5)

(a) Chelate ring nomenclature is described in Figure 4.2(b). Rings within each series are numbered with increasing oxygen number.

(b) Bond lengths are given in Ångstroms and bond angles are given in degrees. Estimated standard deviations in the least significant digits are given in parentheses.

Table 6.7 Chelate Ring[a] Conformational Parameters[b] for $Ca[Er(EGTA)(OH_2)]_2 \cdot 12H_2O \cdot (CH_3)_2CO$

Glycinate Rings

	Ring Type	Bridging[c] Interaction	N-Er-O-C	Er-O-C-C'	O-C-C'-N	C-C'-N-Er	C'-N-Er-O	ΔC_s,min[d] ΔC_s,max	ΔC_2,min ΔC_2,max
G1	δ	0	-9.1(6)	-3.1(10)	21.5(10)	-26.7(7)	18.6(5)	10.5(N) 29.6(O)	4.7(O) 38.7(N)
G2	λ	3	26.3(5)	-16.3(9)	-15.3(10)	34.4(8)	-30.0(5)	8.4(N) 48.4(C)	5.8(C) 54.2(N)
G3	δ	0	-30.5(5)	21.0(8)	15.4(9)	-36.3(6)	33.5(4)	10.9(N) 53.8(C)	5.7(C) 60.7(Er)
G4	λ	3	-10.6(6)	15.9(10)	-11.2(11)	2.5(9)	3.0(5)	6.6(C) 15.9(N)	.6(N) 21.3(C)
G5	δ	0	-7.2(6)	-3.9(11)	19.2(11)	-23.1(7)	16.4(4)	9.3(C') 26.4(O)	3.1(O) 33.6(N)
G6	λ	3	26.4(6)	-17.5(10)	-13.1(10)	31.8(7)	-28.9(4)	9.6(N) 46.5(C)	4.9(C) 52.4(Er)
G7	δ	0	-29.2(5)	20.1(9)	14.9(10)	-34.2(7)	31.5(4)	10.1(Er) 51.2(C)	5.1(C) 57.6(Er)
G8	λ	3	-7.2(6)	9.6(10)	-5.2(11)	-0.6(8)	3.2(5)	2.2(O) 9.9(C')	3.0(N) 13.3(O)

Amino-Ether Rings

	Ring Type	O-Er-N-C	Er-N-C-C'	N-C-C'-O	C-C'-O-Er	C'-O-Er-N	ΔC_s,min ΔC_s,max	ΔC_2,min ΔC_2,max
A1	λ	-23.2(4)	53.6(6)	-61.1(8)	36.7(8)	-7.6(5)	10.9(C) 67.5(Er)	16.3(Er) 91.5(C)
A2	λ	-12.0(4)	38.5(8)	-52.9(9)	43.5(9)	-17.1(5)	16.5(C') 61.5(Er)	5.1(Er) 78.7(C')
A3	λ	-24.1(4)	54.0(6)	-61.0(7)	35.2(7)	-6.7(4)	9.3(C) 66.7(Er)	18.1(Er) 91.5(C)
A4	λ	-16.3(4)	44.3(7)	-55.3(7)	41.6(7)	-14.4(4)	19.5(C) 64.5(Er)	2.3(Er) 81.5(C)

Table 6.7 (continued)

		Diether Rings						
	Ring Type	O'-Er-O-C	Er-O-C-C'	O-C-C'-O'	C-C'-O'-Er	C'-O'-Er-O	ΔC_s,min ΔC_s,max	ΔC_2,min ΔC_2,max
E1	δ	13.8(5)	-38.6(9)	48.8(9)	-39.9(8)	15.2(5)	17.7(C') 59.2(Er)	1.4(Er) 73.4(C')
E2	δ	16.8(4)	-43.0(7)	52.1(8)	-41.5(7)	14.3(4)	18.6(C) 63.7(Er)	2.1(Er) 78.9(C)

(a) Chelate ring nomenclature is described in Figure 4.2(b). Rings within each series are numbered with increasing oxygen number.
(b) Torsion angles are given in degrees. Estimated standard deviations in the least significant digits are given in parentheses.
(c) The bridge types are schematically depicted in Figure 4.2(a). Type 0 implies no interaction.
(d) The symmetry unique atom of the summation is given in parentheses.

distances than are N1 and N3 (Er-N1/N3 = 2.54(2) Å, Er-N2/N4 = 2.597(3) Å). This may be associated with the unusual conformation at the ether oxygen atoms, O6 and O16, which are adjacent to N2 and N4 in the two complexes. Additionally, the ether oxygen atoms bound in the "planar" mode exhibit shorter Er-O(ether) distances than those that are not bound in the planar fashion (Er-O5/O15 = 2.46(1) Å, Er-O6/O16 = 2.37(3) Å). This is consistent with the bonding behavior of the "planar" oxygen atoms of complexes **b** and **c** in $[Ba(EGTA)]^{2-}$, although the differences seen in that case were smaller (0.03 Å for complex **b** and 0.08 Å for complex **c**).

The only conformational irregularities observed for $[Er(EGTA)(OH_2)]^-$ are associated with the A1 and A3 amino-ether rings. The minimum asymmetry parameters associated with those two rings correspond to a mirror plane through the carbon atom bound to the nitrogen atom (instead of the usual conformation involving a C_2 axis passing through the metal ion). These effects are similar to those observed in the case of the barium complex of $EGTA^{4-}$ (**5**). The inter-ring torsion angles (see Table 6.8) are characteristic of the planar mode of coordination of the N-O-O-N belt and the meridional and bent conformations of the iminodiacetate portion of the molecule.

Table 6.8 Inter-ring Torsion Angles[a] for $Ca[Er(EGTA)(OH_2)]_2 \cdot 12H_2O \cdot (CH_3)_2CO$

	complex a	complex b
C2-C1-N1-C5	91.0(8)	94.1(8)
C4-C3-N1-C5	-81.5(7)	-83.1(7)
C12-C11-N2-C10	-155.3(7)	-151.7(7)
C14-C13-N2-C10	124.4(8)	120.2(7)
C2-C1-N1-C3	-147.3(6)	-145.2(7)
C4-C3-N1-C1	155.3(6)	155.2(7)
C12-C11-N2-C13	83.1(8)	85.1(8)
C14-C13-N2-C11	-113.2(8)	-115.6(8)
C1-N1-C5-C6	-66.0(8)	-67.2(7)
C3-N1-C5-C6	171.4(6)	171.5(5)
C11-N2-C10-C9	154.0(7)	159.2(7)
C13-N2-C10-C9	-83.5(9)	-77.9(8)
C5-C6-O5-C7	173.1(7)	171.3(6)
C10-C9-O6-C8	-146.3(8)	-143.2(6)
C6-O5-C7-C8	-175.7(7)	179.8(6)
C9-O6-C8-C7	150.0(7)	143.2(6)

(a) Torsion angles are given in degrees. Estimated standard deviations in the least significant digits are given in parentheses.

Structure of a Ten-Coordinate Neodymium Chelate of $EGTA^{4-}$, $Ca[Nd(EGTA)(OH_2)]\cdot 9H_2O$ (8)

As expected (see above), an increase in coordination number from nine to ten is observed on going from the erbium to the neodymium chelate of $EGTA^{4-}$. Ten-coordination is achieved in the solid state by binding to a carboxylate oxygen atom from an adjacent complex ion, as well as to a water molecule (see Figure 6.8(a)). The structure of **8** is such that only one complex anion resides in the asymmetric unit. The ligand atoms about the Nd^{3+} ion occupy the vertices of a distorted bicapped square antiprism (see Figures 6.8(b) and (c)). The two square faces of the antiprism are made up of O1-w1-O3-O5 and O10a-O7-O6-O9. The nitrogen atoms, N1 and N2, cap the square faces.

Each neodymium chelate engages in three type 2 carboxylate bridging interactions. Two of these interactions involve bridging to two different calcium counterions (see Figure 6.9(a)). The third interaction involves bridging to an adjacent neodymium complex in the unit cell. The calcium counterion occupies a special position of $\bar{1}$ symmetry in the unit cell. This complex anion-cation network is propagated in the $\underline{y}$-$\underline{z}$ plane to produce polymeric sheets, which are linked together by hydrogen bonding interactions with the occluded water molecules (see Figure 6.9(b)).

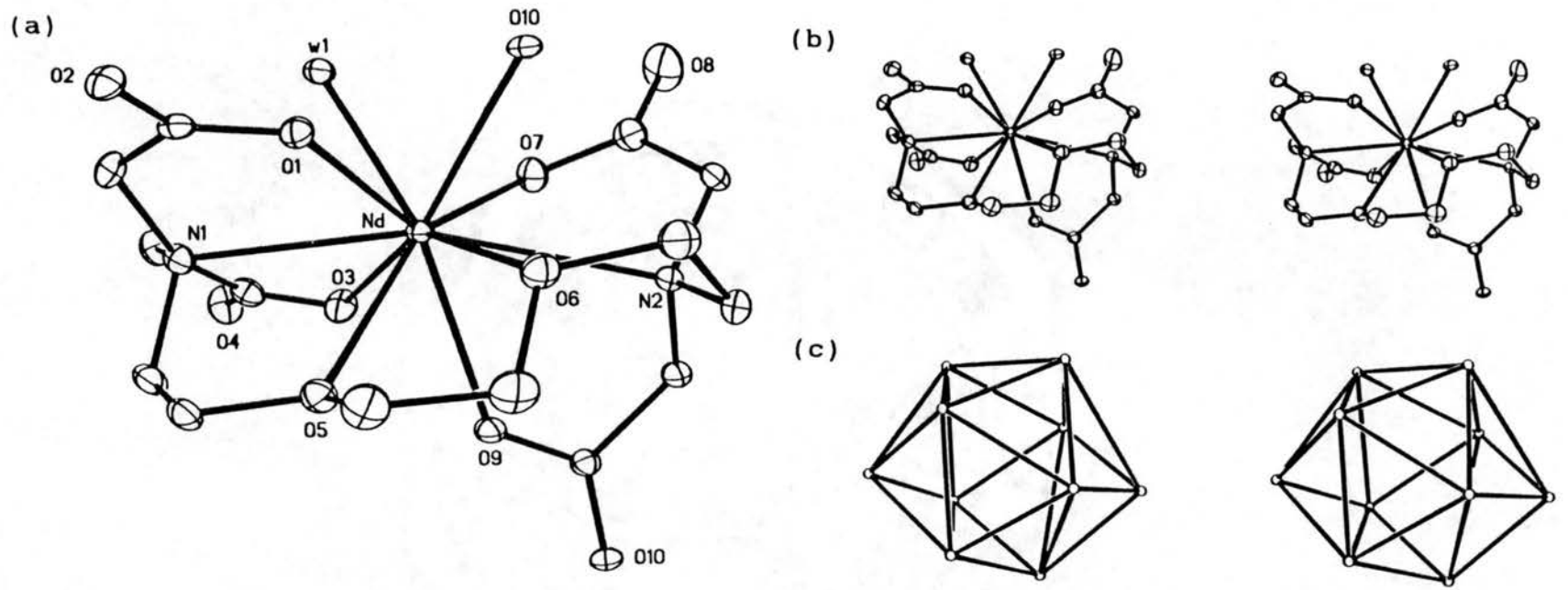

Figure 6.8 (a) A thermal ellipsoid plot (30%) of the ten coordinate $[Nd(EGTA)(OH_2)]^-$ complex anion. For details of the numbering scheme, see Figure 4.1(a). (b) Stereoview of $[Nd(EGTA)(OH_2)]^-$. (c) Stereoview of the coordination polyhedron formed by the ligand atoms about Nd (see text).

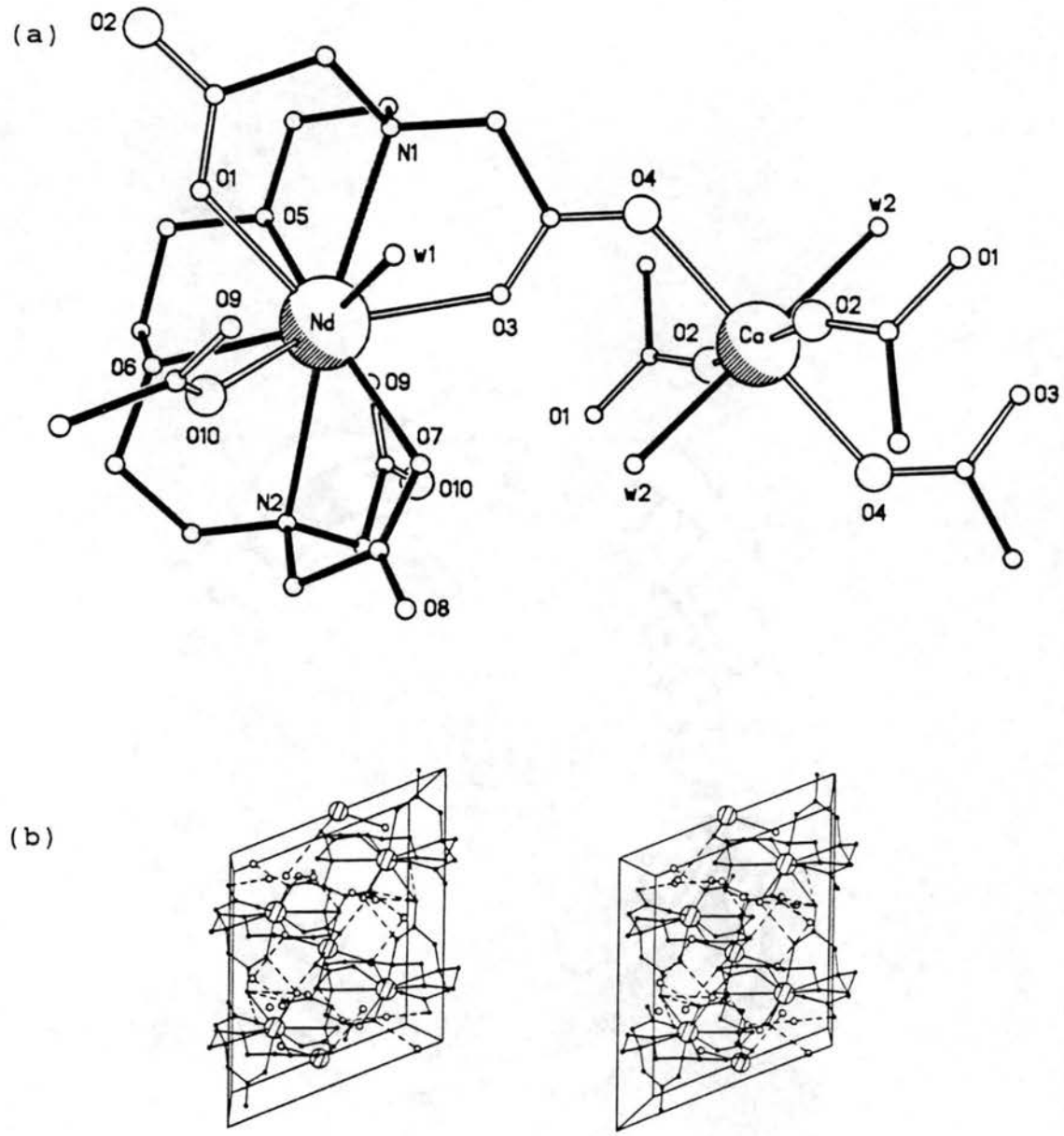

Figure 6.9 (a) Ball and stick plot depicting all the unique interionic interactions in the lattice of $Ca[Nd(EGTA)(OH_2)]_2 \cdot 9H_2O$ (9). Conventions regarding ionic radii of the atoms are described in the caption of Figure 4.3(a). (b) Unit cell of 9 viewed along b.

The crystallographically required $\bar{1}$ symmetry of the calcium ion is satisfied by the octahedral coordination of the calcium ion. In addition to the oxygen atoms of four bridging carboxylate groups, two water molecules are coordinated to the calcium ion. The bridging distance to O4 (Ca-O4 = 2.348(3) Å) is similar to the type 2 bridging distances seen in **2**, while the bridge from O2 is considerably shorter (Ca-O2 = 2.273(3) Å). The single unique water molecule is also bound at a typical distance.[89] The bonding parameters for the calcium and neodymium ions are summarized in Table 6.9.

The mode of wrapping the $EGTA^{4-}$ ligand about the neodymium ion is not a simple perturbation on the erbium ion complex structure. The extra coordination sites in the neodymium complex are obtained by twisting the meridional iminodiacetate portion of the $EGTA^{4-}$ ligand about the Nd-N bond (see Figure 6.8(d)). This results in the ether oxygen atom occupying the coordination position which was occupied by the water molecule in the erbium structure. The water molecule and the bridging carboxylate group occupy sites vacated by the twisting. The meridional/bent conformations which characterized the iminodiacetate ends of the $EGTA^{4-}$ ligand in **7** (and **2**) are maintained in **8**.

The oxygen atom donated through a type 2 carboxylate bridge is bound at a distance intermediate in the range of intrachelate Nd-O(carb) distances (Nd-O(carb) = 2.446(3)-2.480(3) Å, Nd-O10a = 2.467(2) Å). These carboxylate oxygen

Table 6.9 Metal-Ligand Distances (Å) and Angles (deg)[a] for $Ca[Nd(EGTA)(OH_2)]_2 \cdot 9H_2O$

(a) Complex Ion

Nd-N1	2.757(3)	Nd-O6	2.642(3)
Nd-N2	2.862(3)	Nd-O7	2.449(2)
Nd-O1	2.446(3)	Nd-O9	2.481(3)
Nd-O3	2.453(2)	Nd-w1	2.533(3)
Nd-O5	2.687(2)	Nd-O10a	2.468(2)

N1-Nd-N2	161.9(1)	O1-Nd-O9	130.9(1)
N1-Nd-O1	63.8(1)	O3-Nd-O9	71.0(1)
N2-Nd-O1	127.7(1)	O5-Nd-O9	65.1(1)
N1-Nd-O3	62.0(1)	O6-Nd-O9	78.4(1)
N2-Nd-O3	107.4(1)	O7-Nd-O9	89.8(1)
O1-Nd-O3	124.8(1)	N1-Nd-w1	66.7(1)
N1-Nd-O5	63.5(1)	N2-Nd-w1	126.8(1)
N2-Nd-O5	105.9(1)	O1-Nd-w1	76.0(1)
O1-Nd-O5	66.8(1)	O3-Nd-w1	74.4(1)
O3-Nd-O5	96.9(1)	O5-Nd-w1	127.0(1)
N1-Nd-O6	118.5(1)	O6-Nd-w1	136.8(1)
N2-Nd-O6	62.0(1)	O7-Nd-w1	72.4(1)
O1-Nd-O6	70.7(1)	O9-Nd-w1	144.7(1)
O3-Nd-O6	148.3(1)	N1-Nd-O10a	124.6(1)
O5-Nd-O6	61.7(1)	N2-Nd-O10a	73.2(1)
N1-Nd-O7	123.8(1)	O1-Nd-O10a	70.7(1)
N2-Nd-O7	59.4(1)	O3-Nd-O10a	138.5(1)
O1-Nd-O7	138.3(1)	O5-Nd-O10a	123.4(1)
O3-Nd-O7	71.2(1)	O6-Nd-O10a	70.1(1)
O5-Nd-O7	154.8(1)	O7-Nd-O10a	74.6(1)
O6-Nd-O7	117.7(1)	O9-Nd-O10a	131.9(1)
N1-Nd-O9	102.0(1)	w1-Nd-O10a	73.4(1)
N2-Nd-O9	60.0(1)		

(b) Counterion

Ca-O4	2.348(3)
Ca-w2	2.390(3)
Ca-O2a	2.273(3)

O4-Ca-w2	90.2(1)
O4-Ca-O2a	91.1(1)
w2-Ca-O2a	92.5(1)

(c) Interionic Angles

C2-O2-Caa	147.9(3)
Ca-O4-C4	129.9(3)
C14-O10-Nda	139.1(2)

(a) Estimated standard deviations in the least significant digits are given in parentheses.

distances are similar to those observed in the low-quality structure determination of $[Nd(EDTA)(OH_2)_3]^-$ (Nd-N = 2.8 Å, Nd-O(carb) = 2.5 Å),[14] and in the nine-coordinate neodymium ion in $Ba[Nd(DTPA)(OH_2)]\cdot 2H_2O$ (Nd-O(carb,ave) = 2.45(6) Å).[45]

The Nd-N distance in a nine-coordinate $[Nd(IDA)(OH_2)_3]^+$ complex is 2.67(2) Å.[132] For the nine-coordinate Nd^{3+} ion in $Na_3[Nd(ODA)_3]$, Nd-O(ether) = 2.523(10) Å, Nd-O(carb) = 2.428(6) Å.[133] In the $[Nd(DTPA)(OH_2)]^-$ complex mentioned above, Nd-N(ave) = 2.76(7) Å. Although the carboxylate oxygen atoms appear to be bonded at the expected distances, the amine nitrogen atoms and ether oxygen atoms appear to bonded at a considerably longer distance than would be expected (Nd-N(ave) = 2.81(7) Å, Nd-O(ether,ave) = 2.67(3) Å in 9), based on these results.

The difference in the ionic radius of nine-coordinate erbium ion and ten-coordinate neodymium ion is ~0.14 Å.[118] The difference in the mean metal-carboxylate bond distances between the erbium and neodymium chelates (0.15 Å) is compatible with this difference in ionic radii. For both the amine nitrogen atoms and ether oxygen atoms, this difference in mean metal-ligand distance between the two chelates is considerably larger (0.24 Å and 0.25 Å, respectively). Apparently the binding preferences of the favored ligands are satisfied to the detriment of the weaker ligands' binding.

The difference in the chemically equivalent Nd-N distances, relative to the erbium chelate, is larger; the corresponding difference in the Nd-O(ether) distances is smaller for Nd^{3+} than for Er^{3+}. These differences, once again, must be associated with the constraints of wrapping the $EGTA^{4-}$ ligand around the relatively small ten-coordinate metal ion (compared to Ba^{2+}, for instance).

The chelate ring bonding and conformational parameters are summarized in Tables 6.10 and 6.11, respectively. Distinctly irregular conformations are observed for the amino-ether rings in the neodymium chelate. For A1, the O-Nd-N-C and Nd-N-C-C' torsion angles are abnormally high and the C-C'-O-Nd and C'-O-Nd-N torsion angle are abnormally low; for A2 the converse is true. The irregularities are not associated with a "planar" mode of coordination for the ether oxygen atom, as was the case for the barium and erbium chelates. Instead, the strange conformation adopted by the N-O-O-N belt as a result of the twisted iminodiacete unit seems to be responsible for the unusual conformational parameters and minimum asymmetry parameters (minimum asymmetry parameters correspond to mirror planes associated with C and C', instead of a C_2 associated with the metal ion). The glycinate ring conformational parameters are not unusual.

The inter-ring torsion angles (see Table 6.12) describing the conformation of the N-O-O-N belt are similar to those observed for the calcium chelate. The torsion

Table 6.10 Chelate Ring[a] Bonding Parameters[b] for $Ca[Nd(EGTA)(OH_2)]_2 \cdot 9H_2O$

Glycinate Rings

	C-C'	C'-N	C-O	C-O'	C-C'-N	O-C-O'	C'-C-O	C'-C-O'	Nd-N-C'	Nd-O-C
G1	1.522(5)	1.474(5)	1.259(5)	1.251(5)	113.0(3)	124.9(3)	117.8(3)	117.3(3)	109.9(2)	128.2(2)
G2	1.525(6)	1.479(5)	1.260(5)	1.246(4)	111.5(4)	125.6(4)	117.9(3)	116.4(4)	109.2(2)	127.1(3)
G3	1.512(6)	1.458(5)	1.271(4)	1.239(5)	111.6(3)	124.4(4)	117.6(3)	118.0(3)	104.4(2)	122.6(2)
G4	1.517(4)	1.469(5)	1.263(5)	1.253(5)	111.3(3)	125.7(3)	116.6(4)	117.7(4)	106.8(2)	129.7(2)

Amino-Ether Rings

	C-C'	C-N	C'-O	C-C'-O	C'-C-N	C"-N-C†	C-N-C"	C-N-C†	Nd-N-C	Nd-O-C'
A1	1.495(6)	1.475(5)	1.432(5)	108.8(3)	113.1(3)	111.7(3)	111.4(3)	107.9(3)	106.6(2)	119.2(2)
A2	1.495(6)	1.470(5)	1.446(4)	110.2(3)	111.5(4)	110.2(3)	112.2(3)	109.9(3)	113.2(2)	116.2(2)

Diether Ring

	C-C'	C'-O'	C-O	C'-C-O	C-C'-O'	C'-O'-C†	C"-O-C	Nd-O-C	Nd-O'-C'
E1	1.487(6)	1.428(5)	1.441(5)	108.7(3)	108.0(4)	112.2(3)	110.7(3)	116.8(2)	117.2(2)

(a) Chelate ring nomenclature is described in Figure 4.2(b). Rings within each series are numbered with increasing oxygen number.
(b) Bond lengths are given in Ångstroms and bond angles are given in degrees. Estimated standard deviations in the least significant digits are given in parentheses.

Table 6.11 Chelate Ring[a] Conformational Parameters[b] for $Ca[Nd(EGTA)(OH_2)]_2 \cdot 9H_2O$

Glycinate Rings

	Ring Type	Bridging[c] Interaction	N-Nd-O-C	Nd-O-C-C'	O-C-C'-N	C-C'-N-Nd	C'-N-Nd-O	ΔC_s,min[d] ΔC_s,max	ΔC_2,min ΔC_2,max
G1	δ	2	-4.3(3)	-10.5(5)	28.0(5)	-28.9(3)	17.7(2)	5.1(C') 34.0(O)	8.5(O) 44.9(C')
G2	λ	2	24.8(3)	-15.0(5)	-17.1(5)	34.0(3)	-28.9(2)	6.5(N) 47.4(C)	6.7(C) 53.4(N)
G3	δ	0	-40.8(3)	35.8(5)	9.8(5)	-38.1(3)	38.3(2)	2.4(Nd) 64.4(C)	18.5(C) 76.5(Nd)
G4	δ	2	-22.8(3)	8.2(4)	27.1(5)	-40.8(3)	31.3(2)	7.4(N) 51.4(C)	18.5(C) 62.0(N)

Amino-Ether Rings

	Ring Type	O-Nd-N-C	Nd-N-C-C'	N-C-C'-O	C-C'-O-Nd	C'-O-Nd-N	ΔC_s,min ΔC_s,max	ΔC_2,min ΔC_2,max
A1	λ	-27.3(2)	57.0(4)	-59.2(5)	29.0(4)	-1.0(2)	2.0(C) 64.3(O)	27.2(Nd) 91.3(C)
A2	δ	2.9(2)	-30.8(3)	56.6(4)	-56.0(4)	27.3(3)	2.5(C') 65.0(Nd)	24.8(Nd) 89.6(C')

Diether Ring

	Ring Type	O'-Nd-O-C	Nd-O-C-C'	O-C-C'-O'	C-C'-O'-Nd	C'-O'-Nd-O	ΔC_s,min ΔC_s,max	ΔC_2,min ΔC_2,max
E1	δ	12.5(3)	-41.7(5)	58.3(4)	-49.5(4)	20.3(3)	16.4(C') 68.5(Nd)	7.8(Nd) 87.9(C')

(a) Chelate ring nomenclature is described in Figure 4.2(b). Rings within each series are numbered with increasing oxygen number.
(b) Torsion angles are given in degrees. Estimated standard deviations in the least significant digits are given in parentheses.
(c) The bridge types are schematically depicted in Figure 4.2(a). Type 0 implies no interaction.
(d) The symmetry unique atom of the summation is given in parentheses.

Table 6.12 Inter-ring Torsion Angles[a] for $Ca[Nd(EGTA)(OH_2)]_2 \cdot 9H_2O$

C2-C1-N1-C5	89 0(3)	C4-C3-N1-C5	-81.5(4)
C12-C11-N2-C10	-161.0(4)	C14-C13-N2-C10	82.3(4)
C2-C1-N1-C3	-150.3(3)	C4-C3-N1-C1	155.8(3)
C12-C11-N2-C13	76.3(4)	C14-C13-N2-C11	-153.6(3)
C1-N1-C5-C6	-63.0(4)	C3-N1-C5-C6	174.1(4)
C11-N2-C10-C9	87.1(4)	C13-N2-C10-C9	-150.0(3)
C5-C6-O5-C7	168.7(3)	C10-C9-O6-C8	82.8(4)
C6-O5-C7-C8	177.5(4)	C9-O6-C8-C7	172.2(3)

(a) Torsion angles are given in degrees. Estimated standard deviations in the least significant digits are given in parentheses.

angle at the N2 end is near 90°, while the other three are near 180°. The torsion angles of the iminodiacetate terminii are characteristic of the meridional and bent conformations observed.

Conclusions

Distinct differences in ligand atom preferences and coordination number preference are observed for the "probe" ions when substituted into the highly calcium-selective $EGTA^{4-}$ ligand environment. The difference in the affinity of cadmium ion, in comparison to calcium ion, for the neutral ether oxygen atom donors may be important in explaining NMR results for cadmium ion in the cadmium-substituted protein sites. The higher coordination numbers exhibited by the lanthanide ions, despite their similarity to calcium ion in size, would imply that they are unlikely to have the same coordination number as calcium ion when substituted into a protein site.

CHAPTER 7

TRANSITION METAL COMPLEXES OF $EGTA^{4-}$

Introduction

Eight-coordination is not common for metal ions of the first transition series. To explore structural variations in complexes of such metal ions with $EGTA^{4-}$, the structures of the Mn(II) and Cu(II) complexes of $EGTA^{4-}$ have been determined.

High-spin manganese(II) ion, with an eight-coordinate ionic radius of 0.96 Å, is the largest of the dipositive first row transition metal ions.[118] Octadentate coordination, if possible for such metal ions, is most likely for this case.

A structure of a complex of the smaller copper(II) ion (ionic radius = 0.73 Å for a six coordinate ion[605]) with the octadentate ligand, $DTPA^{5-}$, has been determined.[134] The chelate was crystallized as the neutral, triprotonated species, $[Cu(H_3DTPA)]$, and contained an octahedral complex with two noncoordinated carboxylic acid groups. It is not clear how the copper(II) ion would achieve its desired lower coordination number with $EGTA^{4-}$, given the rather weak coordinating power of the ether oxygen atoms.

The Eight-Coordinate Manganese Chelate of $EGTA^{4-}$

Structure of $Sr[Mn(EGTA)]\cdot 7H_2O$ (10)

Both calcium ion (r_{ionic} = 1.12 Å)[118] and cadmium ion (r_{ionic} = 1.10 Å)[118] form eight-coordinate chelates with $EGTA^{4-}$. The mean metal-ligand distance, which is representative of the size of the metal ion within the chelate, is smaller for the case of cadmium (Ca-L(ave) = 2.46 Å, Cd-L(ave) = 2.43 Å), as expected. This small size difference between the two ions is sufficient to result in a different coordination number in the $EDTA^{4-}$ chelates; $[Ca(EDTA)]^{2-}$ is eight-coordinate in the solid state, whereas $[Cd(EDTA)]^{2-}$ is seven-coordinate. The ionic radius of Mn(II) is 0.14 Å smaller than that of the Cd(II) ion, and represents a decrease in available surface area on the metal ion of approximately 34%. If the coordinating atoms of the $EGTA^{4-}$ ligand bind to the Mn^{2+} ion at a distance consistent with the expected ionic radius, a lower coordination number might be expected for Mn(II). This expectation is not realized, however, as the strontium salt of $[Mn(EGTA)]^{2-}$ crystallizes isomorphously with $Sr[Cd(EGTA)]\cdot 7H_2O$ (7); the coordination sphere of the Mn(II) ion is dodecahedral, utilizing all eight possible ligand atoms of the $EGTA^{4-}$ ligand (see Figure 7.1(a)). As implied by the isomorphous nature of the crystals of 7 and 10, the complex anion and the partially aquated cation engage in an identical pattern of bridging interactions,

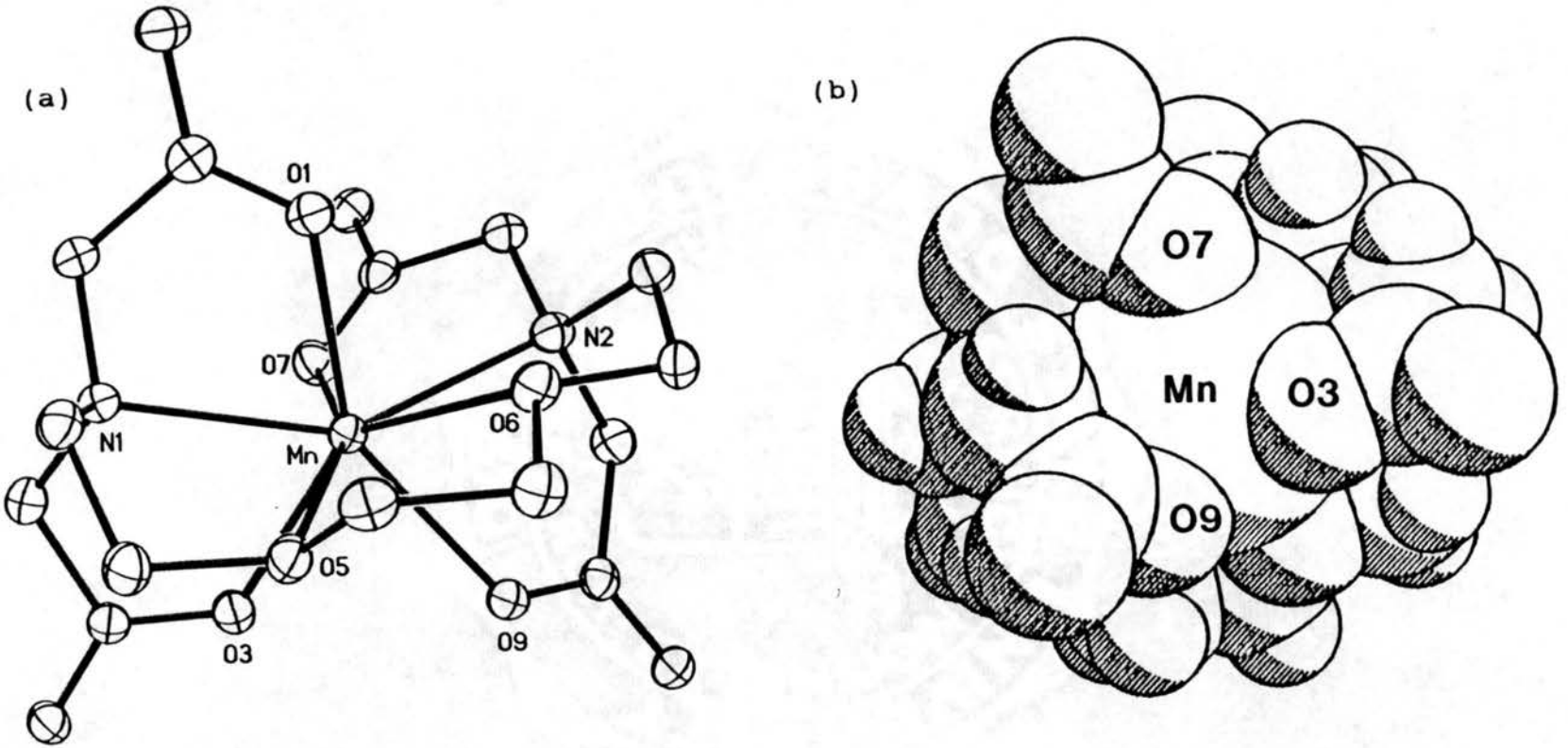

Figure 7.1 (a) A thermal ellipsoid plot (40%) of $[Mn(EGTA)]^{2-}$. (b) Space-filling plot of $[Mn(EGTA)]^{2-}$.

although there are differences in the individual bridging bond lengths and angles (see Table 7.1). The largest disparity occurs for the type 1 bridge to strontium involving O7 (Sr-O7 = 3.162(3) Å in **10**; Sr-O7 = 2.995(3) Å in $Sr[Cd(EGTA)]\cdot 7H_2O$).

The manganese(II) ion and the cadmium(II) ion exhibit similar ligand atom preferences. The carboxylate oxygen atoms are bound at the shortest distances (Mn-O(carb,ave) = 2.25(3) Å), followed by the amine nitrogen atoms (Mn-N(ave) = 2.426(1) Å), and the ether oxygen atoms (Mn-O(ether,ave) = 2.51(3) Å). In seven-coordinate $Mn[Mn(HEDTA)]_2\cdot 10H_2O$,[25] the mean Mn-O(carb) distance (Mn-O(carb,ave) = 2.24(2) Å) is nearly identical with that found in **10**, while the mean Mn-N distance (Mn-N(ave) = 2.38(3) Å) is shorter by 0.05 Å than in **10**. The Mn-O(carb) bond lengths in the $HEDTA^{3-}$ chelate do not seem to be influenced by the presence of the proton, which is involved in a strong hydrogen bond between carboxylate groups connecting the two $[Mn(HEDTA)]^-$ complex anions. Unfortunately, no good comparative data exist for the bond lengths from manganese(II) to ether oxygen atoms.

The differences in the mean metal-ligand bonding parameters exhibited for the manganese and cadmium $EGTA^{4-}$ chelates are not uniform between each ligand atom class. The amine nitrogen atoms are bound at the same distance in the two complex anions, while the carboxylate oxygen atoms and ether oxygen atoms are bound at average distances 0.10 Å and 0.09 Å shorter, respectively, in **10**. Based on the

Table 7.1 Metal-Ligand Distances (Å) and Angles (deg)[a] for $Sr[Mn(EGTA)]\cdot 7H_2O$

(a) Complex Ion

Mn-N1	2.426(3)
Mn-N2	2.427(3)
Mn-O1	2.211(3)
Mn-O3	2.256(3)
Mn-O5	2.493(3)
Mn-O6	2.529(3)
Mn-O7	2.285(3)
Mn-O9	2.233(3)
N1-Mn-N2	146.2(1)
N1-Mn-O1	71.0(1)
N2-Mn-O1	82.4(1)
N1-Mn-O3	70.6(1)
N2-Mn-O3	128.3(1)
O1-Mn-O3	140.4(1)
N1-Mn-O5	71.8(1)
N2-Mn-O5	132.4(1)
O1-Mn-O5	94.9(1)
O3-Mn-O5	81.7(1)
N1-Mn-O6	119.1(1)
N2-Mn-O6	69.4(1)
O1-Mn-O6	72.7(1)
O3-Mn-O6	136.4(1)
O5-Mn-O6	64.7(1)
N1-Mn-O7	89.3(1)
N2-Mn-O7	69.7(1)
O1-Mn-O7	89.6(1)
O3-Mn-O7	81.0(1)
O5-Mn-O7	157.8(1)
O6-Mn-O7	137.0(1)
N1-Mn-O9	140.6(1)
N2-Mn-O9	72.3(1)
O1-Mn-O9	143.5(1)
O3-Mn-O9	75.7(1)
O5-Mn-O9	83.9(1)
O6-Mn-O9	74.0(1)
O7-Mn-O9	105.2(1)

(b) Counterion

Sr-O9	2.781(3)
Sr-O10	2.660(3)
Sr-w1	2.547(4)
Sr-w2	2.697(3)
Sr-w3	2.552(3)
Sr-w4	2.531(3)
Sr-O7a	3.163(3)
Sr-O8a	2.596(3)
Sr-O10a	2.558(3)
O9-Sr-O10	47.9(1)
O9-Sr-w1	66.0(1)
O10-Sr-w1	78.9(1)
O9-Sr-w2	125.0(1)
O10-Sr-w2	94.3(1)
w1-Sr-w2	68.7(1)
O9-Sr-w3	147.2(1)
O10-Sr-w3	164.6(1)
w1-Sr-w3	108.6(1)
w2-Sr-w3	76.7(1)
O9-Sr-w4	71.6(1)
O10-Sr-w4	119.4(1)
w1-Sr-w4	80.7(1)
w2-Sr-w4	128.8(1)
w3-Sr-w4	75.6(1)
O9-Sr-O7a	109.5(1)
O10-Sr-O7a	116.9(1)
w1-Sr-O7a	155.5(1)
w2-Sr-O7a	124.5(1)
w3-Sr-O7a	61.2(1)
w4-Sr-O7a	75.3(1)
O9-Sr-O8a	74.8(1)
O10-Sr-O8a	73.4(1)
w1-Sr-O8a	140.8(1)
w2-Sr-O8a	139.6(1)
w3-Sr-O8a	105.3(1)
w4-Sr-O8a	89.3(1)
O7a-Sr-O8a	44.3(1)
O9-Sr-O10a	121.5(1)
O10-Sr-O10a	76.9(1)
w1-Sr-O10a	128.2(1)
w2-Sr-O10a	68.3(1)
w3-Sr-O10a	88.1(1)
w4-Sr-O10a	150.6(1)
O7a-Sr-O10a	75.4(1)
O8a-Sr-O10a	71.4(1)

(c) Interionic Angles

Mn-O7-Sra	161.3(1)
C12-O7-Sra	80.2(2)
C12-O8-Sra	107.1(2)
Mn-O9-Sr	148.2(1)
Sr-O9-C14	91.7(2)
Sr-O10-C14	97.5(2)
Sr-O10-Srb	103.1(1)
C14-O10-Srb	149.5(2)

(a) Estimated standard deviations in the least significant digits are given in parentheses.

difference in ionic radius between cadmium and manganese ions, these differences should be on the order of 0.14 Å. Since the carboxylate oxygen atoms are bound at a "normal" distance (based on the $EDTA^{4-}$ structure), the strain associated with achieving eight-coordination about high spin Mn(II) is accommodated in the N-O-O-N belt of the chelate.

The bonding and conformational parameters for the rings in 10 are summarized in Table 7.2 and 7.3. The ring conformations for 10 are nearly identical with those for the cadmium chelate (see Table 7.3). The slight differences in the torsion angles that describe the five-membered rings are not sufficient to result in different minimum asymmetry parameters. The inter-ring torsion angles (see Table 7.4) also are essentially identical to those for $[Cd(EGTA)]^{2-}$ (and for $[Ca(EGTA)]^{2-}$). For two chelates that are conformationally similar, differences in the metal-ligand angular parameters must be expected to result from the observed differences in bond lengths. In 10, Mn-O(carb)-C > Cd-O(carb)-C, and Mn-O(ether)-C > Cd-O(ether)-C; these results are as expected, given the tighter binding of the ether oxygen atoms and carboxylate oxygen atoms to the manganese ion. The corresponding angles involving the nitrogen atoms are nearly identical for the two complexes.

Table 7.2 Chelate Ring[a] Bonding Parameters[b] for $Sr[Mn(EGTA)]\cdot 7H_2O$

Glycinate Rings

	C-C'	C'-N	C-O	C-O'	C-C'-N	O-C-O'	C'-C-O	C'-C-O'	Mn-N-C'	Mn-O-C
G1	1.528(5)	1.462(5)	1.262(5)	1.249(5)	111.0(3)	125.4(4)	117.8(3)	116.9(3)	104.0(2)	119.2(2)
G2	1.509(5)	1.470(5)	1.255(5)	1.257(4)	112.6(3)	124.5(3)	117.0(3)	118.3(3)	110.7(2)	123.7(2)
G3	1.523(6)	1.456(5)	1.258(5)	1.257(5)	112.2(3)	125.2(4)	118.1(3)	116.6(3)	106.9(2)	118.3(2)
G4	1.515(6)	1.470(5)	1.262(5)	1.257(5)	113.7(3)	122.8(3)	118.9(3)	118.3(3)	104.6(2)	118.4(2)

Amino-Ether Rings

	C-C'	C-N	C'-O	C-C'-O	C'-C-N	C"-N-C†	C-N-C"	C-N-C†	Mn-N-C	Mn-O-C'
A1	1.492(6)	1.485(5)	1.446(5)	109.5(3)	111.6(3)	113.0(3)	109.7(3)	110.9(3)	108.2(2)	110.7(2)
A2	1.506(6)	1.484(5)	1.426(5)	106.7(3)	112.8(3)	110.8(3)	110.5(3)	111.7(3)	112.0(2)	113.3(2)

Diether Ring

	C-C'	C'-O'	C-O	C'-C-O	C-C'-O'	C'-O'-C†	C"-O-C	Mn-O-C	Mn-O'-C'
E1	1.498(6)	1.420(5)	1.450(5)	106.7(3)	106.4(3)	112.7(3)	112.1(3)	116.3(2)	116.3(2)

(a) Chelate ring nomenclature is described in Figure 4.2(b). Rings within each series are numbered with increasing oxygen number.
(b) Bond lengths are given in Ångstroms and bond angles are given in degrees. Estimated standard deviations in the least significant digits are given in parentheses.

Table 7.3 Chelate Ring[a] Conformational Parameters[b] for $Sr[Mn(EGTA)]\cdot 7H_2O$

Glycinate Rings

	Ring Type	Bridging[c] Interaction	N-Mn-O-C	Mn-O-C-C'	O-C-C'-N	C-C'-N-Mn	C'-N-Mn-O	ΔC_s,min[d] ΔC_s,max	ΔC_2,min ΔC_2,max
G1	δ	0	-26.1(3)	11.6(4)	23.2(5)	-40.2(3)	34.2(2)	4.7(N) 52.9(C)	12.9(C) 63.1(N)
G2	λ	0	2.0(3)	11.4(5)	-24.7(5)	24.6(4)	-14.7(2)	2.3(C') 29.4(O)	9.7(O) 39.4(C')
G3	δ	1	-28.1(3)	17.8(4)	14.6(5)	-35.3(3)	32.1(2)	9.8(N) 50.3(C)	5.6(C) 56.8(Mn)
G4	δ	1,2	-22.9(2)	11.2(4)	18.6(5)	-33.9(3)	28.8(2)	4.7(N) 45.4(C)	9.4(C) 53.2(N)

Amino-Ether Rings

	Ring Type		O-Mn-N-C	Mn-N-C-C'	N-C-C'-O	C-C'-O-Mn	C'-O-Mn-N	ΔC_s,min ΔC_s,max	ΔC_2,min ΔC_2,max
A1	δ		19.6(2)	-49.3(4)	61.4(4)	-39.4(3)	10.5(2)	16.4(C) 66.2(Mn)	9.5(Mn) 88.7(C)
A2	λ		-13.3(2)	42.9(4)	-57.9(4)	43.5(3)	-17.3(2)	20.8(C') 64.8(Mn)	2.9(Mn) 83.4(C')

Diether Ring

	Ring Type		O'-Mn-O-C	Mn-O-C-C'	O-C-C'-O'	C-C'-O'-Mn	C'-O'-Mn-O	ΔC_s,min ΔC_s,max	ΔC_2,min ΔC_2,max
E1	δ		17.3(2)	-47.1(3)	59.4(4)	-46.7(3)	17.1(2)	22.5(C) 70.6(Mn)	.3(Mn) 87.9(C)

(a) Chelate ring nomenclature is described in Figure 4.2(b). Rings within each series are numbered with increasing oxygen number.
(b) Torsion angles are given in degrees. Estimated standard deviations in the least significant digits are given in parentheses.
(c) The bridge types are schematically depicted in Figure 4.2(a). Type 0 implies no interaction.
(d) The symmetry unique atom of the summation is given in parentheses.

Table 7.4 Inter-ring Torsion Angles[a] for $Sr[Mn(EGTA)]\cdot 7H_2O$

C2-C1-N1-C5	75.3(4)	C4-C3-N1-C5	-95.4(4)
C12-C11-N2-C10	-157.5(3)	C14-C13-N2-C10	87.5(4)
C2-C1-N1-C3	-160.3(3)	C4-C3-N1-C1	140.9(3)
C12-C11-N2-C13	78.1(4)	C14-C13-N2-C11	-148.7(3)
C1-N1-C5-C6	-162.2(3)	C3-N1-C5-C6	72.2(4)
C11-N2-C10-C9	162.0(3)	C13-N2-C10-C9	-74.1(4)
C5-C6-O5-C7	92.4(4)	C10-C9-O6-C8	178.3(3)
C6-O5-C7-C8	-176.0(3)	C9-O6-C8-C7	179.9(3)

(a) Torsion angles are given in degrees. Estimated standard deviations in the least significant digits are given in parentheses.

molecules has been used in the calculation of secondary sphere contributions to water proton relaxation rates.[136]

Solid State and Solution EPR Spectra of **10**

The X-band EPR spectrum for solid $Sr[Mn(EGTA)]\cdot 7H_2O$ (doped at 1% into $Sr[Cd(EGTA)]\cdot 7H_2O$) is shown in Figure 7.2, as is the solution spectrum at two different temperatures. The complex splitting pattern observed is typical for a high spin Mn(II) ion in a ligand field of low symmetry. The magnetic susceptibility also indicates that the Mn(II) is high spin ($\mu_{s.o.}$ = 5.90). The zero field splitting observed in the solid spectrum is approximately 350 G. The complexity of the solution EPR spectrum at room temperature indicates that the $[Mn(EGTA)]^{2-}$ molecules must have a long correlation time, and that motional averaging is incomplete. Upon increasing the temperature to 67° C, peaks in the outer wings of the spectrum are seen to coalesce. These results are in partial agreement with the previously reported solution EPR spectrum of $[Mn(EGTA)]^{2-}$.[137] That room temperature spectrum did not exhibit the broadening at room temperature seen in experiments with **10**. The fact that the experimental conditions utilized were not identical may explain this fact. The strontium salt of the manganese chelate was used in preparation of of solutions that yielded the spectra in Figure 7.2; no adjustments of pH were made. In the previous experiments, an excess of ligand was added, and the pH was

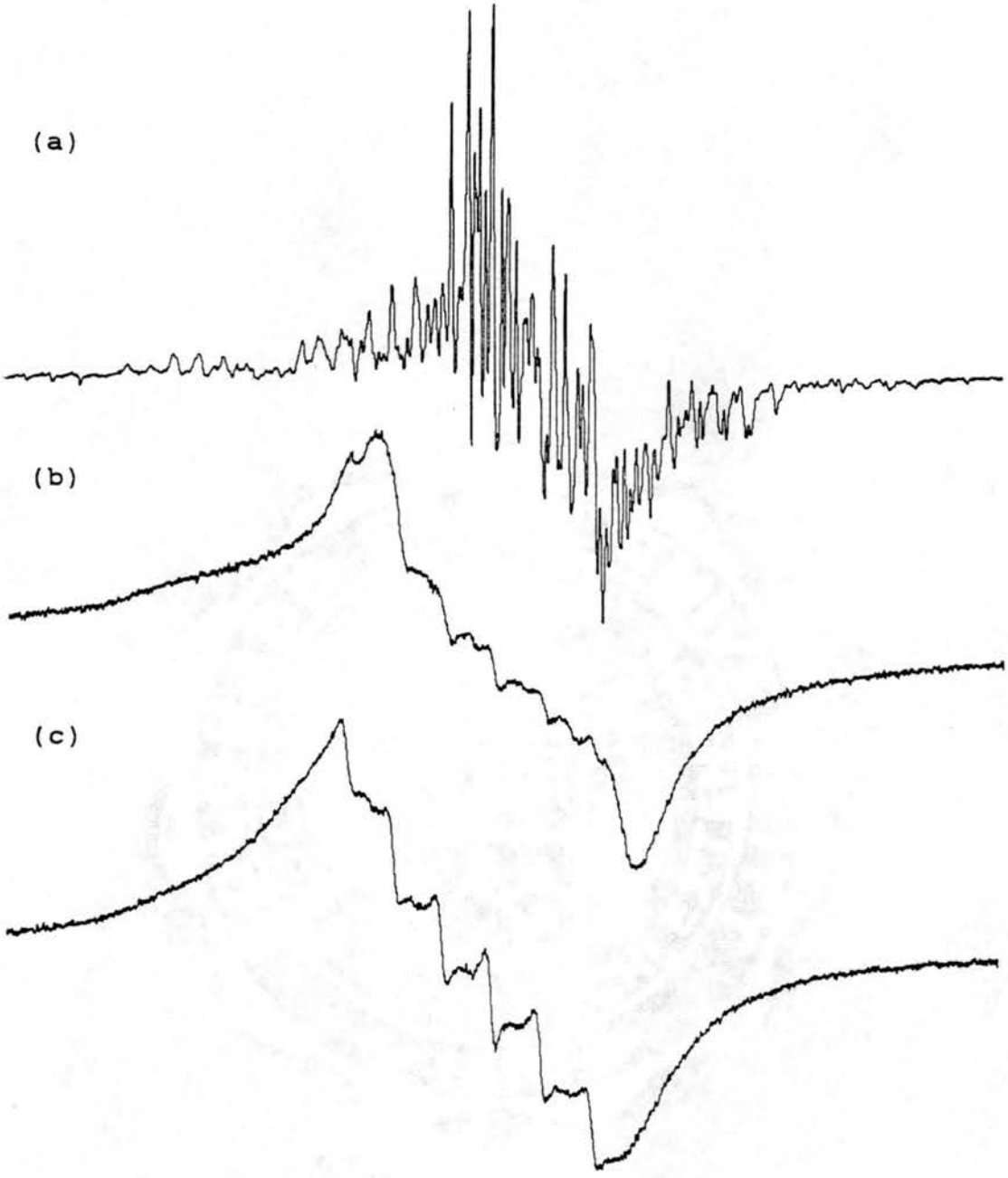

Figure 7.2 (a) EPR spectrum of a powdered sample of $Sr[Mn(EGTA)]\cdot 7H_2O$. (b) Solution EPR spectrum of $[Mn(EGTA)]^{2-}$ at room temperature. (c) Solution EPR spectrum of $[Mn(EGTA)]^{2-}$ at 340 K.

adjusted to 7.5-8.0 utilizing KOH as a base. The frozen solution spectrum[137] does not show as large a zero field splitting (212 G) as the solid state spectrum of 10 does. This may indicate a different coordination geometry in solution compared to the solid state.

Structure of a Dinuclear Copper(II) Complex of $EGTA^{4-}$, $[Cu_2(EGTA)(OH_2)_2]\cdot 2H_2O$ (11)

In attempts to crystallize a copper chelate of $EGTA^{4-}$, crystals of 11 were obtained. Only half of this dinuclear species is crystallographically unique, the other half being generated by a center of inversion at the midpoint of the C7-C7' bond. Each copper(II) ion exhibits a square pyramidal coordination array, with the ligand atom set consisting of a single water molecule, together with the ether oxygen atom, amine nitrogen atom, and the oxygen atoms of two carboxylate groups at one end of the $EGTA^{4-}$ ligand. The structure of this dinuclear copper(II) complex (see Figure 7.3(a)) is quite different from that of the dinuclear magnesium complex (6), in which the ether oxygen atoms are not utilized in coordination to the metal ion. In addition, the oxygen atoms of the carboxylate groups occupy cis coordination sites in 6; they occupy trans sites in 11.

The analogous dinuclear copper(II) $EDTA^{4-}$ complex has been characterized;[138] the coordination mode for the iminodiacetate portion of the molecule is identical with

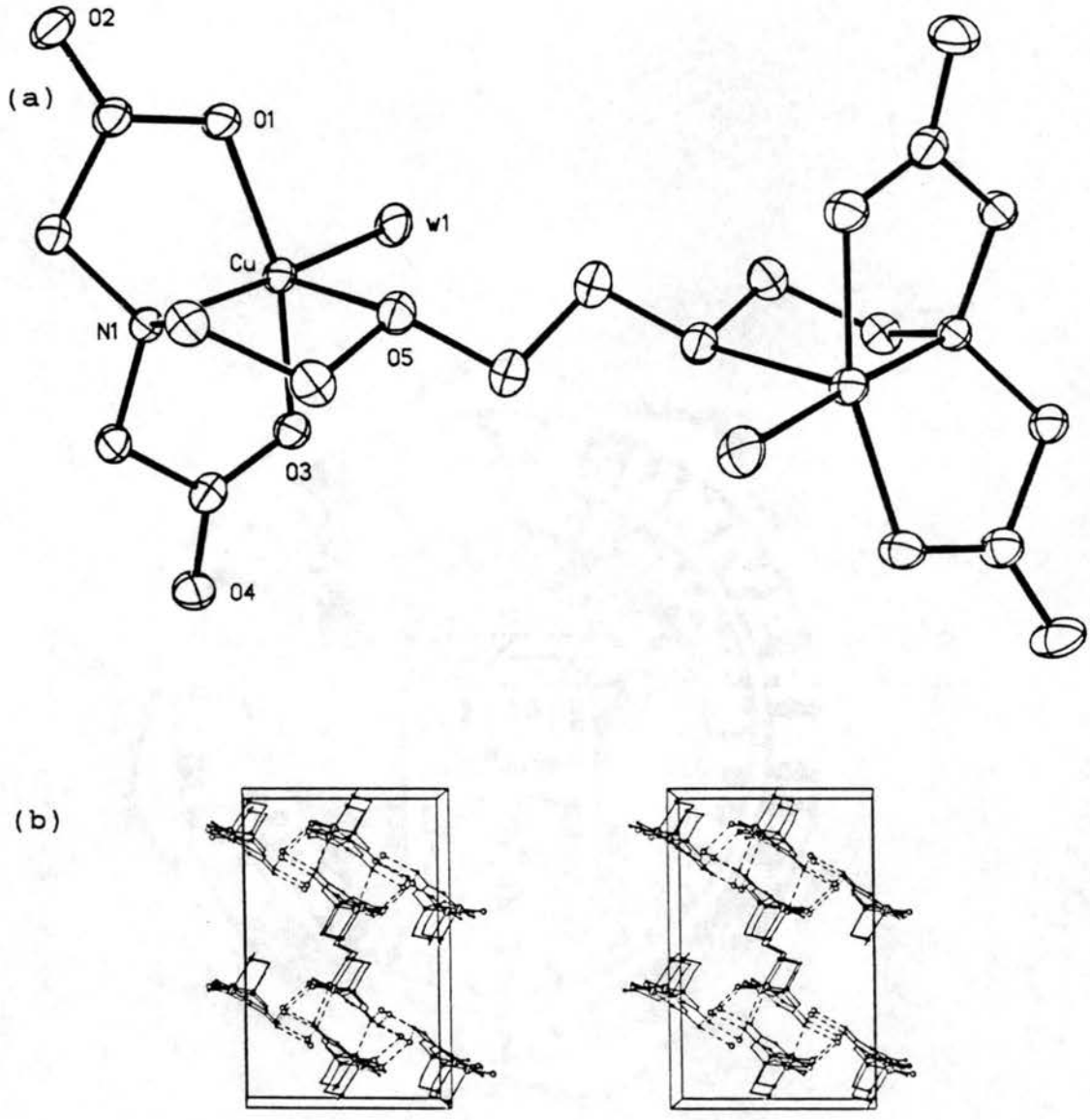

Figure 7.3 (a) A thermal ellipsoid plot (40%) of $[Cu_2(EGTA)(OH_2)_2]$. (b) View of the unit cell of $[Cu_2(EGTA)(OH_2)_2]\cdot 2H_2O$ taken along the b axis.

that of 11. In the $EDTA^{4-}$ complex, the copper(II) ions achieve square pyramidal coordination through the binding of two water molecules.

The water molecule and the carboxylate groups are bound at approximately the same distance (Cu-O = 1.928(2)-1.939(2) Å, see Table 7.5). These distances are slightly shorter than those seen for the strong bonds in the six-coordinate H_3DTPA^{2-},[134] NTA^{3-},[139,140] IDA^{2-},[141] and ODA^{2-}[142] copper complexes (Cu-O = 1.941(3)-1.991(3) Å). Hydrogen bonding interactions between water molecules and carboxylate oxygen atoms function to stitch the lattice of 10 together (see Figure 7.3(b))

The amine nitrogen atom is bound at a slightly longer distance than are the oxygen atom donors (1.992(2) Å) a distance which is also shorter than the corresponding distance in the NTA^{3-} and IDA^{2-}, and H_3DTPA^{2-} complexes (Cu-N = 2.014(3)-2.086(5) Å).[134, 139-141] The structures of octahedral $[Cu(EDTA)]^{2-}$ [33,34] and $[Cu_2(EDTA)(OH_2)_4]$[138] were not drawn upon for structural comparison because the structures are of very low relative precision.

The ether oxygen atom occupies the weakly bound apical site of the square pyramid. As expected, the bond to the copper(II) ion is long (Cu-O(ether) = 2.408(2) Å), but it is still shorter than the bond to the ether oxygen atom of ODA^{2-} (Cu-O(ether) = 2.488(7) Å).

In six-coordinate $Cu(IDA)(OH_2)_2$[141] and $Cu(ODA)(OH_2)_3$,[142] the carboxylate oxygen atoms of the IDA^{2-} and

Table 7.5 Metal-Ligand Distances (Å) and Angles (deg)[a] for $[Cu_2(EGTA)(OH_2)_2]\cdot 2H_2O$

(a) Complex Ions

Cu-N1	1.992(2)
Cu-O1	1.928(2)
Cu-O3	1.939(2)
Cu-O5	2.408(2)
Cu-w1	1.938(2)

N1-Cu-O1	85.2(1)
N1-Cu-O3	86.0(1)
O1-Cu-O3	163.1(1)
N1-Cu-O5	81.9(1)
O1-Cu-O5	103.5(1)
O3-Cu-O5	89.5(1)
N1-Cu-w1	177.2(1)
O1-Cu-w1	92.1(1)
O3-Cu-w1	96.4(1)
O5-Cu-w1	99.5(1)

(a) Estimated standard deviations in the least significant digits are given in parentheses.

ODA^{2-} ligands occupy *cis* coordination sites. The adoption of a *trans* geometry must occur to maintain the nitrogen atom and the carboxylate oxygen atoms in the basal coordination plane, where bonds to the metal are strong, and to restrict the weakly coordinating ether oxygen atom to the apical site of the square pyramid. The closest approach of a ligand to the potential sixth coordination site is ~3 Å (Cu-O4' = 3.012(2) Å, see Figure 7.3(b)). The ring conformations are similar to those observed for the magnesium complex (see Tables 7.6 and 7.7), indicating that small metal ions have similar conformational preferences.

The log of the equilibrium constant for protonation of the ML^{2-} species does not vary substantially between copper (4.36) and manganese (4.1).[48] Thus, it is likely that the $EGTA^{4-}$ ligand wraps around the Cu(II) ion in solution, utilizing both amine nitrogen atoms in coordinating to the metal ion (as seen for Mn^{2+} ion). Preferential crystallization of **11** must be attributed to the low solubility of the neutral dinuclear species, and to the adoption of an especially favorable coordination environment about the copper(II) ion. The equilibrium constant for the formation of the dinuclear copper(II) complex has been measured[143] ($Cu^{2+} + L^{4-} \rightleftharpoons CuL^{2-}$, log K = 17.6; $CuL^{2-} + Cu^{2+} \rightleftharpoons Cu_2L$, log K = 4.31). Only very small amounts of the dinuclear species should be present in a solution which contains a 1:1 stoichiometric ratio of metal to ligand.

Table 7.6 Chelate Ring[a] Bonding Parameters[b] for $[Cu_2(EGTA)(OH_2)_2]\cdot 2H_2O$

Glycinate Rings

	C-C'	C'-N	C-O	C-O'	C-C'-N	O-C-O'	C'-C-O	C'-C-O'	Cu-N-C'	Cu-O-C
G1	1.536(4)	1.478(4)	1.279(4)	1.218(4)	109.9(2)	123.6(3)	117.0(3)	119.4(3)	104.7(2)	112.9(2)
G2	1.521(4)	1.486(4)	1.271(4)	1.240(4)	111.4(2)	124.1(3)	118.3(3)	117.5(3)	107.6(2)	114.0(2)

Amino-Ether Ring

	C-C'	C-N	C'-O	C-C'-O	C'-C-N	C"-N-C[†]	C-N-C"	C-N-C[†]	Cu-N-C	Cu-O-C'
A1	1.498(5)	1.499(4)	1.434(4)	108.5(3)	111.8(3)	114.4(2)	110.6(2)	111.0(2)	108.2(2)	100.0(2)

Diether Ring

	C-C'	C'-C-O	C"-O-C	Cu-O-C
E1	1.502(7)	107.4(4)	112.0(2)	119.2(2)

(a) Chelate ring nomenclature is described in Figure 4.2(b). Rings within each series are numbered with increasing oxygen number.

(b) Bond lengths are given in Ångstroms and bond angles are given in degrees. Estimated standard deviations in the least significant digits are given in parentheses.

Table 7.7 Chelate Ring[a] Conformational Parameters[b] for $[Cu_2(EGTA)(OH_2)_2]\cdot 2H_2O$

Glycinate Rings

	Ring Type	Bridging[c] Interaction	N-Cu-O-C	Cu-O-C-C'	O-C-C'-N	C-C'-N-Cu	C'-N-Cu-O	ΔC_s,min[d] ΔC_s,max	ΔC_2,min ΔC_2,max
G1	δ	0	-22.0(2)	8.8(3)	15.8(4)	-30.2(3)	28.6(2)	4.5(N) 40.8(C)	7.6(C) 49.4(N)
G2	λ	0	13.2(2)	-7.7(3)	-5.0(4)	14.3(3)	-14.8(2)	4.8(Cu) 21.4(C)	2.1(C) 25.2(Cu)

Amino-Ether Ring

	Ring Type	O-Cu-N-C	Cu-N-C-C'	N-C-C'-O	C-C'-O-Cu	C'-O-Cu-N	ΔC_s,min ΔC_s,max	ΔC_2,min ΔC_2,max
A1	δ	15.1(2)	-46.2(3)	63.8(3)	-42.6(3)	15.6(2)	23.1(C) 66.4(Cu)	2.6(Cu) 87.8(C)

(a) Chelate ring nomenclature is described in Figure 4.2(b). Rings within each series are numbered with increasing oxygen number.
(b) Torsion angles are given in degrees. Estimated standard deviations in the least significant digits are given in parentheses.
(c) The bridge types are schematically depicted in Figure 4.2(a). Type 0 implies no interaction.
(d) The symmetry unique atom of the summation is given in parentheses.

Conclusions

Two different coordination possibilities for the $EGTA^{4-}$ ligand with first row transition metals of different size have been established . A coordination mode in which an arm of the $EGTA^{4-}$ ligand is not coordinated to the metal ion, similar to that commonly observed in $EDTA^{4-}$ chelates,[45] has yet to be observed.

CHAPTER 8

TRENDS AND CORRELATIONS AMONG STRUCTURAL PARAMETERS OF $EGTA^{4-}$ CHELATES

Introduction

In this dissertation, structural results have been reported for a variety of metal ion complexes of $EGTA^{4-}$. The complexed metal ions span a large range in size (ionic radius = 0.68 Å (Cu^{2+})-1.52 Å (Ba^{2+}), ligand atom preferences, and coordination number preferences (5 (Cu^{2+}) -10 (Ba^{2+} and Nd^{3+})). To explore trends and correlations among the observed structural parameters, scatter plots and histograms may be utilized. Such trends and correlations were explored for $EDTA^{4-}$ complexes in a recent review;[45] results for $EGTA^{4-}$ chelates can now be compared with those for $EDTA^{4-}$ chelates.

Metal-Ligand Distance Correlations

If the preferred metal-ligand distance were simply a function of the size of the metal ion, a plot of the metal-ligand distance versus the ionic radius of the metal ion (for the appropriate coordination number) would be linear. Figure 8.1(a-c) shows such plots for the three ligand atom types in metal-EGTA complexes. The correlation

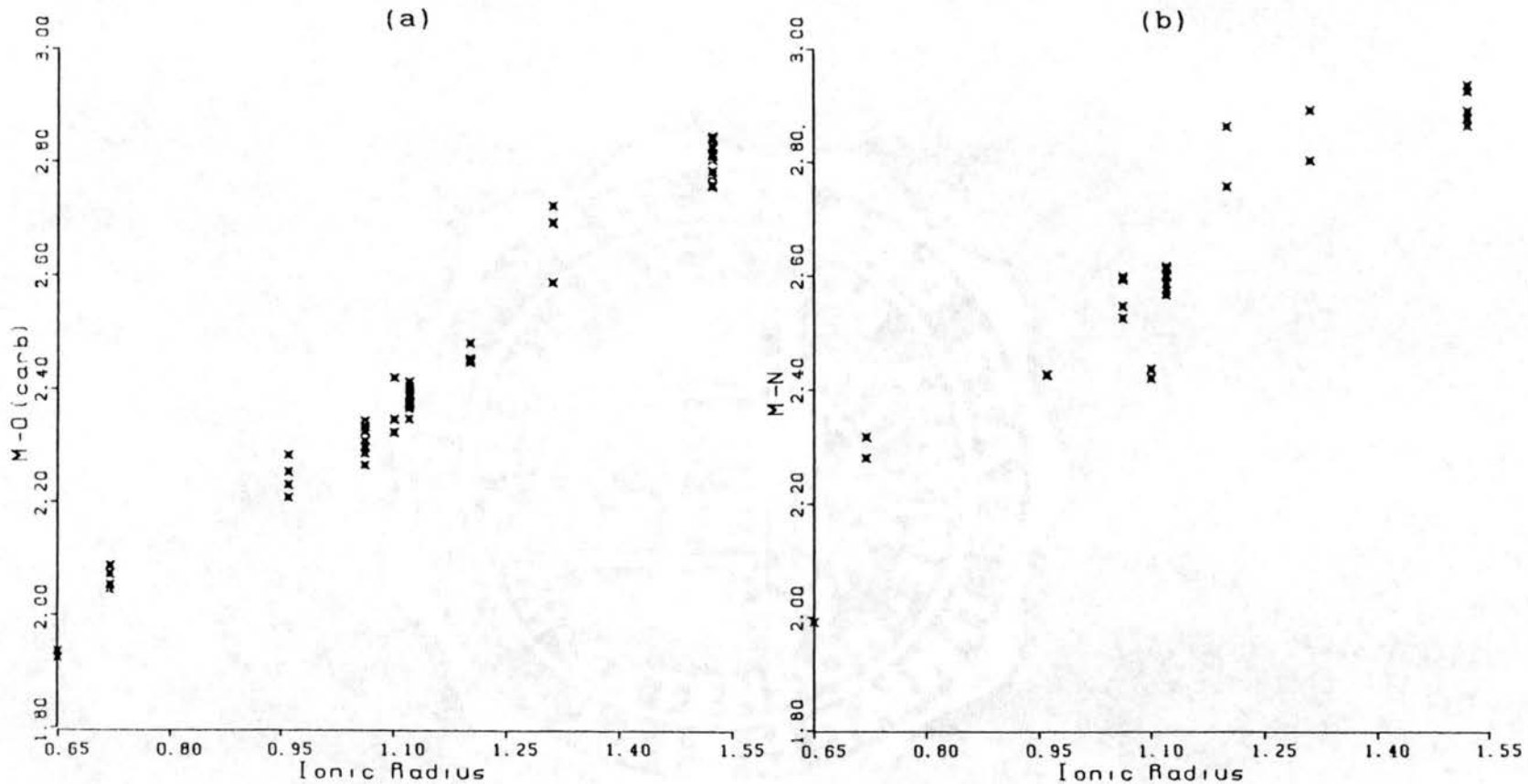

Figure 8.1 Correlations of metal-ligand distances (Å) with ionic radii (Å). The ionic radii utilized are Ba (1.52), Sr (1.31), Nd (1.20), Ca (1.12), Cd (1.10), Mn (0.96), Mg (0.72), Cu (0.65). (a) M-O(carb) distance versus ionic radius. (b) M-N distance versus ionic radius.

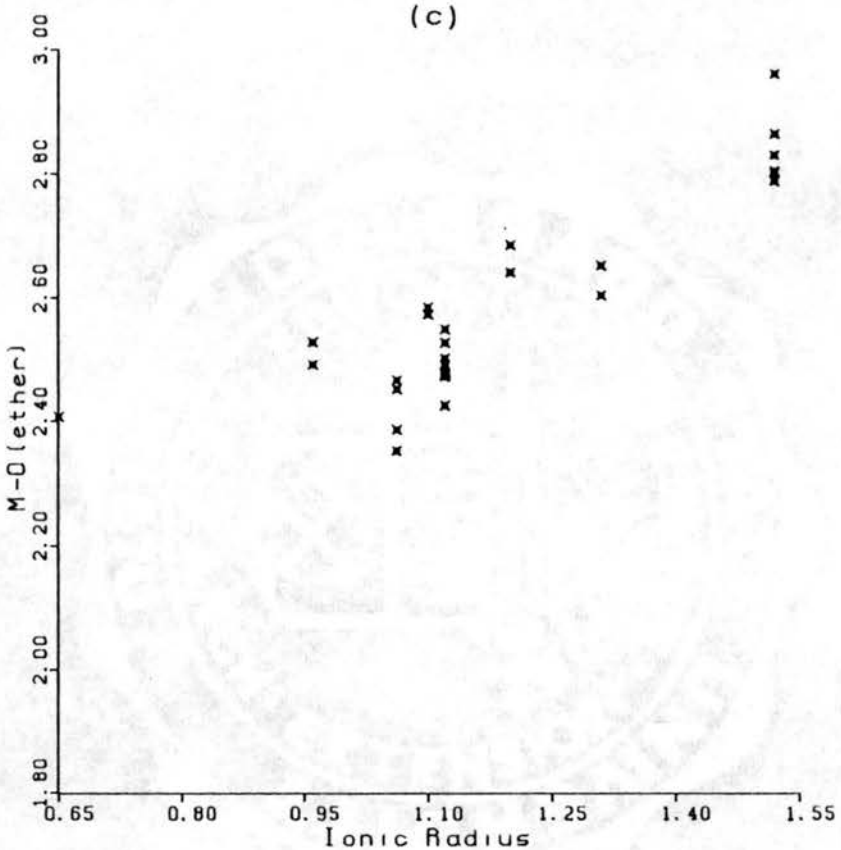

Figure 8.1 (continued) (c) M-O(ether) distance versus ionic radius.

coefficients for the best straight line fit in each case are displayed in Table 8.1. The plot relating ionic radius to the mean metal-O(carboxylate) distance gives the best linear fit of the three (c.c. = 0.96); the plots attempting to relate the ionic radius to the M-N and M-O(ether) distances give a less satisfactory linear fits (c.c = 0.87 and 0.76, respectively).

If metal ion size were the only factor important in determining the metal-ligand bond distance, linear correlations would also be expected among metal-ligand distances. The correlation between the M-N distances and M-O(carb) distances for $[M(EDTA)]^{n-}$ complexes is not impressive (c.c = 0.37),[45] although it is much better for the limited selection of compounds present in this thesis (c.c. = 0.89, see Figure 8.2(a)). Plots relating <M-O(carb)> and <M-N> distances to <M-O(ether)> distances for the seven complexes which contained amino-ether rings or diether rings are displayed in Figure 8.2(b,c). These plots do not appear to be distinctly linear (c.c = 0.57, and 0.74, respectively), although there is not sufficient data to make a definite conclusion.

Qualitatively, it appears that the ligand preferences exhibited by the metal ions (as expressed in metal-ligand distances) are associated with hard/soft character. For example, calcium ion, which would be considered a hard metal ion, exhibits a distinct preference to bind the ether oxygen atoms at a much shorter distance than the amine

Table 8.1 Correlations Between Selected Structural Parameters in Metal-EGTA Complexes

x	y	# of Observ.	b[a]	m[b]	c.c[c]
Ionic radius	M-O(carb)	58	1.29	0.99	0.97
Ionic radius	M-N	29	1.61	0.87	0.87
Ionic radius	M-O(ether)	27	1.80	0.66	0.76
M-N	M-O(carb)	9	0.13	0.88	0.89
M-N	M-O(ether)	8	1.62	0.37	0.57
M-O(ether)	M-O(carb)	8	1.65	1.58	0.74
M-N	N-M-O(ether)	27	129	-23.5	0.91
M-O(ether)	N-M-O(ether)	27	132	-25.2	0.61
without Cu included		26	123	-22.1	0.68
<M-N, M-O(e)>	N-M-O(ether)	27	140	-28.3	0.89
<M-O(ether)>	O(e)-M-O(e)	13	119	-21.7	0.97
M-O(carb)	N-M-O(carb)	58	129	-25.8	0.87
M-N	N-M-O(carb)	58	143	-29.4	0.96
<M-N, M-O(c)>	N-M-O(carb)	58	138	-28.5	0.95

(a) b = intercept

(b) m = slope

(c) c.c. = correlation coefficient

$$= \frac{b\,\Sigma y_i + m\,\Sigma x_i y_i - (1/n)(\Sigma y_i)^2}{\Sigma(y_i^2) - (1/n)(\Sigma y_i)^2}$$

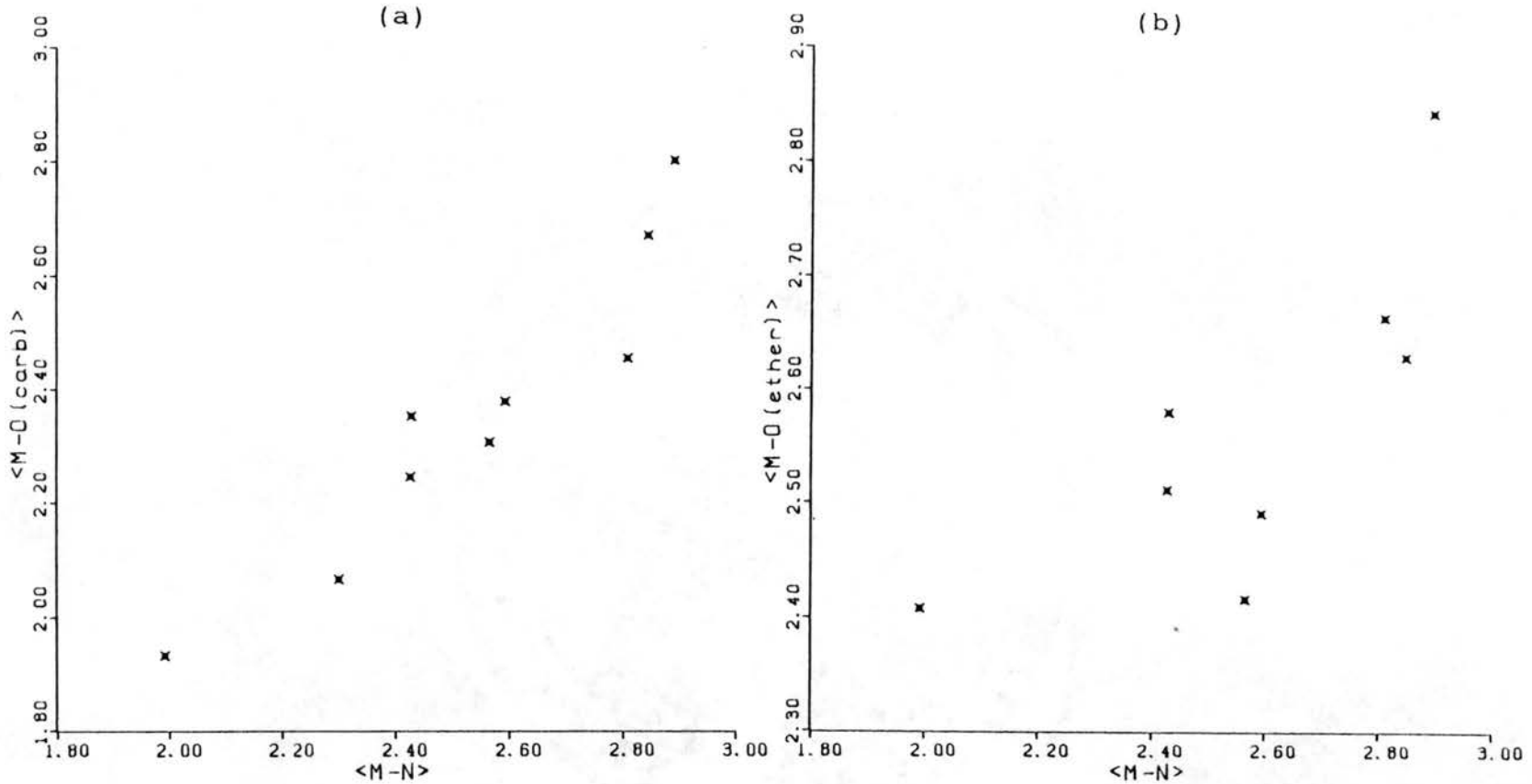

Figure 8.2 Correlations among metal-ligand distances (Å). (a) Mean M-O(carb) distance versus mean M-N distance. (b) Mean M-O(ether) distance versus mean M-N distance.

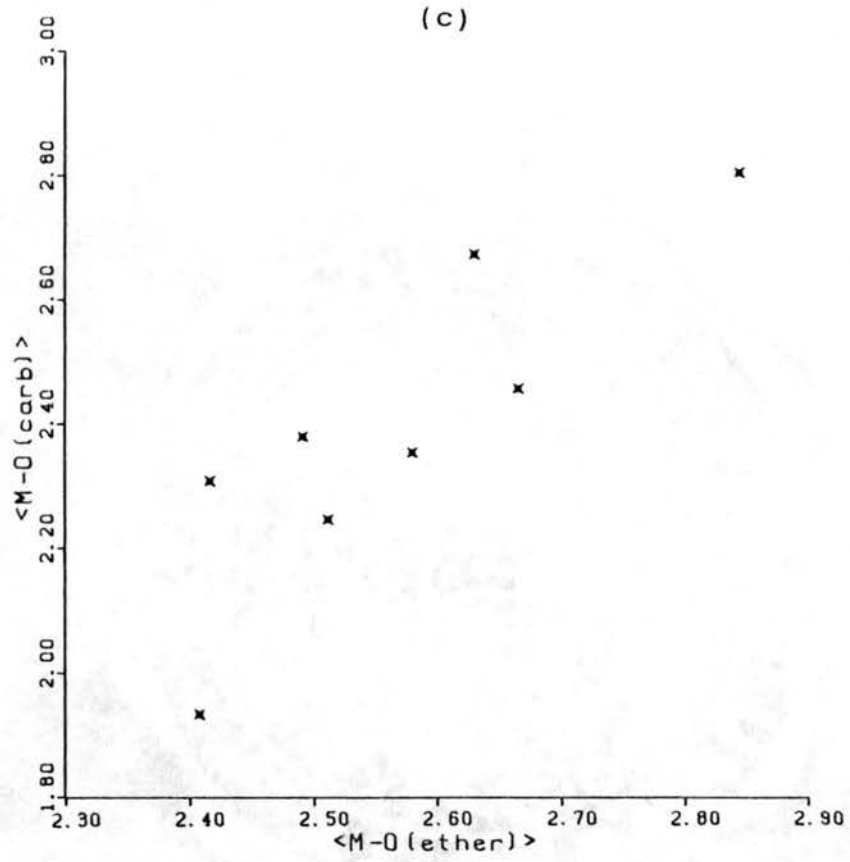

Figure 8.2 (continued) (c) Mean M-O(carb) distance versus mean M-O(ether) distance.

nitrogen atoms. In contrast, cadmium ion, a soft metal ion essentially equal in size to the calcium ion, binds the amine nitrogen atoms at a shorter distance than the ether oxygen atoms.

A quantitative scale is available for the softness of a metal ion (see Table 8.2).[144] The quantities $E_n^{\neq}$, which range from approximately -5 for soft metal ions to +6 for hard metal ions, agree well with the qualitative description of hardness and softness given by Pearson.[145] Correlations have been explored between these softness parameters and the ligand atom preferences of the metal ions. The ligand atom preference is defined as the difference in the mean metal-ligand bond distance exhibited by a particular metal ion for two different ligand atom types of the $EGTA^{4-}$ ligand. Plots of the softness parameter versus the three possible ligand atom preference parameters are shown in Figure 8.3(a, b, c). Corresponding results for $EDTA^{4-}$ complexes have also been utilized in construction of Figure 8.3(a) for metal ions where both structural information and softness parameters are available. In all structurally characterized $EGTA^{4-}$ chelates, the carboxylate oxygen atoms are, on average, bound at shorter distances than are the amine nitrogen atoms. Consequently, the difference (<M-N> - <M-O(carb)>) is always greater than zero. The soft metal ions (Cd^{2+}, Cu^{2+}) display a smaller preference to bind the carboxylate

Table 8.2 Softness Character Parameters

Metal Ion	$E_n^{\neq}$, ev
Al^{3+}	6.01
La^{3+}	4.51
Ti^{4+}	4.35
Be^{2+}	3.75
Mg^{2+}	2.42
Ca^{2+}	2.33
Fe^{3+}	2.22
Sr^{2+}	2.21
Cr^{3+}	2.06
Ba^{2+}	1.89
Ga^{3+}	1.45
Cr^{2+}	0.91
Fe^{2+}	0.69
Li^{+}	0.49
H^{+}	0.42
Ni^{2+}	0.29
Na^{+}	0
Cu^{2+}	-0.55
Tl^{+}	-1.88
Cd^{2+}	-2.04
Cu^{+}	-2.30
Ag^{+}	-2.82
Tl^{3+}	-3.37
Au^{+}	-4.35
Hg^{2+}	-4.64

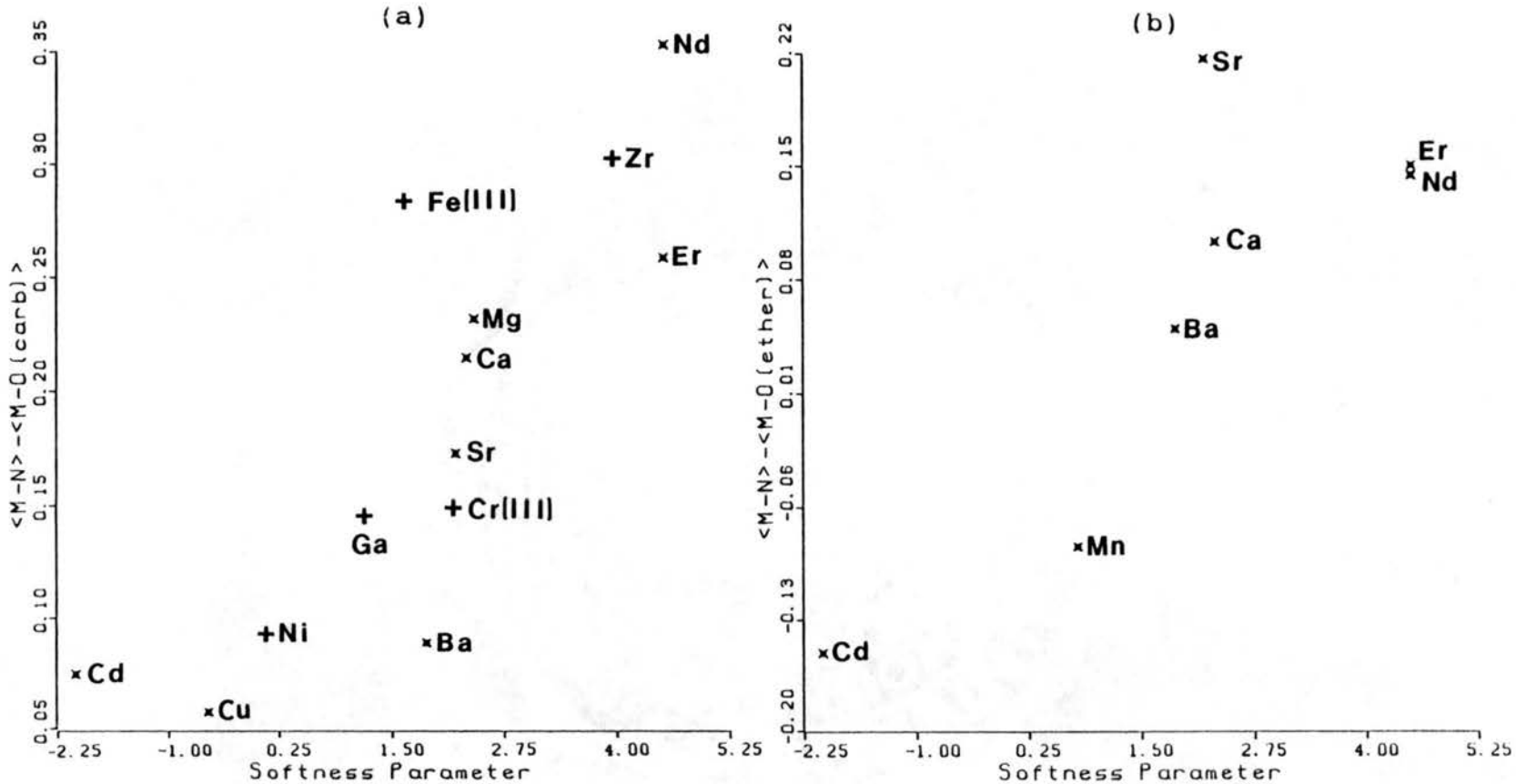

Figure 8.3 Correlations between ligand atom preference parameters (Å) and a softness parameter (ev, see text). (a) The difference between the mean M-O(ether) distance and the mean M-O(carb) distance versus the "softness " parameter. (b) The difference between the mean M-N distance and the mean M-O(carb) distance versus the "softness" parameter.

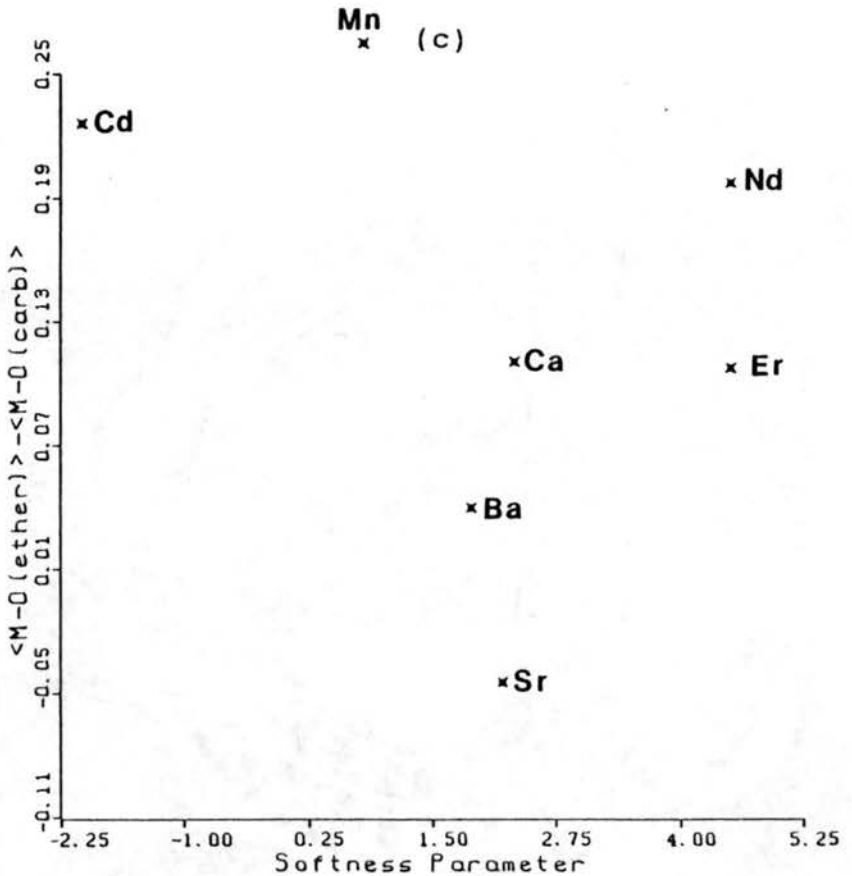

Figure 8.3 (continued) (c) The difference between the mean M-O(ether) distance and the mean M-O(carb) distance versus the "softness" parameter.

oxygen atoms over the amine nitrogen atoms than do the hard metal ions (Ca^{2+}, Nd^{3+}, Er^{3+}).

There is less data available involving ether oxygen atom coordination. The observed trends behave roughly as one might expect. In Figure 8.3(b), the quantity (<M-N> - <M-O(ether)>) is less than zero for the soft metal ions, and is greater than zero for the hard metal ions. Thus, the hard metal ions prefer to bind to the harder ether oxygen atoms, despite the higher intrinsic basicity of the amine nitrogen atoms.

The plot relating the quantity (<M-O(ether)> - <M-O(carb)>) to the softness parameter displays the poorest correlation. It is unclear if a correlation between these two distances would be expected. Both carboxylate oxygen and ether oxygen are "hard" oxygen atom donors. The greater intrinsic basicity of the anionic carboxylate oxygen donors must be the dominant factor in determining the preferred bond distance. Additionally, in discussion of the individual structures, the point has been made several times in earlier chapters that when a metal ion needs to make concessions in bonding to one of the ligand atom types, the metal-O(carboxylate) linkage proves less yielding. Some of the trends observed in this plot may relate to that factor. For example, the fact that the manganese chelate has shorter intraligand contacts than does the cadmium chelate may be responsible for the

anomalously long ether oxygen bond lengths to manganese ion.

Metal-Ligand Angular Correlations

In the discussions of individual structures, trends relating bond distances to bond angles have been mentioned. Correlation plots for relating metal-ligand distances to the corresponding angles have been constructed for the amino-ether rings, the diether rings, and the glycinate rings.

The correlation plots for the amino-ether rings are depicted in Figure 8.4. The N-M-O(ether) angle correlates equally well with the average of the M-N and M-O(ether) bond distances for an individual ring (c.c. = 0.89), as it does with the M-N distance (c.c. = 0.91). The correlation is considerably worse for the M-O(ether) bond length (c.c. = 0.68, excluding the Cu point). The correlation plot for the diether rings is shown in Figure 8.5. Although fewer data are available for this plot, a good correlation between mean M-O(ether) bond distance and the observed O(ether)-M-O(ether) angle is observed (c.c. = 0.97). The behavior of the amino-ether and diether rings in these respects is similar to that of the diamine rings present in $EDTA^{4-}$ chelates.[45]

As in the case of $EDTA^{4-}$ chelates, the N-M-O(carb) angle for the glycinate ring correlates better with the M-N

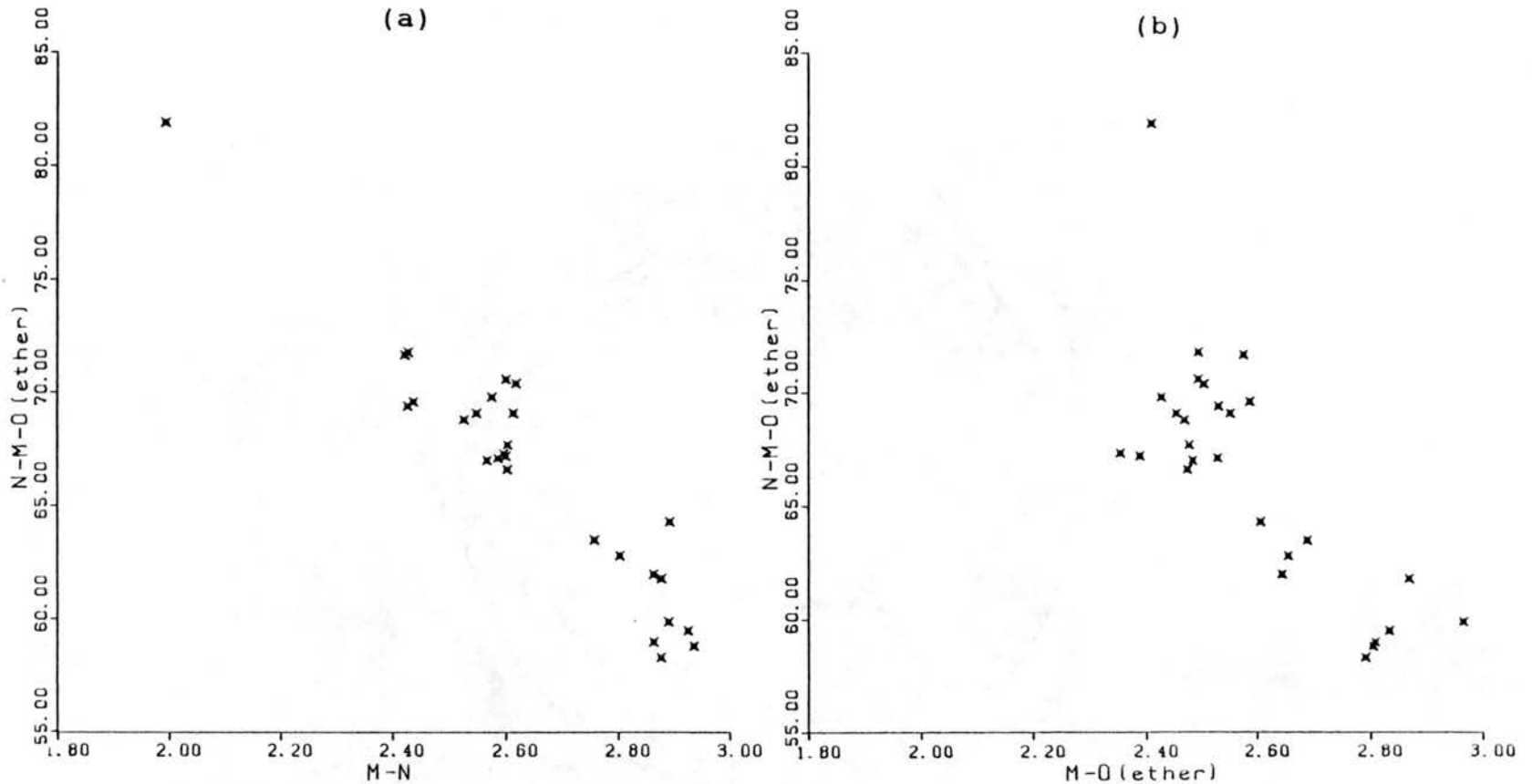

Figure 8.4 Angle (deg)--bond length (Å) correlations for amino-ether rings. (a) N-M-O(carb) angles versus M-N distance. (b) N-M-O(ether) angle versus M-O(ether) distance.

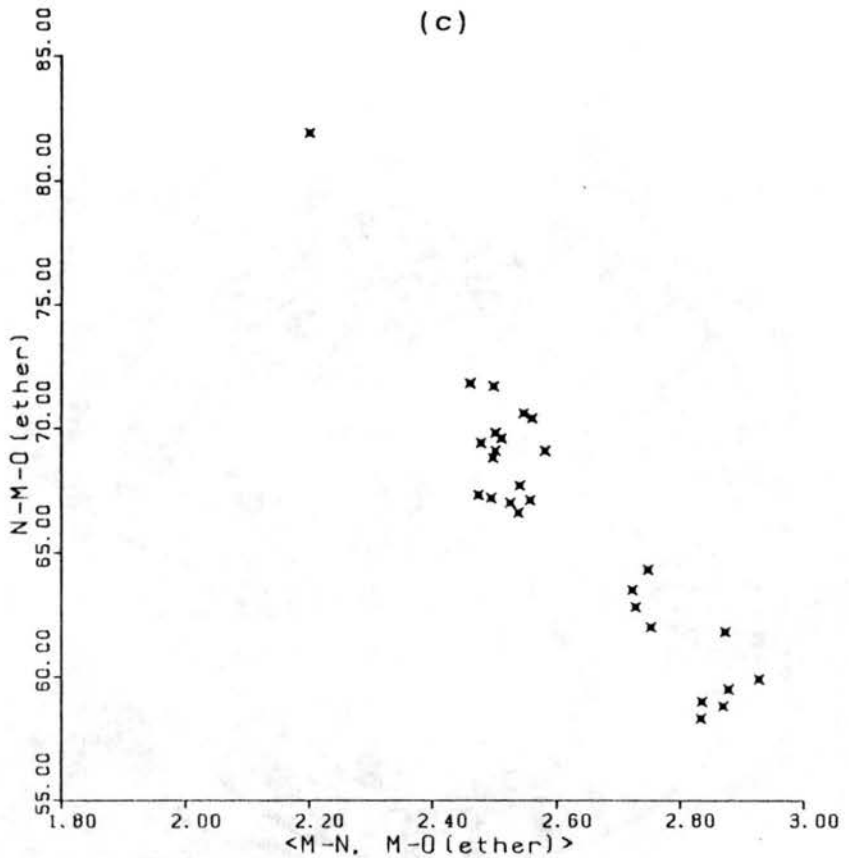

Figure 8.4 (continued) (c) N-M-O(ether) angle versus the average of the M-N and M-O(ether) distances.

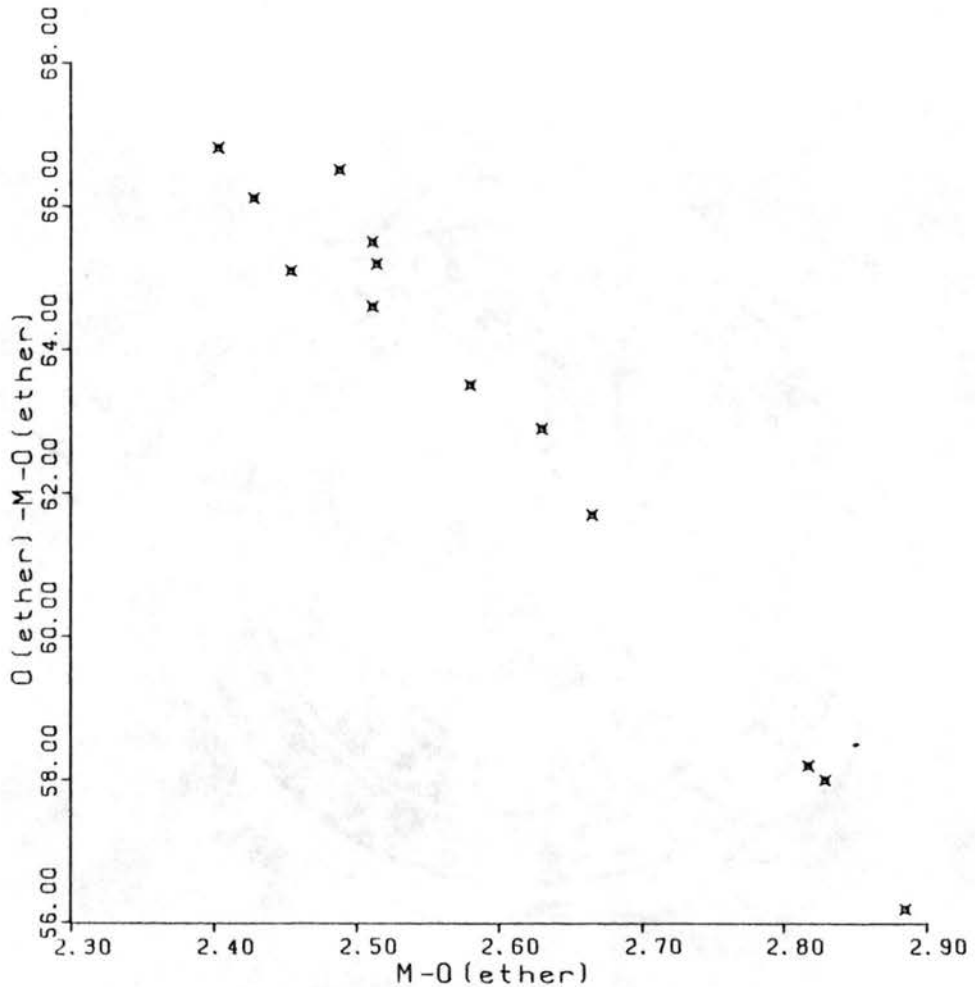

Figure 8.5 Angle (deg)--bond length (Å) correlations for diether rings. O(ether)-M-O(ether) angle versus average M-O(ether) bond distance.

bond distance than with the M-O(carb) bond distance or with the average of the two distances (see Figure 8.6). This may be due to the influence of bridging interactions on the M-O(carb) distances.

Distributions of Conformational Parameters

Instead of plotting distributions of minimum asymmetry parameters, as was done in conformational analysis of the $EDTA^{4-}$ chelates,[45] an analysis of the distribution of the torsion angles which contribute to the asymmetry parameters has been performed. The torsion angles for the amino-ether rings and diether rings (assuming 2-fold symmetry for the amino-ether ring) are plotted collectively in Figure 8.7. Distinct angular ranges are observed for each torsion angle. The average values for the N(O)-C-C'-O, M-N(O)-C-C', and O-M-N(O)-C torsion angles are ~59°, ~45°, and ~16°, respectively. Given the rather narrow distribution of these conformational parameters, it is not surprising that the minimum asymmetry parameters associated with these rings typically corresponds to an idealized C_2 ring symmetry, with the C_2 axis through the metal ion. Rings that exhibit torsion angles well outside of these distributions are conformationally irregular and do not have the typical minimum asymmetry parameter. Such conformational irregularities are not generally seen in the diamine rings in $EDTA^{4-}$ chelates, and seem to be associated

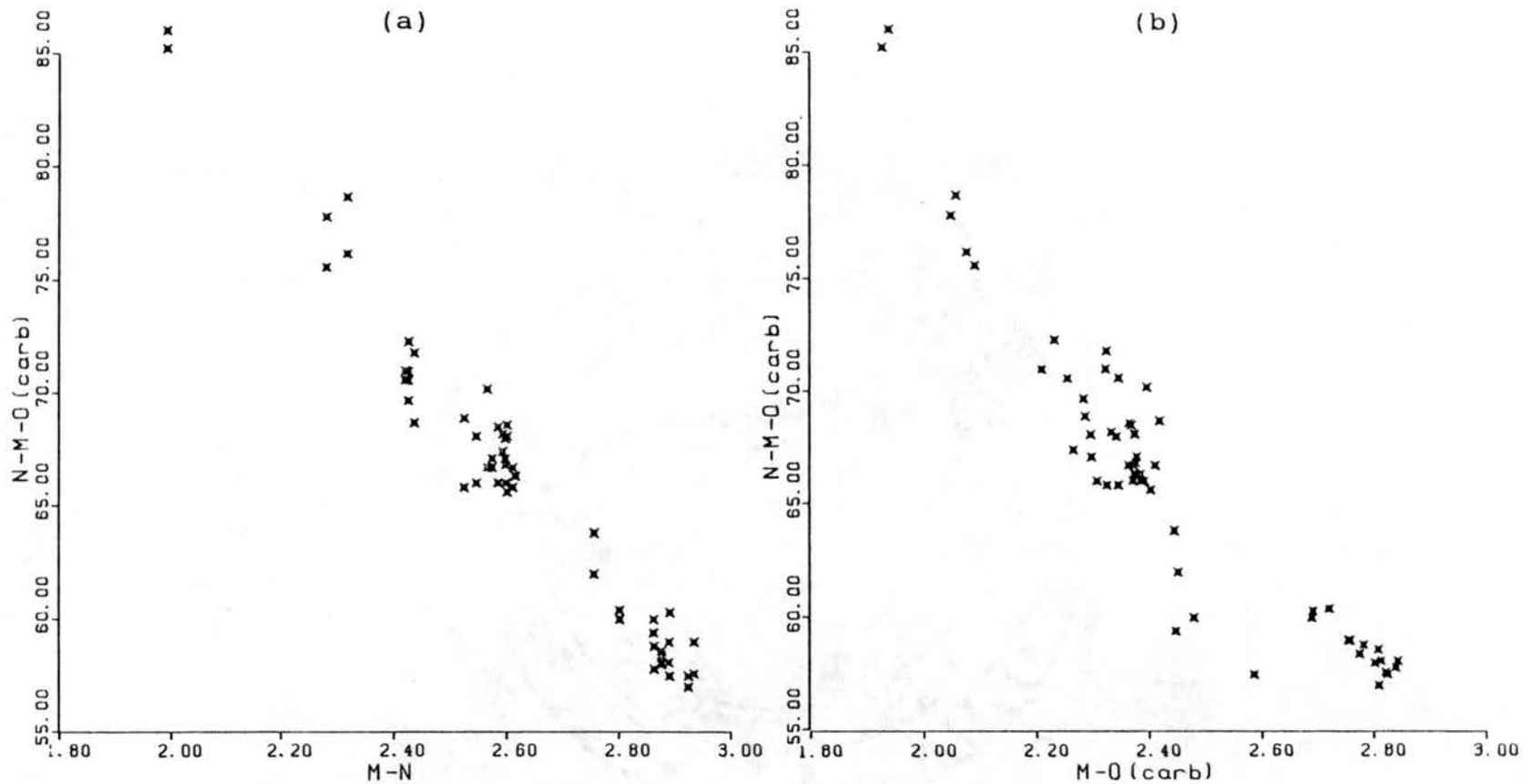

Figure 8.6 Angle (deg)--Bond length (Å) correlations for glycinate rings. (a) N-M-O(carb) angle versus M-N distance. (b) N-M-O(carb) angle versus M-O(carb) distance.

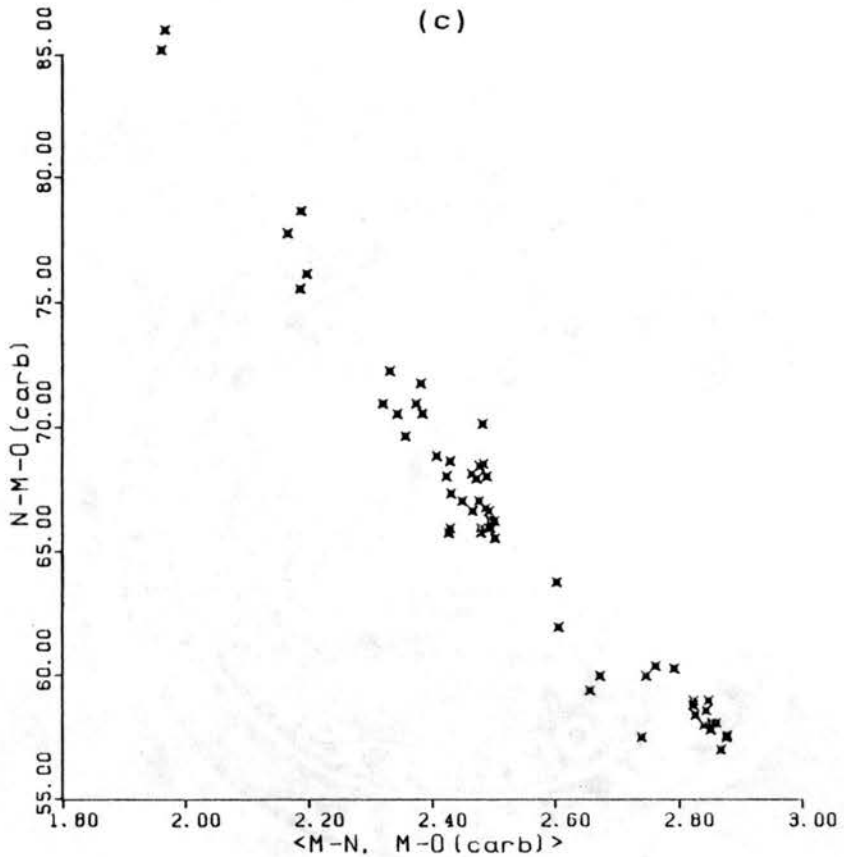

Figure 8.6 (continued) (c) N-M-O(carb) angle versus the average of the M-N and M-O(carb) distances.

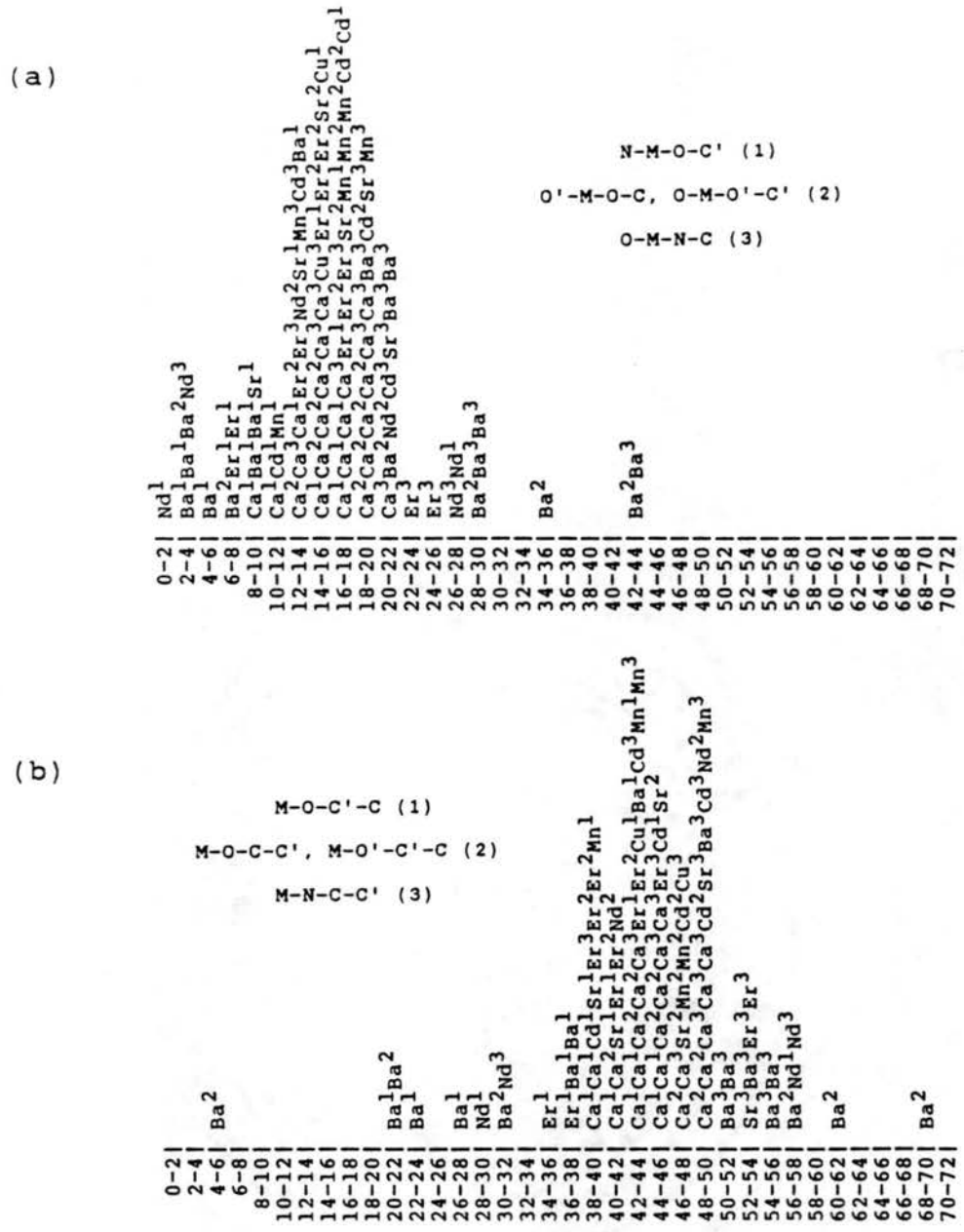

Figure 8.7 Distributions of torsion angles (deg) for amino-ether and diether rings plotted collectively; two-fold symmetry is assumed for the amino-ether rings. The symbols for the elements are used to construct the histograms. (a) Amino-ether N-M-O-C' (type 1) and O-M-N-C (type 3) torsion angles plotted together with diether O'-M-O-C/O-M-O'-C' (type 2) torsion angles. (b) Amino-ether M-N-C-C' (type 1) and M-O-C'-C (type 3) torsion angles plotted together with diether M-O-C-C'/M-O'-C'-C (type 2) torsion angles.

(c)

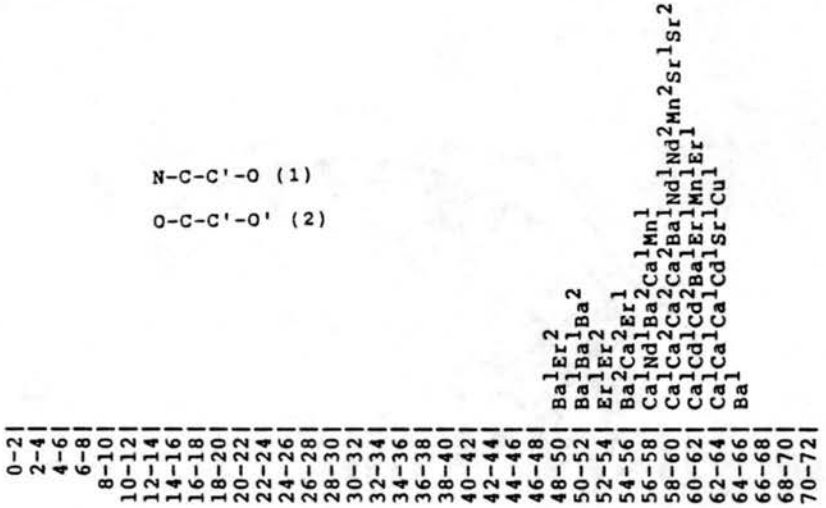

Figure 8.7 (continued) (c) Amino-ether N-C-C'-O (type 1) torsion angles plotted together with diether O-C-C'-O' (type 2) torsion angles.

with the flexible bonding available through the ether oxygen atoms of the diether ring (see below).

The distributions of the five unique torsion angles of the glycinate rings are plotted in Figure 8.8. In contrast to the amino-ether and diether rings, the observed distributions of torsion angles for the glycinate rings are quite broad. This is consistent with the observation of a wide variety of minimum asymmetry parameters for these rings. Clearly, carboxylate bridging interactions must have a considerable influence on the conformations of these rings. There are not enough carboxylate groups that are not involved in bridging interactions to assess the potential influences of bridging to counterions.

Flexibility of Ether Oxygen Binding

When a water molecule binds to a metal ion, it can orient itself along the dipole axis of the water molecule, or along the axis of one of the lone pairs. In a recent survey of the geometry of water molecules in crystalline hydrates,[146] approximately half of the water molecules only involved in one coordinate bond formed a bond oriented along the lone pair axis, while the remaining water molecules formed bonds oriented along the dipole of the water molecule. Ether oxygen atom coordination possibilites resemble those of a water molecule. Two views of the distribution of ether oxygen atom positions are shown in Figure 8.9. As discussed for the erbium and

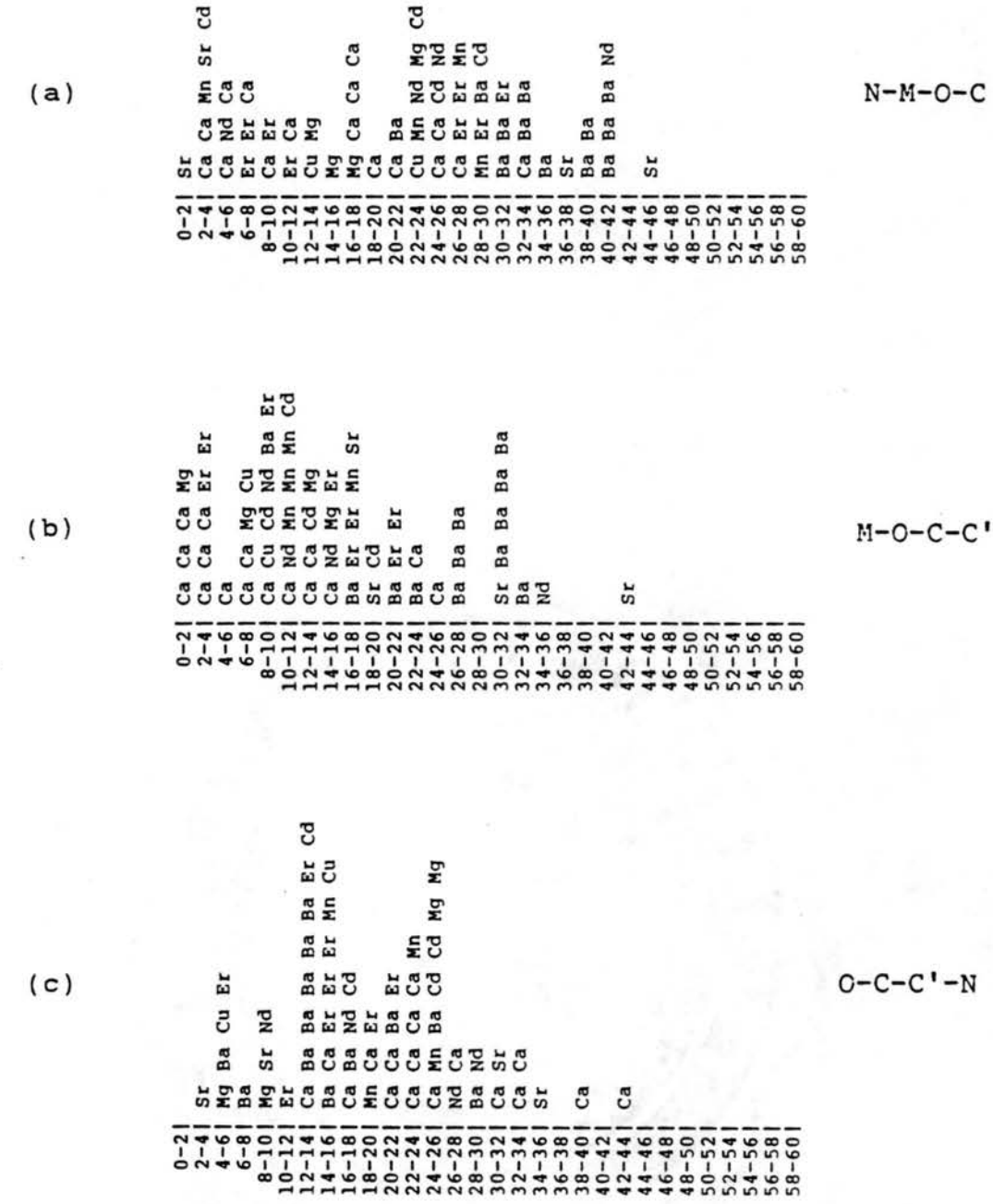

Figure 8.8 Distributions of torsion angles for glycinate rings. The symbols for the elements are used to construct the histograms. (a) N-M-O-C torsion angles. (b) M-O-C-C' torsion angles. (c) O-C-C'-N torsion angles.

(d)

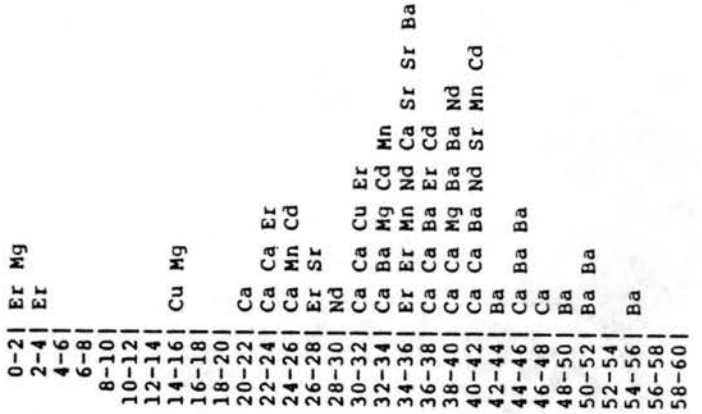

(e)

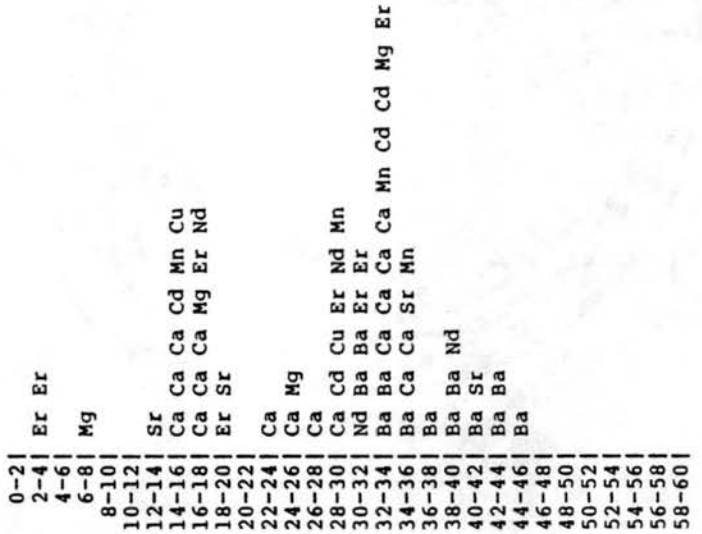

Figure 8.8 (continued) (d) C-C'-N-M torsion angles. (e) C'-N-M-O torsion angles.

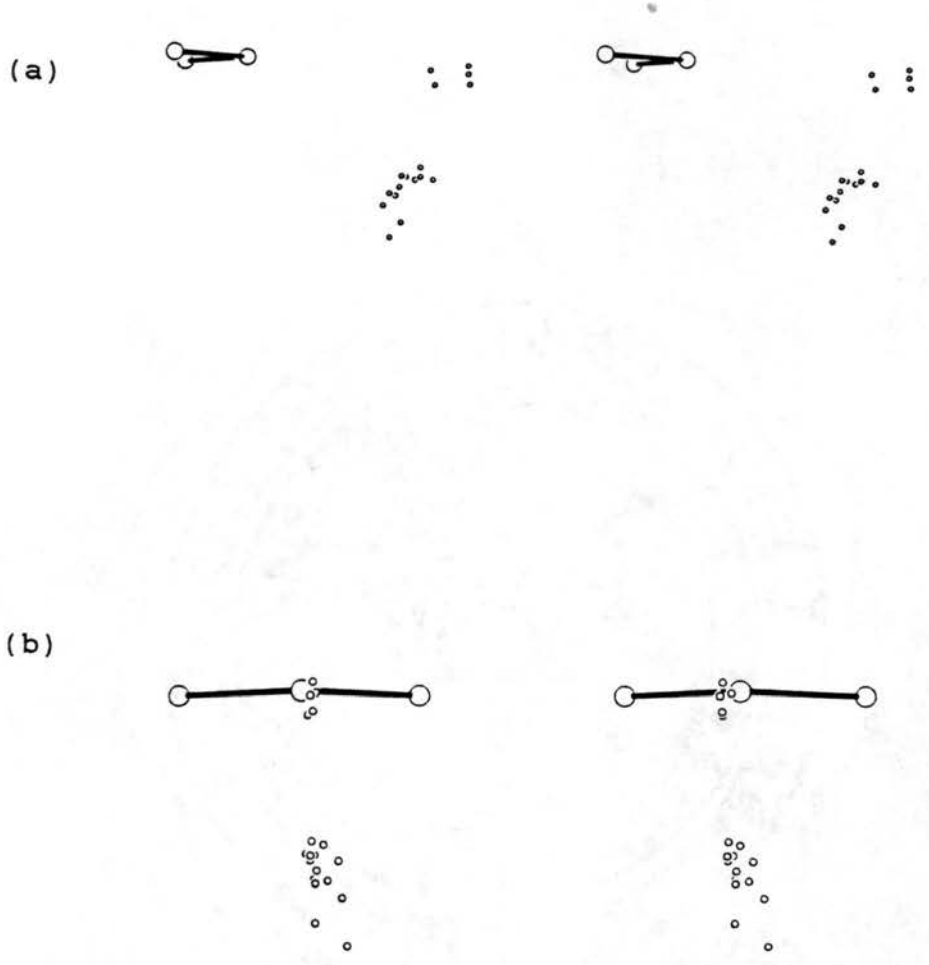

Figure 8.9 Two stereoviews of metal atom positions relative to a fragment of the $EGTA^{4-}$ ligand containing an ether oxygen atom and the two carbon atoms bound to it.

barium structures, a "planar" mode of coordination is seen for one of M-O(ether) bonds in the chelates of these metal ions, while the majority of the M-O(ether) bonds are coincident with a lone pair of the ether oxygen atom. The conformational flexibility associated with the potential of the "planar" coordination mode appears to be invoked when necessary to facilitate organization of the chelate about a metal ion. This feature endows the $EGTA^{4-}$ ligand with greater conformational flexibility than that exhibited by $EDTA^{4-}$ chelates.

Conclusions

In general, the structural parameters observed for $EGTA^{4-}$ chelates do not differ greatly from those observed for $EDTA^{4-}$ chelates. In cases where disparities are observed, the greater flexibility in the bonding associated with the ether oxygen atoms is implicated. The large number of conformational degrees of freedom may be associated with attainment of higher coordination numbers than would be possible with less flexible ligands (see, for example, the Nd and Er chelates). Preferences among the metal ions toward the available ligand atom types appear to be governed by the hard/soft characteristics of the metal ions. These preferences are also operative in choosing a ligand atom type to bind more weakly if the steric constraints of the bonding demand that such a choice be made.

REFERENCES

1. Barnett, B.L.; Uchtman, V.A. Inorg. Chem. **1979**, 18, 2674.

2. Passer, E.; White, J.G.; Cheng, K.L. Inorg. Chim. Acta **1977**, 24, 13.

3. Stezowski, J.J.; Countryman, R.; Hoard, J.L. Inorg. Chem. **1973**, 12, 1749.

4. Ze-Ying, Z.; Mei-Cheng, S.; Xiang-Ling, J. Acta Chim. Sin. **1981**, 39, 829.

5. Solans, X.; Gali, S.; Font-Altaba, M.; Oliva, J.; Herrera, J. Acta Crystallogr., Sect. C: Cryst. Struct. Commun. **1983**, 39, 438.

6. Shao, M.C.; Tang, Z.-R.; Liu, T.-C.; Song, S.-Y.; Tang, Y.-Q. Sci. Sin. **1979**, 22, 912.

7. Templeton, L.K.; Templeton, D.H.; Zalkin, A.; Ruben, H.W. Acta Crystallogr., Sect. B: Struct. Sci. **1982**, 38, 2155.

8. Nassimbeni, L.R.; Wright, M.R.W.; van Niekerk, J.C.; McCallum, P.A. Acta Crystallogr., Sect. B: Struct. Sci. **1979**, 35, 1341.

9. Engel, D.W. Acta Crystallogr., Sect. C: Cryst. Struct. Commun. **1984**, 40, 1687.

10. Lee, B. Ph.D. Dissertation, Cornell University, Ithaca, N.Y., Feb. 1967.

11. Lind, M.D.; Lee, B.; Hoard, J.L. J. Am. Chem. Soc. **1965**, 87, 1611.

12. Hoard, J.L.; Lee, B.; Lind, M.D. J. Am. Chem. Soc. **1965**, 87, 1612.

13. Filippova, T.V.; Polynova, T.N.; Il'inskii, A.L.; Porai-Koshits, M.A.; Martynenko, L.I. Zh. Strukt. Khim. **1977**, 18, 1127.

14. Nesterova, Ya.M.; Zbryskaya, S.G.; Polynova, T.N.; Porai-Koshits, M.A. Zh. Strukt. Khim. **1972**, 13, 739.

15. Sysoeva, T.F.; Agre, V.M.; Trunov, V.K.; Dyatlova, N.M.; Fridman, A.Ya.; Barkhanova, N.N. Zh. Strukt. Khim. **1981**, 22, 99.

16. Agre, V.M.; Sysoeva, T.F.; Trunov, V.K.; Fridman, A.Ya.; Barkhanova, N.N. Zh. Strukt. Khim. **1981**, 22, 114.

17. Agre, V.M.; Sysoeva, T.F.; Trunov, V.K.; Efremov, V.A.; Fridman, A.Ya.; Barkhanova, N.N. Zh. Strukt. Khim. **1980**, 21, 110.

18. Nesterova, Ya. M.; Porai-Koshits, M.A.; Logvinenko, V.A. Zh. Strukt. Khim. **1980**, 21, 171.

19. Filippova, T.V.; Polynova, T.N.; Il'inskii, A.L.; Porai-Koshits, M.A.; Martynenko, L.I. Zh. Neorg. Khim. **1981**, 26, 1140.

20. Porai-Koshits, M.A.; Nesterova, Ya.M.; Polynova, T.N.; Turk De Garcia Banus, D.T. Koord. Khim. **1975**, 1, 682.

21. Smith, G.S.; Hoard, J.L. J. Am. Chem. Soc. **1959**, 81, 556.

22. McCandlish, E.F.K.; Michael, T.K.; Neal, J.A.; Lingafelter, E.C.; Rose, N.J. Inorg. Chem. **1978**, 17 1383.

23. Pozhidaev, A.I.; Nesterova, Ya.M.; Polynova, T.N.; Porai-Koshits, M.A.; Logvinenko, V.A. Zh. Strukt. Khim. **1977**, 18, 408.

24. Nesterova, Ya.M.; Porai-Koshits, M.A.; Logvinenko, V.A. Zh. Neorg. Khim. **1981**, 26, 1141.

25. Richards, S.; Pederson, B.; Silverton, J.V.; Hoard, J.L. Inorg. Chem. **1964**, 3, 27.

26. Weakliem, H.A.; Hoard, J.L. J. Am. Chem. Soc. **1959**, 81, 549.

27. Gerdom, L.E.; Baenziger, N.A.; Goff, H.M. Inorg. Chem. **1981**, 20, 1606.

28. Stein, J.; Fackler, J.P., Jr.; McClune, G.J.; Fee, J.A.; Chan, L.T. Inorg. Chem. **1979**, 18, 3511.

29. Lis, T.; Acta Crystallogr., Sect. B: Struct. Sci. **1978**, 34, 1342.

30. Lind, M.D.; Hamor, M.J.; Hamor, T.A.; Hoard, J.L. Inorg. Chem. **1964**, 3, 34.

31. Novozhilova, N.V.; Polynova, T.N.; Porai-Koshits, M.A. Zh. Strukt. Khim. **1975**, 16, 865.

32. Cohen, G.H.; Hoard, J.L. J. Am. Chem. Soc. **1966**, 88, 3228.

33. Novozhilova, N.V.; Polynova, T.N.; Porai-Koshits, M.A.; Martynenko, I.I. Zh. Strukt. Khim. **1967**, 8, 553.

34. Nesterova, Ya.M.; Porai-Koshits, M.A.; Logvinenko, V.A. Zh. Neorg. Khim. **1979**, 24, 2273.

35. Stephens, F.S.; J. Chem. Soc., A **1969**, 1723.

36. Agre, V.M.; Kozlova, N.P.; Trunov, V.K.; Ershova, S.D. Zh. Strukt. Khim. **1981**, 22, 138.

37. Lin, G.H.Y.; Leggett, J.D.; Wing, R.M. Acta Crystallogr., Sect. B: Struct. Sci. **1973**, 29, 1023.

38. Hoard, J.L.; Scheidt, W.R.; Countryman, R. J. Am. Chem. Soc. **1971**, 93, 3878.

39. Shimoi, M.; Orita, Y.; Uehiro, T.; Kita, I.; Iwamoto, T.; Ouchi, A.; Yoshino, Y. Bull. Chem. Soc. Jpn. **1980**, 53, 3189.

40. Shields, K.G.; Seccombe, R.C.; Kennard, C.H.L. J. Chem. Soc., Dalton Trans. **1973**, 741.

41. van Remoortere, F.P.; Flynn, J.J.; Boer, F.P. Inorg. Chem. **1971**, 10, 2313.

42. Kennard, C.H.L. Inorg. Chim. Acta **1967**, 1, 347.

43. Polynova, T.N.; Bel'skaya, N.P.; Turk de Garcia Banus, D.; Porai-Koshits, M.A.; Martynenko, L.I. Zh. Strukt. Khim. **1970**, 11, 164.

44. Pozhidaev, A.I.; Porai-Koshits, M.A.; Polynova, T.N. Zh. Strukt. Khim. **1974**, 15, 644.

45. Stezowski, J.J.; Hoard, J.L. Isr. J. Chem. **1984**, 24, 323.

46. Spirlet, M.-R.; Rebizant, J.; Desreux, J.F.; Loncin, M.-F. Inorg. Chem. **1984**, 23, 359.

47. Spirlet, M.-R.; Rebizant, J.; Loncin, M.-F.; Desreux, J.F. Inorg. Chem. **1984**, 23, 4278.

48. Martell, A.E.; Smith, R.M. "Critical Stability Constants"; Plenum Press: New York, 1974; Vol I.

49. Spiro, T.G., Ed. "Calcium in Biology", Metal Ions in Biology **1983**, 6.

50. Sigel, H., Ed. "Calcium and Its Role in Biology", Metal Ions in Biological Systems **1984**, 17.

51. Cheung, W.Y. Science **1980**, 207, 19.

52. Cheung, W.Y., Ed. "Calcium and Cell Function"; Acad. Press: New York, 1980; Vol. 1.

53. Cheung, W.Y., Ed. "Calcium and Cell Function"; Acad. Press: New York, 1982; Vol. 2.

54. Campbell, A.K. "Intracellular Calcium"; John Wiley & Sons Limited: New York, 1983.

55. DeBernard, B.; Sottocasa, G.L.; Sandri, G.; Carafoli, E.; Taylor, A.N.; Vanaman, T.C.; Williams, R.J.P., Eds. "Calcium Binding Proteins, 1983", Developments in Biochemistry **1983**, 25.

56. Siegel, F.L.; Carafoli, E.; Kretsinger, R.H.; Maclennan, D.H.; Wasserman, R.H., Eds. "Calcium Binding Proteins: Structure and Function", Developments in Biochemistry **1980**, 14.

57. Kretsinger, R.H. Crit. Rev. Biochem. **1980**, 8, 119.

58. Watterson, D.M.; Vincenzi, F.F., Eds. "Calmodulin and Cell Function", Ann. New York Acad. Sci. **1980**, 356.

59. Means, A.R.; Tash, J.R.; Chafouleas, J.G. Physiol. Rev. **1982**, 62, 1.

60. Ashley, C.C. In ref. 49, Ch. 3, p 107.

61. Cormier, M.J. In ref. 49, Ch. 2, p 53.

62. Rubin, R.P. In ref. 49, Ch. 4, p 175.

63. Creutz, C.E. In ref. 50, Ch. 8, p 319.

64. Ref. 54, Chapter 2.

65. Seamon, K.B.; Kretsinger, R.H. In ref. 49, Ch. 1, p 1.

66. Sundaralingam, M.; Drendel, W.; Greaser, M. Annual Meeting of the American Crystallographic Association, Stanford, California, August 1985; American Crystallographic Association: New York, New York, 1985; Abstr. PB12.

67. Babu, Y.S.; Sack, J.S.; Greenhough, T.J.; Bugg, C.E.; Means, A.R.; Cook, W.J. Nature **1985**, 315, 37.

68. Moews, P.C.; Kretsinger, R.H. J. Mol. Biol. **1975**, 91, 201.

69. Armitage, I.M.; Boulanger, Y. "NMR of Newly Accessible Nuclei", Lazlo, P., Ed.; Acad. Press: New York, 1983; Vol 2, Ch. 13, p 337.

70. Ellis, P.D.; Science **1983**, 221, 1141.

71. Martin, R.B. in ref. 49, Ch. 6, p 235.

72. Nieboer, E. Struct. Bonding (Berlin) **1975**, 22, 1.

73. Horrocks, W.DeW., Jr.; Albin, M. Prog. Inorg. Chem. **1984**, 31, 1.

74. Richardson, F.S. Chem. Rev. **1982**, 82, 541.

75. Bryson, A.; Nancollas, G.H. Chem. Ind. (London) **1965**, 654.

76. Reed, G.H.; Kula, R.J. Inorg. Chem. **1971**, 10, 2050.

77. Sheldrick, G.M. "SHELXTL", Revision 4, Nicolet XRD: 1983.

78. "International Tables for X-Ray Crystallography"; Kynoch Press: Birmingham, England, 1974; Vol. IV, p 99.

78. Ibid, p 149.

80. Abrahams, S.C. Acta Crystallogr., Sect. B: Struct. Sci. **1974**, 30, 261.

81. Lawton, S.L. "TRACER", April, 1967.

82. Birnbaum, G.I. Acta Crystallogr., Sect. B: Struct. Sci. **1967**, 23, 526.

83. Emsley, J. Chem. Soc. Rev. **1981**, 91.

84. Manojlovic, L.; Speakman, J.C. J. Chem. Soc., A **1967**, 971.

85. Hamilton, W.C.; Ibers, J.A. "Hydrogen Bonding in Solids"; Benjamin: New York, 1968.

86. Cotrait, M. Acta Crystallogr., Sect. B: Struct. Sci. **1972**, 28, 781.

87. Novak, A. Struct. Bonding. (Berlin) **1974**, 18, 177.

88. Novak, A.; Cotrait, M.; Joussot-Dubien, J.; Lascombe, J. Bull. Soc. Chim. Fr. (Mem.) **1965**, 1440.

89. Einspahr, H.; Bugg, C.E. In ref. 50, Ch. 2, p 51.

90. Einspahr, H.; Bugg, C.E. In "Calcium Binding Proteins and Calcium Function"; Wasserman, R.H.; Corradino, R.A.; Carafoli, E.; Kretsinger, R.H.; MacLennan, D.H.; Siegel, F.L., Eds.; Elsevier North-Holland: 1977; p 13.

91. Ancillotti, F.; Boschi, G.; Perego, G.; Zazzetta, A. J. Chem. Soc., Dalton Trans. **1977**, 901.

92. Mirti, P.; Gennaro, M.C. J. Inorg. Nucl. Chem. **1981**, 43, 3221.

93. Mirti, P. J. Inorg. Nucl. Chem. **1979**, 41, 323.

94. Uchtman, V.A.; Oertel, R.P. J. Am. Chem. Soc. **1973**, 95, 1802.

95. Metz, B.; Moras, D.; Weiss, R. Acta Crystallogr., Sect. B: Struct. Sci. **1973**, 29, 1377.

96. Duax, W.L.; Norton, D.A. "Atlas of Steroid Structure"; IFI/Plenum: New York, 1975; Vol I, p 17.

97. Dalley, N.K. In "Synthetic Multidentate Macrocyclic Componds"; Izatt, R.M.; Christensen, J.T., Eds.; Acad. Press: New York, 1978; Ch. 4, p 207.

98. Day, R.J.; Reilley, C.N. Anal. Chem. **1965**, 37, 1326.

99. Day, R.J.; Reilley, C.N. Anal. Chem. **1964**, 36, 1073.

100. Haiech, J.; Klee, C.B.; Demaille, J.G. Biochemistry **1981**, 20, 3890.

101. Nancollas, G.H. Coord. Chem. Rev. **1970**, 5, 379.

102. Wright, D.L.; Holloway, J.H.; Reilley, C.N. Anal. Chem. **1965**, 37, 884.

103. Anderegg, G. Helvet. Chim. Acta **1964**, 47, 1801.

104. Bozhidaev, A.I.; Polynova, T.N.; Porai-Koshits, M.A. Acta Crystallogr., Sect A: Found. Crystallogr. **1972**, 28, S76.

105. Hughes, D.L.; Mortimer, C.L.; Truter, M.R. Inorg. Chim. Acta **1978**, 29, 43.

106. Fenton, D.E.; Parkin, D.; Newton, R.F.; Nowell, I.W.; Walker, P.E. J.Chem.Soc., Dalton Trans. **1982**, 327.

107. Briggman, B.; Oskarsson, Å. Acta Crystallogr., Sect. B: Struct. Sci. **1977**, B33, 1900.

108. Voegele, J.C.; Fischer, J.; Weiss, R. Acta Crystallogr., Sect. B: Struct. Sci. **1974**, 30, 66.

109. Metz, B; Moras, D.; Weiss, R. Acta Crystallogr., Struct. Sci. **1973**, 29, 1382.

110. Metz, B; Moras, D.; Weiss, R. Acta Crystallogr., Sect. B: Struct. Sci, **1973**, 29, 1388.

111. Tsien, R.Y. Biochemistry **1980**, 19, 2396.

112. Vogel, H.J.; Drakenberg, T.; Forsén, S. In "NMR of Newly Accessible Nuclei"; Lazlo, P., Ed.; Acad. Press: New York, 1983; Vol. 1, Ch. 7, p 157.

113. Andersson, T.; Drakenberg, T.; Forsén, S.; Thulin, E.; Sward, M. J. Am. Chem. Soc. **1982**, 104, 576.

114. Sudnick, D.R.; Horrocks, W.DeW., Jr. Biochim. Biophys. Acta **1979**, 578, 135.

115. Horrocks, W.DeW.; Sudnick, D.R. J. Am. Chem. Soc. **1979**, 101, 334.

116. Moews, P.C.; Kretsinger, R.H. J. Mol. Biol. **1975**, 91, 229.

117. Sowadski, J.; Cornick, G.; Kretsinger, R.H. J. Mol. Biol. **1978**, 124, 123.

118. Shannon, R.D. Acta Crystallogr., Sect. A: Found. Crystallogr. **1976**, 32, 751.

119. Boman, C.-E. Acta Crystallogr., Sect. B: Struct. Sci. **1977**, 33, 838-843.

120. Iwamoto, R.; Wakano, H. J. Am. Chem. Soc. **1976**, 98, 3764.

121. Frey, C.M.; Stuehr, J. Metal Ions in Biological Systems **1974**, 1, 69.

122. Keller, A.D.; Drakenberg, T.; Briggs, R.W.; Armitage, I.M. Inorg. Chem. **1985**, 24, 1170.

123. Murphy, P.D.; Gerstein, B.C. J. Am. Chem. Soc. **1981**, 103, 3282.

124. Cheung, T.T.P.; Worthington, L.E.; DuBois Murphy, P.; Gerstein, B.C.; J. Magn. Reson. **1980**, 41, 158.

125. Mennitt, P.G.; Shatlock, M.P.; Bartuska, V.J.; Maciel, G.E. J. Phys. Chem. **1981**, 85, 2087.

126. Honkonen, R.S.; Doty, F.D.; Ellis, P.D. J. Am. Chem. Soc. **1983**, 105, 4163.

127. Honkonen, R.S.; Ellis, P.D. J. Am. Chem. Soc. **1984**, 106, 5488.

128. Jensen, C.F.; Deshmukh, S.; Jakobsen, H.J.; Inners, R.R.; Ellis, P.D. J. Am. Chem. Soc. **1981**, 103, 3659.

129. Grenthe, I. Acta Chem. Scand. **1971**, 25, 3721.

130. Elding, I. Acta Chem. Scand., Ser. A **1977**, 31, 75.

131. Albertsson, J.; Elding, I. Acta Chem. Scand., Ser. A **1977**, 31, 21.

132. Oskarsson, Å. Acta Chem. Scand. **1971**, 25, 1206.

133. Albertsson, J. Acta Chem. Scand. **1970**, 24, 3527.

134. Seccombe, R.C.; Lee, B.; Henry, G.M. Inorg. Chem. **1975**, 14, 1147.

135. Zetter, M.S.; Grant, M.W.; Wood, E.J.; Dodgen, H.W.; Hunt, J.P. Inorg. Chem. **1972**, 11, 2701.

136. Oakes, J.; Smith, E.G. J. Chem. Soc., Faraday Trans. **1981**, 77, 299.

137. Reed, G.H.; Leigh, J.S., Jr.; Pearson, J.E. J. Chem. Phys. **1971**, 55, 3311.

138. Filippova, T.V.; Polynova, T.N.; Porai-Koshits, M.A.; Novozhilova, N.V.; Martynenko, L.I. Zh. Strukt. Khim. **1973**, 14, 280.

139. Whitlow, S.H. Inorg. Chem. **1973**, 12, 2286.

140. Fomenko, V.V.; Kopaneva, L.I.; Porai-Koshits, M.A.; Polynova, T.N. Zh. Strukt. Khim. **1974**, 15, 268.

141. Podder, A.; Dattagupta, J.K.; Saha, N.N.; Saenger, W. Acta Crystallogr., Sect. B: Struct. Sci. **1979**, 35, 53.

142. Whitlow, S.H.; Davey, G. J. Chem. Soc., Dalton Trans. **1975**, 1228.

143. Ohzeki, K.; Saruhashi, M.; Kambara, T. Bull. Chem. Soc. Jpn. **1980**, 53, 2548.

144. Klopman, G. J. Am. Chem. Soc. **1968**, 90, 223.

145. Pearson, R.G. J. Chem. Educ. **1968**, 45, 581.

146. Chiari, G.; Ferraris, G. Acta Crystallogr., Sect. B: Struct. Sci. **1982**, 38, 2331.

APPENDIX A

ATOMIC COORDINATES AND THERMAL PARAMETERS

For the tables contained in this Appendix, estimated standard deviations in the least significant digit(s) are given in parentheses. If no standard deviation is given, the quantity was not refined.

The anisotropic thermal parameter exponent takes the form: $-2\pi^2(\underline{h}^2\underline{a}^{*2}\underline{U}_{11} + \underline{k}^2\underline{b}^{*2}\underline{U}_{22} + \ldots + 2\underline{hk}a^*b^*\underline{U}_{12})$.

Table A.1 Atomic Coordinates (x 10^4) and Thermal Parameters ($Å^2$ x 10^3) for H_4EGTA

atom	x	y	z	U_{11}	U_{22}	U_{33}	U_{23}	U_{13}	U_{12}
C1	2215(3)	10095(3)	8800(2)	20(1)	26(1)	32(1)	-11(1)	12(1)	-6(1)
C2	2121(3)	12130(3)	9314(2)	26(1)	22(1)	23(1)	-3(1)	5(1)	-6(1)
C3	5010(3)	10210(3)	6807(2)	27(1)	33(1)	22(1)	-3(1)	8(1)	-9(1)
C4	7383(3)	9899(3)	6532(2)	30(1)	31(1)	30(1)	-9(1)	6(1)	-14(1)
C5	4497(4)	6827(3)	7885(2)	33(1)	25(1)	42(1)	-14(1)	10(1)	-10(1)
C6	6732(4)	5434(4)	7478(2)	39(1)	29(1)	41(1)	-11(1)	12(1)	-3(1)
C7	9692(4)	4835(4)	5751(3)	28(1)	46(1)	44(1)	-17(1)	7(1)	0(1)
N1	4392(3)	9019(2)	8098(2)	20(1)	22(1)	22(1)	-7(1)	6(1)	-5(1)
O1	213(3)	13339(2)	9562(2)	29(1)	28(1)	50(1)	-14(1)	3(1)	-0(1)
O2	3747(2)	12448(2)	9481(2)	31(1)	29(1)	36(1)	-7(1)	1(1)	-10(1)
O3	8059(3)	10403(3)	5287(2)	33(1)	54(1)	30(1)	-1(1)	11(1)	-20(1)
O4	8419(3)	9311(3)	7461(2)	34(1)	59(1)	35(1)	-6(1)	1(1)	-22(1)
O5	7479(3)	5897(3)	6092(2)	31(1)	42(1)	37(1)	-15(1)	9(1)	-1(1)
H1	5290(36)	8970(33)	8649(22)	21(5)					
Ha1	0	15000	10000	103(17)					
Ha2	10000	10000	5000	55(11)					
H1a	1226	10384	8172	32					
H1b	1823	9197	9559	32					
H3a	4617	9737	6066	36					
H3b	4268	11666	6879	36					
H5a	3686	6895	7181	42					
H5b	3877	6227	8718	42					
H6a	6738	4006	7615	50					
H6b	7652	5648	8030	50					
H7a	10500	5385	6212	59					
H7b	9961	3372	6014	59					

Table A.2 Atomic Coordinates (x 10^4) and Thermal Parameters ($Å^2$ x 10^3) for $Ca[Ca(EGTA)]\cdot(22/3)H_2O$

atom	x	y	z	U_{11}	U_{22}	U_{33}	U_{23}	U_{13}	U_{12}
Ca1	1538(1)	11479(1)	4187(1)	26(1)	24(1)	27(1)	-0(1)	3(1)	2(1)
Ca2	1611(1)	8445(1)	1149(1)	26(1)	24(1)	23(1)	2(1)	1(1)	-2(1)
Ca3	4707(1)	11366(1)	2465(1)	32(1)	30(1)	43(1)	-5(1)	9(1)	-3(1)
Ca4	-24(1)	12459(1)	162(1)	29(1)	24(1)	24(1)	0(1)	2(1)	-4(1)
Ca5	465(1)	9934(1)	2529(1)	34(1)	30(1)	25(1)	1(1)	3(1)	1(1)
Ca6	3788(1)	9675(1)	3169(1)	27(1)	27(1)	46(1)	1(1)	-1(1)	2(1)
C1	2399(3)	11382(4)	2906(3)	34(3)	46(4)	42(4)	-11(3)	11(3)	6(3)
C2	2656(2)	10908(4)	3514(3)	29(3)	32(3)	52(4)	-12(3)	10(3)	0(3)
C3	1681(3)	12360(4)	2587(3)	43(4)	42(4)	28(3)	2(3)	13(3)	3(3)
C4	1127(2)	12592(3)	2822(3)	37(3)	22(3)	34(3)	-2(2)	6(3)	2(2)
C5	2419(3)	12678(4)	3460(4)	36(4)	41(4)	54(4)	-4(3)	14(3)	-7(3)
C6	2123(3)	13242(4)	3909(3)	45(4)	35(3)	47(4)	-3(3)	11(3)	-3(3)
C7	2302(3)	12822(4)	5114(3)	48(4)	42(4)	46(4)	-17(3)	-6(3)	-6(3)
C8	2053(3)	12353(4)	5675(3)	46(4)	48(4)	37(4)	-18(3)	-9(3)	3(3)
C9	1764(3)	11038(4)	5927(3)	54(4)	49(4)	25(3)	-3(3)	-6(3)	2(3)
C10	1737(3)	10224(4)	5578(3)	50(4)	37(4)	34(3)	4(3)	-8(3)	11(3)
C11	1458(3)	9538(3)	4488(3)	48(4)	25(3)	31(3)	4(2)	2(3)	11(3)
C12	1172(2)	9677(3)	3758(3)	35(3)	24(3)	27(3)	-4(2)	1(2)	5(2)
C13	782(3)	10243(3)	5115(3)	45(4)	24(3)	30(3)	1(2)	5(3)	1(3)
C14	555(2)	11076(3)	5186(3)	28(3)	28(3)	22(3)	1(2)	3(2)	1(2)
C15	2452(3)	8530(4)	2606(3)	41(4)	36(3)	33(3)	-2(3)	-2(3)	-13(3)
C16	2697(2)	9047(4)	2055(3)	30(3)	34(3)	36(3)	-5(3)	2(3)	0(3)
C17	1744(2)	7524(4)	2757(3)	33(3)	42(3)	27(3)	5(3)	3(2)	-7(3)
C18	1207(3)	7278(3)	2390(3)	41(4)	24(3)	30(3)	0(2)	9(3)	-0(2)
C19	2504(3)	7243(4)	2040(3)	39(4)	40(4)	39(3)	6(3)	-1(3)	4(3)
C20	2219(3)	6673(4)	1528(3)	50(4)	32(3)	41(4)	3(3)	3(3)	8(3)
C21	2373(3)	7065(4)	354(4)	46(4)	39(4)	50(4)	-12(3)	11(3)	2(3)
C22	2137(3)	7561(4)	-243(3)	51(4)	40(4)	36(3)	-13(3)	5(3)	-3(3)

Table A.2 (continued)

atom	x	y	z	U_{11}	U_{22}	U_{33}	U_{23}	U_{13}	U_{12}
C23	1919(3)	8922(4)	-493(3)	56(4)	38(4)	30(3)	2(3)	12(3)	-6(3)
C24	1918(3)	9725(4)	-133(3)	46(4)	35(3)	30(3)	6(3)	12(3)	-11(3)
C25	1575(3)	10391(3)	891(3)	41(3)	20(3)	33(3)	-1(2)	2(3)	-6(3)
C26	1245(2)	10240(3)	1514(3)	30(3)	26(3)	32(3)	-2(2)	1(2)	-9(2)
C27	941(3)	9763(3)	51(3)	49(4)	21(3)	34(3)	3(2)	-5(3)	-5(3)
C28	657(2)	8963(3)	-35(3)	29(3)	32(3)	22(3)	4(2)	1(2)	-0(2)
C29	5006(5)	11445(5)	786(4)	133(9)	57(5)	55(5)	-18(4)	38(5)	-39(5)
C30	5209(4)	12218(4)	1124(4)	87(6)	46(4)	57(5)	-20(4)	22(4)	-25(4)
C31	4578(3)	10190(4)	1029(4)	54(4)	39(4)	57(4)	-6(3)	-5(4)	-3(3)
C32	4335(3)	9737(4)	1606(4)	30(3)	28(3)	57(4)	-1(3)	6(3)	1(3)
C33	5523(4)	10419(7)	1418(6)	43(5)	126(9)	112(9)	-62(8)	8(5)	14(5)
C34	5635(6)	10086(9)	2022(9)	52(8)	66(9)	87(11)	-10(8)	0(8)	37(7)
C34'	5941(8)	10673(14)	1997(11)	46(12)	69(14)	62(13)	-26(11)	-0(10)	2(11)
C35	6012(4)	11035(7)	3039(7)	59(6)	139(10)	147(11)	47(9)	16(7)	56(7)
C36	5796(4)	11434(5)	3648(5)	61(6)	74(6)	94(7)	3(5)	-30(5)	14(5)
C37	5156(3)	12465(4)	3888(4)	55(5)	58(5)	49(4)	1(4)	-10(4)	-20(4)
C38	4747(3)	13002(4)	3495(4)	49(4)	41(4)	46(4)	-8(3)	-5(3)	-4(3)
C39	4023(3)	13036(4)	2564(4)	60(5)	29(3)	51(4)	-1(3)	-4(3)	2(3)
C40	3708(3)	12537(4)	1997(4)	49(4)	48(4)	53(4)	3(4)	-5(3)	2(3)
C41	3919(3)	12210(4)	3582(4)	40(4)	42(4)	47(4)	-7(3)	17(3)	-4(3)
C42	4092(3)	11426(4)	3901(3)	39(4)	41(4)	36(3)	-4(3)	3(3)	-10(3)
N1	2064(2)	12043(3)	3142(3)	23(3)	35(3)	36(3)	-6(2)	10(2)	-1(2)
N2	1364(2)	10220(3)	4938(2)	33(3)	24(2)	25(2)	-2(2)	-1(2)	9(2)
N3	2135(2)	7859(3)	2279(2)	27(3)	36(3)	29(3)	-3(2)	-1(2)	-6(2)
N4	1495(2)	9732(3)	392(2)	37(3)	30(3)	25(2)	-1(2)	2(2)	-10(2)
N5	4984(2)	10788(3)	1287(3)	47(3)	33(3)	54(3)	-5(3)	14(3)	-8(2)
N6	4309(2)	12556(3)	3108(3)	42(3)	27(3)	39(3)	1(2)	4(2)	-3(2)
O1	2401(2)	10858(3)	4062(2)	36(3)	56(3)	48(3)	2(2)	10(2)	14(2)
O2	3105(2)	10570(3)	3434(3)	31(2)	53(3)	77(3)	-14(3)	11(2)	12(2)
O3	987(2)	12314(2)	3405(2)	33(2)	38(2)	33(2)	6(2)	6(2)	8(2)
O4	825(2)	13014(3)	2422(2)	50(3)	54(3)	37(2)	12(2)	7(2)	23(2)
O5	1913(2)	12828(2)	4505(2)	40(3)	38(2)	37(2)	-7(2)	-2(2)	-4(2)

Table A.2 (continued)

atom	x	y	z	U_{11}	U_{22}	U_{33}	U_{23}	U_{13}	U_{12}
O6	1952(2)	11565(2)	5410(2)	45(3)	38(2)	34(2)	-8(2)	-2(2)	-1(2)
O7	1136(2)	10379(2)	3524(2)	49(3)	22(2)	30(2)	2(2)	-6(2)	1(2)
O8	989(2)	9090(2)	3414(2)	61(3)	27(2)	34(2)	-3(2)	-7(2)	-0(2)
O9	733(2)	11617(2)	4803(2)	31(2)	26(2)	39(2)	9(2)	7(2)	2(2)
O10	175(2)	11177(2)	5580(2)	35(2)	36(2)	35(2)	6(2)	12(2)	6(2)
O11	2474(2)	9030(3)	1435(2)	35(2)	46(3)	32(2)	3(2)	-6(2)	-14(2)
O12	3087(2)	9503(3)	2244(2)	34(2)	43(3)	44(3)	-3(2)	-5(2)	-14(2)
O13	1062(2)	7584(2)	1797(2)	31(2)	38(2)	32(2)	7(2)	-2(2)	-10(2)
O14	909(2)	6809(3)	2710(2)	51(3)	44(3)	43(3)	13(2)	5(2)	-19(2)
O15	2006(2)	7076(2)	901(2)	42(2)	38(2)	34(2)	-6(2)	5(2)	1(2)
O16	2066(2)	8341(2)	28(2)	53(3)	35(2)	25(2)	-7(2)	11(2)	-2(2)
O17	1211(2)	9533(2)	1742(2)	45(3)	26(2)	36(2)	4(2)	12(2)	-2(2)
O18	1001(2)	10810(2)	1789(2)	61(3)	27(2)	39(2)	-2(2)	13(2)	5(2)
O19	814(2)	8394(2)	355(2)	38(2)	28(2)	28(2)	6(2)	-4(2)	-5(2)
O20	257(2)	8903(3)	-486(2)	38(2)	40(2)	36(2)	11(2)	-13(2)	-12(2)
O21	5156(2)	12312(3)	1772(2)	70(3)	41(3)	47(3)	-11(2)	21(2)	-16(2)
O22	5406(3)	12718(3)	729(3)	180(7)	53(3)	65(4)	-11(3)	55(4)	-46(4)
O23	4321(2)	10067(3)	2208(2)	31(2)	41(2)	52(3)	-11(2)	9(2)	-8(2)
O24	4154(2)	9061(3)	1466(3)	45(3)	40(3)	64(3)	-15(2)	11(2)	-8(2)
O25	5576(2)	10664(4)	2638(3)	72(4)	98(5)	66(4)	3(3)	1(3)	47(3)
O26	5369(2)	11949(3)	3375(3)	42(3)	50(3)	69(3)	3(3)	-13(2)	1(2)
O27	3859(2)	11824(3)	1930(3)	55(3)	47(3)	53(3)	-7(2)	-5(2)	2(2)
O28	3338(3)	12868(3)	1624(3)	84(4)	68(4)	74(4)	3(3)	-39(3)	18(3)
O29	4291(2)	10914(2)	3498(2)	49(3)	30(2)	48(3)	1(2)	10(2)	-1(2)
O30	3999(2)	11298(3)	4529(3)	87(4)	66(3)	40(3)	6(3)	9(3)	-4(3)
w1	-686(2)	12664(3)	1016(2)	45(3)	38(2)	43(2)	-2(2)	19(2)	3(2)
w2	-451(2)	13271(3)	-788(2)	54(3)	36(2)	35(2)	4(2)	-10(2)	-5(2)
w3	428(2)	11698(3)	-718(2)	55(3)	38(2)	44(3)	-8(2)	15(2)	-8(2)
w4	640(2)	12206(3)	1119(2)	47(3)	37(2)	41(3)	-1(2)	-11(2)	1(2)
w5	120(2)	11258(3)	2879(3)	45(3)	38(3)	82(4)	-16(3)	1(3)	8(2)
w6	-304(2)	9655(3)	3207(3)	61(3)	78(4)	50(3)	25(3)	27(3)	17(3)
w7	176(2)	8582(3)	2156(3)	41(3)	39(3)	77(3)	-13(2)	11(2)	-7(2)

Table A.2 (continued)

atom	x	y	z	U_{11}	U_{22}	U_{33}	U_{23}	U_{13}	U_{12}
w8	-242(2)	10112(3)	1604(3)	58(3)	86(4)	49(3)	31(3)	-17(2)	-16(3)
w9	3327(3)	8963(4)	4087(3)	122(5)	66(4)	55(3)	18(3)	1(3)	-14(4)
w10	4582(3)	9250(4)	3900(4)	98(5)	52(4)	173(7)	9(4)	-80(5)	4(3)
w11	3946(2)	8321(3)	2721(3)	57(3)	37(3)	87(4)	-2(3)	21(3)	6(2)
w12	3083(2)	759(3)	1237(3)	70(4)	57(3)	63(3)	11(3)	-10(3)	-15(3)
w13	3051(2)	4446(4)	1592(3)	70(4)	72(4)	86(4)	-4(3)	-12(3)	-3(3)
w14	3132(2)	172(4)	5098(3)	59(4)	125(5)	60(4)	-13(4)	2(3)	5(4)
w15	3321(3)	8725(5)	476(4)	55(4)	156(7)	127(6)	-87(5)	20(4)	-19(4)
w16	3721(3)	2378(5)	272(3)	133(6)	129(6)	58(4)	8(4)	15(4)	-46(5)
w17	3420(3)	4157(5)	4863(4)	124(6)	122(6)	80(5)	-19(4)	14(4)	-16(5)
w18	2380(3)	4933(5)	2663(4)	74(5)	167(8)	123(6)	15(6)	14(4)	21(5)
w19	3097(3)	5218(6)	3863(5)	82(5)	166(8)	170(8)	-9(7)	37(5)	11(5)
w20	1270(3)	5072(6)	2736(6)	77(6)	176(9)	212(10)	68(8)	38(6)	14(6)
w21	3561(5)	7425(10)	4618(8)	175(10)	388(19)	368(19)	283(17)	198(12)	194(12)
w22	4443(8)	4802(11)	357(11)	320(22)	216(17)	355(25)	-196(18)	-201(20)	121(17)
w23	6660(12)	11943(18)	1488(17)	55(18)	75(20)	99(24)	-1(18)	-39(16)	-26(15)
H1a	2169	11036	2612	49					
H1b	2686	11594	2640	49					
H3a	1845	12823	2393	42					
H3b	1626	11960	2228	42					
H5a	2713	12434	3746	56					
H5b	2569	12975	3087	56					
H6a	1821	13477	3631	49					
H6b	2372	13652	4080	49					
H7a	2640	12579	4996	56					
H7b	2373	13357	5274	56					
H8a	1713	12594	5790	51					
H8b	2302	12333	6089	51					
H9a	2018	11031	6337	47					
H9b	1407	11195	6060	47					
H10a	1609	9843	5904	46					
H10b	2099	10078	5455	46					

Table A.2 (continued)

atom	x	y	z	U_{11}	U_{22}	U_{33}	U_{23}	U_{13}	U_{12}
H11a	1846	9473	4448	42					
H11b	1311	9067	4692	42					
H13a	563	9971	4751	35					
H13b	755	9970	5555	35					
H15a	2212	8849	2869	40					
H15b	2744	8322	2918	40					
H17a	1910	7065	2986	42					
H17b	1672	7918	3104	42					
H19a	2799	7496	1815	49					
H19b	2652	6949	2443	49					
H20a	1921	6422	1747	50					
H20b	2478	6274	1401	50					
H21a	2723	7277	525	49					
H21b	2420	6528	196	49					
H22a	1789	7348	-422	52					
H22b	2384	7574	-614	52					
H23a	2182	8921	-846	45					
H23b	1560	8808	-710	45					
H24a	1836	10133	-478	43					
H24b	2274	9823	101	43					
H25a	1958	10431	1045	37					
H25b	1456	10878	665	37					
H27a	721	10098	329	38					
H27b	962	9992	-408	38					
H29a	5250	11299	432	86					
H29b	4643	11530	569	86					
H31a	4286	10456	756	57					
H31b	4756	9819	734	57					
H33a	5794	10825	1365	113					
H33b	5555	10017	1065	113					
H35a	6278	10641	3200	126					
H35b	6184	11420	2753	126					

Table A.2 (continued)

atom	x	y	z	U_{11}	U_{22}	U_{33}	U_{23}	U_{13}	U_{12}
H36a	6081	11735	3900	97					
H36b	5651	11048	3959	97					
H37a	4978	12159	4233	64					
H37b	5448	12773	4118	64					
H38a	4937	13317	3167	52					
H38b	4586	13347	3827	52					
H39a	3767	13376	2780	55					
H39b	4288	13356	2343	55					
H41a	3875	12580	3958	54					
H41b	3572	12137	3317	54					

Table A.3 Atomic Coordinates (x 10^4) and Thermal Parameters ($Å^2$ x 10^3) for $Sr[Ca(EGTA)]\cdot 6H_2O$

atom	x	y	z	U_{11}	U_{22}	U_{33}	U_{23}	U_{13}	U_{12}
Ca	7601(1)	2627(1)	-2603(1)	31(1)	23(1)	19(1)	2(1)	-12(1)	-7(1)
Sr	10989(1)	5069(1)	-1597(1)	45(1)	39(1)	23(1)	3(1)	-11(1)	-21(1)
C1	5946(5)	1780(4)	-4335(3)	40(3)	29(2)	34(3)	2(2)	-18(2)	-11(2)
C2	6119(5)	717(3)	-3645(3)	28(2)	23(2)	38(3)	3(2)	-11(2)	-4(2)
C3	6815(6)	3710(4)	-4794(4)	53(3)	29(2)	32(3)	6(2)	-21(2)	-11(2)
C4	7238(5)	4717(4)	-4261(3)	37(2)	27(2)	28(3)	3(2)	-11(2)	-9(2)
C5	8899(5)	1834(4)	-5022(3)	42(3)	35(2)	22(3)	-3(2)	-11(2)	-9(2)
C6	10381(5)	2285(4)	-4864(3)	39(3)	44(3)	25(3)	-3(2)	-5(2)	-11(2)
C7	11435(6)	955(4)	-3695(4)	38(3)	40(3)	43(3)	-4(2)	-13(2)	-0(2)
C8	11392(5)	874(4)	-2609(4)	32(3)	46(3)	37(3)	-3(2)	-11(2)	1(2)
C9	9439(6)	892(4)	-1007(4)	45(3)	45(3)	35(3)	6(2)	-21(2)	-1(2)
C10	7580(5)	980(4)	-511(4)	38(3)	43(3)	29(3)	12(2)	-13(2)	-6(2)
C11	4790(5)	1992(4)	-578(4)	30(2)	37(2)	36(3)	8(2)	-13(2)	-11(2)
C12	3864(5)	2901(4)	-1171(3)	35(2)	31(2)	31(3)	-6(2)	-13(2)	-3(2)
C13	6632(5)	3159(4)	-143(3)	37(3)	44(3)	24(3)	1(2)	-7(2)	-16(2)
C14	8030(5)	3826(4)	-634(3)	33(2)	30(2)	26(3)	2(2)	-15(2)	-6(2)
N1	7266(4)	2499(3)	-4408(3)	35(2)	23(2)	26(2)	3(2)	-14(2)	-10(1)
N2	6544(4)	2118(3)	-730(3)	27(2)	30(2)	30(2)	5(2)	-14(2)	-9(1)
O1	6863(4)	791(3)	-2984(2)	57(2)	33(2)	43(2)	12(1)	-31(2)	-19(1)
O2	5469(4)	-137(3)	-3777(3)	59(2)	30(2)	61(3)	9(2)	-31(2)	-23(2)
O3	7590(4)	4494(3)	-3438(2)	72(2)	30(2)	29(2)	5(1)	-26(2)	-16(2)
O4	7145(4)	5722(3)	-4659(2)	66(2)	26(2)	34(2)	10(1)	-19(2)	-16(1)
O5	10450(4)	2111(2)	-3837(2)	36(2)	35(2)	28(2)	-5(1)	-10(1)	-8(1)
O6	9670(4)	989(3)	-2056(2)	34(2)	40(2)	31(2)	3(1)	-15(1)	-3(1)
O7	4705(4)	3461(3)	-1844(3)	42(2)	43(2)	42(2)	19(2)	-16(2)	-7(1)
O8	2279(4)	3011(3)	-941(2)	28(2)	58(2)	38(2)	-4(2)	-12(2)	-2(1)
O9	8704(4)	3689(3)	-1569(2)	43(2)	40(2)	21(2)	4(1)	-12(1)	-20(1)
O10	8432(4)	4524(3)	-95(2)	52(2)	50(2)	27(2)	-4(1)	-14(2)	-24(2)

Table A.3 (continued)

atom	x	y	z	U_{11}	U_{22}	U_{33}	U_{23}	U_{13}	U_{12}
w1	9298(5)	6089(3)	-2821(3)	98(3)	50(2)	72(3)	2(2)	-55(3)	-13(2)
w2	9587(4)	7343(3)	-983(3)	58(2)	53(2)	45(2)	-4(2)	-17(2)	-6(2)
w3	13622(4)	5875(3)	-2418(3)	48(2)	49(2)	63(3)	12(2)	1(2)	-16(2)
w4	12080(4)	3885(3)	-3317(2)	57(2)	48(2)	32(2)	-1(2)	-10(2)	-18(2)
w5	14478(5)	2424(3)	3204(3)	71(2)	42(2)	56(3)	8(2)	-4(2)	-24(2)
w6	12599(6)	1425(3)	2121(3)	122(4)	49(2)	79(3)	19(2)	-60(3)	-13(2)
H1a	4856	2294	-4074	38					
H1b	6044	1475	-4995	38					
H3a	7413	3698	-5495	43					
H3b	5621	3885	-4717	43					
H5a	9007	996	-4854	42					
H5b	8924	1911	-5719	42					
H6a	10261	3131	-5001	45					
H6b	11406	1846	-5313	45					
H7a	10965	317	-3883	47					
H7b	12581	885	-4102	47					
H8a	11851	1514	-2415	51					
H8b	12032	106	-2491	51					
H9a	10063	128	-870	51					
H9b	9823	1536	-756	51					
H10a	7401	938	205	46					
H10b	7228	311	-750	46					
H11a	4789	1189	-792	44					
H11b	4204	2116	125	44					
H13a	5574	3724	-24	43					
H13b	6796	2873	489	43					

Table A.4 Atomic Coordinates (x 10^4) and Thermal Parameters ($Å^2$ x 10^3) for $Mg[Sr(EGTA)(OH_2)]\cdot 7H_2O$

atom	x	y	z	U_{11}	U_{22}	U_{33}	U_{23}	U_{13}	U_{12}
Sr	1166(1)	1149(1)	3892(1)	26(1)	27(1)	27(1)	0(1)	0(1)	-1(1)
Mg1	0	0	5000	29(2)	24(2)	33(2)	4(2)	7(2)	-2(1)
Mg2	2500	2500	3010(2)	29(2)	31(2)	29(2)	0	0	-4(2)
C1	-30(3)	2548(4)	4655(5)	42(4)	26(4)	39(4)	-1(4)	8(4)	2(4)
C2	-156(3)	1758(4)	5116(5)	26(4)	26(4)	37(4)	0(3)	4(3)	-0(3)
C3	602(3)	3215(4)	3501(5)	38(5)	26(4)	52(5)	6(4)	8(4)	-2(4)
C4	1190(3)	3110(4)	2928(5)	29(4)	34(4)	37(4)	2(3)	-1(4)	-10(4)
C5	-150(3)	2199(4)	3055(5)	37(5)	43(5)	43(5)	5(4)	1(4)	6(4)
C6	151(4)	1932(4)	2164(5)	39(5)	46(5)	34(4)	4(4)	-3(4)	1(4)
C7	835(4)	954(4)	1523(5)	43(5)	54(6)	31(4)	5(4)	-7(4)	-8(4)
C8	1128(4)	185(4)	1724(5)	43(5)	52(5)	32(4)	-6(4)	0(4)	4(4)
C9	1940(4)	-421(4)	2620(5)	49(5)	44(5)	41(5)	-11(4)	5(4)	-0(4)
C10	2401(3)	-229(4)	3374(5)	33(5)	38(4)	43(5)	-2(4)	1(4)	11(4)
C11	1853(3)	-706(4)	4747(5)	37(4)	29(4)	41(5)	0(4)	-3(4)	2(4)
C12	1348(3)	-516(4)	5448(5)	27(4)	32(4)	37(4)	1(4)	-1(3)	-3(3)
C13	2533(4)	426(4)	4865(5)	38(4)	40(4)	32(4)	9(4)	-5(4)	-0(4)
C14	2672(3)	1289(4)	4599(5)	29(4)	35(4)	34(4)	-2(3)	-0(3)	-9(3)
N1	295(2)	2464(3)	3772(3)	27(3)	24(3)	31(3)	5(3)	6(3)	-3(3)
N2	2090(3)	4(3)	4255(4)	31(3)	24(3)	41(4)	2(3)	4(3)	1(3)
O1	99(2)	1151(3)	4750(3)	31(3)	28(2)	37(3)	3(2)	6(2)	4(2)
O2	-484(2)	1736(3)	5842(3)	58(3)	37(3)	38(3)	2(2)	20(3)	-2(3)
O3	1520(2)	2509(3)	3052(3)	25(2)	27(2)	43(3)	8(2)	-3(2)	1(2)
O4	1318(2)	3666(3)	2369(4)	47(4)	47(4)	71(4)	27(3)	18(3)	9(3)
O5	527(2)	1244(3)	2352(3)	39(3)	41(3)	27(3)	1(2)	-2(2)	4(3)
O6	1566(2)	286(3)	2464(3)	37(3)	39(3)	38(3)	-8(3)	-7(3)	12(2)
O7	968(2)	38(3)	5238(3)	32(3)	34(3)	41(3)	8(2)	0(2)	4(2)
O8	1319(2)	-932(3)	6167(4)	50(3)	41(3)	44(3)	11(3)	5(3)	4(2)
O9	2384(2)	1569(3)	3908(3)	31(3)	32(2)	31(3)	3(2)	-6(3)	-1(2)

Table A.4 (continued)

atom	x	y	z	U_{11}	U_{22}	U_{33}	U_{23}	U_{13}	U_{12}
O10	3055(3)	1634(3)	5096(4)	70(4)	54(3)	56(4)	13(3)	-30(3)	-27(3)
w1	1388(2)	1936(3)	5377(4)	45(3)	53(3)	39(3)	-7(3)	1(3)	-10(3)
w2	285(2)	-199(3)	3608(3)	38(3)	31(3)	29(3)	1(2)	8(2)	-3(2)
w3	2475(3)	1644(3)	1958(3)	47(3)	48(3)	35(3)	-8(3)	-3(3)	-2(3)
w4	1543(4)	7383(5)	3559(5)	143(7)	111(6)	83(5)	-12(5)	3(5)	30(6)
w5	708(2)	5091(3)	2554(4)	47(3)	45(3)	46(3)	1(3)	-1(3)	7(3)
w6	580(3)	5323(4)	4565(4)	94(5)	90(5)	67(5)	-0(4)	-6(4)	3(4)
w7	1846(3)	7420(4)	1603(4)	68(4)	66(4)	76(4)	-15(4)	7(4)	-13(4)
w8	1548(3)	8552(4)	143(5)	74(5)	87(5)	112(6)	6(5)	1(5)	-16(4)
H1a	223	2865	5064	44					
H1b	-423	2811	4547	44					
H3a	308	3522	3144	45					
H3b	709	3500	4058	45					
H5a	-387	1762	3302	49					
H5b	-427	2633	2916	49					
H6a	410	2351	1922	46					
H6b	-167	1801	1717	46					
H7a	532	892	1034	55					
H7b	1150	1328	1331	55					
H8a	1342	-6	1180	52					
H8b	812	-192	1905	52					
H9a	1677	-854	2810	54					
H9b	2159	-562	2060	54					
H10a	2662	203	3170	47					
H10b	2656	-690	3488	47					
H11a	1685	-1070	4297	46					
H11b	2197	-953	5067	46					
H13a	2363	424	5483	46					
H13b	2922	138	4858	46					

Table A.5 Atomic Coordinates (x 10^4) and Thermal Parameters ($Å^2$ x 10^3) for $Mg[Ba(EGTA)]\cdot(8/3)H_2O\cdot(1/3)(CH_3)_2CO$

atom	x	y	z	U_{11}	U_{22}	U_{33}	U_{23}	U_{13}	U_{12}
Ba1	6110(1)	8036(1)	9189(1)	18(1)	13(1)	17(1)	1(1)	-0(1)	-1(1)
Ba2	5066(1)	4704(1)	7468(1)	16(1)	14(1)	19(1)	-1(1)	-1(1)	-0(1)
Ba3	6965(1)	1348(1)	7398(1)	17(1)	13(1)	16(1)	1(1)	-0(1)	0(1)
Mg1	5439(1)	5714(1)	9142(1)	20(1)	13(1)	19(1)	1(1)	-0(1)	-1(1)
Mg2	7280(1)	9049(1)	8025(1)	21(1)	15(1)	19(1)	1(1)	2(1)	1(1)
Mg3	5440(1)	2405(1)	6919(1)	19(1)	12(1)	19(1)	-0(1)	-1(1)	0(1)
C1	5238(2)	9439(3)	8091(3)	22(2)	15(2)	33(2)	3(2)	1(2)	5(2)
C2	5897(2)	9512(3)	7830(2)	19(2)	18(2)	16(2)	-1(1)	-2(1)	-1(1)
C3	5031(2)	7952(3)	7892(2)	23(2)	21(2)	29(2)	4(2)	-11(2)	-2(2)
C4	5011(2)	7018(3)	8140(2)	15(2)	19(2)	28(2)	4(2)	-3(2)	1(1)
C5	4532(2)	8674(3)	8811(3)	19(2)	26(2)	38(3)	12(2)	1(2)	-1(2)
C6	4615(2)	9246(3)	9408(3)	27(2)	26(2)	44(3)	10(2)	9(2)	6(2)
C7	5174(3)	9351(3)	10421(3)	38(3)	25(2)	31(2)	-3(2)	14(2)	-1(2)
C8	5806(2)	9230(3)	10694(2)	41(3)	24(2)	25(2)	-4(2)	13(2)	-6(2)
C9	6508(2)	8142(3)	11047(2)	38(3)	28(2)	21(2)	-1(2)	-1(2)	-10(2)
C10	6828(2)	7347(3)	10774(2)	35(2)	22(2)	19(2)	4(2)	-4(2)	-4(2)
C11	7576(3)	8053(3)	10069(2)	41(3)	34(2)	23(2)	3(2)	-9(2)	-20(2)
C12	7700(2)	8476(3)	9399(2)	28(2)	18(2)	27(2)	3(2)	1(2)	-3(2)
C13	7241(2)	6619(3)	9813(2)	25(2)	21(2)	26(2)	4(2)	-6(2)	-1(2)
C14	6718(2)	6007(3)	9663(2)	25(2)	22(2)	23(2)	1(2)	-2(2)	-2(2)
C15	6409(2)	6096(3)	7221(2)	32(2)	13(2)	20(2)	2(1)	3(2)	-3(2)
C16	6293(2)	6150(3)	7967(2)	20(2)	16(2)	22(2)	-0(1)	0(2)	1(1)
C17	6695(2)	4609(3)	7100(2)	21(2)	17(2)	29(2)	-1(2)	1(2)	-2(2)
C18	6477(2)	3677(3)	6995(2)	23(2)	18(2)	16(2)	1(1)	1(1)	-0(1)
C19	6206(2)	5326(3)	6184(2)	30(2)	26(2)	19(2)	2(2)	2(2)	-2(2)
C20	5664(2)	5847(3)	5948(2)	34(2)	25(2)	19(2)	4(2)	-4(2)	-7(2)
C21	4592(2)	5949(3)	6008(3)	37(3)	31(2)	27(2)	5(2)	-8(2)	9(2)
C22	4042(2)	5391(3)	6057(3)	34(3)	40(3)	29(2)	-1(2)	-11(2)	7(2)

Table A.5 (continued)

atom	x	y	z	U_{11}	U_{22}	U_{33}	U_{23}	U_{13}	U_{12}
C23	3400(2)	4814(3)	6921(3)	21(2)	30(2)	36(3)	-7(2)	-6(2)	3(2)
C24	3420(2)	4036(3)	7374(3)	22(2)	29(2)	42(3)	-6(2)	-5(2)	-0(2)
C25	3629(2)	4741(3)	8435(3)	18(2)	26(2)	36(2)	-8(2)	2(2)	-2(2)
C26	4121(2)	5047(3)	8921(2)	21(2)	31(2)	31(2)	-9(2)	1(2)	-4(2)
C27	3962(2)	3269(3)	8225(3)	27(2)	22(2)	31(2)	-1(2)	8(2)	-4(2)
C28	4310(2)	2643(3)	7766(2)	19(2)	19(2)	35(2)	-0(2)	2(2)	-0(2)
C29	6472(2)	2748(2)	8785(2)	32(2)	11(2)	22(2)	-3(1)	-6(2)	5(1)
C30	5941(2)	2802(2)	8287(2)	26(2)	15(2)	17(2)	3(1)	-3(2)	-2(1)
C31	6509(2)	1267(3)	9094(2)	27(2)	19(2)	20(2)	-1(2)	2(2)	4(2)
C32	6739(2)	334(3)	8968(2)	23(2)	20(2)	16(2)	-1(1)	-3(2)	-1(2)
C33	7445(2)	2085(3)	9045(2)	31(2)	19(2)	26(2)	-3(2)	-10(2)	3(2)
C34	7870(2)	2624(3)	8617(3)	27(2)	23(2)	36(2)	-5(2)	-11(2)	-6(2)
C35	8312(2)	2702(3)	7549(3)	23(2)	34(2)	46(3)	1(2)	-5(2)	-11(2)
C36	8535(2)	2154(4)	6981(3)	22(3)	61(4)	45(3)	-6(3)	3(2)	-12(2)
C37	8192(2)	1372(3)	6044(2)	19(2)	34(2)	29(2)	6(2)	8(2)	5(2)
C38	7782(2)	599(3)	5899(2)	30(2)	27(2)	24(2)	4(2)	9(2)	3(2)
C39	6877(2)	1397(3)	5577(2)	23(2)	24(2)	18(2)	2(2)	4(2)	-0(2)
C40	6283(2)	1809(3)	5803(2)	20(2)	17(2)	19(2)	-1(1)	-2(1)	-3(1)
C41	6788(2)	-42(3)	6041(2)	32(2)	17(2)	20(2)	-2(2)	3(2)	2(2)
C42	6973(2)	-676(3)	6582(2)	32(2)	17(2)	23(2)	-1(2)	11(2)	1(2)
C43	10551(6)	1583(7)	5796(8)	97(9)	56(6)	192(15)	46(8)	-102(10)	-16(6)
C44	10104(4)	1834(5)	5284(5)	59(5)	50(4)	88(6)	-8(4)	-3(4)	1(3)
C45	10369(7)	2200(9)	4658(7)	117(11)	120(11)	83(8)	-10(8)	29(8)	-65(9)
N1	5092(2)	8612(2)	8406(2)	20(2)	14(1)	29(2)	1(1)	-0(1)	-1(1)
N2	7057(2)	7458(2)	10090(2)	27(2)	17(1)	22(2)	2(1)	-4(1)	-5(1)
N3	6240(2)	5271(2)	6917(2)	22(2)	16(1)	17(2)	-1(1)	1(1)	-3(1)
N4	3855(2)	4130(2)	7928(2)	20(2)	19(2)	29(2)	-5(1)	-4(1)	2(1)
N5	6838(2)	1953(2)	8744(2)	21(2)	17(1)	18(2)	-2(1)	-6(1)	0(1)
N6	7136(2)	769(2)	6052(2)	19(2)	19(1)	21(2)	3(1)	3(1)	3(1)
O1	6287(1)	8952(2)	8014(2)	21(1)	15(1)	20(1)	-0(1)	-2(1)	1(1)
O2	6001(1)	10157(2)	7476(2)	21(1)	19(1)	25(1)	3(1)	2(1)	1(1)
O3	5187(1)	6882(2)	8732(2)	25(2)	15(1)	24(2)	3(1)	-2(1)	3(1)

Table A.5 (continued)

atom	x	y	z	U_{11}	U_{22}	U_{33}	U_{23}	U_{13}	U_{12}
O4	4845(2)	6467(2)	7729(2)	31(2)	20(1)	34(2)	-2(1)	-10(1)	1(1)
O5	5146(2)	8979(2)	9765(2)	28(2)	24(1)	32(2)	-5(1)	5(1)	1(1)
O6	5981(2)	8329(2)	10639(2)	30(2)	26(1)	24(2)	-2(1)	2(1)	-6(1)
O7	7331(1)	8389(2)	8920(2)	20(2)	16(1)	24(1)	1(1)	-2(1)	-1(1)
O8	8168(2)	8947(3)	9378(2)	30(2)	51(2)	31(2)	3(2)	-3(1)	-18(2)
O9	6178(1)	6309(2)	9633(2)	22(1)	18(1)	22(1)	0(1)	-3(1)	-1(1)
O10	6853(2)	5233(2)	9564(2)	26(2)	20(1)	58(2)	-4(2)	-10(2)	4(1)
O11	5958(1)	5576(2)	8237(2)	22(1)	14(1)	20(1)	1(1)	-2(1)	-1(1)
O12	6523(1)	6795(2)	8249(2)	28(2)	19(1)	25(2)	-4(1)	1(1)	-7(1)
O13	5909(1)	3560(2)	6878(2)	19(1)	16(1)	24(1)	1(1)	-1(1)	0(1)
O14	6878(1)	3110(2)	7054(2)	19(1)	15(1)	36(2)	3(1)	-0(1)	-1(1)
O15	5123(2)	5461(2)	6187(2)	30(2)	26(1)	25(2)	4(1)	-4(1)	2(1)
O16	4006(2)	5036(2)	6723(2)	23(2)	47(2)	31(2)	9(2)	-5(1)	3(1)
O17	4675(1)	5041(2)	8747(2)	21(2)	20(1)	23(1)	-3(1)	4(1)	-3(1)
O18	3931(2)	5327(3)	9470(2)	27(2)	89(3)	40(2)	-37(2)	10(2)	-12(2)
O19	4670(1)	2971(2)	7349(2)	20(1)	18(1)	26(2)	-0(1)	1(1)	1(1)
O20	4220(2)	1859(2)	7859(2)	29(2)	18(1)	60(2)	2(2)	19(2)	-2(1)
O21	5891(1)	2219(2)	7841(1)	21(1)	16(1)	18(1)	-2(1)	1(1)	2(1)
O22	5604(2)	3448(2)	8342(2)	30(2)	21(1)	23(2)	-6(1)	-5(1)	6(1)
O23	7105(1)	222(2)	8484(2)	23(2)	14(1)	22(1)	2(1)	0(1)	1(1)
O24	6528(2)	-234(2)	9341(2)	33(2)	16(1)	23(2)	-0(1)	5(1)	-4(1)
O25	8002(1)	2162(2)	8014(2)	25(2)	26(1)	32(2)	-1(1)	-3(1)	-5(1)
O26	8047(1)	1680(2)	6702(2)	20(2)	35(2)	28(2)	0(1)	0(1)	-5(1)
O27	6122(1)	1732(2)	6407(1)	22(1)	17(1)	15(1)	0(1)	-0(1)	2(1)
O28	5992(2)	2205(2)	5364(2)	29(2)	33(2)	20(1)	8(1)	0(1)	4(1)
O29	7248(1)	-378(2)	7095(2)	24(2)	17(1)	22(1)	-0(1)	5(1)	2(1)
O30	6833(2)	-1458(2)	6491(2)	62(2)	18(1)	23(2)	-2(1)	1(2)	-5(1)
O31	9572(3)	1780(5)	5355(4)	31(3)	116(6)	109(6)	26(5)	7(4)	-4(3)
w1	5761(1)	4498(2)	9404(2)	27(2)	17(1)	18(1)	-0(1)	-1(1)	4(1)
w2	4948(1)	5910(2)	9992(2)	29(2)	24(1)	22(1)	-6(1)	4(1)	-0(1)
w3	7325(1)	7841(2)	7569(2)	29(2)	15(1)	30(2)	-4(1)	7(1)	0(1)
w4	8219(1)	9284(2)	8090(2)	21(2)	20(1)	33(2)	1(1)	6(1)	-2(1)

Table A.5 (continued)

atom	x	y	z	U_{11}	U_{22}	U_{33}	U_{23}	U_{13}	U_{12}
w5	5038(1)	2728(2)	5990(2)	23(2)	21(1)	24(1)	5(1)	-4(1)	3(1)
w6	10049(1)	8817(2)	7037(2)	23(2)	16(1)	22(1)	1(1)	-2(1)	4(1)
w7	7722(2)	3395(3)	5945(2)	30(2)	49(2)	50(2)	15(2)	2(2)	1(2)
w8	7772(2)	4078(3)	9805(2)	29(2)	48(2)	63(3)	18(2)	6(2)	8(2)
H1a	4962	9520	7725	28					
H1b	5175	9890	8413	28					
H3a	4659	8063	7652	31					
H3b	5375	8006	7596	31					
H5a	4209	8906	8541	32					
H5b	4421	8104	8960	32					
H6a	4261	9202	9690	37					
H6b	4665	9835	9266	37					
H7a	5081	9958	10397	36					
H7b	4882	9068	10704	36					
H8a	5812	9399	11153	37					
H8b	6089	9581	10448	37					
H9a	6784	8627	11042	36					
H9b	6378	8033	11496	36					
H10a	6543	6873	10778	31					
H10b	7169	7214	11058	31					
H11a	7502	8505	10387	39					
H11b	7937	7737	10195	39					
H13a	7460	6723	9406	29					
H13b	7508	6342	10127	29					
H15a	6838	6191	7144	25					
H15b	6176	6546	7008	25					
H17a	7056	4699	6836	25					
H17b	6794	4682	7562	25					
H19a	6574	5593	6022	29					
H19b	6173	4751	6007	29					
H20a	5657	5858	5471	33					
H20b	5694	6428	6115	33					

Table A.5 (continued)

atom	x	y	z	U_{11}	U_{22}	U_{33}	U_{23}	U_{13}	U_{12}
H21a	4550	6434	6303	36					
H21b	4634	6154	5559	36					
H22a	4070	4929	5740	43					
H22b	3681	5729	5968	43					
H23a	3219	5293	7153	37					
H23b	3160	4681	6535	37					
H24a	3536	3540	7116	36					
H24b	3017	3948	7555	36					
H25a	3465	5238	8212	32					
H25b	3310	4461	8684	32					
H27a	4196	3343	8625	31					
H27b	3571	3016	8331	31					
H29a	6304	2786	9225	26					
H29b	6740	3230	8707	26					
H31a	6542	1379	9562	27					
H31b	6086	1294	8963	27					
H33a	7393	2373	9464	30					
H33b	7631	1529	9117	30					
H34a	8245	2731	8853	33					
H34b	7677	3165	8512	33					
H35a	8036	3136	7385	43					
H35b	8655	2976	7762	43					
H36a	8842	1760	7141	52					
H36b	8710	2523	6647	52					
H37a	8117	1821	5724	32					
H37b	8615	1202	6024	32					
H38a	7919	118	6163	32					
H38b	7817	455	5436	32					
H39a	7173	1848	5508	28					
H39b	6801	1102	5165	28					
H41a	6361	93	6095	29					
H41b	6850	-314	5617	29					

Table A.5 (continued)

atom	x	y	z	U_{11}	U_{22}	U_{33}	U_{23}	U_{13}	U_{12}
H43a	10944	1522	5587	148					
H43b	10387	1021	5896	148					
H43c	10595	1908	6200	148					
H45a	10799	2332	4669	144					
H45b	10149	2677	4468	144					
H45c	10304	1690	4394	144					

Table A.6 Atomic Coordinates (x 10^4) and Thermal Parameters ($Å^2$ x 10^3) for $[Mg_2(EGTA)(OH_2)_6]\cdot 5H_2O$

atom	x	y	z	U_{11}	U_{22}	U_{33}	U_{23}	U_{13}	U_{12}
Mg1	8876(1)	6742(1)	3088(1)	19(1)	33(1)	21(1)	-1(1)	1(1)	-2(1)
Mg2	6146(1)	6556(1)	10902(1)	20(1)	28(1)	19(1)	-0(1)	1(1)	1(1)
C1	7808(3)	7440(4)	4677(3)	30(2)	52(3)	23(2)	-0(2)	2(2)	18(2)
C2	7297(3)	7799(3)	3888(3)	18(2)	30(2)	33(2)	-3(2)	-4(2)	-1(2)
C3	9527(3)	7406(4)	4832(3)	29(2)	44(3)	28(2)	-4(2)	-3(2)	-5(2)
C4	9862(3)	8245(4)	4196(3)	27(2)	31(2)	37(3)	-6(2)	6(2)	-0(2)
C5	8644(4)	5704(4)	4875(3)	42(3)	39(2)	28(2)	4(2)	7(2)	2(2)
C6	8762(4)	5597(4)	5820(4)	45(3)	56(3)	30(3)	14(3)	3(2)	9(2)
C7	7173(4)	5687(5)	6328(3)	48(3)	58(3)	21(2)	-6(2)	7(2)	-16(3)
C8	6579(5)	6401(6)	6859(4)	45(4)	59(5)	31(3)	-0(3)	4(3)	2(3)
C8'	7109(18)	4779(15)	7007(11)	88(16)	29(9)	11(7)	-14(7)	18(10)	-18(10)
C9	6461(5)	5597(6)	8148(4)	59(4)	110(5)	27(3)	-22(3)	2(3)	17(4)
C10	6631(4)	5726(4)	9102(3)	36(2)	61(3)	23(2)	-11(2)	5(2)	6(2)
C11	7070(3)	7598(4)	9383(3)	23(2)	46(3)	26(2)	6(2)	1(2)	-5(2)
C12	7624(3)	7855(3)	10171(3)	15(2)	28(2)	29(2)	1(2)	1(2)	4(2)
C13	5426(3)	7151(4)	9204(3)	23(2)	40(2)	21(2)	4(2)	-2(2)	-2(2)
C14	5007(3)	7939(4)	9831(3)	18(2)	32(2)	32(2)	3(2)	3(2)	-2(2)
N1	8693(2)	6816(3)	4534(2)	22(2)	30(2)	19(2)	-2(1)	2(1)	3(1)
N2	6358(2)	6762(3)	9491(2)	17(1)	28(2)	22(2)	-4(1)	-1(1)	0(1)
O1	7566(2)	7462(3)	3191(2)	26(1)	51(2)	26(2)	-3(2)	-4(1)	6(1)
O2	6615(3)	8412(3)	4012(2)	31(2)	57(2)	38(2)	-4(2)	-5(1)	19(2)
O3	9653(2)	8091(3)	3437(2)	30(2)	36(2)	32(2)	-0(1)	3(1)	-6(1)
O4	10351(3)	9013(3)	4465(3)	51(2)	47(2)	49(2)	-12(2)	1(2)	-20(2)
O5	8087(2)	6180(3)	6306(2)	41(2)	51(2)	26(2)	-4(2)	0(1)	-11(2)
O6	6869(3)	6389(4)	7724(3)	46(3)	43(3)	30(2)	-7(2)	3(2)	-6(2)
O6'	7287(8)	5180(10)	7796(7)	33(6)	34(7)	17(6)	-9(5)	-0(5)	9(5)
O7	7399(2)	7390(3)	10848(2)	22(1)	46(2)	22(1)	3(1)	-2(1)	-6(1)
O8	8277(2)	8548(3)	10100(2)	25(2)	38(2)	38(2)	4(1)	-2(1)	-9(1)

Table A.6 (continued)

atom	x	y	z	U_{11}	U_{22}	U_{33}	U_{23}	U_{13}	U_{12}
O9	5286(2)	7869(2)	10585(2)	24(1)	34(2)	22(1)	-1(1)	3(1)	2(1)
O10	4414(2)	8599(3)	9570(2)	38(2)	42(2)	42(2)	9(2)	-5(2)	14(2)
w1	10140(2)	5937(3)	3100(2)	26(1)	37(2)	50(2)	-8(2)	-6(2)	3(1)
w2	8212(2)	5274(3)	2978(3)	30(2)	48(2)	48(2)	-8(2)	12(2)	-14(2)
w3	8928(2)	7071(3)	1847(2)	26(2)	77(2)	23(2)	8(2)	-1(1)	1(2)
w4	4924(2)	5612(2)	10763(2)	24(1)	33(2)	41(2)	-0(1)	-2(1)	-1(1)
w5	6846(2)	5100(3)	10983(3)	38(2)	37(2)	40(2)	7(2)	5(2)	13(1)
w6	6052(2)	6804(3)	12156(2)	29(2)	56(2)	24(2)	-6(2)	3(1)	1(2)
w7	8654(2)	4684(3)	418(3)	34(2)	50(2)	44(2)	-4(2)	4(2)	3(2)
w8	3517(3)	5384(3)	8600(3)	37(2)	46(2)	55(2)	-13(2)	-10(2)	4(2)
w9	9067(4)	3840(4)	2010(3)	75(3)	80(3)	61(3)	-14(3)	9(3)	12(3)
w10	6220(5)	3559(4)	12043(4)	121(5)	67(3)	89(4)	28(3)	-13(4)	-29(3)
w11	10849(3)	3796(4)	2873(3)	54(2)	70(3)	46(2)	12(2)	7(2)	-3(2)
H1a	7381	6997	4997	43					
H1b	7967	8072	4995	43					
H3a	9371	7764	5349	39					
H3b	10031	6902	4929	39					
H5a	8038	5408	4728	41					
H5b	9137	5289	4613	41					
H6a	9384	5852	5966	57					
H6b	8709	4847	5963	57					
H7a	6914	5642	5772	49					
H7b	7212	4978	6566	49					
H9a	6435	5660	8748	69					
H9b	5868	5325	7943	69					
H10a	7299	5631	9196	45					
H10b	6288	5165	9385	45					
H11a	7509	7366	8959	39					
H11b	6757	8245	9199	39					
H13a	5498	7503	8671	34					
H13b	5004	6547	9144	34					

Table A.7 Atomic Coordinates (x 10^4) and Thermal Parameters ($Å^2$ x 10^3) for $Sr[Cd(EGTA)]\cdot 7H_2O$

atom	x	y	z	U_{11}	U_{22}	U_{33}	U_{23}	U_{13}	U_{12}
Cd	7566(1)	617(1)	106(1)	29(1)	34(1)	31(1)	0(1)	6(1)	-5(1)
Sr	9211(1)	5310(1)	804(1)	35(1)	40(1)	33(1)	-3(1)	9(1)	-10(1)
C1	6360(3)	-1953(5)	535(2)	40(2)	34(2)	42(2)	4(2)	5(2)	-9(2)
C2	6166(2)	-1746(4)	-333(2)	32(2)	30(2)	45(2)	1(2)	8(2)	0(2)
C3	7078(3)	-801(5)	1697(2)	44(2)	48(2)	38(2)	5(2)	6(2)	-11(2)
C4	7804(3)	205(5)	1910(2)	39(2)	37(2)	32(2)	2(2)	10(2)	2(2)
C5	5974(3)	613(5)	948(3)	39(2)	41(2)	55(3)	-5(2)	17(2)	-8(2)
C6	6252(3)	2288(5)	1117(3)	44(2)	45(2)	47(2)	-8(2)	18(2)	-2(2)
C7	6188(3)	3648(5)	-80(3)	40(2)	37(2)	60(3)	-1(2)	5(2)	5(2)
C8	6700(3)	4046(5)	-688(3)	43(2)	33(2)	54(3)	4(2)	5(2)	2(2)
C9	7528(3)	2786(5)	-1504(2)	49(3)	39(2)	36(2)	10(2)	2(2)	-1(2)
C10	7816(3)	1161(5)	-1694(2)	47(2)	40(2)	31(2)	4(2)	6(2)	-2(2)
C11	8291(3)	-1369(5)	-1190(2)	45(2)	32(2)	38(2)	-1(2)	7(2)	-3(2)
C12	8428(2)	-2396(5)	-473(2)	29(2)	38(2)	43(2)	1(2)	3(2)	-4(2)
C13	9051(2)	990(5)	-808(2)	31(2)	37(2)	44(2)	0(2)	12(2)	-2(2)
C14	9089(2)	2373(4)	-259(2)	29(2)	32(2)	32(2)	7(2)	4(2)	-2(2)
N1	6658(2)	-490(4)	926(2)	35(2)	33(2)	37(2)	-0(1)	5(1)	-5(1)
N2	8248(2)	325(4)	-1026(2)	38(2)	29(2)	31(2)	-2(1)	3(1)	-2(1)
O1	6523(2)	-653(4)	-648(2)	49(2)	47(2)	42(2)	3(1)	2(1)	-12(1)
O2	5687(2)	-2695(4)	-670(2)	47(2)	42(2)	52(2)	-1(1)	-4(1)	-12(1)
O3	8155(2)	765(4)	1386(2)	40(2)	65(2)	36(2)	1(1)	6(1)	-19(2)
O4	8048(2)	367(4)	2607(2)	43(2)	62(2)	36(2)	-0(1)	5(1)	-5(1)
O5	6690(2)	2869(3)	528(2)	34(2)	37(2)	49(2)	-1(1)	8(1)	-3(1)
O6	6992(2)	2591(3)	-944(2)	37(2)	33(1)	46(2)	1(1)	5(1)	-1(1)
O7	8348(2)	-1794(4)	161(2)	51(2)	43(2)	36(2)	5(1)	6(1)	4(1)
O8	8597(2)	-3826(3)	-571(2)	49(2)	31(1)	54(2)	5(1)	5(1)	3(1)
O9	8514(2)	2622(3)	117(2)	33(1)	37(1)	38(1)	-1(1)	9(1)	-6(1)
O10	9713(2)	3207(3)	-182(2)	35(1)	39(2)	48(2)	-1(1)	11(1)	-9(1)

Table A.7 (continued)

atom	x	y	z	U_{11}	U_{22}	U_{33}	U_{23}	U_{13}	U_{12}
w1	9365(3)	2885(6)	1675(2)	107(3)	102(3)	81(3)	50(3)	-46(3)	-67(3)
w2	10657(2)	5257(4)	1714(2)	46(2)	49(2)	57(2)	5(2)	6(2)	-3(1)
w3	9140(2)	7590(5)	1756(2)	60(2)	69(2)	77(2)	-28(2)	-1(2)	16(2)
w4	7806(2)	5039(4)	1195(2)	45(2)	57(2)	54(2)	-14(2)	18(2)	-16(2)
w5	5292(2)	5967(5)	1922(2)	68(2)	58(2)	74(2)	1(2)	-5(2)	9(2)
w6	4464(2)	2966(4)	2178(2)	74(2)	62(2)	54(2)	-4(2)	0(2)	-2(2)
w7	10581(2)	3917(5)	3123(2)	63(2)	80(3)	50(2)	10(2)	-5(2)	6(2)
H1a	6763	-2757	636	36					
H1b	5882	-2278	736	36					
H3a	6710	-613	2062	42					
H3b	7241	-1890	1722	42					
H5a	5646	590	460	42					
H5b	5664	272	1339	42					
H6a	6593	2311	1598	43					
H6b	5794	2951	1146	43					
H7a	5759	2957	-284	43					
H7b	5968	4597	108	43					
H8a	7139	4707	-482	42					
H8b	6388	4583	-1105	42					
H9a	7254	3276	-1955	42					
H9b	7975	3432	-1301	42					
H10a	8170	1267	-2077	37					
H10b	7359	538	-1893	37					
H11a	7795	-1684	-1483	37					
H11b	8724	-1543	-1485	37					
H13a	9389	165	-572	36					
H13b	9253	1338	-1266	36					

Table A.8 Atomic Coordinates (x 10^4) and Thermal Parameters ($Å^2$ x 10^3) for $Ca[Er(EGTA)(OH_2)]_2 \cdot 12H_2O \cdot (CH_3)_2CO$

atom	x	y	z	U_{11}	U_{22}	U_{33}	U_{23}	U_{13}	U_{12}
Er1	2966(1)	3896(1)	1534(1)	11(1)	12(1)	15(1)	-1(1)	4(1)	-1(1)
Er2	7329(1)	5017(1)	4668(1)	11(1)	9(1)	18(1)	-2(1)	5(1)	0(1)
Ca1	4452(1)	5144(1)	3436(1)	13(1)	11(1)	17(1)	-1(1)	5(1)	0(1)
C1	268(6)	3677(7)	754(4)	16(3)	17(4)	31(4)	-6(3)	3(3)	-1(3)
C2	836(6)	3240(6)	168(5)	20(4)	18(4)	28(4)	2(3)	10(3)	3(3)
C3	724(6)	4299(7)	2103(4)	13(3)	25(4)	33(4)	-4(3)	4(3)	-1(3)
C4	1674(6)	4597(7)	2787(4)	16(3)	26(4)	24(4)	-5(3)	9(3)	2(3)
C5	878(6)	5583(7)	1109(5)	20(4)	22(4)	34(5)	0(4)	1(3)	10(3)
C6	1299(7)	5772(8)	409(5)	32(5)	23(4)	38(5)	6(4)	4(4)	5(4)
C7	2902(7)	5502(8)	-20(5)	36(5)	45(5)	24(4)	17(4)	4(4)	-8(4)
C8	4052(7)	5112(8)	234(5)	39(5)	39(5)	30(4)	1(4)	17(4)	-6(5)
C9	4890(8)	3327(9)	624(7)	31(5)	50(6)	62(7)	-18(5)	28(5)	-11(5)
C10	4423(8)	2214(8)	648(6)	40(5)	41(6)	50(6)	-20(5)	30(5)	-5(4)
C11	3088(6)	1257(7)	1159(5)	32(4)	17(4)	27(4)	-5(3)	9(3)	2(3)
C12	2261(6)	1427(7)	1634(5)	23(4)	25(4)	26(4)	0(3)	-1(3)	-0(3)
C13	4818(7)	1810(8)	2028(5)	33(5)	32(5)	35(5)	-19(4)	-6(4)	15(4)
C14	4945(6)	2555(6)	2724(4)	18(4)	12(4)	25(4)	-3(3)	6(3)	-1(3)
C15	8499(5)	6559(6)	6274(5)	13(3)	14(4)	32(4)	-8(3)	5(3)	0(3)
C16	9319(6)	5724(7)	6123(5)	24(4)	22(4)	24(4)	8(3)	9(3)	-2(3)
C17	6694(6)	7245(7)	5567(4)	18(4)	19(4)	19(4)	-10(3)	3(3)	1(3)
C18	5745(5)	6993(6)	4853(4)	16(3)	20(4)	20(4)	-6(3)	9(3)	2(3)
C19	6843(6)	5592(7)	6335(4)	19(4)	21(4)	21(4)	-7(3)	6(3)	-5(3)
C20	7384(6)	4472(7)	6535(4)	19(4)	32(4)	14(4)	7(3)	3(3)	-0(3)
C21	7889(6)	2888(6)	5918(5)	23(4)	13(4)	36(4)	5(3)	11(3)	-0(3)
C22	7695(6)	2365(6)	5129(5)	24(4)	10(4)	37(5)	8(3)	13(3)	1(3)
C23	8434(7)	2826(7)	4020(5)	33(4)	17(4)	37(5)	-5(4)	20(4)	1(4)
C24	9204(5)	3732(7)	3950(4)	15(3)	16(4)	30(4)	-3(3)	8(3)	3(3)
C25	9378(6)	5740(7)	3981(5)	11(3)	24(4)	42(5)	1(4)	11(3)	-3(3)

Table A.8 (continued)

atom	x	y	z	U_{11}	U_{22}	U_{33}	U_{23}	U_{13}	U_{12}
C26	8832(6)	6759(7)	4192(5)	22(4)	17(4)	33(5)	1(4)	10(3)	-3(3)
C27	8007(5)	4866(8)	2926(4)	11(3)	31(5)	27(4)	3(4)	8(3)	3(3)
C28	6784(5)	5027(7)	2777(4)	13(3)	8(3)	30(4)	-5(3)	7(3)	-4(3)
N1	986(5)	4406(6)	1356(4)	18(3)	24(4)	20(3)	-5(3)	4(3)	-1(3)
N2	3946(5)	2093(5)	1322(4)	20(3)	22(4)	23(3)	-4(3)	4(3)	7(3)
N3	7361(4)	6243(5)	5837(3)	17(3)	10(3)	21(3)	-3(3)	1(2)	1(2)
N4	8627(4)	4802(5)	3775(3)	16(3)	19(4)	16(3)	-0(3)	4(2)	0(3)
O1	1884(4)	3231(4)	376(3)	23(3)	23(3)	21(3)	-9(2)	4(2)	-7(2)
O2	257(4)	2897(5)	-466(3)	26(3)	27(3)	23(3)	-9(2)	3(2)	-3(2)
O3	2603(4)	4647(4)	2642(3)	11(2)	20(3)	22(3)	-1(2)	6(2)	-2(2)
O4	1505(4)	4738(6)	3426(3)	17(3)	75(5)	27(3)	-12(3)	12(2)	-5(3)
O5	2433(4)	5479(4)	641(3)	29(3)	19(3)	25(3)	5(2)	7(2)	4(2)
O6	4068(4)	4124(5)	650(3)	23(3)	32(4)	29(3)	-4(3)	14(2)	-5(2)
O7	2248(4)	2358(5)	1963(3)	23(3)	22(3)	22(3)	2(2)	7(2)	4(2)
O8	1615(5)	666(5)	1658(4)	40(3)	17(3)	57(4)	-10(3)	25(3)	-12(3)
O9	4425(4)	3460(4)	2620(3)	21(3)	13(3)	16(3)	-5(2)	3(2)	-1(2)
O10	5585(4)	2268(5)	3350(3)	30(3)	19(3)	21(3)	-2(2)	-3(2)	10(2)
O11	9040(4)	5100(4)	5533(3)	15(2)	12(3)	27(3)	-4(2)	5(2)	1(2)
O12	10258(4)	5750(5)	6582(3)	13(2)	31(3)	27(3)	-9(2)	2(2)	-3(2)
O13	5780(4)	6080(4)	4514(3)	15(2)	8(2)	29(3)	-3(2)	7(2)	1(2)
O14	5040(4)	7707(4)	4633(3)	22(3)	17(3)	24(3)	-4(2)	1(2)	14(2)
O15	7252(4)	3912(5)	5808(3)	17(2)	14(2)	22(2)	3(2)	5(2)	2(2)
O16	7918(4)	3192(4)	4608(3)	23(3)	12(3)	30(3)	-0(2)	15(2)	2(2)
O17	7924(4)	6656(4)	4334(3)	17(3)	16(3)	28(3)	-6(2)	7(2)	-2(2)
O18	9334(5)	7654(5)	4226(4)	30(3)	21(3)	69(4)	0(3)	25(3)	-4(3)
O19	6372(3)	5013(4)	3344(3)	15(2)	12(2)	22(2)	-2(2)	9(2)	1(2)
O20	6251(4)	5133(5)	2079(3)	19(2)	36(3)	17(2)	4(3)	7(2)	4(3)
w1	4197(4)	5458(4)	2007(3)	12(2)	13(2)	18(3)	-1(2)	2(2)	-1(2)
w2	5663(3)	3873(4)	4354(3)	15(2)	9(2)	18(2)	-0(2)	3(2)	3(2)
w3	3507(4)	5045(5)	4393(3)	17(2)	28(3)	25(3)	-4(3)	10(2)	1(3)
w4	3951(4)	7004(5)	3210(3)	34(3)	21(3)	24(3)	4(2)	6(2)	14(3)
w5	2453(7)	7584(7)	8417(5)	74(5)	42(5)	72(5)	-19(4)	37(4)	-15(4)

Table A.8 (continued)

atom	x	y	z	U_{11}	U_{22}	U_{33}	U_{23}	U_{13}	U_{12}
w6	3827(4)	5141(5)	6001(3)	34(3)	27(3)	27(3)	-5(3)	12(2)	-3(3)
w7	2771(6)	8812(8)	9775(4)	50(4)	63(5)	54(4)	-18(4)	22(3)	-2(4)
w8	1643(4)	4702(5)	5753(4)	26(3)	33(4)	45(4)	-5(3)	12(3)	-6(3)
w9	6248(4)	2653(5)	8304(3)	31(3)	25(3)	32(3)	-11(3)	1(2)	-2(3)
w10	441(5)	6367(8)	8119(4)	37(4)	93(7)	48(4)	-25(4)	6(3)	-13(4)
w11	2853(7)	792(7)	9108(4)	81(5)	77(6)	38(4)	-2(4)	37(4)	15(5)
w12	8209(4)	3665(5)	8947(4)	20(3)	27(4)	44(3)	6(3)	0(2)	3(2)
w13	422(5)	3465(7)	7152(4)	42(4)	53(5)	57(5)	11(4)	4(3)	5(3)
w14	1276(11)	2246(10)	-1563(6)	176(11)	110(9)	87(7)	49(7)	90(8)	101(9)
C29	3481(8)	3037(9)	7407(7)	39(5)	31(6)	82(8)	-18(5)	-16(5)	5(5)
C30	3723(7)	3987(8)	7964(5)	31(4)	34(5)	35(5)	4(4)	4(4)	-4(4)
C31	2880(7)	4825(9)	7926(6)	31(5)	48(7)	46(5)	-10(5)	12(4)	-4(5)
O21	4614(5)	4074(6)	8453(4)	33(3)	43(4)	58(4)	-8(4)	3(3)	2(3)
H1a	43	3064	1014	28					
H1b	-364	4088	477	28					
H3a	122	4776	2101	29					
H3b	520	3551	2163	29					
H5a	121	5788	981	31					
H5b	1288	6030	1534	31					
H6a	1215	6531	256	42					
H6b	910	5319	-19	42					
H7a	2486	5032	-427	43					
H7b	2884	6241	-214	43					
H8a	4502	5652	565	40					
H8b	4319	4985	-215	40					
H9a	5108	3414	151	50					
H9b	5513	3425	1067	50					
H10a	3860	2093	171	49					
H10b	4990	1677	694	49					
H11a	2707	1284	613	37					
H11b	3421	548	1284	37					
H13a	4674	1082	2184	45					

Table A.8 (continued)

atom	x	y	z	U_{11}	U_{22}	U_{33}	U_{23}	U_{13}	U_{12}
H13b	5498	1814	1890	45					
H15a	8661	7273	6104	24					
H15b	8556	6580	6824	24					
H17a	6410	7510	5982	24					
H17b	7149	7800	5432	24					
H19a	6898	5989	6812	26					
H19b	6086	5485	6065	26					
H20a	7036	4067	6865	30					
H20b	8147	4559	6798	30					
H21a	8652	3047	6129	27					
H21b	7650	2406	6266	27					
H22a	6950	2124	4946	27					
H22b	8175	1748	5157	27					
H23a	8828	2154	4180	32					
H23b	7896	2713	3529	32					
H24a	9528	3556	3536	22					
H24b	9766	3792	4434	22					
H25a	9974	5538	4420	28					
H25b	9655	5908	3542	28					
H27a	8290	5473	2695	27					
H27b	8127	4194	2677	27					
H29a	2811	2634	7330	67					
H29b	4088	2563	7634	67					
H29c	3543	3305	6912	67					
H31a	2616	4968	7375	49					
H31b	3118	5502	8197	49					
H31c	2304	4511	8111	49					

Table A.9 Atomic Coordinates (x 10^4) and Thermal Parameters ($Å^2$ x 10^3) for $Ca[Nd(EGTA)(OH_2)]_2 \cdot 9H_2O$

atom	x	y	z	U_{11}	U_{22}	U_{33}	U_{23}	U_{13}	U_{12}
Nd	2322(1)	2324(1)	2582(1)	16(1)	14(1)	10(1)	-0(1)	5(1)	1(1)
Ca	5000	5000	5000	32(1)	23(1)	22(1)	10(1)	16(1)	8(1)
C1	5365(4)	1592(2)	2575(3)	22(2)	21(2)	26(2)	-2(2)	13(2)	2(2)
C2	4211(4)	1112(2)	1825(3)	26(2)	19(2)	14(2)	3(1)	9(2)	1(1)
C3	5782(4)	2726(2)	3694(3)	17(2)	22(2)	23(2)	-3(1)	1(2)	-2(1)
C4	5059(4)	3302(2)	4128(3)	26(2)	24(2)	17(2)	-3(2)	3(2)	-2(2)
C5	5334(4)	1619(2)	4504(3)	26(2)	30(2)	15(2)	2(2)	3(2)	8(2)
C6	4524(4)	934(2)	4359(3)	28(2)	26(2)	18(2)	5(2)	7(2)	12(2)
C7	2311(4)	478(2)	3547(4)	39(2)	22(2)	42(2)	11(2)	20(2)	3(2)
C8	879(4)	700(2)	3139(4)	37(2)	23(2)	38(2)	8(2)	17(2)	-4(2)
C9	-772(4)	1389(2)	1663(3)	26(2)	29(2)	26(2)	-3(2)	8(2)	-10(2)
C10	-1158(4)	1969(2)	2322(3)	16(2)	34(2)	23(2)	2(2)	8(2)	-1(2)
C11	-878(4)	3135(2)	1501(3)	18(2)	30(2)	14(2)	1(2)	3(1)	6(2)
C12	168(4)	3673(2)	1451(3)	28(2)	22(2)	28(2)	6(2)	12(2)	9(2)
C13	-189(4)	3003(2)	3544(3)	20(2)	30(2)	16(2)	1(2)	8(1)	5(2)
C14	909(4)	2656(2)	4565(3)	18(2)	22(2)	15(2)	-0(1)	5(1)	-4(1)
N1	5031(3)	2027(2)	3421(3)	22(2)	18(2)	18(1)	-1(1)	6(1)	3(1)
N2	-330(3)	2631(2)	2467(3)	16(2)	25(2)	12(1)	0(1)	5(1)	2(1)
O1	3037(2)	1323(1)	1645(2)	19(1)	21(1)	18(1)	-2(1)	8(1)	0(1)
O2	4505(3)	538(1)	1424(2)	31(1)	21(1)	20(1)	-4(1)	12(1)	6(1)
O3	3838(3)	3198(1)	3940(2)	24(1)	26(1)	24(1)	-11(1)	9(1)	-2(1)
O4	5722(3)	3854(2)	4599(2)	27(1)	25(1)	31(1)	-12(1)	4(1)	-5(1)
O5	3132(3)	1125(1)	3912(2)	27(1)	20(1)	23(1)	6(1)	11(1)	5(1)
O6	634(3)	1214(1)	2223(2)	24(1)	22(1)	25(1)	2(1)	11(1)	-3(1)
O7	1377(3)	3559(1)	2113(2)	22(1)	19(1)	28(1)	2(1)	9(1)	3(1)
O8	-208(3)	4193(2)	769(3)	40(2)	43(2)	65(2)	34(2)	20(2)	14(2)
O9	1843(3)	2341(1)	4365(2)	23(1)	25(1)	14(1)	0(1)	8(1)	6(1)
O10	837(3)	2725(1)	5533(2)	22(1)	29(1)	12(1)	-0(1)	8(1)	1(1)

Table A.9 (continued)

atom	x	y	z	U_{11}	U_{22}	U_{33}	U_{23}	U_{13}	U_{12}
w1	3550(2)	2968(1)	1481(2)	20(1)	25(1)	15(1)	2(1)	6(1)	-1(1)
w2	2761(3)	4724(2)	3731(2)	39(2)	22(1)	24(1)	-1(1)	-2(1)	-4(1)
w3	4250(3)	4423(2)	1826(3)	55(2)	32(2)	32(2)	-5(1)	18(1)	-18(1)
w4	1894(3)	5185(2)	1194(3)	37(2)	62(2)	36(2)	-12(2)	6(1)	2(2)
w5	1101(3)	394(2)	15(3)	45(2)	51(2)	58(2)	-22(2)	29(2)	-18(2)
w6	2615(9)	9160(5)	1553(8)	83(6)	54(5)	93(7)	8(5)	36(5)	1(5)
H1a	5604	1923	2088	27					
H1b	6115	1282	2982	27					
H3a	6651	2638	4277	27					
H3b	5881	2908	3013	27					
H5a	6266	1489	4800	28					
H5b	5154	1933	5044	28					
H6a	4750	695	5090	29					
H6b	4707	609	3834	29					
H7a	2486	244	2934	39					
H7b	2510	144	4181	39					
H8a	696	925	3756	33					
H8b	316	278	2868	33					
H9a	-942	1564	900	33					
H9b	-1295	956	1622	33					
H10a	-1043	1780	3067	28					
H10b	-2081	2097	1915	28					
H11a	-1204	2857	800	26					
H11b	-1604	3404	1581	26					
H13a	27	3510	3494	25					
H13b	-1022	2970	3654	25					

Table A.10 Atomic Coordinates (x 10^4) and Thermal Parameters ($Å^2$ x 10^3) for $Sr[Mn(EGTA)]\cdot 7H_2O$

atom	x	y	z	U_{11}	U_{22}	U_{33}	U_{23}	U_{13}	U_{12}
Mn	7564(1)	608(1)	105(1)	19(1)	23(1)	19(1)	-0(1)	3(1)	-3(1)
Sr	9228(1)	5210(1)	821(1)	23(1)	29(1)	20(1)	-2(1)	5(1)	-7(1)
C1	6361(2)	-2013(5)	532(2)	25(2)	24(2)	26(2)	-3(2)	2(2)	-5(2)
C2	6189(2)	-1729(5)	-337(2)	22(2)	22(2)	29(2)	1(2)	2(2)	3(2)
C3	7085(2)	-869(5)	1710(2)	33(2)	29(2)	25(2)	2(2)	5(2)	-7(2)
C4	7817(2)	192(5)	1902(2)	24(2)	20(2)	24(2)	-1(2)	4(2)	2(2)
C5	5961(2)	548(5)	977(2)	25(2)	29(2)	31(2)	-3(2)	8(2)	-5(2)
C6	6249(2)	2202(5)	1154(2)	24(2)	31(2)	29(2)	-0(2)	7(2)	-1(2)
C7	6181(2)	3610(5)	-49(2)	26(2)	25(2)	32(2)	-2(2)	2(2)	2(2)
C8	6704(2)	4022(5)	-663(2)	28(2)	23(2)	31(2)	2(2)	5(2)	4(2)
C9	7509(2)	2766(5)	-1519(2)	27(2)	25(2)	22(2)	4(2)	4(2)	-2(2)
C10	7792(2)	1135(5)	-1721(2)	26(2)	27(2)	24(2)	1(2)	3(2)	-1(2)
C11	8264(2)	-1409(5)	-1200(2)	29(2)	23(2)	26(2)	-3(2)	4(2)	-4(2)
C12	8395(2)	-2383(5)	-459(2)	19(2)	28(2)	29(2)	3(2)	1(2)	-3(2)
C13	9054(2)	936(5)	-834(2)	23(2)	28(2)	27(2)	-0(2)	5(2)	2(2)
C14	9084(2)	2323(5)	-278(2)	22(2)	23(2)	21(2)	5(2)	1(1)	1(2)
N1	6653(2)	-562(4)	937(2)	25(2)	22(2)	22(2)	-2(1)	2(1)	-5(1)
N2	8232(2)	290(4)	-1047(2)	24(2)	21(2)	24(2)	-1(1)	2(1)	-1(1)
O1	6550(2)	-588(3)	-617(2)	29(1)	26(2)	25(1)	0(1)	1(1)	-5(1)
O2	5712(2)	-2675(4)	-714(2)	30(1)	29(2)	31(2)	-3(1)	-2(1)	-4(1)
O3	8140(2)	746(4)	1344(2)	27(1)	36(2)	23(1)	-1(1)	4(1)	-7(1)
O4	8090(2)	386(3)	2600(2)	27(1)	31(2)	22(1)	-1(1)	3(1)	-1(1)
O5	6698(2)	2767(3)	548(2)	23(1)	26(1)	25(1)	1(1)	4(1)	-3(1)
O6	6998(2)	2559(3)	-926(2)	26(1)	20(1)	29(2)	2(1)	5(1)	2(1)
O7	8289(2)	-1710(3)	164(2)	31(1)	31(2)	23(1)	2(1)	2(1)	0(1)
O8	8579(2)	-3822(3)	-528(2)	28(1)	23(2)	35(2)	3(1)	3(1)	-0(1)
O9	8494(2)	2532(3)	106(1)	22(1)	25(1)	21(1)	-1(1)	4(1)	-3(1)
O10	9707(2)	3191(3)	-205(2)	24(1)	28(2)	26(1)	-0(1)	4(1)	-4(1)

Table A.10 (continued)

atom	x	y	z	U_{11}	U_{22}	U_{33}	U_{23}	U_{13}	U_{12}
w1	9435(2)	2685(4)	1627(2)	52(2)	56(2)	44(2)	20(2)	-15(2)	-28(2)
w2	10680(2)	5233(3)	1715(2)	26(1)	28(2)	33(2)	0(1)	2(1)	-4(1)
w3	9104(2)	7554(4)	1727(2)	34(2)	37(2)	38(2)	-9(1)	4(1)	5(1)
w4	7814(2)	4937(4)	1222(2)	30(1)	36(2)	31(2)	-8(1)	10(1)	-9(1)
w5	5249(2)	5970(4)	1931(2)	38(2)	33(2)	36(2)	1(1)	-3(1)	3(1)
w6	4480(2)	2963(4)	2222(2)	36(2)	34(2)	31(2)	-2(1)	2(1)	0(1)
w7	10596(2)	3914(4)	3121(2)	32(2)	43(2)	28(2)	3(1)	-1(1)	2(1)
H1a	6768	-2826	629	31					
H1b	5868	-2354	721	31					
H3a	6715	-696	2084	35					
H3b	7263	-1956	1734	35					
H5a	5622	544	489	34					
H5b	5649	195	1374	34					
H6a	6597	2213	1637	33					
H6b	5789	2882	1189	33					
H7a	5736	2944	-259	34					
H7b	5971	4559	158	34					
H8a	7151	4681	-453	33					
H8b	6388	4569	-1080	33					
H9a	7208	3252	-1964	30					
H9b	7968	3421	-1337	30					
H10a	8151	1239	-2110	31					
H10b	7325	516	-1919	31					
H11a	7760	-1728	-1491	32					
H11b	8706	-1614	-1495	32					
H13a	9395	104	-597	32					
H13b	9262	1285	-1296	32					

Table A.11 Atomic Coordinates (x 10^4) and Thermal Parameters ($Å^2$ x 10^3) for $[Cu_2(EGTA)(OH_2)_2]\cdot 2H_2O$

atom	x	y	z	U_{11}	U_{22}	U_{33}	U_{23}	U_{13}	U_{12}
Cu	3712(1)	2799(1)	4361(1)	31(1)	16(1)	23(1)	-2(1)	3(1)	-1(1)
C1	3441(2)	6276(4)	4875(2)	37(2)	20(2)	26(2)	-0(1)	5(1)	3(1)
C2	3746(2)	6266(4)	3851(2)	37(2)	22(2)	26(2)	-0(1)	2(1)	-1(1)
C3	3111(2)	3979(4)	6092(2)	26(2)	19(2)	30(2)	-1(1)	5(1)	-2(1)
C4	2969(2)	2014(4)	5928(2)	26(2)	23(2)	32(2)	3(1)	-2(1)	1(1)
C5	4238(1)	4833(4)	5944(2)	26(2)	29(2)	30(2)	-5(1)	-0(1)	-4(1)
C6	4532(2)	3070(5)	6196(2)	28(2)	36(2)	28(2)	-2(1)	-1(1)	2(1)
C7	4849(2)	336(5)	5464(3)	36(2)	30(2)	42(2)	6(2)	2(2)	11(1)
N1	3610(1)	4625(3)	5413(2)	23(1)	17(1)	23(1)	-1(1)	3(1)	-1(1)
O1	3953(1)	4772(3)	3536(2)	47(1)	21(1)	27(1)	-1(1)	11(1)	-1(1)
O2	3768(1)	7641(3)	3377(2)	79(2)	20(1)	33(1)	5(1)	12(1)	2(1)
O3	3241(1)	1224(3)	5219(2)	35(1)	19(1)	30(1)	-1(1)	5(1)	-3(1)
O4	2584(1)	1293(3)	6487(2)	42(1)	26(1)	45(1)	3(1)	18(1)	-6(1)
O5	4671(1)	2158(3)	5295(2)	32(1)	28(1)	29(1)	2(1)	0(1)	6(1)
w1	3810(1)	1115(3)	3290(2)	51(1)	21(1)	30(1)	-6(1)	3(1)	3(1)
w2	2976(1)	2114(3)	1893(2)	55(2)	32(1)	32(1)	1(1)	7(1)	1(1)
H1a	2986	6352	4802	60					
H1b	3596	7284	5242	60					
H3a	3256	4147	6761	60					
H3b	2727	4652	5980	60					
H5a	4173	5486	6543	60					
H5b	4524	5481	5529	60					
H6a	4238	2377	6575	60					
H6b	4918	3247	6573	60					
H7a	5148	263	6006	60					
H7b	4478	-358	5610	60					

APPENDIX B

LEAST SQUARES PLANES

Estimated standard deviations in the least significant digit(s) for the coefficients in the equation of the least squares planes are given in parentheses. Deviations of selected atoms from the planes are given in units of 0.01 Å. Dihedral angles between planes are given in degrees.

Table B.1 Selected Least Squares Planes for $Ca[Ca(EGTA)]\cdot(22/3)H_2O$ (2)

(a) Equations of least squares planes ($\underline{a}x + \underline{b}y + \underline{c}z = \underline{d}$)

		a	b	c	d
P1:	N2, O5, O6, O7	22.3(5)	-5.43(8)	-5.8(2)	-5.25(9)
P2:	O9, O3, N1, O1	8.9(6)	12.65(9)	9.9(3)	20.0(1)
P3:	O19, O13, N3, O11	-10.5(5)	12.5(1)	10.3(5)	10.07(8)
P4:	O17, N4, O16, O15	21.0(4)	5.12(8)	6.6(7)	8.49(7)
P5:	O27, N6, O26, O25	11.4(1)	10.50(6)	-12.5(2)	14.35(7)
P6:	O21, N5, O23, O29	20.5(2)	-6.07(9)	6.5(4)	4.4(1)
P7:	O19, O20, w2, w4	16.2(6)	-6.40(3)	-13.1(5)	-8.21(3)
P8:	O9, O10, w1, w3	14.3(4)	-6.25(2)	12.9(3)	-7.60(2)
P9:	O7, O8, w7, w8	18.8(5)	-0.14(4)	-13.1(1)	-2.66(4)
P10:	O17, O18, w5, w6	14.8(9)	0.07(7)	14.2(3)	4.24(7)
P11:	O23, O29, w10	23.75(2)	3.70(1)	-1.88(3)	13.57(1)
P12:	O2, O12, w9	24.08(3)	2.33(1)	-2.45(3)	9.10(1)
P13:	O2, O29, w9, w10	-0.5(2)	5.69(9)	17.9(2)	12.12(9)
P14:	O12, O23, w9, w10	-4.7(2)	15.5(1)	6.6(3)	14.9(1)
P15:	O2, O12, O23, O29	5.0(2)	-13.45(7)	10.4(2)	-8.99(7)

(b) Deviations of selected atoms from planes

Plane 1: Ca1(-1), N2(-15), O5(-9), O6(15), O7(8)
Plane 2: Ca1(3), N1(18), O1(-11), O3(-17), O9(10)
Plane 3: Ca2(-3), N3(-15), O11(9), O13(14), O19(-8)
Plane 4: Ca2(-4), N4(-12), O15(-7), O16(13), O17(7)
Plane 5: Ca3(-11), N6(-12), O25(-7), O26(12), O27(7)
Plane 6: Ca3(1), N5(16), O21(-10), O23(-16), O29(10)
Plane 7: Ca4(-1), O19(-6), O20(6), w2(3), w4(-3)
Plane 8: Ca4(-1), O9(4), O10(-4), w1(2), w3(-2)
Plane 9: Ca5(9), O7(5), O8(7), w7(5), w8(-3)
Plane 10: Ca5(11), O17(10), O18(-14), w5(11), w6(-7)
Plane 13: O2(-12), O29(13), w9(12), w10(-12)

Table B.1 (continued)

Plane 14: O12(-13), O23(14), w9(13), w10(-14)
Plane 15: O2(-10), O12(9), O23(-9), O29(10)

(c) Selected dihedral angles between planes

1-2(92.5), 3-4(86.2), 5-6(94.6), 7-8(86.2), 9-10(91.9), 11-12(5.0), 11-13(88.5), 11-14(89.7), 11-15(89.6), 12-13(91.7), 12-14(94.8), 12-15(86.7), 13-14(50.9), 13-15(75.3), 14-15(126.2)

Table B.2 Selected Least Squares Planes for $Sr[Ca(EGTA)]\cdot 6H_2O$ (3)

(a) Equations of least squares planes ($\underline{a}x + \underline{b}y + \underline{c}z = \underline{d}$)

		a	b	c	d
P1:	N1, O2, O3, O9	6.8(2)	1.9(4)	-3.0(4)	5.6(1)
P2:	N2, O5, O6, O7	4.8(1)	9.5(5)	6.3(5)	4.5(1)
P3:	w1, w2, w3	1.106(9)	9.64(2)	-6.75(5)	8.80(1)
P4:	O10, w1, w3, O10'	-1.1(2)	10.1(4)	3(1)	3.9(2)
P5:	O8, O10, O10'	-0.756(9)	4.93(2)	-12.3(2)	1.71(1)
P6:	O8, w3, w4, O10	7.6(3)	-2.6(7)	2(2)	7.9(3)
P7:	O8, O10, w1, w4	6.0(2)	9.0(4)	5.3(9)	9.3(2)

(b) Deviations of selected atoms from planes

Plane 1: Ca(-10), N1(23), O1(-14), O3(-22), O9(13)
Plane 2: Ca(1), N2(12), O6(-20), O7(-11), O5(12))
Plane 4: O10(-31), w1(25), w3(-30), O10', (37), Sr(55), w2(210)
Plane 5: O8(50), w3(42), w4(-44), O10'(-46). Sr(-118), O7(200)
Plane 7: O8(28), O10(-23), w1(26), w4(-31), Sr(100), O9(-159)

Table B.2 (continued)

(c) Selected dihedral angles between planes

1-2(86.8), 3-5(33.2), 3-4(52.5), 3-6(100.4), 3-7(56.8), 4-5(80.6), 4-6(122.8), 4-7(53.1), 5-6(100.6), 5-7(86.7), 6-7(69.8)

Table B.3 Selected Least Squares Planes for $Mg[Sr(EGTA)(OH_2)]\cdot 7H_2O$ (**4**)

(a) Equations of least squares planes ($\underline{a}x + \underline{b}y + \underline{c}z = \underline{d}$)

		a	b	c	d
P1:	O9, O6, O7	14.81(6)	-11.8(1)	2.13(3)	2.51(1)
P2:	O3, O5, O1	14.2(1)	-12.29(6)	2.06(3)	-0.29(1)
P3:	O9, O3, O6,	10(1)	4(1)	-12.4(6)	-1.7(2)
P4:	O6, O7, O1, O5	12.8(5)	12.8(6)	3.4(1)	3.16(5)
P5:	O7, O1, O3, O9	2.5(7)	9.7(7)	11.6(2)	6.5(1)

(b) Deviations of selected atoms from planes

Plane 1: N2(149), Sr(-131)
Plane 2: N1(-154), Sr(134)
Plane 3: O3(29), O5(-28), O6(25), O9(-26), Sr(-159)
Plane 4: O1(8), O5(-8), O6(7), O7(-7), Sr(115), w2(-180)
Plane 5: O1(15), O3(-15), O7(-15), O9(15), Sr(-60), w1(196)

(c) Selected dihedral angles between planes

1-2(2.2), 3-1(87.7), 3-2(88.5), 4-1(94.8), 4-2(97.0), 4-3(76.3), 5-1(101.9), 5-2(103.2), 5-3(121.0), 5-4(45.0)

Table B.4 Selected Least Squares Planes for $Mg[Ba(EGTA)]\cdot(8/3)H_2O)\cdot(1/3)(CH_3)_2CO$ (6)

(a) Equations of least squares planes ($ax + by + cz = d$)

		a	b	c	d
P1:	O6, O7, O9	15.85(2)	-4.64(1)	12.42(1)	18.83(1)
P2:	O3, O5, O1	16.77(2)	-5.10(1)	11.01(1)	14.80(1)
P3:	O9, O3, O6, O5	15.41(8)	6.53(6)	-11.41(5)	2.59(5)
P4:	O5, O6, O1, O7	5.82(5)	14.54(4)	4.12(4)	20.02(3)
P5:	O1, O7, O3, O9	-7.54(2)	9.23(2)	14.55(2)	15.16(1)
P6:	O19, O16, O17	19.69(2)	4.35(2)	-6.52(1)	5.69(1)
P7:	O13, O15, O11	18.80(2)	4.89(2)	-7.94(1)	7.39(1)
P8:	O19, O13 O15, O16	4.2(1)	7.3(1)	17.31(8)	16.92(5)
P9:	O15, O16, O11, O17	-5.32(3)	14.93(3)	1.53(2)	6.39(2)
P10:	O17, O11, O19, O13	9.40(2)	-9.27(2)	13.55(1)	11.58(1)
P11:	O29, O26, O27	-2.78(1)	4.71(7)	18.99(2)	11.28(1)
P12:	O23, O25, O21	-1.41(1)	5.23(6)	18.88(1)	15.14(1)
P13:	O29, O23, O26, O25	18.83(6)	-7.1(3)	4.18(6)	16.83(4)
P14:	O26, O25, O21, O27	0.99(2)	14.91(8)	-5.15(2)	-0.13(2)
P15:	O27, O21, O29, O23	17.25(7)	9.4(3)	-1.33(6)	11.27(5)

(b) Deviations of selected atoms from planes

Plane 1: N2(143), Ba1(-146)
Plane 2: N1(-139), Ba1(146)
Plane 3: O3(-6), O5(7), O6(-7), O9(6), Ba7(159)
Plane 4: O1(-5), O5(5), O6(-5), O7(4), Ba1(-100), O24(182)
Plane 5: O1(2), O3(-2), O7(-2), O9(2), Ba1(102), O12(-181)
Plane 6: N4(-148), Ba2(146)
Plane 7: N3(143), Ba2(-149)
Plane 8: O13(7), O15(-7), O16(7), O19(-7), Ba2(157)
Plane 9: O11(2), O15(-2), O16(2), O17(-2), Ba2(93), O4(186)
Plane 10: O11(1), O13(-1), O17(-1), O19(1), Ba2(-106), O22(179)
Plane 11: N6(-141), Ba3(147)

Table B.4 (continued)

Plane 12: N5(143), Ba3(-144)
Plane 13: O23(-6), O25(6), O26(-6), O29(6), Ba3(-157)
Plane 14: O21(-2), O25(2), O26(-2), O27(2), Ba3(-98), O14(181)
Plane 15: O21(-7), O23(7), O27(7), O29(-7), Ba3(103), O2(-177)

(c) Selected dihedral angles between planes

1-2(5.0), 3-1(87.9), 3-2(84.6), 4-1(87.9), 4-2(89.6), 4-3(61.9), 5-1(89.1), 5-2(93.9), 5-3(113.7), 5-5(51.8), 6.7(5.1), 8-6(88.4), 8-7(91.2), 9-6(88.4), 9-7(86.2), 9-8(61.7), 10-6(89.9), 10-7(94.8), 10-8(67.7), 10-9(129.4), 11-12(4.1), 13-11(93.1), 13-12(90.9), 14-11(87.3), 14-12(85.2), 14-13(117.2), 15-11(88.7), 15-12(84.7), 15-13(67.0), 15-14(50.2)

Table B.5 Selected Least Squares Planes for $[Mg_2(EGTA)(OH_2)_6]\cdot 5H_2O$ (6)

(a) Equations of least squares planes ($\underline{a}x + \underline{b}y + \underline{c}z = \underline{d}$)

		a	b	c	d
P1:	N1, O1, w1, w3	6.6(1)	10.9(1)	1.6(3)	13.76(9)
P2:	O1, O3, w1, w2	-0.75(4)	-2.17(5)	15.7(1)	2.85(3)
P3:	w3, N1, w2, O3	12.2(1)	-6.2(2)	0.5(3)	6.7(1)
P4:	N2, O9, w6, w5	11.8(2)	6.7(2)	1.2(1)	13.0(1)
P5:	O7, N2, w4, w6	7.6(1)	-10.4(1)	1.05(9)	-1.10(9)
P6:	O7, O9, w4, w5	-1.54(2)	1.39(2)	15.729(9)	16.94(1)

(b) Deviations of selected atoms from planes

Plane 1: N1(12), O1(-13), w1(-11), w3(12)
Plane 2: O1(-5), O3(5), w1(-5), w2(5)
Plane 3: N1(-16), O3(17), w2(14), w3(-15)
Plane 4: N2(19), O9(-20), w5(-17), w6(18)
Plane 5: N2(-13), O7(15), w4(11), w6(-13)
Plane 6: O7(1), O9(-1), w4(1), w5(-1)

Table B.5 (continued)

(c) Selected dihedral angles between planes

1-2(94.6), 3-1(91.8), 3-2(86.0), 5-4(90.0), 6-4(87.5), 6-5(95.0)

Table B.6 Selected Least Squares Planes for $Sr[Cd(EGTA)]\cdot 7H_2O$ (7)

(a) Equations of least squares planes ($\underline{a}x + \underline{b}y + \underline{c}z = \underline{d}$)

		a	b	c	d
P1:	O5, O6, N2, O7	12.6(2)	4.8(6)	4(2)	9.9(1)
P2:	O1, N1, O3, O9	10.3(2)	-7(1)	-3(2)	7.2(2)
P3:	O10a, O8b, O10	7.24(1)	0.54(2)	-16.7(3)	7.51(1)
P4:	w1, w3, w4	-6.06(1)	-0.58(2)	17.06(6)	-2.98(1)
P5:	O10, O10a, w1, w3	14.6(3)	-0.8(5)	7(2)	14.2(3)
P6:	O8b, O10a, w3, w4	6.7(3)	-7.5(5)	3(3)	1.4(3)
P7:	O8b, w1, w4, O10	9.7(2)	6.0(4)	6(2)	11.5(2)

(b) Deviations of selected atoms from planes

Plane 1: Cd(0), N2(24), O5(14), O6(-24), O7(-14)
Plane 2: Cd(18), N1(-29), O1(18), O3(28), O9(-17)
Plane 5: O10(-41), w1(33), w3(-31), O10a(39)
Plane 6: O8b(-45), w3(-42), w4(42), O10a(45)
Plane 7: O8b(24), O10(-26), w1(25), w4(-23)

(c) Selected dihedral angles between planes

1-2(90.7), 3-4(175.6), 3-5(94.0), 3-6(95.3), 3-7(93.5), 4-5(81.6), 4-6(82.4), 4-7(83.7), 5-6(57.5), 5-7(51.0), 6-7(108.4)

Table B.7 Selected Least Squares Planes for $Ca[Er(EGTA)(OH_2)]\cdot 12H_2O\cdot(CH_3)_2CO$ (8)

(a) Equations of least squares planes ($\underline{a}x + \underline{b}y + \underline{c}z = \underline{d}$)

		a	b	c	d
P1:	O1, O5, O6	-1.49(3)	-1.69(2)	17.4(2)	-0.17(1)
P2:	O3, O7, O9	-2.72(3)	-4.47(3)	16.51(4)	1.57(1)
P3:	O5, O1, O3, O7	12.5(3)	-1.9(2)	-2.6(4)	1.74(6)
P4:	O5, O6, O3, O9	6.9(1)	9.5(1)	2.7(3)	6.97(5)
P5:	O1, O7, O6, O9	-6.0(2)	10.5(2)	5.6(5)	2.34(8)
P6:	O11, O15, O16	6.26(1)	-7.57(2)	8.02(2)	6.24(1)
P7:	O13, O17, O19	3.19(2)	-8.85(2)	9.69(2)	0.84(1)
P8:	O13, O15 O11, O17	-1.9(1)	7.7(1)	13.7(1)	9.70(7)
P9:	O11, O16, O17, O19	10.74(9)	-1.0(1)	-13.1(2)	2.04(7)
P10:	O15, O16, O19, O13	9.86(8)	7.3(1)	0.3(1)	9.92(6)
P11:	w2, w3, O9, O3	6.0(1)	10.4(1)	-6.1(1)	4.70(4)
P12:	w1, w4, O13, O14	9.42(2)	7.59(2)	-7.82(3)	6.52(1)

(b) Deviations of selected atoms from planes

Plane 1: Er(174)
Plane 2: Er(-159)
Plane 3: O1(-10), O3(-8), O5(8), O7(10), Er1(81), N1(-170)
Plane 4: O3(-7), O5(7), O6(-7), O9(7), Er1(-82), w1(164)
Plane 5: O1(12), O6(-10), O7(-12), O9(10), Er1(82), N2(-177)
Plane 6: Er2(-170)
Plane 7: Er2(158)
Plane 8: O11(12), O13(9), O15(-9), O17(-11), Er1(-81), N3(173)
Plane 9: O11(-11), O16(9), O17(11), O19(-9), Er2(-80), N4(179)
Plane 10: O13(8), O15(-8), O16(9), O19(-8), Er2(83), w2(-164)
Plane 11: O3(6), O9(-6), w2(5), w3(-5), Ca1(120)
Plane 12: O13(-18), O19(17), w1(-16), w4(17)

Table B.7 (continued)

(c) Selected dihedral angles between planes

1-2(15.0), 1-3(88.4), 2-3(92.4), 1-4(82.4), 2-4(97.0), 3-7(63.1), 1-5(82.6), 2-5(92.2), 3-5(124.9), 4-5(61.9), 6-7(15.2), 6-8(90.4), 7-8(90.9), 6-9(81.6), 7-9(93.7), 8-9(125.3), 6-10(82.3), 7-10(96.3), 8-10(65.1), 9-10(60.2), 11-12(10.5)

Table B.8 Selected Least Squares Planes for $Ca[Nd(EGTA)(OH_2)]\cdot 9H_2O$ (9)

(a) Equations of least squares planes ($\underline{a}x + \underline{b}y + \underline{c}z = \underline{d}$)

		a	b	c	d
P1:	O1, w1, O3	10.05(3)	-3.33(4)	-0.80(3)	2.47(1)
P2:	O10, O7, O6 O9	10.45(8)	-3.4(4)	-2.8(4)	-0.2(1)

(b) Deviations of selected atoms from planes

Plane 1: O1(1), O3(1), O5(-1), w1(-1)
Plane 2: O6(-16), O7(-14), O9(13), O10(17)

(c) Selected dihedral angles between planes

1-2(9.2)

Table B.9 Selected Least Squares Planes for $Sr[Mn(EGTA)]\cdot 7H_2O$ (10)

(a) Equations of least squares planes ($\underline{a}x + \underline{b}y + \underline{c}z = \underline{d}$)

		a	b	c	d
P1:	N1, O1, O3, O9	10.1(2)	7(1)	-3(2)	7.0(2)
P2:	N2, O5, O6, O7	12.5(2)	4.7(6)	4(2)	9.8(1)
P3:	w1, w2, w3	-0.44(1)	-0.39(2)	17.36(6)	2.30(1)

Table B.9 (continued)

P4:	O10, w1, w3, O10'	15.790(7)	1.02(2)	2.63(6)	15.599(7)
P5:	O8, O10, O10'	6.81(1)	0.78(2)	-16.6(3)	7.20(1)
P6:	O8, w3, w4, O10'	6.9(4)	-7.4(5)	3(3)	1.7(3)
P7:	O8, O10, w1, w4	9.6(2)	5.9(4)	6(2)	11.4(2)

(b) Deviations of selected atoms from planes

Plane 1: Mn(16), N1(-26), O1(16), O3(26), O9(-16)
Plane 2: Mn(2), N2(22), O5(13), O6(-22), O7(-13)
Plane 3 Sr(-149),
Plane 4: O10(-46), w1(36), w3(-34), O10'(44), Sr(-61), w2(207)
Plane 5: Sr(-187)
Plane 6: O8(-47), w3(-45), w4(45), O10'(47), Sr(110), O7(-202)
Plane 7: O8(23), O10(-26), w1(24), w4(-22), Sr(107), O9(-164)

(c) Selected dihedral angles between planes

1-2(90.5), 4-3(62.6), 5-3(157.0), 5-4(94.7), 6-3(75.4), 6-4(57.8), 6-5(96.4), 7-3(69.0), 7-4(48.9), 7-5(93.7), 7-6(106.5)

Table B.10 Selected Least Squares Planes for $[Cu_2(EGTA)(OH_2)_2]\cdot 2H_2O$ (11)

(a) Equations of least squares plane ($\underline{a}x + \underline{b}y + \underline{c}z = \underline{d}$)

		$\underline{a}$	$\underline{b}$	$\underline{c}$	$\underline{d}$
P1:	N1, O1, O3, w1	19.0(2)	-1.7(2)	4.6(2)	8.48(8)

(b) Deviations of selected atoms from the plane

Plane 1: N1(12),O1(-12), O3(-11), w1(11), O5(250), Cu(13)

APPENDIX C

HYDROGEN BONDING DISTANCES

All O...O contacts between the oxygen atoms of a water molecule and the oxygen atom of a carboxylate group or a water molecule not bound to the same metal ion less than 3 Å are specified. Bond distances are given in Å. Estimated standard deviations in the least significant digit(s) are given in parentheses.

Table C.1 Hydrogen Bonding Distances for $Ca[Ca(EGTA)]\cdot(22/3)H_2O$ (2)

w1...O8a	2.751(6)	w1...O14a	2.901(6)
w2...O13a	2.750(6)	w3...O3a	2.778(6)
w4...O4	2.832(6)	w4...O18	2.781(6)
w5...O3	2.881(6)	w5...O14a	2.828(6)
w6...O10a	2.696(6)	w6...w20a	2.939(10)
w7...O13	2.852(6)	w7...O4a	2.790(7)
w8...O20a	2.692(7)	w8...w20a	2.879(10)
w9...w21	2.818(17)	w9...w14a	2.859(9)
w10...O22a	2.668(8)	w10...w22a	2.832(21)
w11...O24	2.769(7)	w11...O21a	2.879(7)
w12...O12a	2.850(7)	w12...O27a	2.856(7)
w12...w17a	2.797(9)	w13...w18	2.821(10)
w13...O28a	2.741(8)	w13...w14b	2.932(8)
w14...O1a	2.807(7)	w15...O11	2.894(8)
w15...O24	2.727(8)	w15...w21b	2.621(18)
w16...O28a	2.915(9)	w16...O30a	2.744(9)
w16...w17a	2.778(11)	w17...w19	2.682(12)
w18...w19	2.815(12)	w18...w20	2.727(11)
w21...O22a	2.691(15)	w22...O30a	2.612(19)

Table C.2 Hydrogen Bonding Distances for $Sr[Ca(EGTA)]\cdot6H_2O$ (3)

w1...O3	2.796(6)	w1...w6b	2.972(5)
w2...O8b	2.754(4)	w2...w6b	2.876(6)
w3...w5c	2.753(5)	w4...O5	2.850(5)
w4...O4b	2.740(5)	w5...w6	2.849(7)
w5...O2b	2.677(4)	w5...O4c	2.797(4)
w6...O1a	2.754(5)		

Table C.3 Hydrogen Bonding Distances for $Mg[Sr(EGTA)(OH_2)]\cdot7H_2O$ (4)

w1...O10b	2.711(7)	w2...O2a	2.733(6)
w2...w5b	2.743(7)	w3...O4a	2.692(7)
w3...O10a	2.905(7)	w4...w7	2.886(10)
w4...O2b	2.834(10)	w4...w8a	2.765(11)
w5...O4	2.737(7)	w5...w6	2.929(8)
w5...O8b	2.769(7)	w6...w6a	2.978(13)
w6...w8a	2.918(10)	w7...w8	2.902(10)
w7...O8b	2.812(8)	w7...w7b	2.803(11)

Table C.4 Hydrogen Bonding Distances for $Mg[Ba(EGTA)]\cdot(8/3)H_2O\cdot(1/3)(CH_3)_2CO$ (5)

w1...O10	2.656(5)	w1...O22	2.703(4)
w2...O18	2.612(5)	w2...w5a	2.907(4)
w3...O12	2.745(4)	w3...O30a	2.650(5)
w4...O8	2.644(5)	w4...O20a	2.844(5)
w5...O28	2.562(4)	w5...O6a	2.846(4)
w6...O2b	2.754(4)	w6...O20a	2.664(5)
w7...O14	2.925(5)	w7...w8a	2.745(6)
w8...O10	2.726(5)	w8...O18a	2.771(6)

Table C.5 Hydrogen Bonding Distances for $[Mg_2(EGTA)(OH_2)_6]\cdot5H_2O$ (6)

w1...w11	2.859(5)	w1...O2b	2.662(5)
w2...w9	2.644(6)	w2...w8c	2.756(5)
w3...w1	2.980(5)	w3...O7a	2.709(4)
w3...O9a	2.776(4)	w4...O4a	2.890(5)
w4...O8a	2.755(4)	w5...w10	2.698(7)
w5...w7a	2.751(5)	w6...O1a	2.817(4)
w6...O3a	2.841(5)	w7...w9	2.804(6)
w7...O10b	2.739(5)	w8...O4a	2.707(5)
w8...O8a	2.752(5)	w8...w2a	2.756(5)
w8...w10a	2.830(8)	w9...w11	2.865(7)
w11...O5a	2.912(6)	w11...O6a	2.920(13)
w11...O10a	2.738(6)		

Table C.6 Hydrogen Bonding Distances for $Sr[Cd(EGTA)]\cdot7H_2O$ (7)

w1...O3	2.711(6)	w1...w5a	2.950(6)
w2...w7	2.746(5)	w2...O8b	2.781(5)
w3...w6b	2.830(5)	w4...O5	2.775(4)
w4...O4a	2.713(5)	w5...w6	2.956(5)
w5...O4a	2.855(5)	w5...w7a	2.890(6)
w6...O2a	2.646(5)	w7...O1a	2.910(5)
w7...O6a	2.993(4)		

Table C.7 Hydrogen Bonding Distances for $Ca[Er(EGTA)(OH_2)]_2 \cdot 12H_2O \cdot (CH_3)_2CO$ (8)

w1...O20	2.608(7)	w1...w9a	2.752(8)
w2..O10	2.627(8)	w2...O14a	2.633(8)
w3..O4	2.682(6)	w3...w6	2.775(7)
w4...O14	2.670(7)	w4...w9a	2.748(8)
w5...w7	2.772(11)	w5...w10	2.876(11)
w6...w8	2.743(8)	w6...O10a	2.846(8)
w7...w11b	2.698(13)	w7...w12c	2.876(10)
w8...O12a	2.881(9)	w8...O18a	2.787(9)
w9...w12	2.735(7)	w9...O21	2.769(9)
w10...O8a	2.878(10)	w10...O12a	2.780(10)
w11...O20a	2.773(10)	w11...w14a	2.694(14)
w12...O2a	2.694(7)	w12...O8b	2.693(9)
w13...O12a	2.944(10)	w13...O18a	2.734(11)
w13...w14a	2.691(13)	w14...O2	2.735(14)

Table C.8 Hydrogen Bonding Distances for $Ca[Nd(EGTA)(OH_2)]_2 \cdot 9H_2O$ (9)

w1...w3	2.746(4)	w1...O9a	2.661(3)
w2...O3	2.986(4)	w2...O7	2.929(3)
w2...w5c	2.833(6)	w3...w4	2.736(5)
w3...O2a	2.922(4)	w4...O8	2.787(5)
w4...O8a	2.700(4)	w5...O1	2.862(4)
w5...w5a	2.761(7)	w6...O4b	2.750(12)

Table C.9 Hydrogen Bonding Distances for $Sr[Mn(EGTA)] \cdot 7H_2O$ (10)

w1...O3	2.689(5)	w1...w5a	2.892(5)
w2...w7	2.712(4)	w2...O8b	2.800(4)
w2...w6b	2.984(4)	w3...w6b	2.811(4)
w4...O5	2.755(4)	w4...O4b	2.714(4)
w5...w6	2.905(4)	w5...O4b	2.809(4)
w5...w7b	2.840(4)	w6...O2a	2.623(4)
w7...O1a	2.909(4)	w7...O6a	2.953(4)

Table C.10 Hydrogen Bonding Distances for $[Cu_2(EGTA)(OH_2)_2]\cdot 2H_2O$ (11)

w1...w2	2.664(3)	w1...O2a	2.615(3)
w2...w1	2.664(3)	w2...O4a	2.775(4)
w2...O4b	2.743(3)		